Workshop

Data-driven damage detection in railway systems

Deteção de dano em sistemas ferroviários com Inteligência Artificial



Cecília **VALE** & Diogo **RIBEIRO** (Editors)

2023

U.PORTO FEUP FACULDADE DE ENGENHARIA UNIVERSIDADE DO PORTO
isep Instituto Superior de Engenharia do Porto
EVOLEO TECHNOLOGIES
WAY4SAFE RAIL
NORTE2020
PORTUGAL 2020
UNIÃO EUROPEIA
Fundo Europeu de Desenvolvimento Regional

Technical sheet

Pagination and assembly: Cecília Vale, Rúben Silva and Diogo Ribeiro

ISBN: 978-989-35087-4-9

© The authors. 2023
© The editors. 2023
© Faculty of Engineering of University of Porto
Rua Dr. Roberto Frias, s/n, 4200-465 Porto
© School of Engineering of Polytechnic of Porto
Rua Dr. António Bernardino de Almeida, 431, 4249-015 Porto

Text prepared from the direct reproduction of the originals prepared by the authors. Despite the attention taken in the preparation of this publication, to guarantee its quality and integrity, the editors assume no responsibility for the content and possible inaccuracies in the text.

U.PORTO FEUP FACULDADE DE ENGENHARIA UNIVERSIDADE DO PORTO
isep Instituto Superior de Engenharia do Porto
EVOLEO TECHNOLOGIES
WAY4SAFE RAIL
NORTE2020
PORTUGAL 2020
UNIÃO EUROPEIA
Fundo Europeu de Desenvolvimento Regional

Preface

This publication is the result of a compilation of presentations by guest speakers from the **Workshop "Data-driven damage detection in railway systems"** held in the facilities of Faculty of Engineering of University of Porto (FEUP) and School of Engineering of Polytechnic of Porto (ISEP), from 27th february till 1st March 2023.

This dissemination event was part of the **WAY4SafeRail project** (WAYside monitoring system FOR Safe Rail Transportation) and aims to train the academic and scientific community, especially researchers and PhD students, with basic skills in the field of damage detection in railway systems using Artificial Intelligence techniques.

The chapters in this book cover various subdomains related to the track and train subsystems, monitoring systems (wayside and onboard), vehicle-track dynamic interaction methodologies, damage identification methodologies based on Artificial Intelligence, and case studies.



Cecília Vale [FEUP]



Diogo Ribeiro [FEUP]

U.PORTO FEUP FACULDADE DE ENGENHARIA UNIVERSIDADE DO PORTO
isep Instituto Superior de Engenharia do Porto
EVOLEO TECHNOLOGIES
WAY4SAFE RAIL
NORTE2020
PORTUGAL 2020
UNIÃO EUROPEIA
Fundo Europeu de Desenvolvimento Regional

Contents

1. Railway track: Components, assessment of the geometrical quality. Typical Damages.
Cecília Vale [FEUP]

2. Vehicle subsystem: Components, dynamic characteristics. Typical Damages.
Diogo Ribeiro [ISEP], Rúben Silva [ISEP], António Guedes [ISEP] & Mohammad Reza [FEUP]

3. Monitoring systems
Araliya Mosleh [FEUP]

4. Vehicle track dynamic interaction
Pedro Montenegro [FEUP]

5. Methodologies for damage detection
Andreia Meixedo [FEUP], Maria de Lurdes Simões [FEUP], Diogo Ribeiro [ISEP], Araliya Mosleh [FEUP], Rúben Silva [FEUP] & António Guedes [ISEP]

U.PORTO FEUP FACULDADE DE ENGENHARIA UNIVERSIDADE DO PORTO
isep Instituto Superior de Engenharia do Porto
EVOLEO TECHNOLOGIES
WAY4SAFE RAIL
NORTE2020
PORTUGAL 2020
UNIÃO EUROPEIA
Fundo Europeu de Desenvolvimento Regional

Railway track: Components, assessment of the geometrical quality.
Typical Damages.

Cecília Vale [FEUP]

Contents

1. Railway tracks systems
2. Geometrical track quality assessment
3. Typical damages
4. Numerical modelling

1. Railway track systems

Types of structural track systems

Structural systems

- ballasted tracks



- slab or ballast less tracks



1. Railway track systems

Ballasted tracks

A high proportion of existing tracks have been constructed by using ballast.



Ballasted tracks have several **advantages** in relation to slab tracks, such:

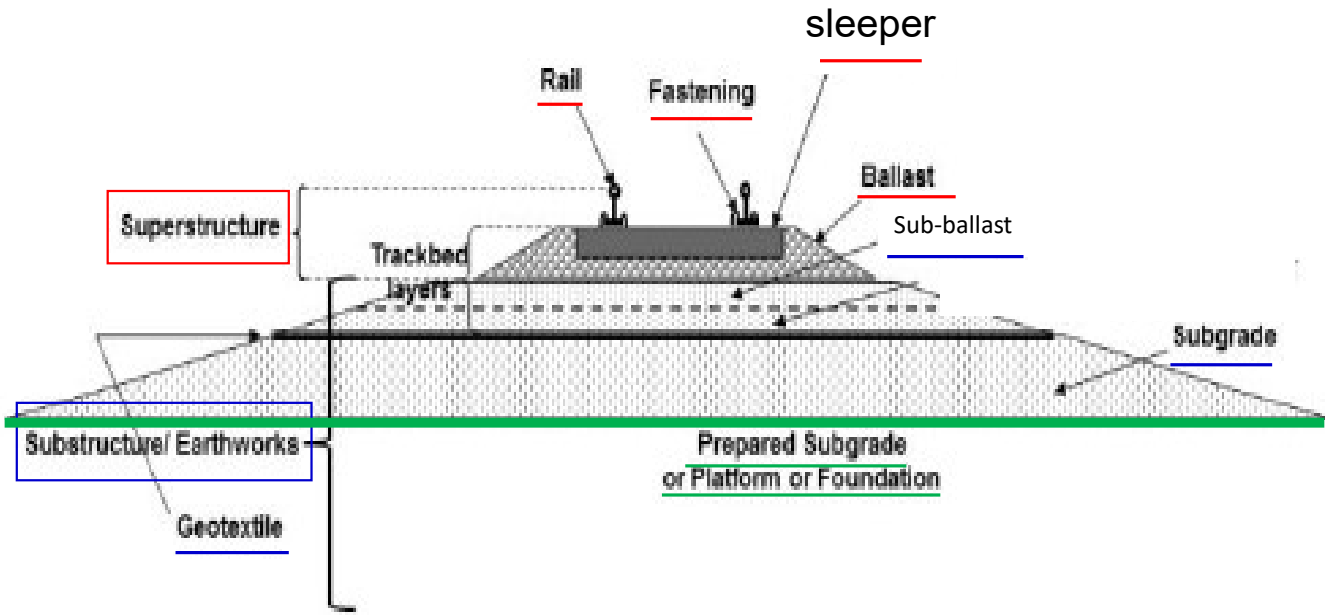
- lower construction cost;
- easier maintenance;
- highest noise and vibration attenuation;
- possibility of reusing the ballast as secondary material in the subgrade;
- easiness of modifying the track layout as can't, intersections, etc.

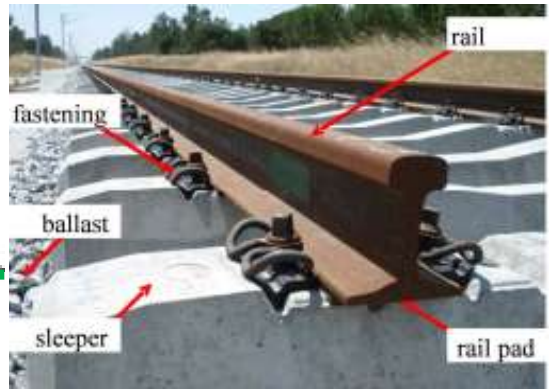
The **disadvantages** in relation to slab tracks are:

- highest maintenance costs during its lifetime;
- ballast wear due to abrasion and fragmentation;
- larger construction volumes given that ballasted track has generally a greater cross section;
- limited lateral resistance.

1. Railway track systems

Ballasted tracks: classical system



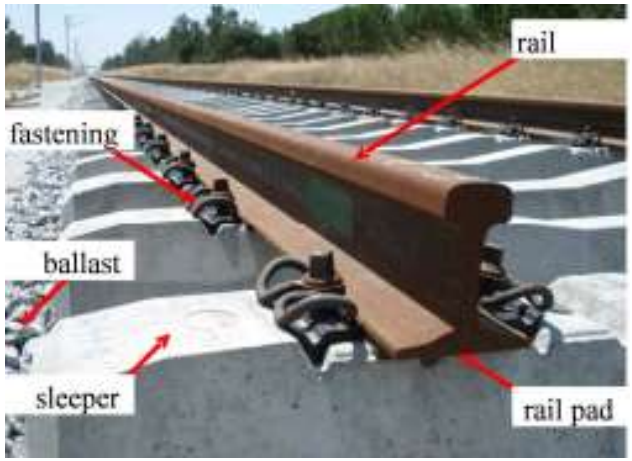


Adapted Figure from Giannakos (2015).

1. Railway track systems

Ballasted tracks: elements

Rail

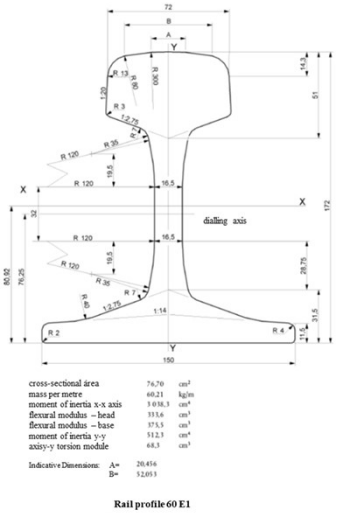


Functions

1. To provide the level and continuous surface.
2. To provide a smooth pathway to trains.
3. To serve as a lateral guide.
4. To carry the stresses from the loads transmitted from the wheels of the rolling stock to the track.

Section rail choice

1. Daily traffic (ton).
2. Vehicle speed.
3. Load per wheel.
4. Expected life cycle.
5. Maintenance.



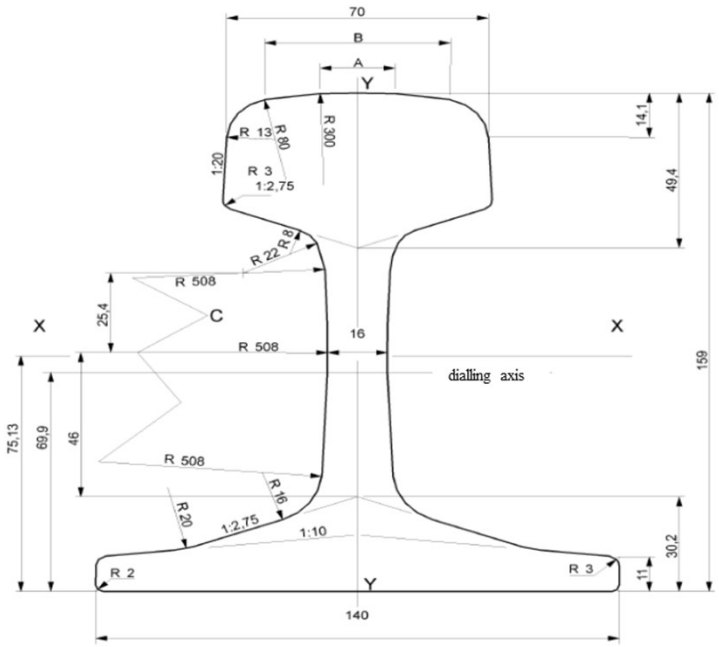
Rail profile 60 E1

European practice: TMD<25000 t – 54E1; TMD>35000 t – 60E1

Most common in Portugal: 54E1 (54kg/m) and 60E1 (60kg/m)

1. Railway track systems

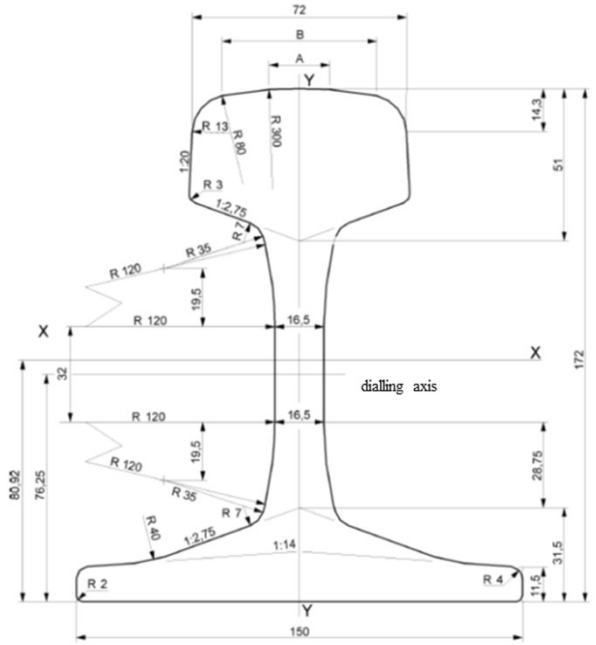
Ballasted tracks: elements



cross-sectional área	69,77	cm²
mass per metre	54,77	kg/m
moment of inertia x-x axis	2 337,9	cm⁴
flexural modulus – head	278,7	cm³
flexural modulus – base	311,2	cm³
moment of inertia y-y	419,2	cm⁴
axisy-y torsion module	59,9	cm³

Indicative Dimensions: A= 20,024
B= 49,727

Rail profile 54 E1



cross-sectional área	76,70	cm²
mass per metre	60,21	kg/m
moment of inertia x-x axis	3 038,3	cm⁴
flexural modulus – head	333,6	cm³
flexural modulus – base	375,5	cm³
moment of inertia y-y	512,3	cm⁴
axisy-y torsion module	68,3	cm³

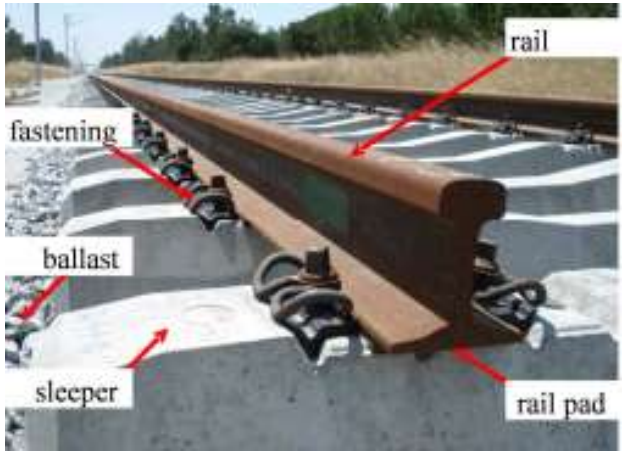
Indicative Dimensions: A= 20,456
B= 52,053

Rail profile 60 E1

1. Railway track systems

Ballasted tracks: elements

Sleepers



Functions

1. To hold the rails strongly and to maintain uniform gauge.
2. To transfer the load from rails to the ballast or ground.
3. To reduce the vibrations coming from the rails.
4. To offer longitudinal and lateral stability.

Types of sleepers according to material:

- Wooden sleepers.
- Concrete sleepers.
- Steel sleepers.
- Composite sleepers.







1. Railway track systems

Ballasted tracks: elements

Wooden sleepers



Benefits

• Wooden sleepers are cheaper than others types and easy to manufacture.
• These sleepers are light in weight so they can be easily transported and handled while installing.
• Fasteners can be easily installed to wooden sleepers.
• Any type of gauge can be maintained by wooden sleepers.
• Wooden sleepers are suitable for all types of rail sections.

Drawbacks

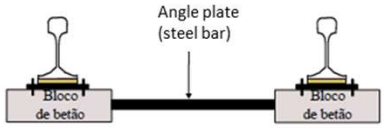
• Life of wooden sleepers is very smaller compared to other type of sleepers.
• Wooden sleepers have weak resistance against fire.
• These sleepers are easily affected by humidity and vermin attack if not properly treated.

1. Railway track systems

Ballasted tracks: elements

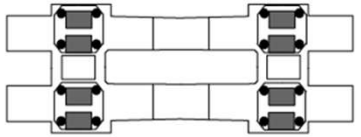
Concrete sleepers

Most of the concrete sleepers are made from pre-stressed concrete.



Two-block concrete sleeper


Monoblock concrete sleeper


Frame concrete sleeper

Benefits

- Concrete sleepers are heavier than all other types which gives good stability to the rails.
- These sleepers have longer life span.
- They have good fire resistance.
- They are not affected by corrosion or vermin attack, hence, they are suitable for all types of soil and moisture conditions.
- Concrete sleepers holds the track strongly and maintains gauge.

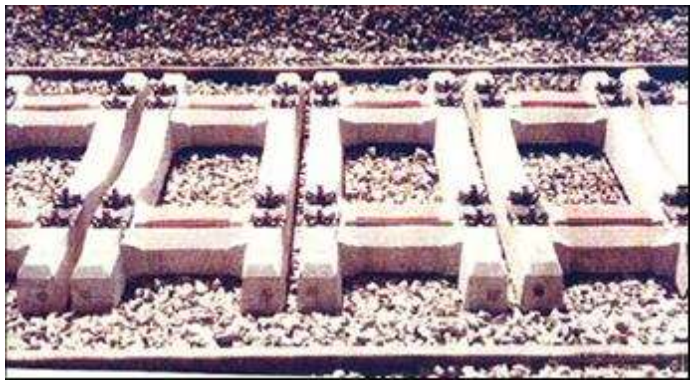
Drawbacks

- Due to their heavy weight, handling is difficult and damage may occur while transporting.
- They may not be suitable for special sections of the track.

1. Railway track systems

Ballasted tracks: elements

Frame Sleepers



These sleepers are double-H prestressed concrete frames whose goals are:

- to transmit the load in a continuous manner into the ballast bed reducing substantially the pressure under the sleepers;
- to increment of lateral resistance.

Usually, an elastic pad is incorporated into the concrete structure at the frame-sleeper-bottom to improve the ballast-concrete interface.

1. Railway track systems

Ballasted tracks: elements

Steel sleepers



Benefits

• Steel sleepers are lighter in weight, so they are easy to transport, to place and to install.
• They are recyclable.
• Their life span is about 30 years.
• They are resistant to fire.
• They are well suitable for high speeds tracks or tracks with larger loads.
•They holds the rail strongly and the connection to the rail is also simple.

Drawbacks

• Steel can be easily affected by chemicals.
• Steel sleepers requires high maintenance.
• If a derailment happens, they damaged very badly and are not suitable for re using.
•These are not suitable for all types of rail sections and gauges.

1. Railway track systems

Ballasted tracks: elements

Composite Sleepers



Composite sleepers are modern type of sleepers which are made from waste plastic and rubber.

Benefits

•Composite sleepers are serviceable for longer spans, about 50 years.
•They are eco-friendly.
•They are light in weight but with great strength.
• They can be resized easily like wooden sleepers, thus they can have any type of rail section.
• They reduce vibrations received from the rails.

Drawbacks

• Composite sleepers are not resistant to fire.
• High cost.

1. Railway track systems

Ballasted tracks: elements

Fastening system + rail pads





Rail fastening systems are used to fasten the rails into the sleepers.

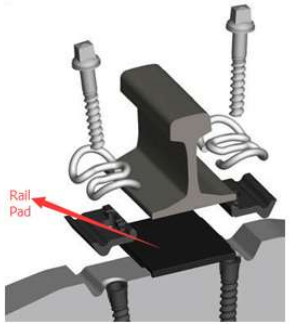
The **functions of the rail fastening** systems are:

- to maintain the gauge;
- to prevent the vertical and horizontal movement of rails relative to the position of the sleeper.

The **functions of the rail pad** are:

- to distribute load to a large surface;
- to reduce the noise and vibration improving the comfort of the passengers;
- to seal the gap between the bottom of the track and the top of the sleeper;
- to reduce the wear of steel rail and rail sleeper.





1. Railway track systems

Ballasted tracks: elements

Ballast

Ballast is a granular material which is placed and packed below and around the railway sleepers.

The main purpose of the ballast is to transmit the load from sleepers to the formation (consolidated track bed) and to provide drainage facilities to the track.



Functions of ballast:

- to provide levelled bed or support for the railway sleepers;
- to transfer the load from sleepers to subgrade and distributes the load uniformly on subgrade;
- to hold the sleepers in a firm position while the trains pass by;
- to prevent the longitudinal and lateral movement of sleepers;
- to offer a good drainage to the track.

1. Railway track systems

Ballasted tracks: elements

Ballast

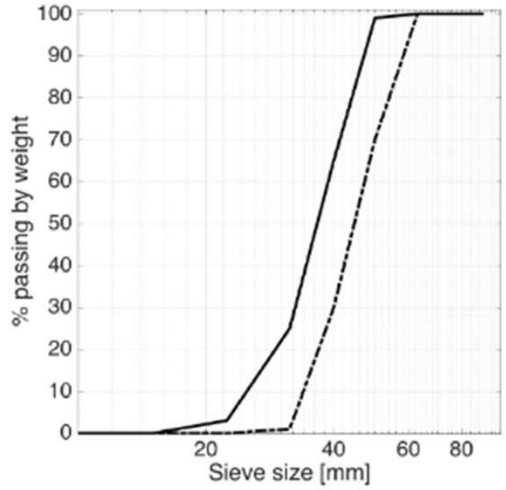
Current ballast thickness (UIC, 2008)

Country	Conventional track		High-speed track	
	Speed (Km/h)	Thickness (mm)	Speed (Km/h)	Thickness (mm)
Germany	< 160	300	> 160	350
Austria	< 160	450-550	> 160	550
Belgium	< 220	300	> 160	350
Spain	< 200	250-300	> 200	300
France	< 220	250	> 220	350
Greece	< 200	300	> 160	350
Hungary	< 160	350	-	-
Norway	< 160	350	= 210	350
Portugal	< 220	300	-	-
United Kingdom	< 200	>300	= 200	>300
Switzerland	< 160	300	> 160	300

1. Railway track systems

Ballasted tracks: elements

Ballast



Gralunometry grades

Sieve opening (mm)	Ballast sizes 31.5 mm to 50 mm			Ballast sizes 31.5 mm to 63 mm		
	Maximum percentage of passes in mass					
	Gralunometric grades					
	A	B	C	D	E	F
80	100	100	100	100	100	100
63	100	97 a 100	95 a 100	97 a 99	95 a 99	93 a 99
50	70 a 99	70 a 99	70 a 99	65 a 99	55 a 99	45 a 70
40	30 a 65	30 a 70	25 a 75	30 a 65	25 a 75	15 a 40
31,5	1 a 25	1 a 25	1 a 25	1 a 25	1 a 25	0 a 7
22,4	0 a 3	0 a 3	0 a 3	0 a 3	0 a 3	0 a 7
31,5 a 50	≥ 50	≥ 50	≥ 50	-	-	-
31,5 a 63	-	-	-	≥ 50	≥ 50	≥ 85

Note 1: *the percentage passing the 22.4 mm sieve requirement applies to ballast sampled at the production site*

Note 2: *in certain circumstances a 25 mm sieve may be used as an alternative to the 22.4 mm sieve, the tolerance then being 0 to 5 (0 to 7 for category F)*

Categories for fine particle content

Sieve opening (mm)	Maximum percentage of passes in mass			
	Category for fines content			
	A	B	declared	C
0,5	0,6	1,0	> 1,0	no required
Note: *this requirement applies to ballast sampled at the production site*				

Categories for fines content

Sieve opening (mm)	Maximum percentage of passes in mass				
	Category for fines content				
	A	B	C	declared	D
0,063	0,5	1,0	1,5	> 1,5	no required
Note: *this requirement applies to ballast sampled at the production site*					

CEN (2013)

1. Railway track systems

Ballasted tracks: variants to the classical track

Ballasted track supported on a bituminous layer

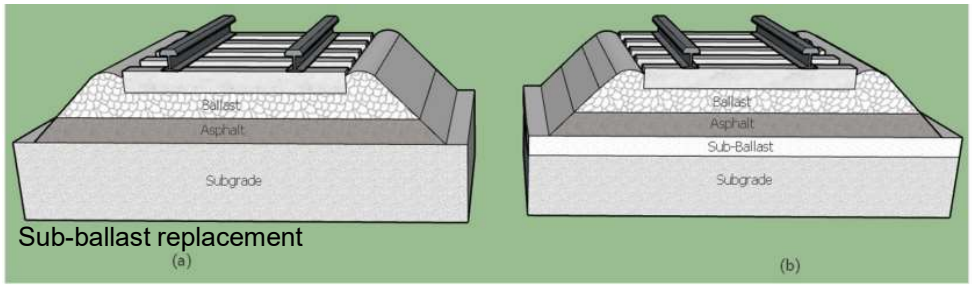


Figure from: Jadidi et al. (2021).

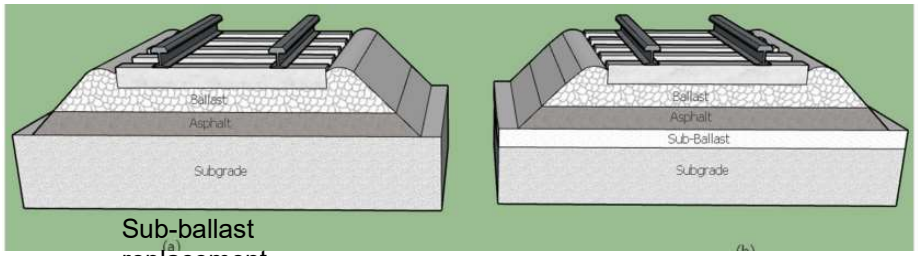
Benefits

- This solution helps improving a substructure's stiffness and bearing capacity.
- It provides an overall improvement of the track performance that minimizes settlement under heavy loads.
- This type of system increases the dynamic characteristics, especially under high-speed train loads.
- It provides waterproofing to the subgrade.
- This solution contributes for protecting the top layers against fine contamination.

1. Railway track systems

Ballasted tracks: variants to the classical track

Ballasted track supported on a bituminous layer



Sub-ballast replacement

Figure from: Jadidi et al. (2021).

Other benefits

- This solution promotes a reduction of the track overall thickness/materials as theoretical analysis suggested an asphalt layer with a thickness of 12 to 14 cm is an alternative to a 30 cm traditional sub-ballast layer.
- It provides a better load distribution with reduction of the amount of pressure on a track's bed, contributing for lower settlements.
- This type of system cam be an improvement in transition zones as asphalt restricts permanent settlement, increases the track modulus, and overcomes the stiffness differences.

1. Railway track systems

Ballasted tracks: variants to the classical track

Ballasted tracks with special sleepers

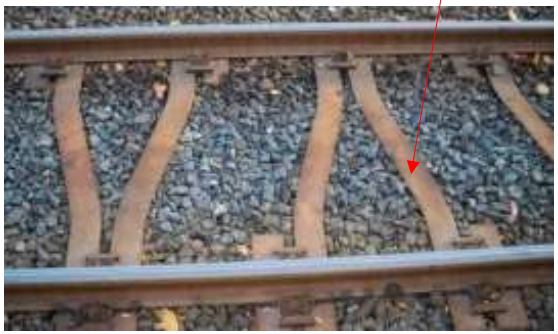
New sleeper designs have been applied to improve the lateral resistance of ballast bed.

Ladder sleepers/Frame sleeper





Y- shape sleepers



Figures from: Guoqing et al. (2021).

1. Railway track systems

Slab tracks: type of families

UIC (2002) considers seven different families of structures, regarding:

i. the type of slab supporting (punctual or continuous),
ii. the construction method (in situ or precast),
iii. the number of resilient levels
iv. the type of the foundation material (plain concrete or bituminous material).

Slab track families:

1. systems without punctual fixing of the rail;
2. systems with punctual fastening of the rail and independent stretches of rail;
3. systems with punctual fastening of the rail on sleepers incorporated in structure by infill concrete;
4. systems with punctual fastening of the rail on sleepers incorporated in structure by vibration;
5. systems with punctual fastening of the rail on sleepers laid and anchored on a supporting structure;
6. systems with punctual fastening of the rail on sleepers separated from supporting structure by a resilient level;
7. systems with punctual fastening of the rail on prefabricated slabs.

UIC (2002)

1. Railway track systems

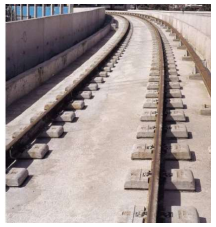
Slab tracks: type of families

F1 Systems without punctual fixing of the rail



F2 to F7 Systems with punctual fixing of the rail

F2 – on the slab or on sleepers



F3 & F4 – sleepers incorporated in structure

F3- by infill concrete

F4 by vibration



F5 – sleepers laid and anchored on a supporting structure



F6 –sleepers separated from supporting structure by a resilient level



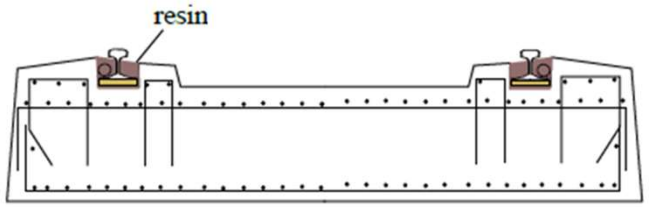
F7 – prefabricated slabs



1. Railway track systems

Slab tracks: type of families

Family 1 - Systems without punctual fixing of the rail



cross-section scheme



general view of the track

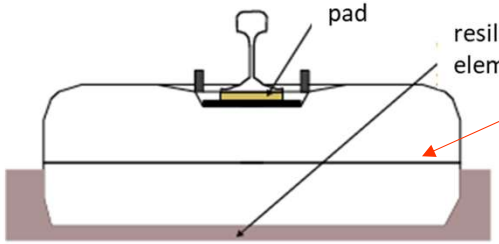
Benefits	Drawbacks
Favorable use on short bridges and tramway tracks.	System to be avoided on large stretches of tracks and on bridges with a length between expansion joints greater than 30 m as there is no neutral temperature control in the rail causing irregular behavior of this type of track, in the longitudinal direction. Maintenance with a long intervention period, due to the temperature-dependent resin polymerization process.

1. Railway track systems

Slab tracks: type of families

Family 2 - systems with punctual fastening of the rail and independent stretches of rail;



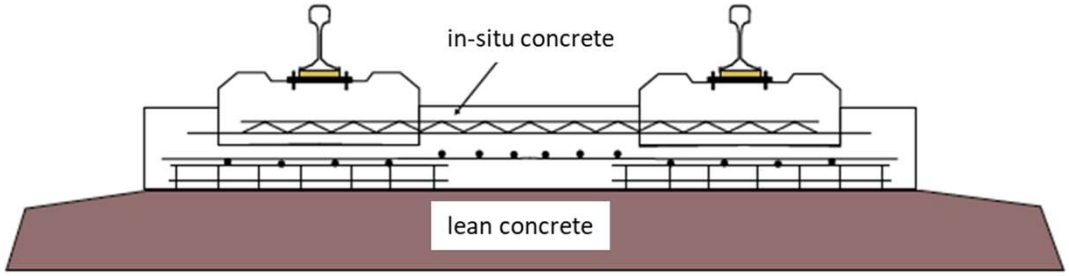


Benefits	Drawbacks
The inexistence of connection between the two rails can contribute for a better aerodynamic behavior of the track, for the electrical isolation between the two rails and for the unblocking of the central part of the track, which allows the circulation of people and vehicles. Variations in gauge and rail inclination is greater than in other systems, as there is no connecting element between the two rails. Possibility to apply one or two resilient levels: at the top and at the bottom of the blocks which allows to reduce noise and vibration.	The gauge and rail inclination is definitive during construction since there is no connection element between the two rails that could allow further adjustments. Track deficient vertical flexibility in systems made up of a single resilient element, which makes it impossible to use this type of track in high-speed railway lines.

1. Railway track systems

Slab tracks: type of families

F3 & F4 – Systems with punctual fastening and sleepers incorporated in structure



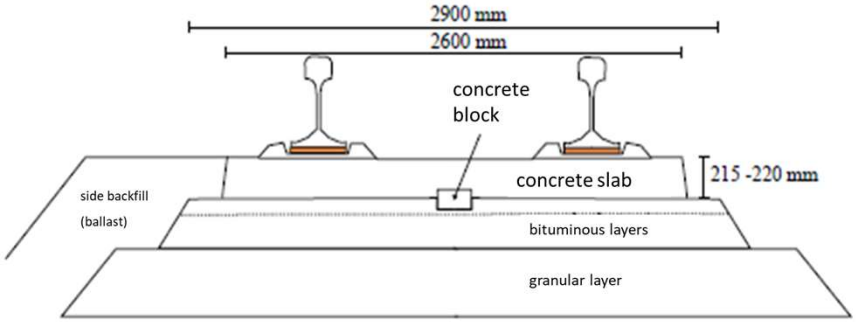


Benefits	Drawbacks
The slab reinforcement ensures: 1) an even distribution of the cracks; 2) cracks opening less than 0.5 mm. Cracking usually occurs where there is a reduction in the slab cross section. Distance between cracks can vary between 0.5 and 4 m with current values between 2 and 2.5 m.	Reinforced or prestressed concrete sleepers are not replaceable in maintenance and /or repair operations as they are incorporated in the slab.

1. Railway track systems

Slab tracks: type of families

Family 5 - Systems with punctual fastening of the rail on sleepers laid and anchored on a supporting structure



GETRAC track

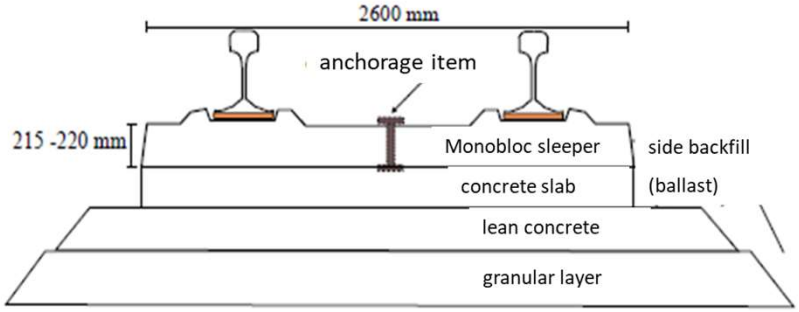




1. Railway track systems

Slab tracks: type of families

Family 5 - Systems with punctual fastening of the rail on sleepers laid and anchored on a supporting structure



BTD track



with no ballast



with ballast between the sleepers

1. Railway track systems

Slab tracks: type of families

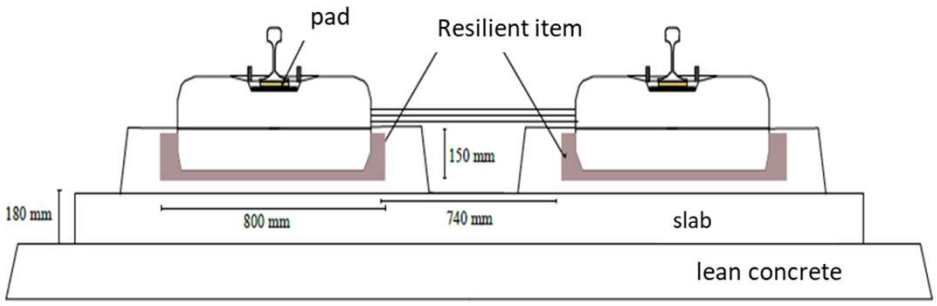
Family 5 - Systems with punctual fastening of the rail on sleepers laid and anchored on a supporting structure

Benefits	Drawbacks
Possibility of sleeper replacement if needed as their anchoring is not definitive. The connection between the sleeper and the bituminous layer is made through a concrete element, called “stopper”, whose function is to transmit horizontal efforts from the sleeper to the bituminous layer resulting from traffic and thermal variations. The support layer can be made of bituminous material or concrete.	Possible slow long-term deformation and distortions in tracks with bituminous layer. Possible cracking in tracks with plain concrete support layer.

1. Railway track systems

Slab tracks: type of families

Family 6 - Systems with punctual fastening of the rail on sleepers separated from supporting structure by a resilient level







Benefits	Drawbacks
The resilient element at the base and at the side faces of the sleeper contributes to the rigidity of the track in the vertical and lateral directions. This type of track is of interest in selectively reducing the range of excitation frequencies: the rail pad filters high frequency vibrations transmitted by the rail to the slab and the elastomer placed under the sleepers absorbs low frequency vibrations.	This system do not allow the circulation of people and vehicles between the rails.

1. Railway track systems

Slab tracks: type of families

Family 7 - Systems with punctual fastening of the rail on prefabricated slabs



OBB-Porr system: independent reinforced slabs with 2 openings from where self-compating concrete is introduced, forming a concrete block that ensures the transfer of forces in horizontal direction.



Bogl system: prestressed slabs in the transversal direction fixed with spindles on a stabilised layer.



Shinkansen system: prestressed slabs with stoppers between adjacent slabs that ensure the transfer of forces.

1. Railway track systems

Slab tracks: type of families

Family 7 - Systems with punctual fastening of the rail on prefabricated slabs



OBB-Porr system: independent reinforced slabs with 2 openings from where self-compating concrete is introduced, forming a concrete block that ensures the transfer of forces in horizontal direction.



Bogl system: prestressed slabs in the transversal direction fixed with spindles on a stabilised layer.



Shinkansen system: prestressed slabs with stoppers between adjacent slabs that ensure the transfer of forces.

2. Geometrical track quality assessment

Track inspection vehicle

The track inspection vehicle runs on a rail track to test several parameters of the track geometry without obstructing the normal railroad operations and circulation.







Usually, these vehicles have:

- a GPS system;
- front and rear camera;
- laser-optical system to measure rail wear;
- Optical system – inertial system - to measure track irregularities;
- Laser system for catenary and transversal profile.

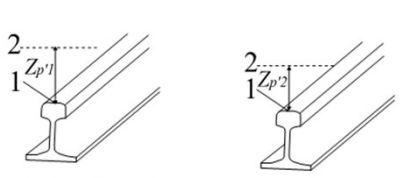
2. Geometrical track quality assessment

Track inspection vehicle



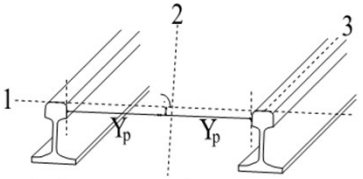
Some of the parameters generally measured are:

- position;
- curvature;
- longitudinal level of both rails;
- track alignment of both rails;
- track gauge;
- cross level;
- twist.



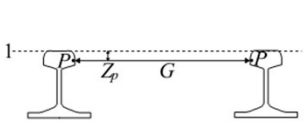
1 - Track centre
2 - Reference line

a) Longitudinal level: deviation Z_P



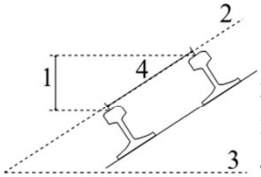
1 - Running surface
2 - Track centre
3 - Axis of running surface

b) Alignment: deviation Y_P



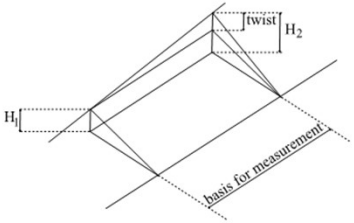
1 - Running Surface

c) Gauge: deviation G



1 - Cross Level
2 - Running surface
3 - Horizontal reference plane
4 - Axis-to-axis distance

d) Cross level: deviation 1



1- Basis for measurement

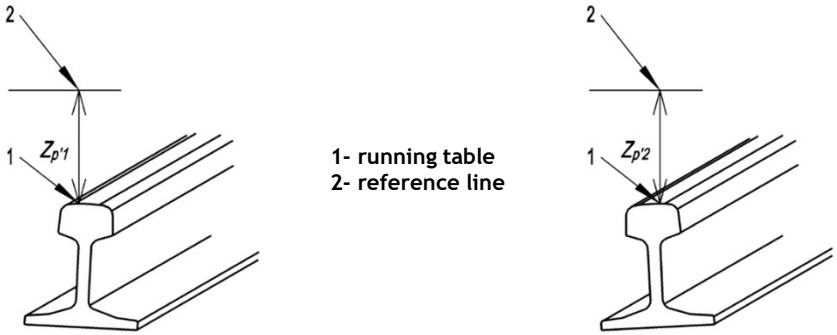
e) Twist: diference between H_2 and H_1

2. Geometrical track quality assessment

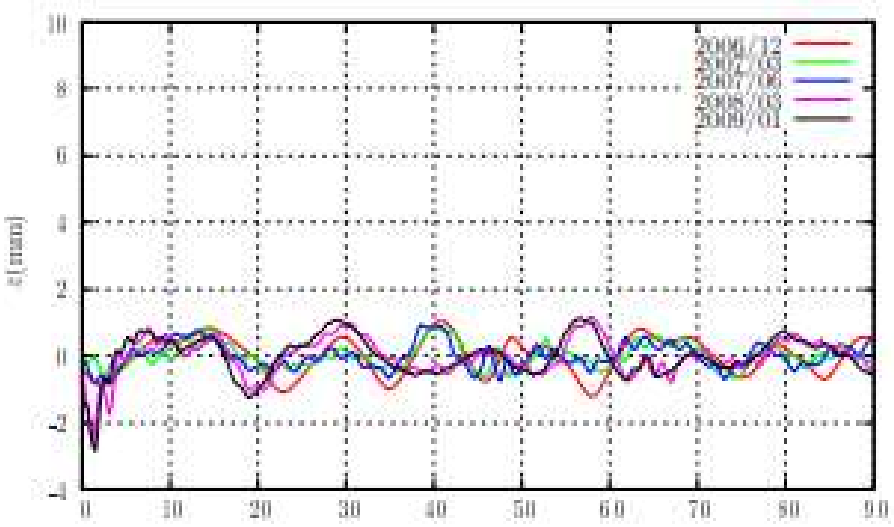
Geometrical track parameters

Longitudinal Level

Deviation Z'_P in Z-direction of consecutive running table levels on any rail.



1- running table
2- reference line

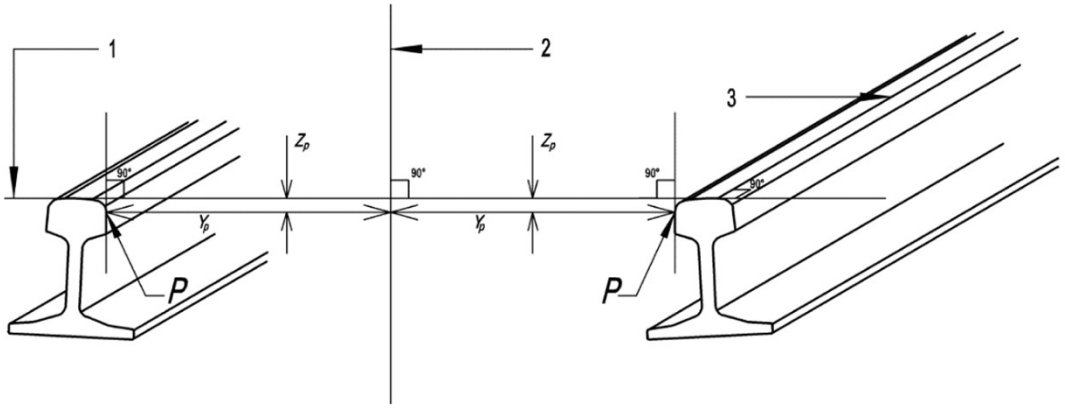


2. Geometrical track quality assessment

Geometrical track parameters

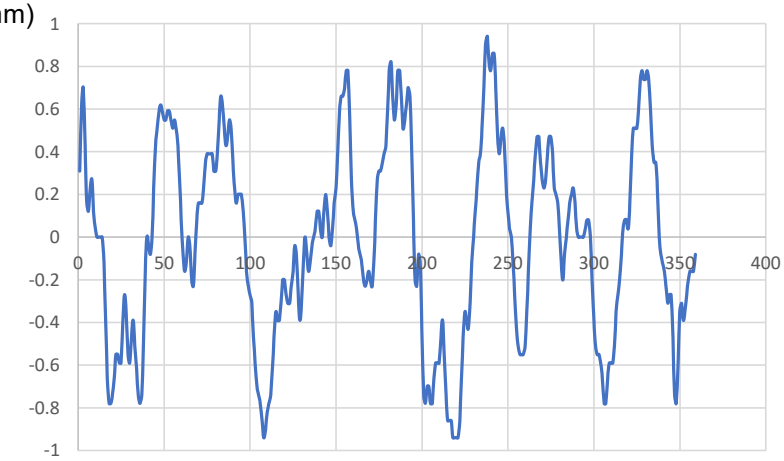
Alignment

Deviation Yp in y-direction of consecutive positions of point P on any rail.



1- running surface
2- reference line
3- center line of running table

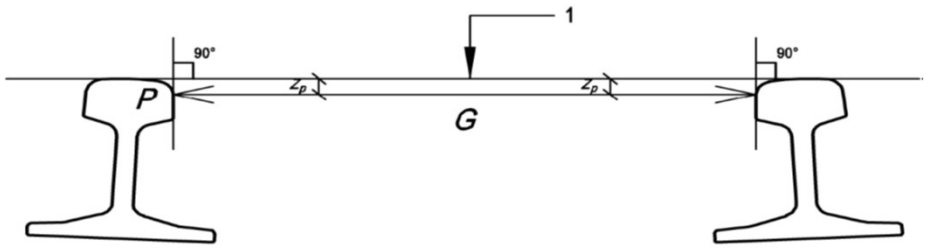
Alignment of left rail (mm)

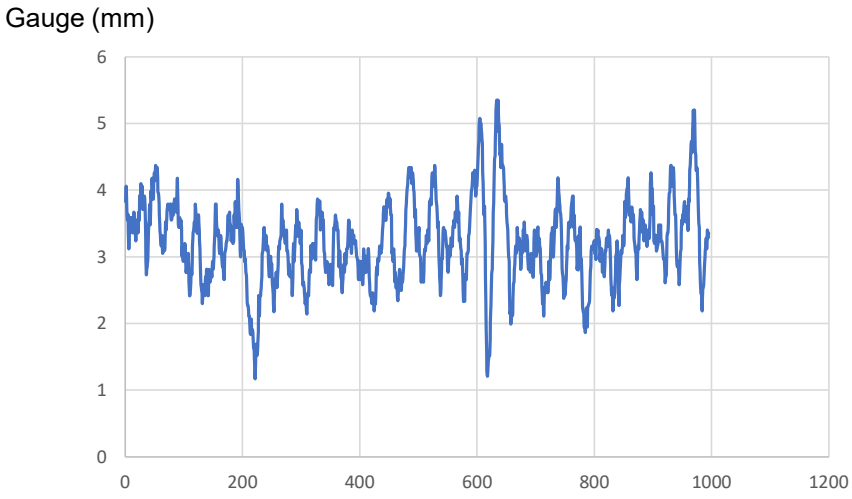


2. Geometrical track quality assessment

Geometrical track parameters

Nominal Gauge - Distance G between the gauge faces of the two adjacent running rails measured at a distance ZP below the running surface 1 . The value Zp shall be equal to (14 +/- 1mm) for a new rail.



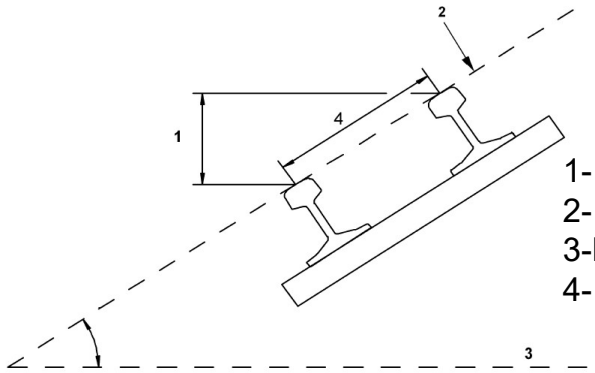


2. Geometrical track quality assessment

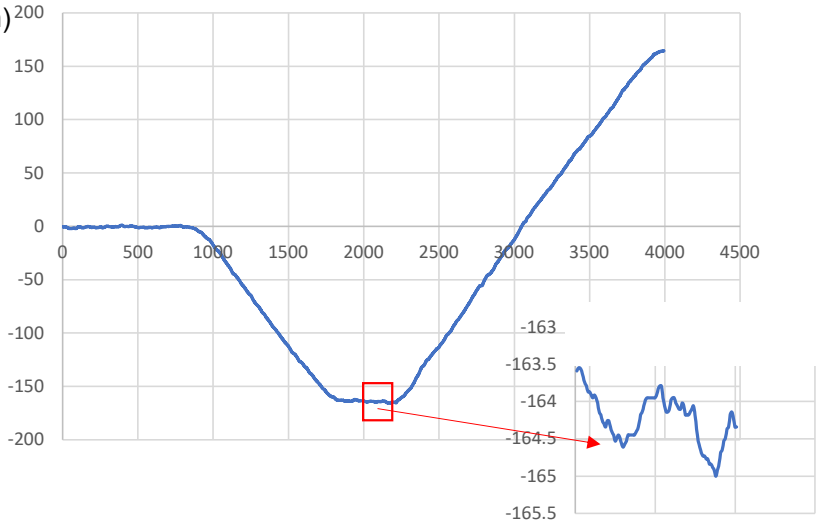
Geometrical track parameters

Cross Level

Difference in height of the adjacent running tables computed from the the angle between the running surface and the horizontal reference plane.
It is expressed as the height of the vertical leg of the right-angled triangle having a hypotenuse that relates to the nominal track gauge plus the width of the rail head rounded to the nearest 10 mm.



1- Cross level
2- running surface
3-Horizont reference plane
4- Hypotenuse

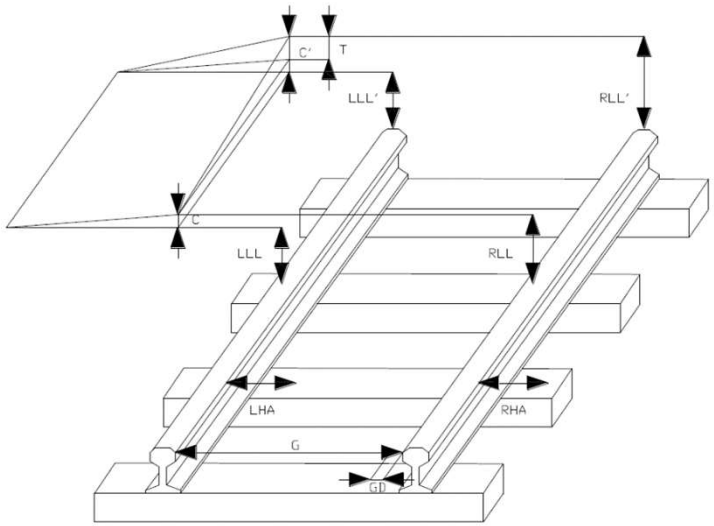


2. Geometrical track quality assessment

Geometrical track parameters

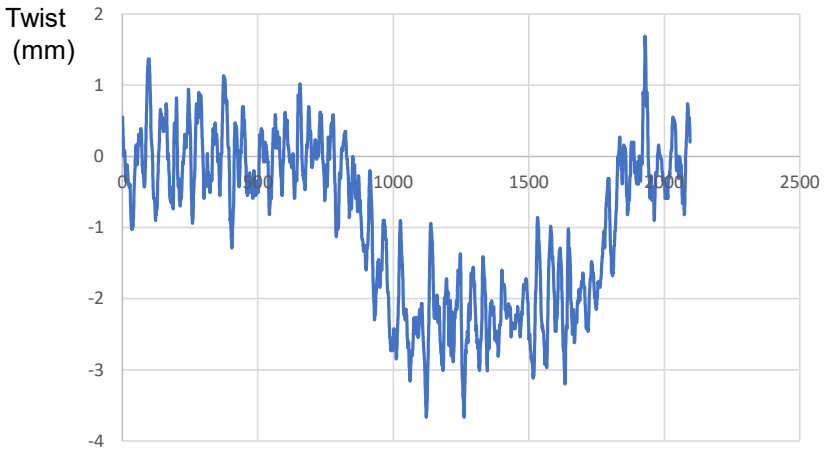
Twist

This parameter is the difference between two cross levels taken at a defined distance apart, expressed as a gradient between the two points of measurements (%º or mm/m)



T – twist

In practice it results from the difference of the cross levels in a defined measurement base (C'-C), usually = 3 m



2. Geometrical track quality assessment

Methodologies for track quality assessment

The assessment of the geometrical track quality can be made by considering :

1) track quality indexes (TQI) that might combine the track irregularities parameters in two or more dimensions.
2) five geometrical indicators separately as proposed by the European Standard EN 13848-5 (2017)

In Europe, the track quality assessment is done according to the European Standard EN 13848-5 (2017), that compares the deviations of longitudinal level, alignment, gauge, cross level and twist with defined thresholds.

(CEN, 2017)

(Vale and Simões, 2022)

(Berawi et al., 2010)

2. Geometrical track quality assessment

Methodologies for track quality assessment

Track quality indexes (TQI)

For the **Federal Railroad Administration (FRA),** the TQI is calculated separately for gauge, alignment, longitudinal level and cross level according to the equation :

$$TQI_s = \left(\frac{L_s}{L_0} - 1\right) \times 10^6$$

where L_0 is the theoretical length of the track section and L_s is the traced length of the space curve calculated by equation (2) being Δx the sample space and Δy the difference between two consecutive measurements.

$$L_s = \sum_{i=1}^{n} \sqrt{\Delta_{xi}^2 + \Delta_{yi}^2}$$

(Vale and Simões, 2022)

(Berawi et al., 2010)

2. Geometrical track quality assessment

Methodologies for track quality assessment

Track quality indexes (TQI)

The J-synthetic coefficient is a track quality indicator developed by the Polish railways and it can be calculated by the following equation:

$$\frac{S_z + S_y + S_w + 0.5S_e}{3.5}$$

where S_z, S_y, S_w and S_e are the standard deviation of the vertical irregularities, horizontal irregularities, twist and gauge respectively.

(Vale and Simões, 2022)

(Berawi et al., 2010)

2. Geometrical track quality assessment

Methodologies for track quality assessment

EN 13848-5 - Railway applications - Track - Track geometry quality

The standard EN 13848-5 refers that the geometrical track quality assessment should be analyzed not only in terms of **distributed irregularities**, but also in terms of **isolated defects** being this type of defect characterized by its wavelength and amplitude.

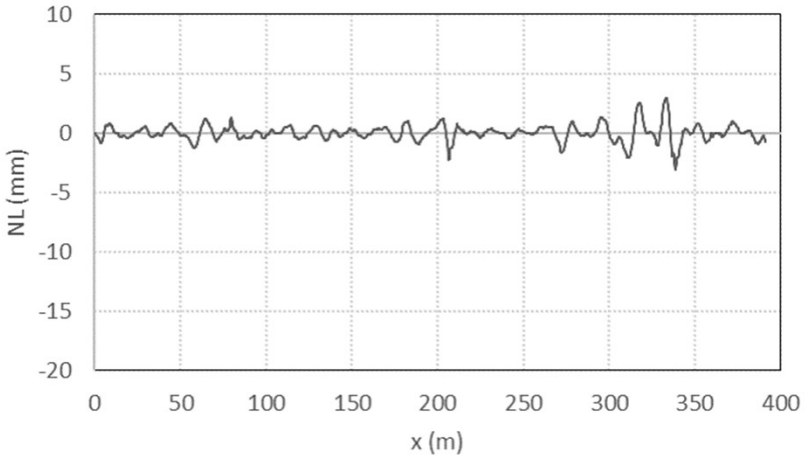


Figure - Distributed irregularity

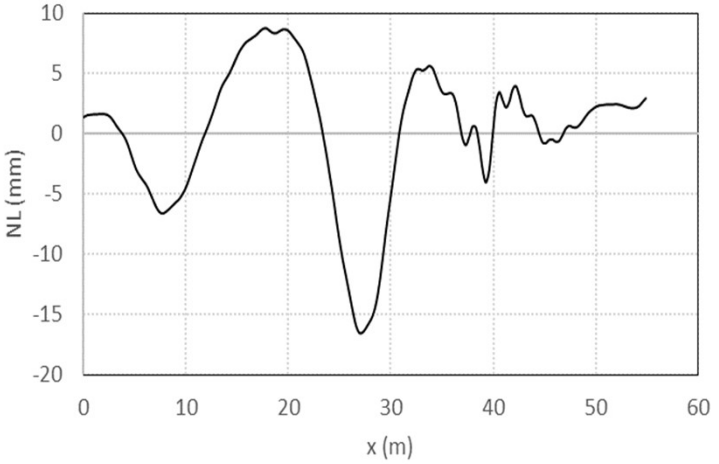


Figure - Isolated irregularity

2. Geometrical track quality assessment

Methodologies for track quality assessment

EN 13848-5 - Railway applications - Track - Track geometry quality

The indicators for the geometrical track quality assessment according to the European standard are, for:

DISTRIBUTED IRREGULARITIES

i. the standard deviation (SD) of the longitudinal level of left and right rails over track segments of 200 m;
ii. the standard deviation (SD) of the alignment of left and right rails over track segments of 200 m;
iii. the mean value in 100 m of track of the gauge

ISOLATED IRREGULARITIES

i. the peak amplitude of longitudinal level defects with wavelength between 3 and 25 m (D1);
ii. the peak amplitude of longitudinal level defects with wavelength between 25 and 70 m (D2);
iii. the peak amplitude of alignment defects with wavelength between 3 and 25 m (D1);
iv. the peak amplitude of alignment defects with wavelength between 25 and 70 m (D2);
v. the peak gauge value;
vi. the peak cross level value;
vii. the peak twist value.

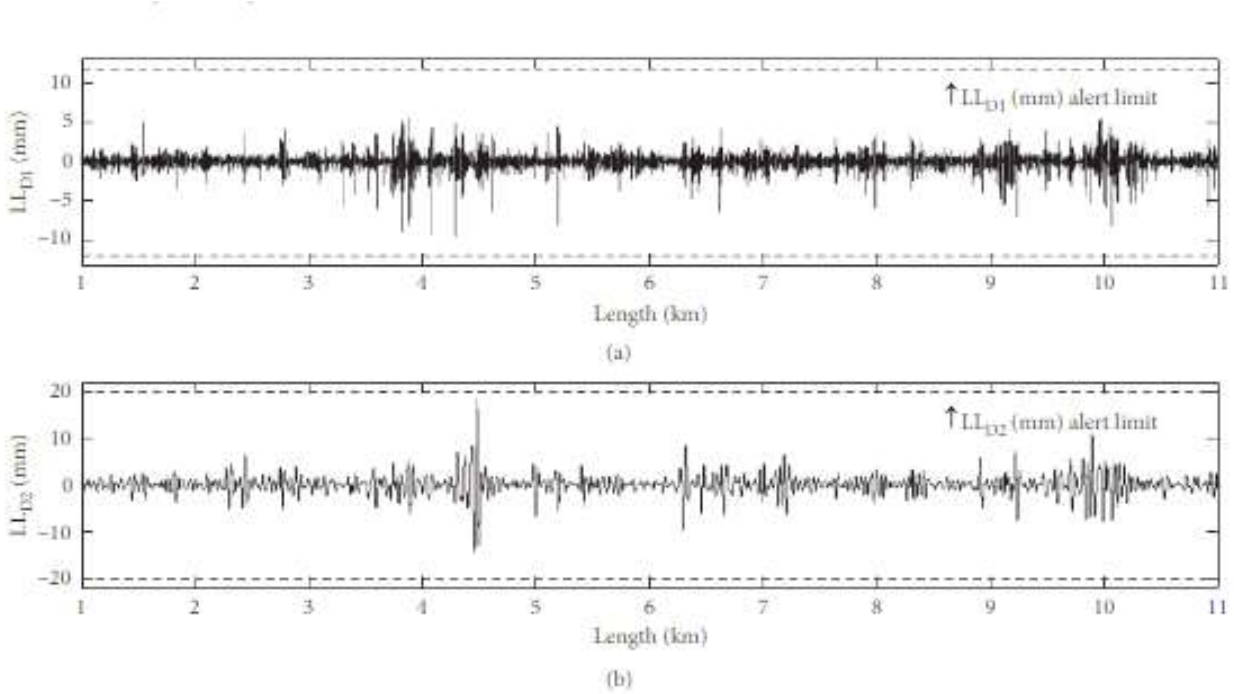
(CEN, 2017)

2. Geometrical track quality assessment

Methodologies for track quality assessment

EN 13848-5 - Railway applications - Track - Track geometry quality

Track longitudinal level for D1 (λ between 3 and 25 m) and D2 (λ between 25 and 70 m)



Figures from: Paixão et al. (2019).

2. Geometrical track quality assessment

Methodologies for track quality assessment

EN 13848-5 - Railway applications - Track - Track geometry quality

EN13848-5 refers three thresholds given as a function of speed:

1) **safety limit**, given only for isolated defects, and if a irregularity exceeds this limit it is required to take immediate measures, such as lowering the maximum speed of trains or closing the line until the defect has been corrected;

2) **intervention limit**, given only for isolated defects, and if an irregularity exceeds this limit it is required corrective maintenance actions in order the safety limit is not reached before the next inspection;

3) **alert limit**, given for both distributed and isolated defects, and if an irregularity exceeds these regular planned maintenance operations needs to be scheduled.

(CEN, 2017)

2. Geometrical track quality assessment

Methodologies for track quality assessment

EN 13848-5 - Railway applications - Track - Track geometry quality

Limits for the standard deviation in 200 m of the **longitudinal level- distributed irregularity**

Design speed (Km/h)	Safety limit		Intervention limit		Alert limit	
	D1	D2	D1	D2	D1	D2
$V \leq 80$	-	-	-	-	$2,3 - 3,0$	-
$80 < V \leq 120$	-	-	-	-	$1,8 - 2,7$	-
$120 < V \leq 160$	-	-	-	-	$1,4 - 2,4$	-
$160 < V \leq 220$	-	-	-	-	$1,2 - 1,9$	-
$220 < V \leq 300$	-	-	-	-	$1,0 - 1,5$	-

D1 (λ between 3 and 25 m)

D2 (λ between 25 and 70 m)

Limits for the peak value of the **longitudinal level- isolated irregularity**

Design speed (Km/h)	Safety limit		Intervention limit		Alert limit	
	D1	D2	D1	D2	D1	D2
$V \leq 80$	29	-	$16 - 20$	-	$12 - 18$	-
$80 < V \leq 120$	26	-	$12 - 18$	-	$10 - 16$	-
$120 < V \leq 160$	24	-	$10 - 17$	-	$8 - 15$	-
$160 < V \leq 220$	20	33	$9 - 14$	$18 - 23$	$7 - 12$	$14 - 20$
$220 < V \leq 300$	17	28	$8 - 12$	$16 - 20$	$6 - 10$	$12 - 18$

(CEN, 2017)

2. Geometrical track quality assessment

Methodologies for track quality assessment

Limits for the standard deviation in 200 m of the **alignment distributed irregularity**

Design speed	Standard deviation
	D1
$V \leq 80$	1,5 a 1,8
$80 < V \leq 120$	1,2 a 1,5
$120 < V \leq 160$	1,0 a 1,3
$160 < V \leq 230$	0,8 a 1,1
$230 < V \leq 300$	0,7 a 1,0

Limits for the peak value of the **aligment isolated irregularity**

Design speed (Km/h)	From average to peak value (mm)					
	LA		*LI*		*LAI*	
	wavelength intervals					
	D1	*D2*	*D1*	*D2*	*D1*	*D2*
$V \leq 80$	12 a 15	N/A	15 a 17	N/A	22	N/A
$80 < V \leq 120$	8 a 11	N/A	11 a 13	N/A	17	N/A
$120 < V \leq 160$	6 a 9	N/A	8 a 10	N/A	14	N/A
$160 < V \leq 230$	5 a 8	10 a 15	7 a 9	14 a 17	12	24
$230 < V \leq 300$	4 a 7	8 a 13	6 a 8	12 a 14	10	20

(CEN, 2017)

2. Geometrical track quality assessment

Methodologies for track quality assessment

Limits for the mean value in 100 m of the **gauge** in 100 m - **distributed irregularity**

Design speed	From average to peak value (mm)					
	LA		*LI*		*LAI*	
	Min	Max	Min	Max	Min	Max
$V \leq 40$	*N/A*	+25	*N/A*	+28	*N/A*	+32
$40 < V \leq 80$	-6	+25	-7	+28	-8	+32
$80 < V \leq 120$	-5	+22	-6	+25	-7	+27
$120 < V \leq 160$	-3	+16	-4	+18	-5	+20
$160 < V \leq 230$	-3	+16	-4	+18	-5	+20
$230 < V \leq 300$	-1	+16	-2	+18	-3	+20

Limits for the peak value of the **gauge- isolated irregularity**

Design speed	From average to peak value (mm)					
	LA		*LI*		*LAI*	
	Min	Max	Min	Max	Min	Max
$V \leq 80$	-7	+25	-9	+30	-11	+35
$80 < V \leq 120$	-7	+25	-9	+30	-11	+35
$120 < V \leq 160$	-6	+25	-8	+30	-10	+35
$160 < V \leq 230$	-4	+20	-5	+23	-7	+28
$230 < V \leq 300$	-3	+20	-4	+23	-5	+28

(CEN, 2017)

2. Geometrical track quality assessment

Methodologies for track quality assessment

EN 13848-5 - Railway applications - Track - Track geometry quality

Limits for the peak value of twist (base of 3 m between sections) - **isolated irregularity**

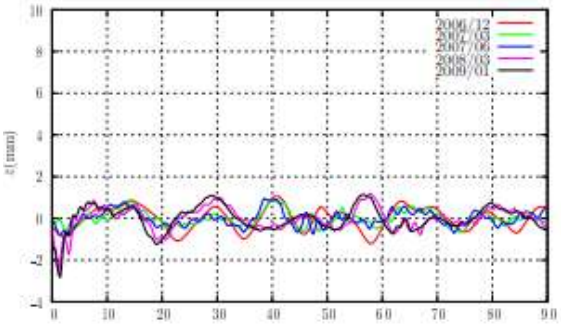
Design speed (Km/h)	From zero to peak value (mm/m)		
	LA	LI	LAI
$V \leq 80$	4	5	7
$80 < V \leq 120$	4	5	7
$120 < V \leq 160$	4	5	7
$160 < V \leq 200$	4	5	7
$200 < V \leq 300$	3	4	5

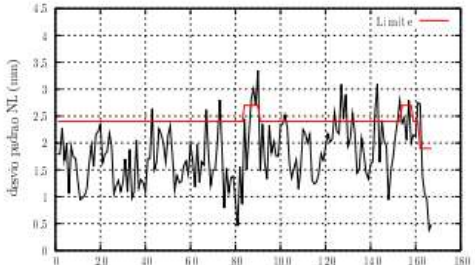
(CEN, 2017)

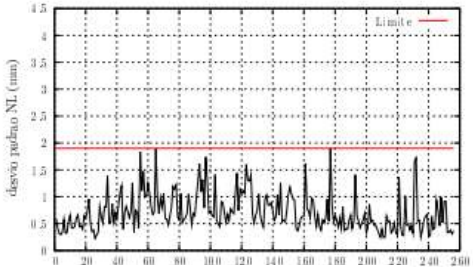
3. Typical damages

Analysis of measured track defects

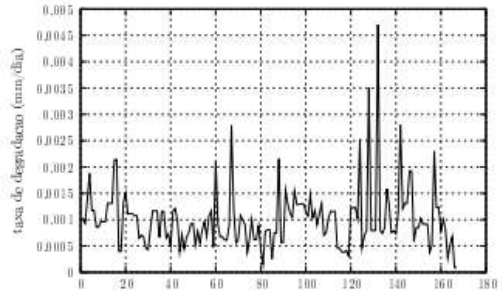
Longitudinal level

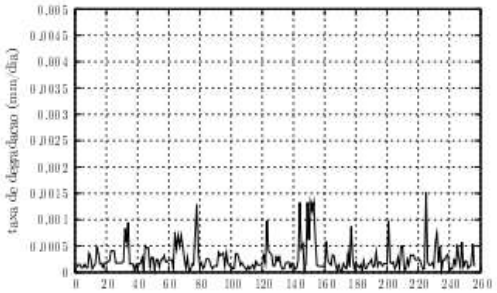






Standard deviation in two railway streches





Degradation rate of the standard deviation in two railway streches

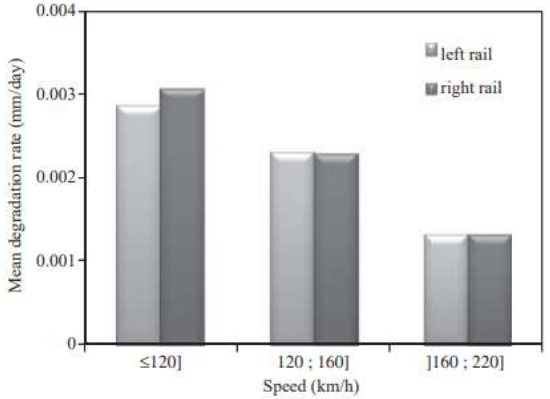


Fig. 4. Mean degradation rate of the standard deviation of the longitudinal level by speed range.

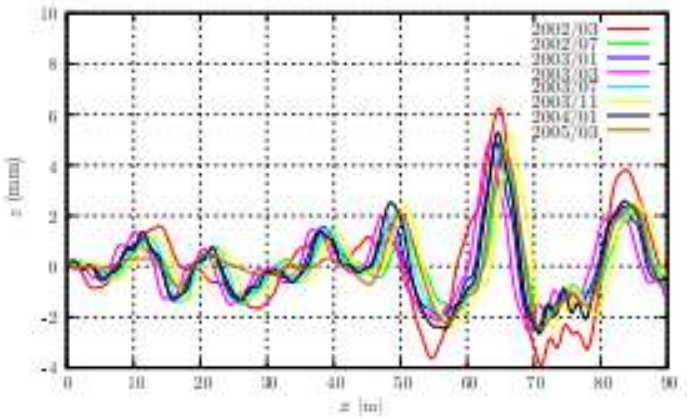
(Vale, 2010)

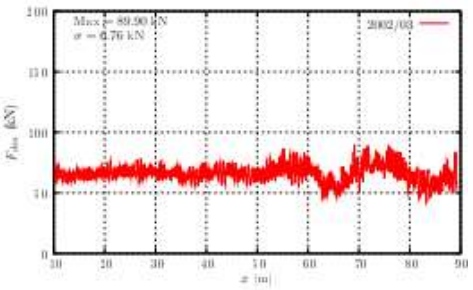
3. Typical damages

Dynamics effects of the track irregularities

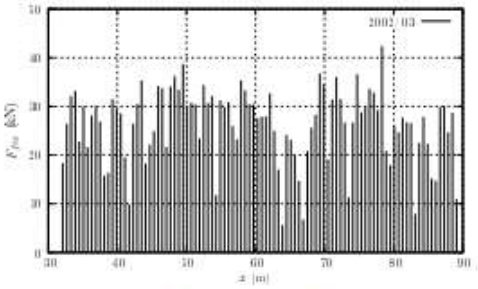
Railway vehicle dynamics is strongly affected by track irregularities and vehicle speed.

Distributed irregularity

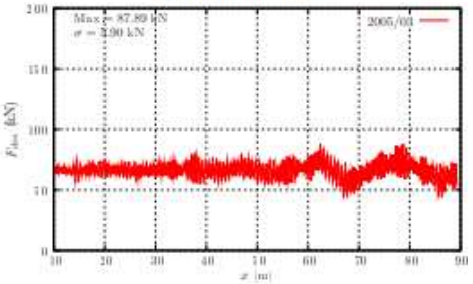




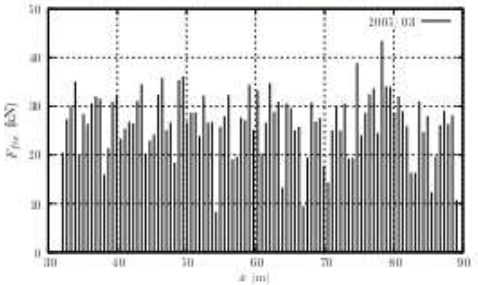
a) March 2002



a) March 2002



c) March 2005



c) March 2005

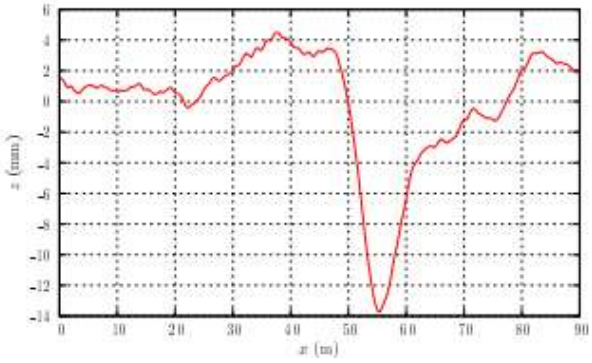
(Vale, 2010)

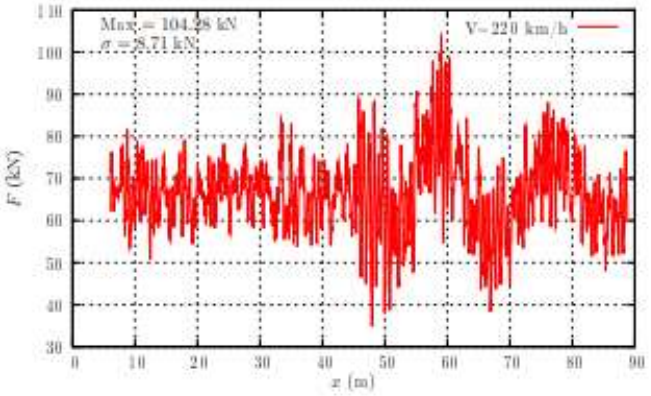
3. Typical damages

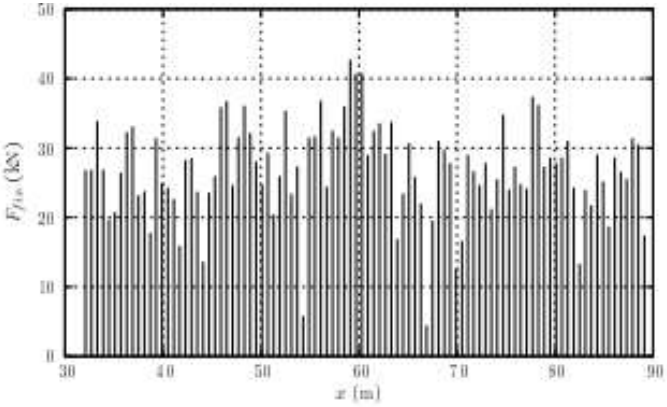
Dynamics effects of the track irregularities

Railway vehicle dynamics is strongly affected by track irregularities and vehicle speed.

Isolated defect







(Vale, 2010)

3. Typical damages

Dynamics effects of the track irregularities

Railway vehicle dynamics is strongly affected by track irregularities, which can influence the safety and the running behavior of the vehicle.

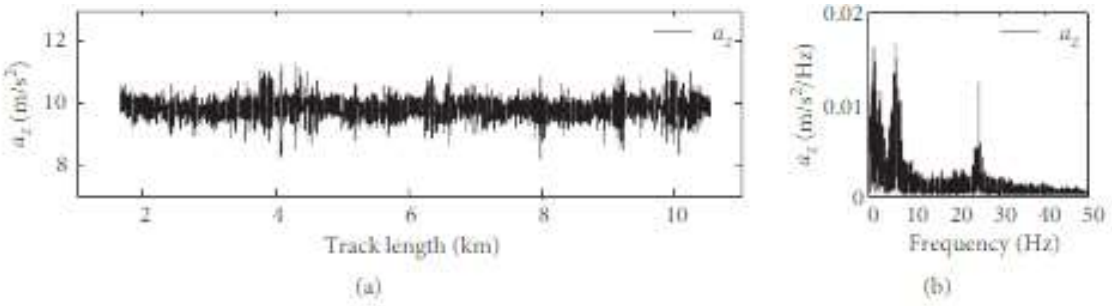


FIGURE 3: Acceleration measurements: (a) measurements along the track; (b) frequency content.

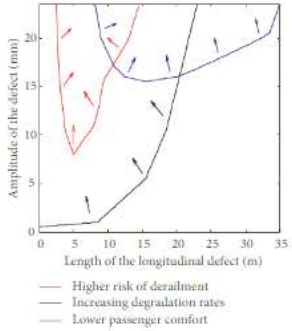


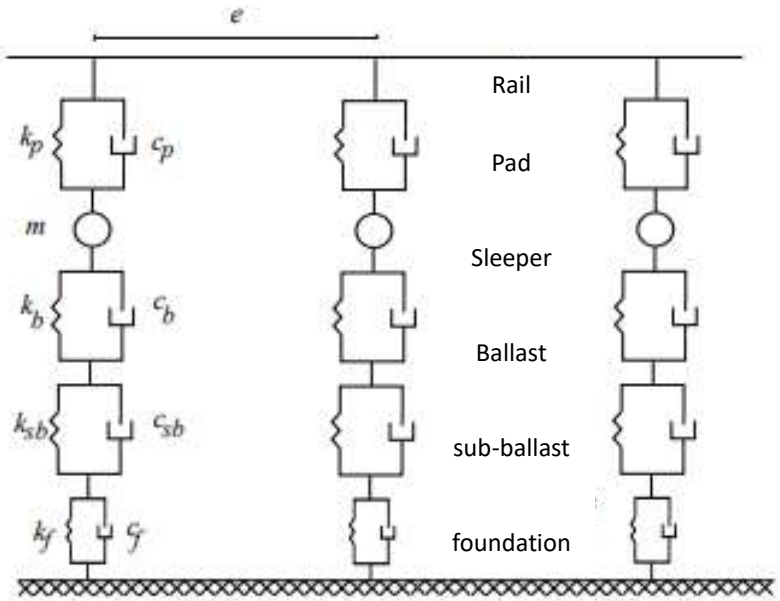
FIGURE 7: Identification of the regions that negatively affect the track performance, analysed in terms of amplitude and length of the defects: (i) regions with higher risk of derailment (lower train running safety) in red, (ii) regions with increasing track degradation rates in black, and (iii) region with lower passenger ride comfort in blue (adapted from [25]).

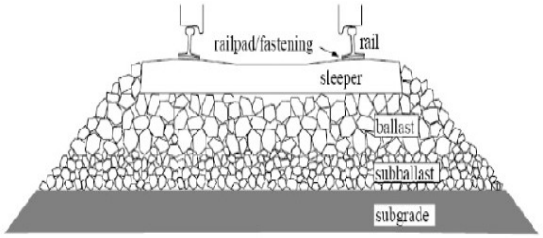
Figures from: Paixão et al. (2019).

4. Numerical modelling

Ballasted track models

2D model: discret support





Rail: beam elements

Pad: Spring + dashopt

Sleeper: pontual mass

Ballast: Spring + dashopt

Sub-ballast: Spring + dashopt

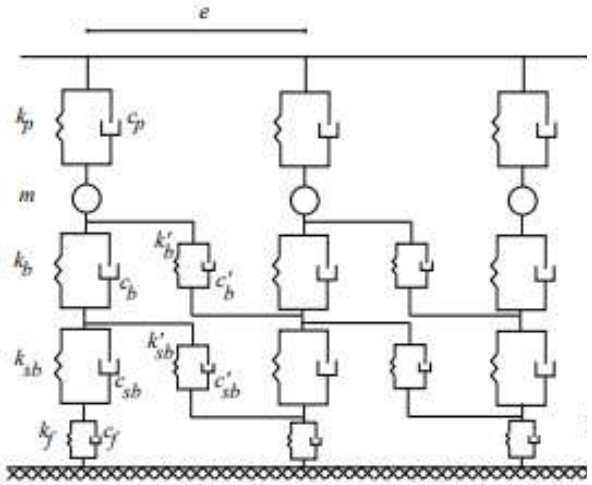
Foundation: Spring + dashopt

(Vale, 2010)

4. Numerical modelling

Ballasted track models

2D model with longitudinal continuity made by bars



Rail

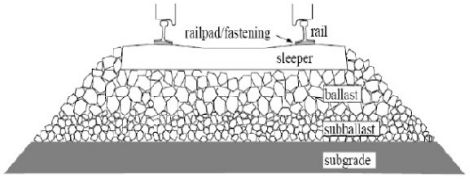
Pad

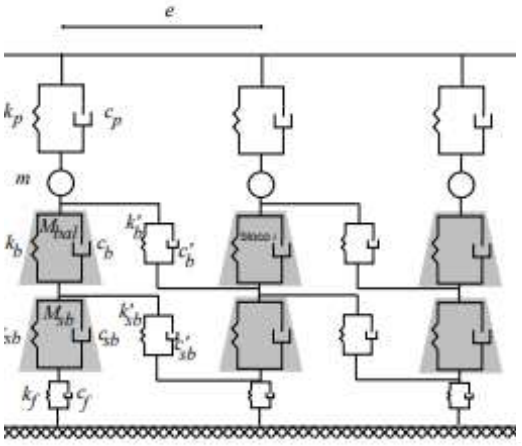
Sleeper

Ballast

sub-ballast

foundation





Rail

Pad

Sleeper

Ballast

sub-ballast

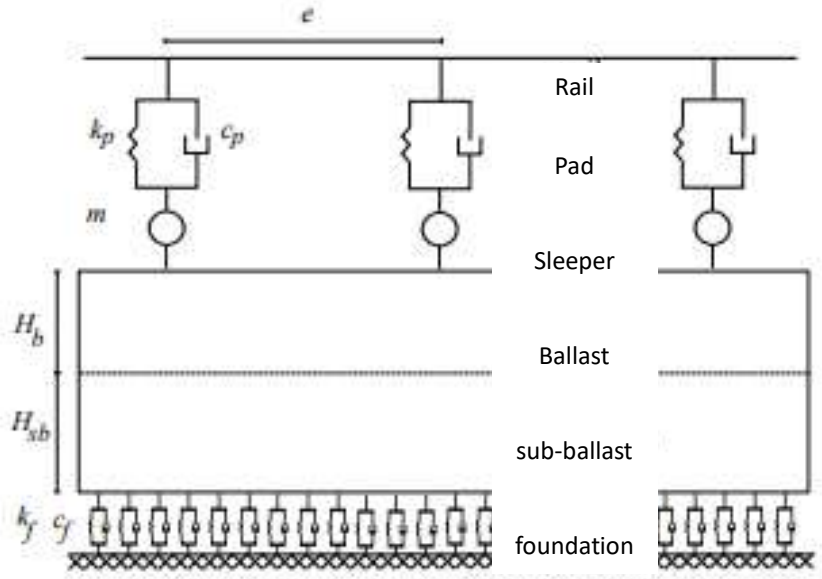
foundation

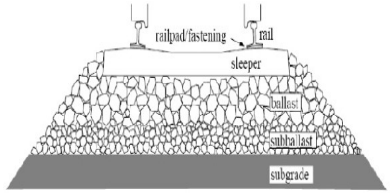
(Vale, 2010)

4. Numerical modelling

Ballasted track models

2D model with longitudinal continuity made with plain stress elements for ballast and sub-ballast layers





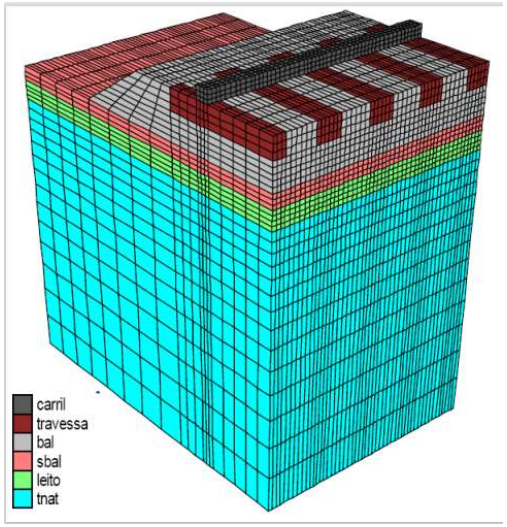
(Vale, 2021)

(Vale, 2010)

4. Numerical modelling

Ballasted track models

3D model



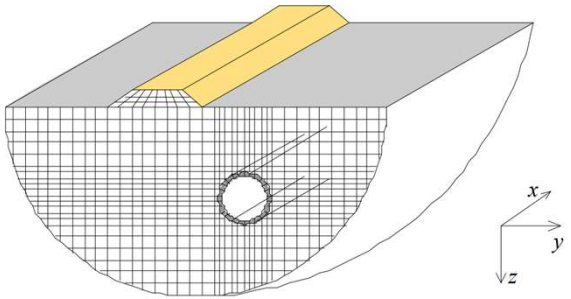
4. Numerical modelling

Ballasted track models

2,5 D model

As an alternative to 3D and empirical models is the use of 2.5D modelling has become an attractive alternative

It only requires the discretisation of the track into a 2D slice, thus reducing the number of degrees of freedom compared to a fully 3D model. However, it still allows for the recovery of the 3D response through the use of a transform.



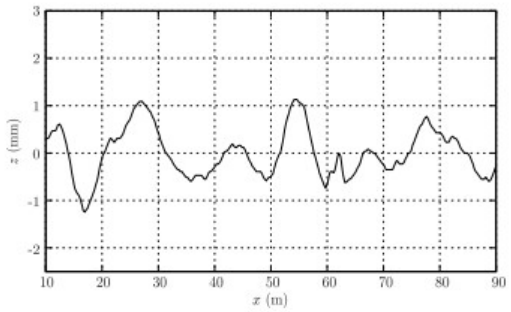
(Connolly et al., 2019)

4. Numerical modelling

Artificial generation of track irregularities for dynamic calculations

When performing numerical calculations, it is possible to artificially define distributed track irregularities by using a spectral density function.

In this table, several functions are indicated.



Power spectral density function S (ω)	Comments
$\frac{A\omega_c^2}{(\omega_r^2+\omega^2)(\omega_c^2+\omega^2)}$	Analytical expression also for track axis alignment $\omega_c = 0,82460$ rad/m, $\omega_r = 0,0206$ rad/m $A = 0,59933 \times 10^{-6}$ rad.m (good quality) $A = 1,58610 \times 10^{-6}$ rad.m
$\frac{A\omega_2^2(\omega^2+\omega_1^2)}{\omega^4(\omega^2+\omega_2^2)}$	Expression definied by FRA with A, ω_1 e ω_2 to be defined according to track quality
$A\omega^{-2}$	Valid expression for $4 \leq \lambda \leq 40$ m e $2 \leq A \leq 4$
$\frac{2,72\times10^{-4}}{(1+1,185\omega^2)(1+14,388\omega^2)}$	Expression used by the old Czechoslovakian railways
$\frac{0,135}{(1+22\omega^2)(1+44000\omega^2)}$	Expression used by the Czech Republic
$\frac{10^{-6}a}{\pi(\omega^2+a^2)}$	Expression used in the former USSR countries for $8 \leq \lambda \leq 250$ m ; $a = 9,54 \times 10^{-3}$ m^{-1}
$\frac{10^{-6}A}{(1+\omega/\omega_0)^3}$	Expression used by SNCF $2 \leq \lambda \leq 40$ m ; $\omega_0 = 0,307$ m^{-1} $A = 160$ (good quality) $A = 550$ (bad quality)

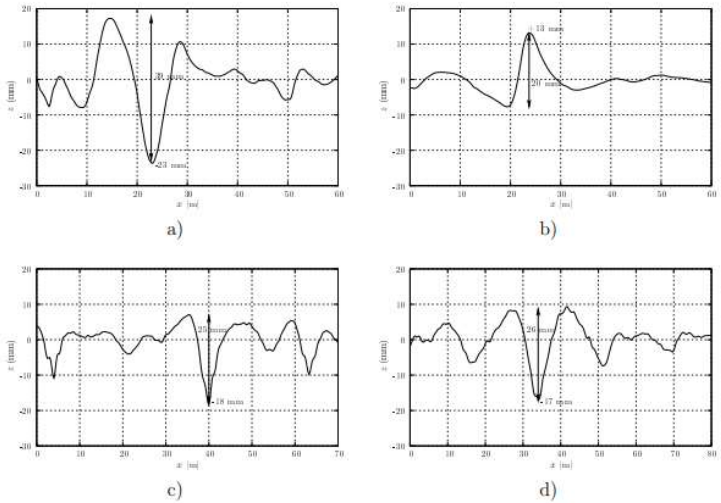
(Vale and Calçada, 2014)

(Vale, 2010)

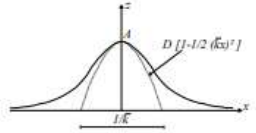
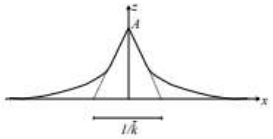
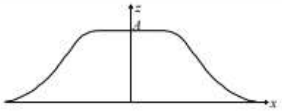
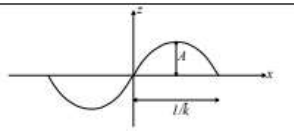
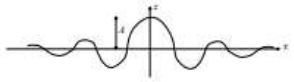
4. Numerical modelling

Artificial generation of track irregularities for dynamic calculations

When performing numerical calculations, it is possible to artificially define the geometry of isolated defects.



Real measured irregularities

Shape	Analytical expression
	$z = Ae^{(-1/2)(\bar{k}x)^2}$
	$z = Ae^{-\bar{k}\lvert x\rvert}$
	$z = (\frac{A^2}{1+(\bar{k}x)^8})^{1/2}$
	$z = A\sin(\pi\bar{k}x)$
	$z = Ae^{-\bar{k}\lvert x\rvert}\cos(\pi\bar{k}x)$

(Vale, 2010)

References

- Berawi, A., Delgado R., Calçada R. Vale C. (2010) “Evaluating Track Geometrical Quality through Different Methodologies”. International Journal of Technology, v. 1, n. 1, p. 38-47, jul. 2010. ISSN 2087-2100., doi:10.14716/ijtech.v1i1.35, Available at: http://ijtech.eng.ui.ac.id/old/index.php/journal/article/view/35.
- CEN (2013) , EN 13450 -Aggregates for railway ballast, CEN.
- CEN (2017) EN 13848-5 - Railway applications - Track - Track geometry quality - Part 5: Geometric quality levels - Plain line, switches and crossings, CEN.
- Connolly, DP, Galvín, P, Olivier, B et al. (2019) “A 2.5D time-frequency domain model for railway induced soil-building vibration due to railway defects”, Soil Dynamics and Earthquake Engineering, 120. pp. 332-344. ISSN 0267-7261.
- Giannakos, K. (2015). “Sensitivity Analysis of Fastenings’ Types on Track's Life-Cycle” International Journal of Railway Reserch. 1. 1-10.
- Guoqing J., Wenli J., Xinyu W., Valeri M., Roar N., Yunlong G. (2021) “Experimental and numerical study on lateral resistance of frictional sleeper with arrowhead groove”, Transportation Geotechnics,Vol. 30, https://doi.org/10.1016/j.trgeo.2021.100638.

References

- Paixão, A. & Fortunato, E. & Calçada, (2019). “Smartphone’s Sensing Capabilities for On-Board Railway Track Monitoring: Structural Performance and Geometrical Degradation Assessment”. Advances in Civil Engineering. 1-13. 10.1155/2019/1729153.
- UIC (2002) Feasibility Study Ballastless Track. UIC.
- UIC (2008) Best Practice Guide for Optimum Track Geometry Durability, UIC.
- Vale C (2010) Influência da qualidade dos sistemas ferroviários no comportamento dinâmico e no planeamento da manutenção preventiva de vias de alta velocidade. Tese de doutoramento. Faculdade de Engenharia da Universidade do Porto.
- Vale C., Calçada R. (2014) “A Dynamic Vehicle-Track Interaction Model for Predicting the Track Degradation Process”, Journal of Infrastructure Systems Volume 20 Issue 3 - September 2014, https://doi.org/10.1061/(ASCE)IS.1943-555X.0000190.
- Jadidi, K., Esmaeili, M., Kalantari, M.; Khalili, M.; Karakouzian, M. (2021). A Review of Different Aspects of Applying Asphalt and Bituminous Mixes under a Railway Track. Materials. 14. 169. 10.3390/ma14010169.

References

- Vale, C. (2021) "Wheel Flats in the Dynamic Behavior of Ballasted and Slab Railway Tracks", *Applied Science 11*, 7127. https://doi.org/10.3390/app11157127.

- Vale, C.; Simões, M.L. (2022) "Prediction of Railway Track Condition for Preventive Maintenance by Using a Data-Driven Approach". *Infrastructures 7*, 34. https://doi.org/10.3390/infrastructures7030034.

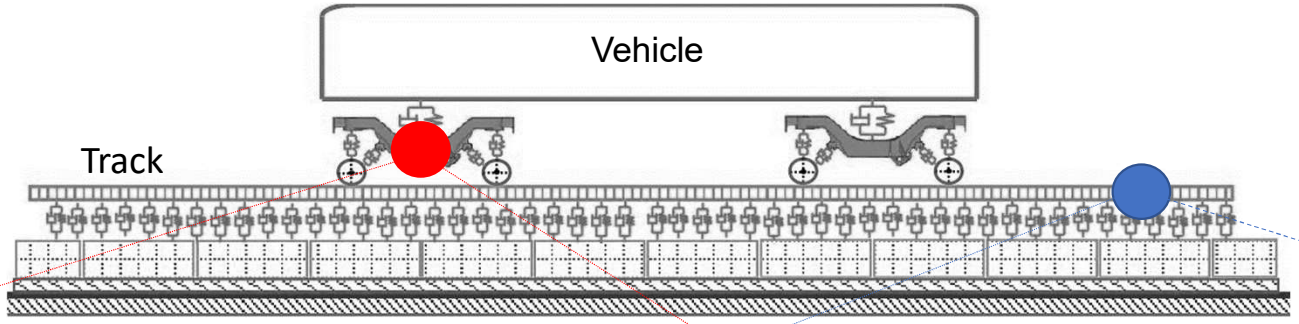
Rolling Stock: Components, Dynamic Characteristics and Typical Damages

Diogo Ribeiro [ISEP], Rúben Silva [FEUP], António Guedes [ISEP]
& Mohammad Reza Mohammadi [FEUP]

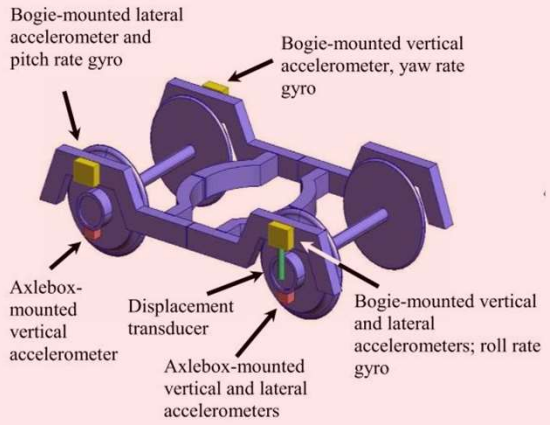
Contents

1. Introduction
2. Passenger vehicles
3. Freight vehicles
4. Anomalies in railway vehicles

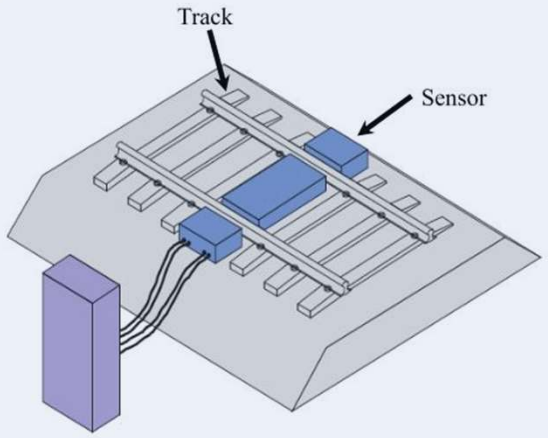
1. Introduction



- Service vehicles and dedicated inspection vehicles
- A running vehicle can monitor an entire railway infrastructure
- V2V and V2I strategies



Onboard monitoring system



- An instrumented track section can monitor the condition of all passing vehicles
- I2I and I2V strategies

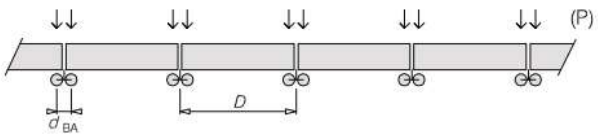
Wayside monitoring system

2. Passenger vehicles

Types

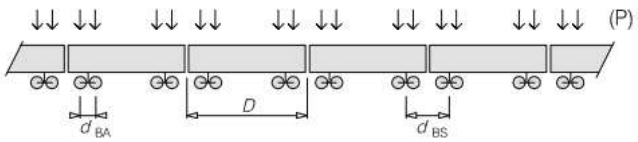
Articulated train
Shared bogies by adjacent cars





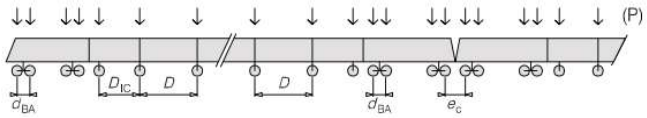
Conventional train
Independent bogies for each car





Regular train
Shared axle by adjacent cars (not a bogie)



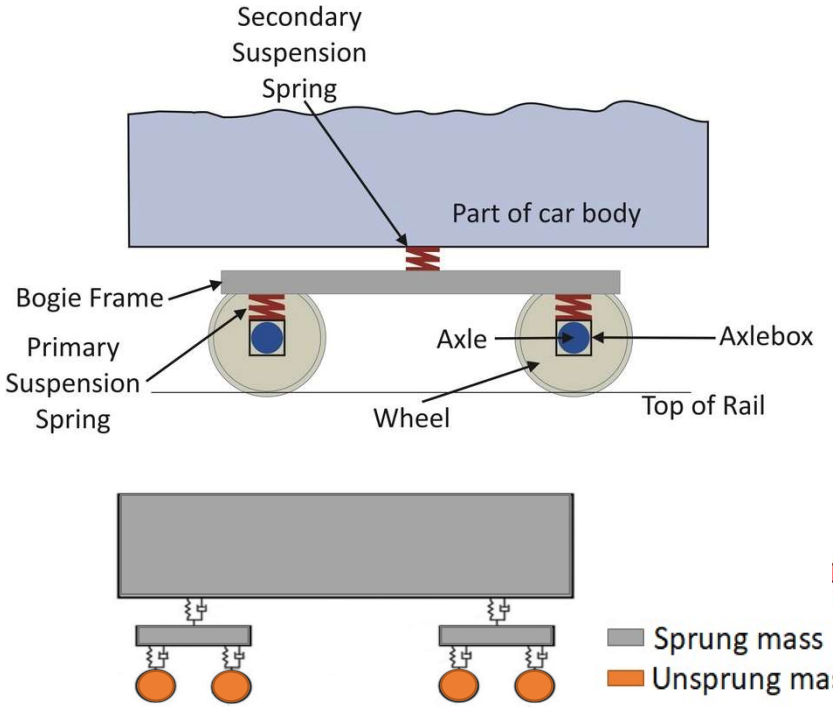


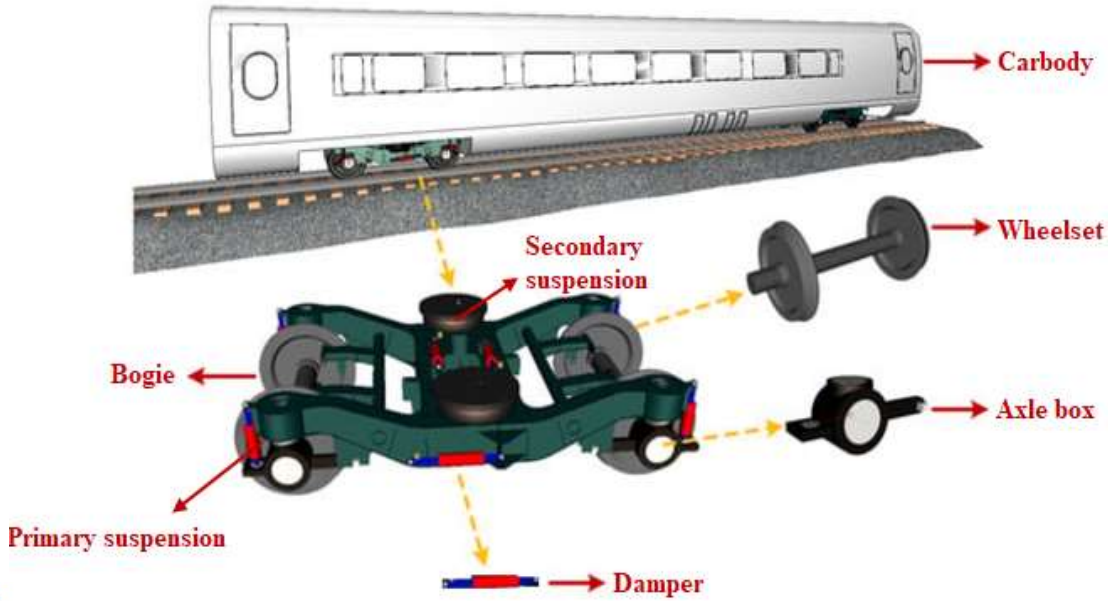
2. Passenger vehicles

Components

Vehicles have two levels of suspension to ensure better passenger comfort:

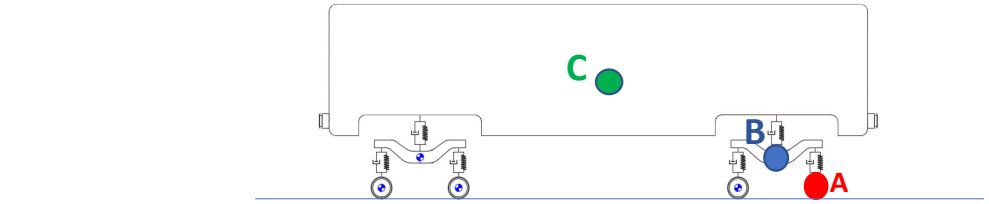
- **Primary suspension** (between axle-boxes and bogies);
- **Secondary suspension** (between bogies and carbody);





2. Passenger vehicles

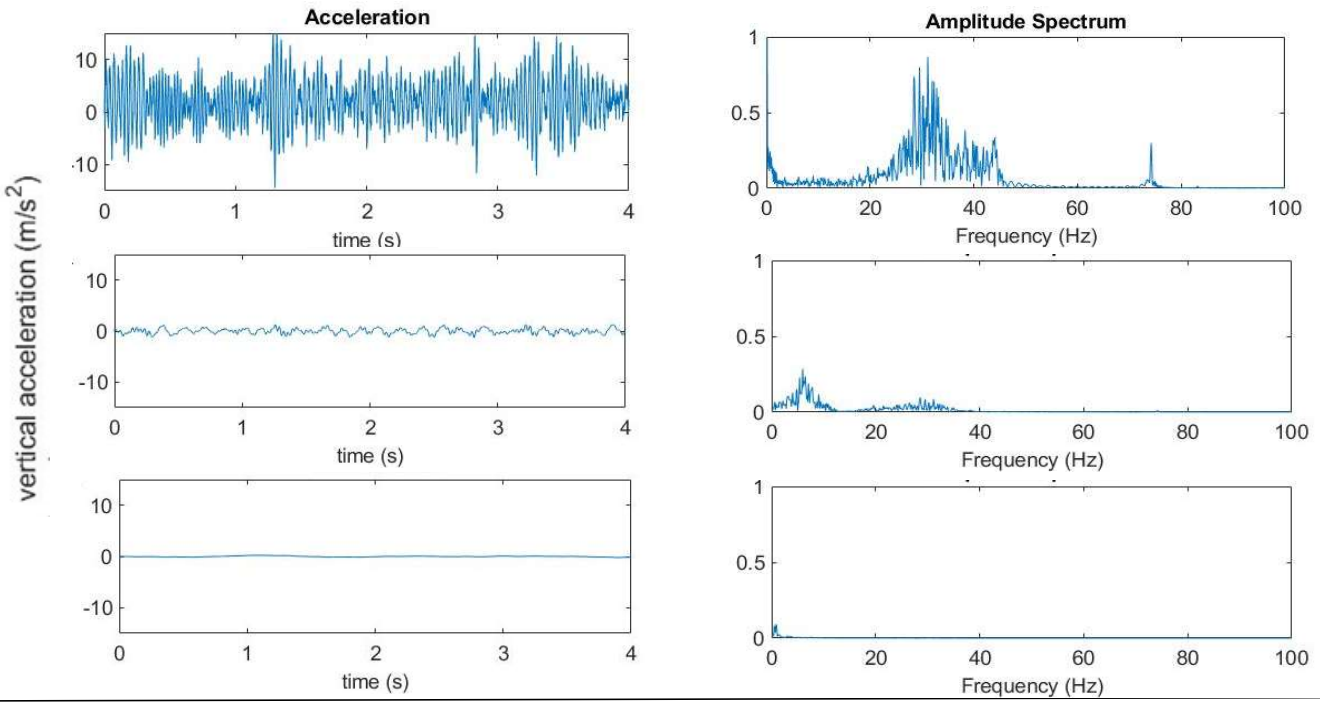
Suspensions filtering effect



A **Axlebox**

B **Bogie**

C **Carbody**



2. Passenger vehicles

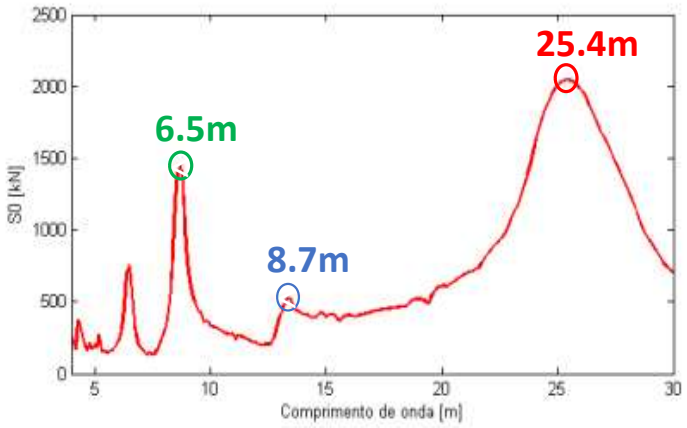
Dynamic Signature

The **dynamic signature** of a train is a reference parameter for representing the parametric dynamic excitation induced by the train, which depends on the values of axle loads P_k and distance between axles x_k, and can be obtained by:

$$S_0(\lambda) = \max_{i=1,N} \sqrt{\left[\sum_{k=0}^{i} P_k \cos\left(\frac{2\pi x_k}{\lambda}\right)\right]^2 + \left[\sum_{k=0}^{i} P_k \sin\left(\frac{2\pi x_k}{\lambda}\right)\right]^2}$$

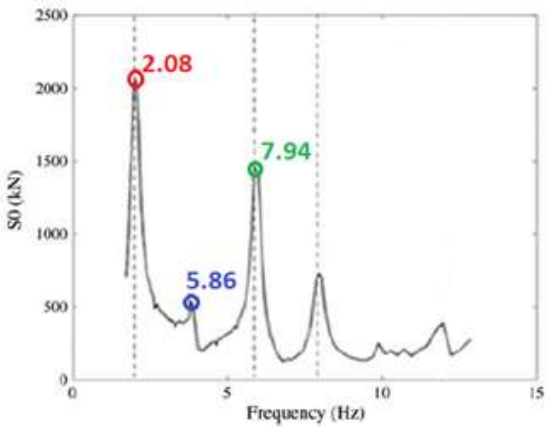
Example: Alfa Pendular (6 cars)





$f = v/\lambda$

v: velocity
λ: wavelength

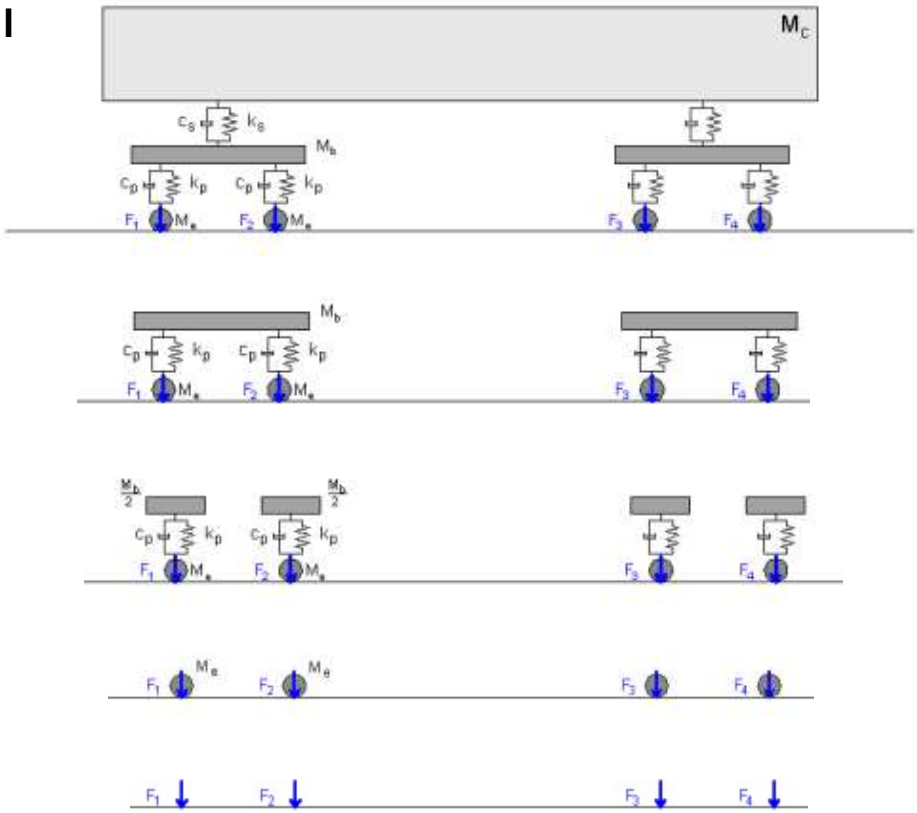


Alfa pendular
185 km/h

2. Passenger vehicles

Numerical modelling

Level of detail



Complete vehicles

Individual bogies

Set of individual bogies

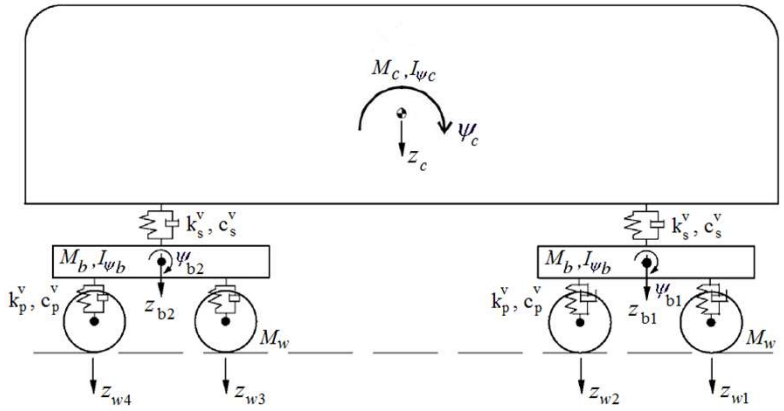
Moving masses

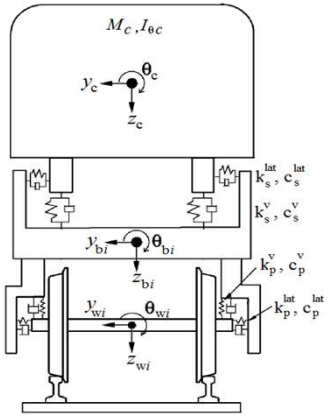
Moving loads

2. Passenger vehicles

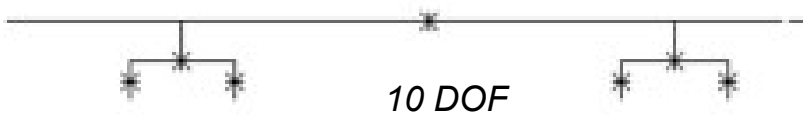
Numerical modelling

Multibody modelling strategies consider separate bodies with their mass and inertial properties that are connected by elastic elements, typically suspensions.



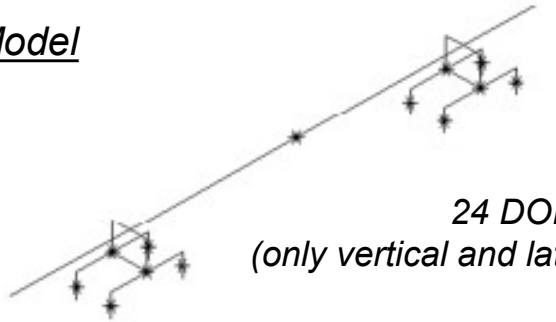


2D Model



10 DOF
(only vertical dynamic)

3D Model

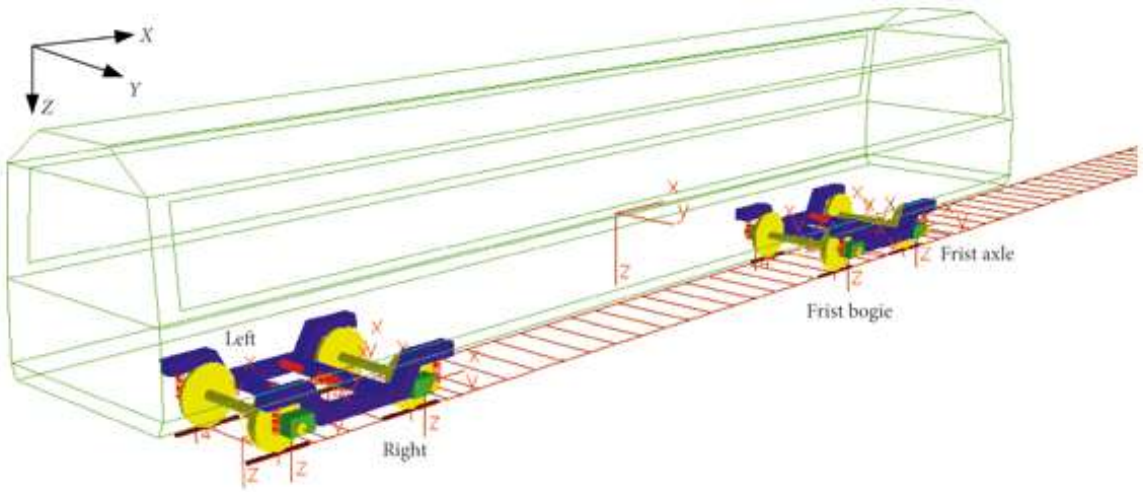


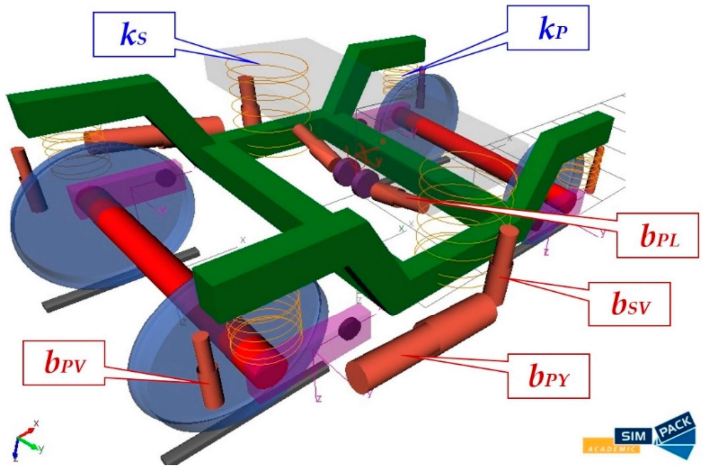
24 DOF
(only vertical and lateral dynamic)

2. Passenger vehicles

Numerical modelling

Simulation packages SIMPACK®
VAMPIRE®
ADAMS-RAIL®





Advantages:
Low computational costs and good accuracy in predicting the global vehicle response

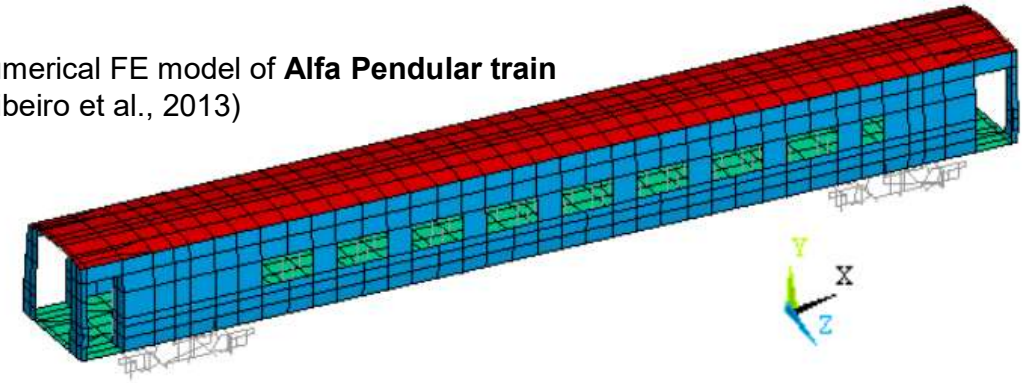
2. Passenger vehicles

Numerical modelling

FEM models

Flexible FE models

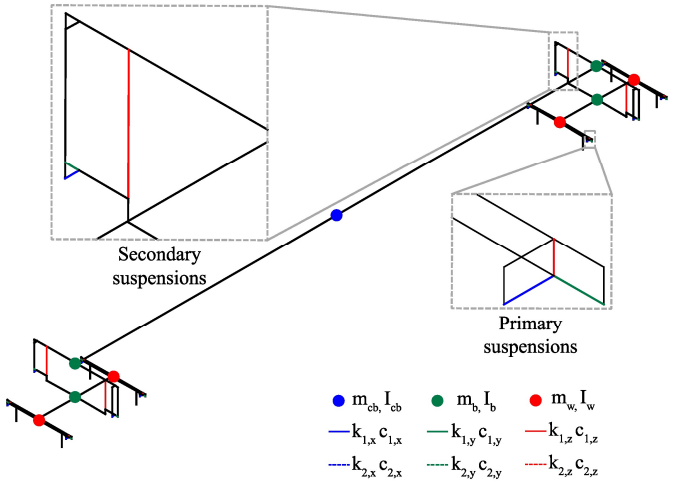
Numerical FE model of **Alfa Pendular train**
(Ribeiro et al., 2013)



Consider the vehicle **components flexibility** through the use of shell, volume and beam elements;
High computational costs and difficulties in finding the vehicle design details;
Good for **passenger comfort** assessment and **fatigue-life** prediction;

Rigid FE models

Numerical FE model of **Alfa Pendular train**
(Meixedo et al., 2014)

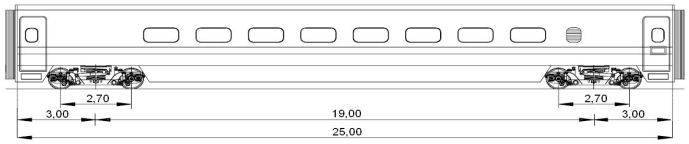


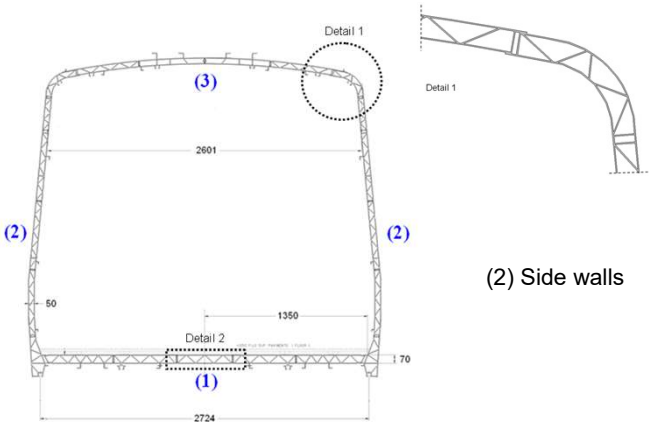
Consider all the **mass** and **inertial properties** in mass elements connected by **rigid beams**;
Low computational costs;

2. Passenger vehicles

Numerical modelling: carbody

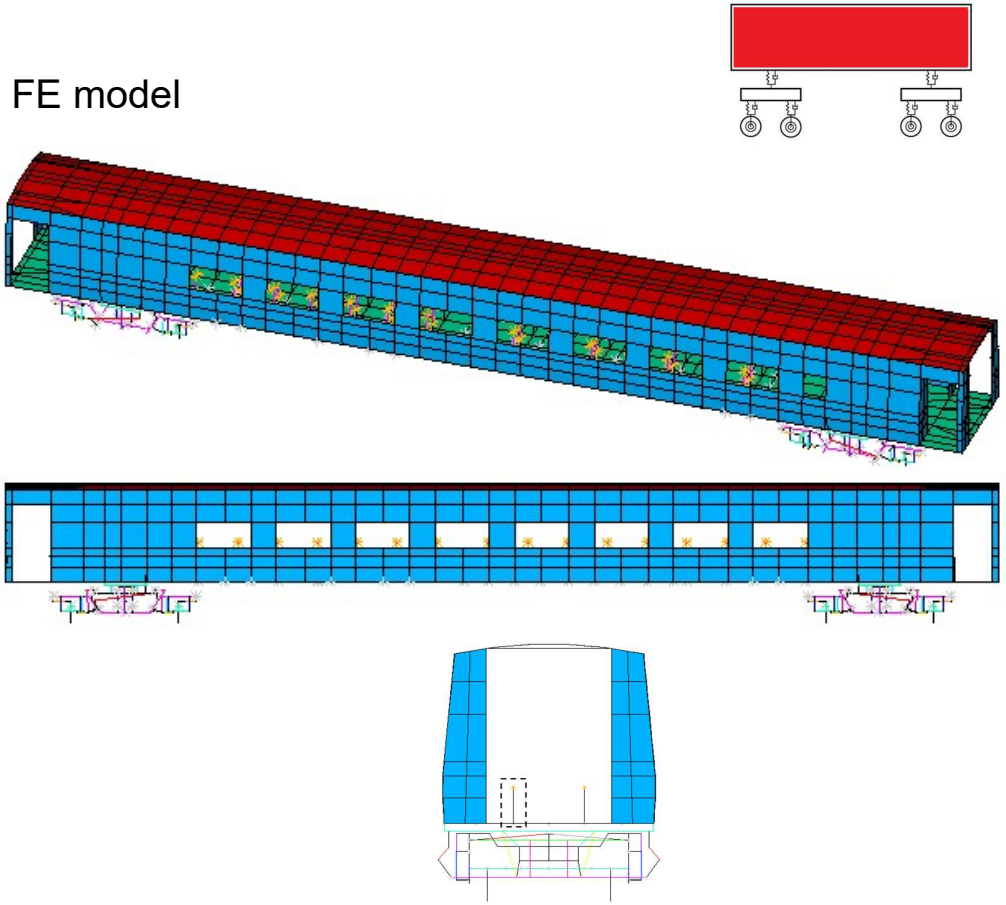
Alfa pendular: Structural details





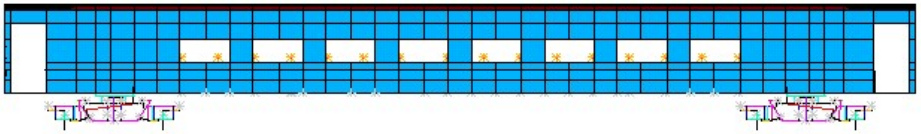
(2) Side walls

FE model



2. Passenger vehicles

Carbody: modal parameters



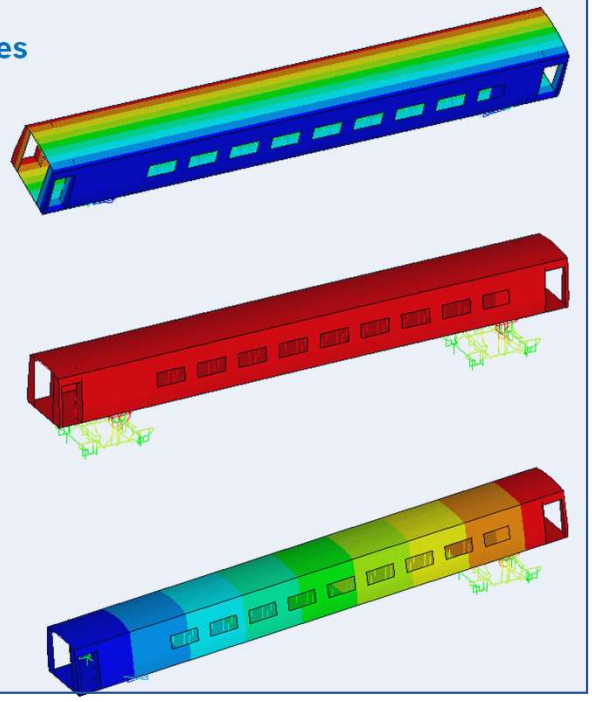
Numerical FE model of **Alfa Pendular train** (Ribeiro et al., 2013)

Rigid body modes

Rolling mode
f = 1.01 Hz

Bouncing mode
f = 1.24 Hz

Pitching mode
f = 1.70 Hz

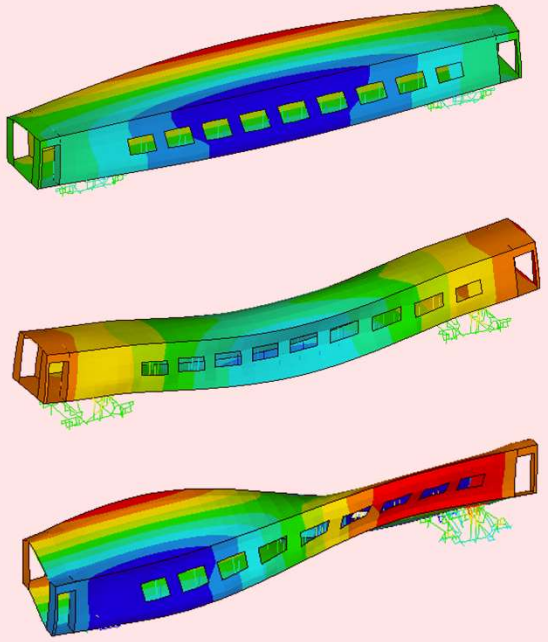


Flexural modes

Distortion mode
f = 8.39 Hz

Bending mode
f = 12.16 Hz

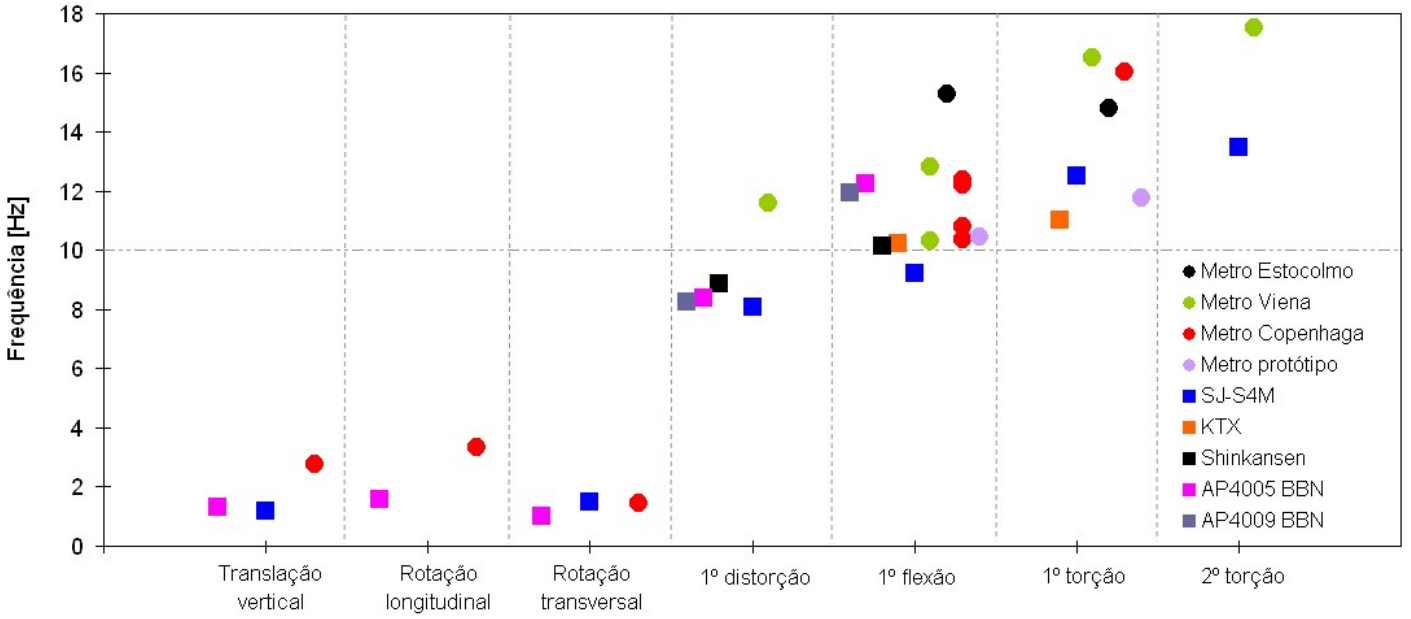
Torsion mode
f = 17.73 Hz



2. Passenger vehicles

Carbody: modal parameters

Typically, the carbody mode shapes are associated to **rigid body movements** and **flexural structural movements**. Rigid body modes present frequency values **below 3.5 Hz**, while structural modes are, for most vehicles, **above 8 Hz**.

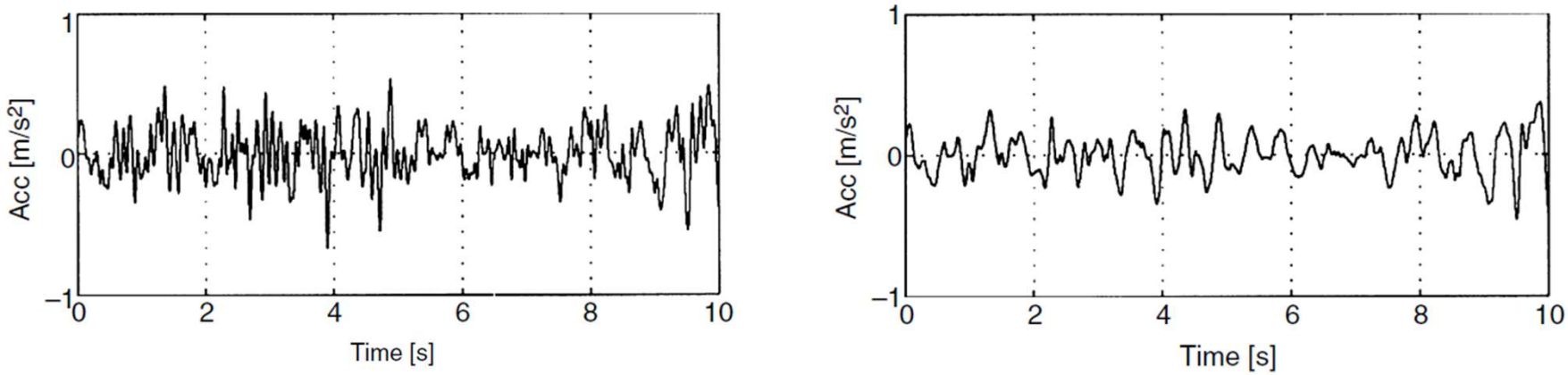


2. Passenger vehicles

Carbody: influence of structural flexibility

The use of models which **consider the deformability of the carbody** becomes more important due to the tendency to use increasingly **lighter and slender structures** in the manufacture of trains to reduce weight and construction costs.

The carbody structural flexibility may contribute, in a large extent, to the accelerations that passengers are subjected to and therefore can have a negative effect on ride comfort.

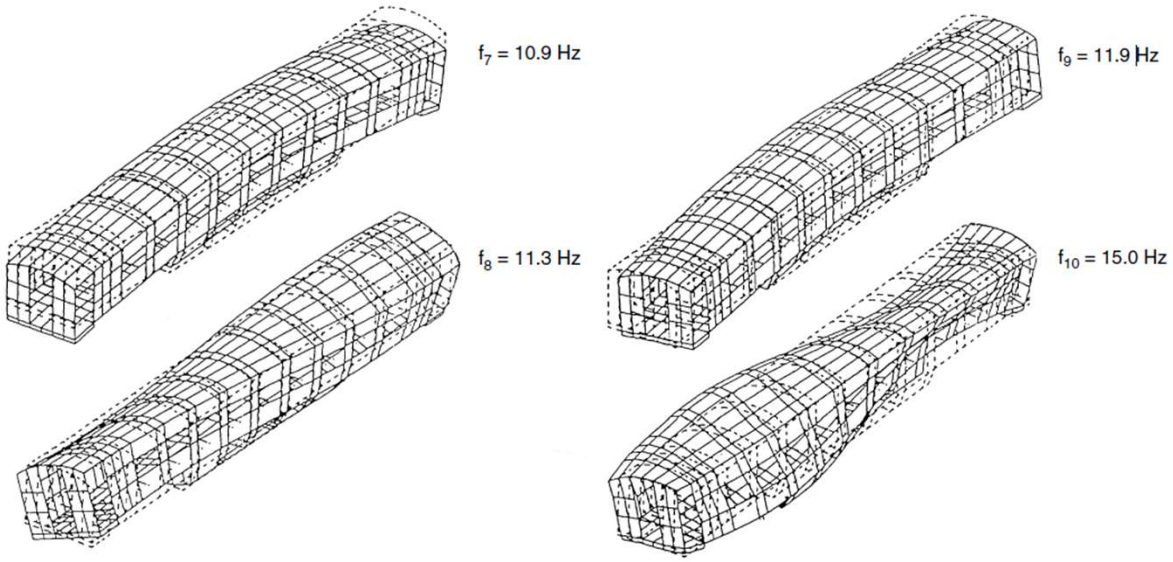


Influence of carbody structural flexibility on carbody accelerations (Carlbom, 2000)

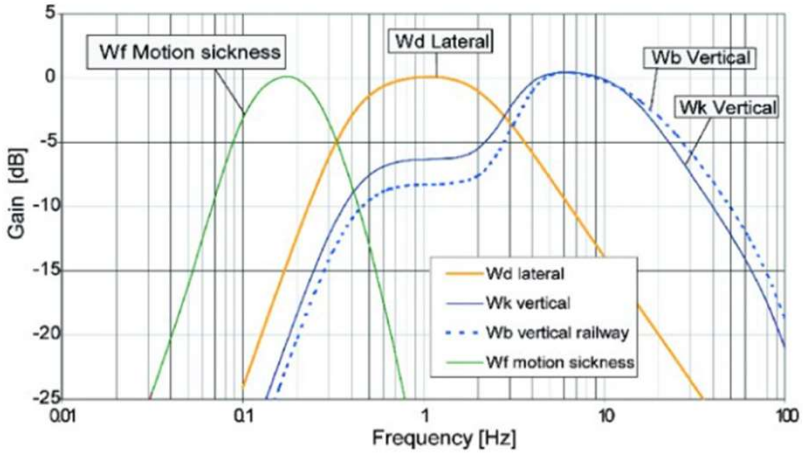
2. Passenger vehicles

Carbody: influence of structural flexibility

Additionally, the frequencies of these vibration modes range from 8.0 Hz to 18 Hz, which is significantly relevant regarding **human beings' sensitivity to vibration** (see frequency weighting curves from ISO 2631).



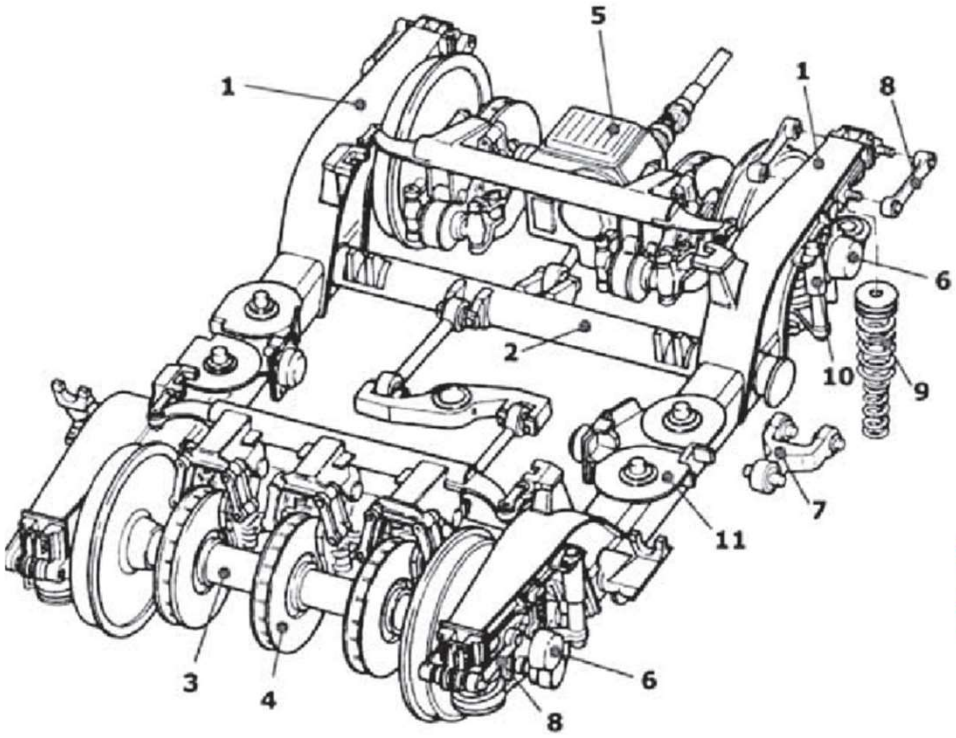
Flexural vibration modes and corresponding natural frequencies (Iwnicki, 2006)

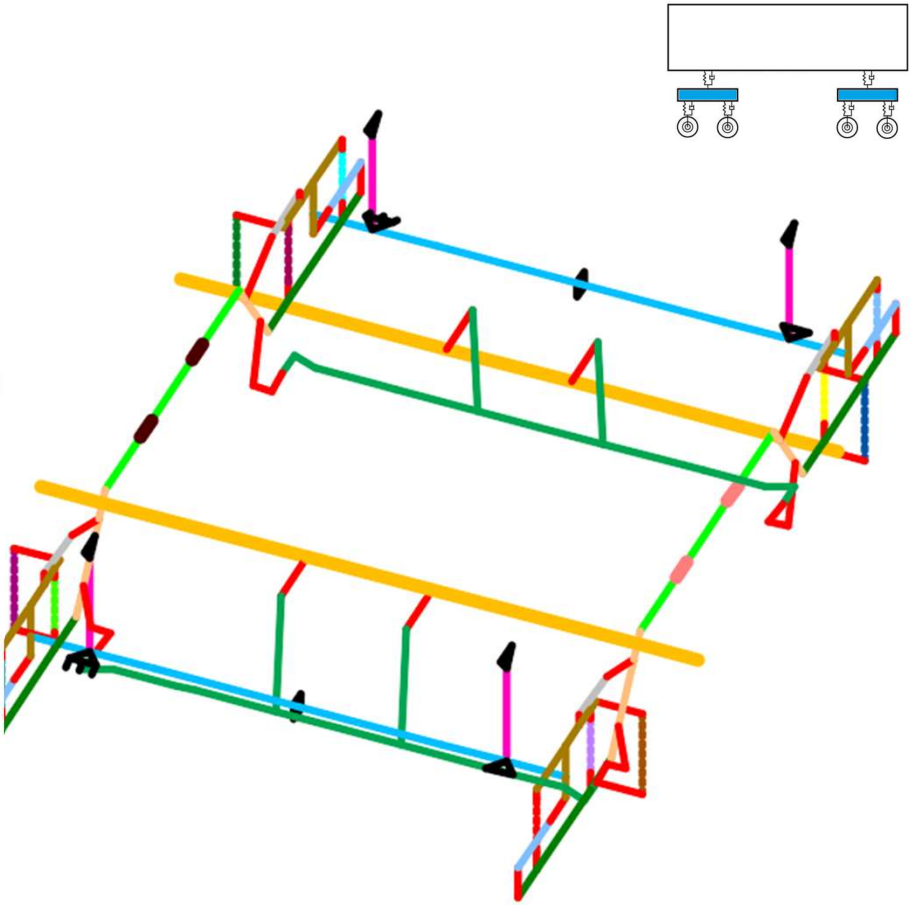


Frequency weighting curves from ISO 2631 (2018)

2. Passenger vehicles

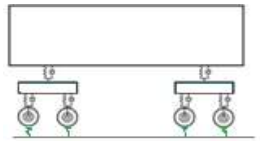
Numerical modelling: bogies





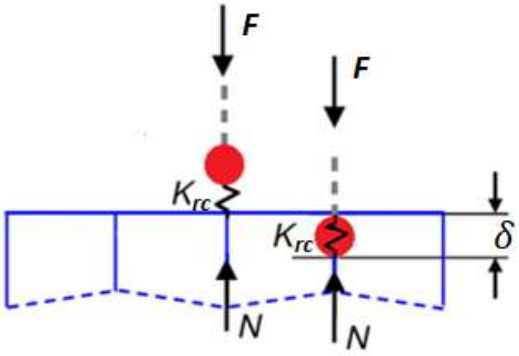
2. Passenger vehicles

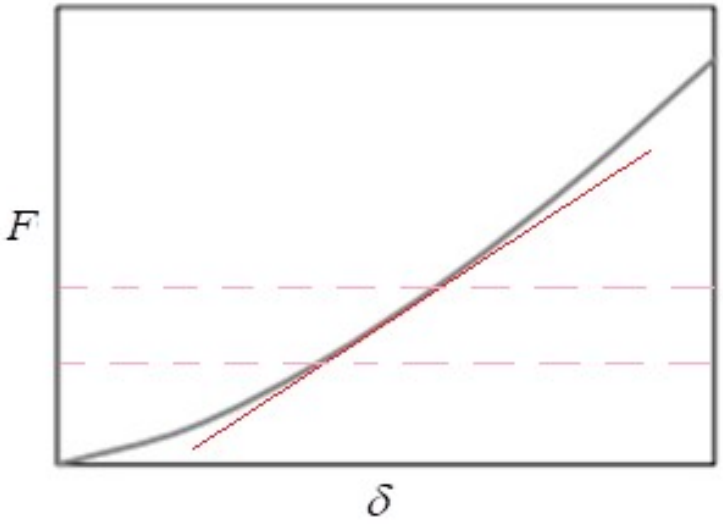
Numerical modelling: wheel-rail contact



The **Hertzian contact model** assumes the contact between two perfectly elastic solids without friction on the interface. The normal contact force *F* is related to the penetration δ, according to:

$$F = c\delta^{\frac{3}{2}}$$ with *c* as the Hertzian constant





Linearized stiffness:

$$F = K_{rc}\delta$$

$$K_{rc} = \frac{3}{2}F^{\frac{1}{3}}\left[\frac{2}{3}\frac{E}{1-\nu^2}\left(r_r r_c\right)^{\frac{1}{4}}\right]^{\frac{2}{3}}$$

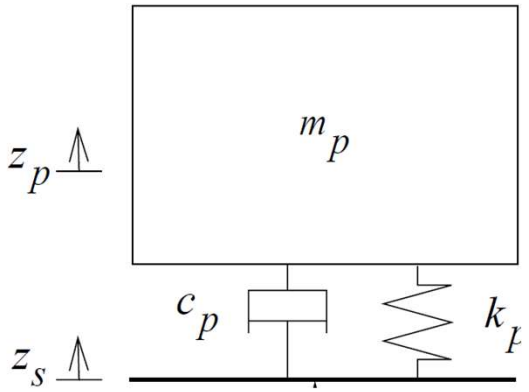
2. Passenger vehicles

Numerical modelling: passenger-seat system

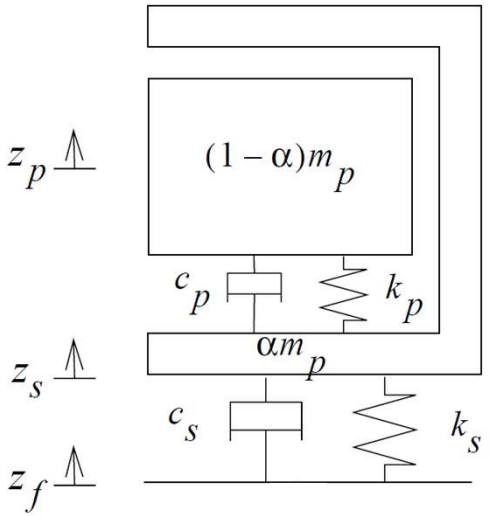
In carbody modelling, equipment and passengers may be modelled as separate bodies suspended to the carbody structure. Explicit introduction of seats and passengers into modelling also promotes evaluation of ride comfort on the seat cushion and not only on the floor.

Concerning the **modeling the passenger-seat system**, different alternatives were proposed associated with different levels of complexity (Carlbom, 2000):

The carbody-seat connection is assumed rigid, and the mass of the seat is coupled to the carbody



1-DOF system



2-DOFs system

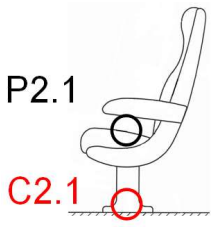
Simulation of the **carbody-seat** interface and **passenger-seat** interface. The value of a lies between 5% and 20% of the passenger's mass.

2. Passenger vehicles

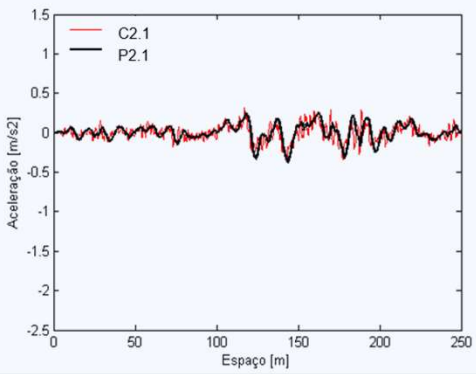
Passenger-seat system: isolation of the seat structure

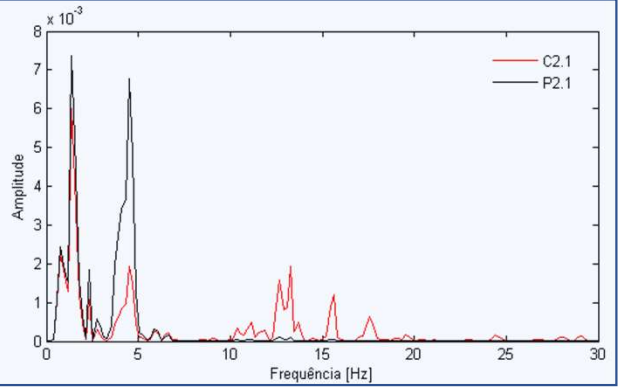
The seat structure has a relevant **isolation effect** of the vibrations derived from the carbody.



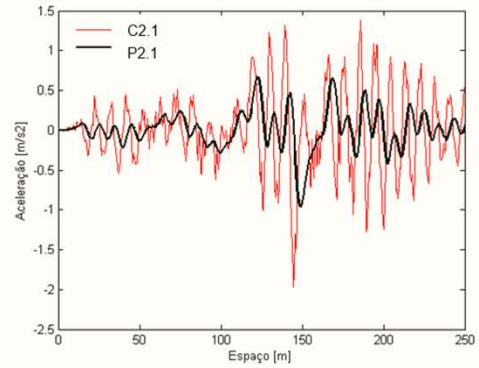


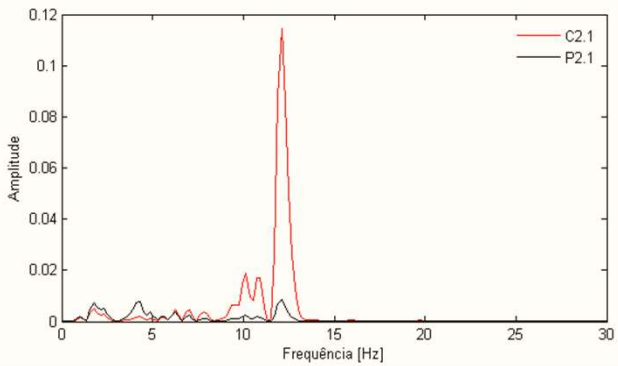
150 km/h





Carbody resonant speed



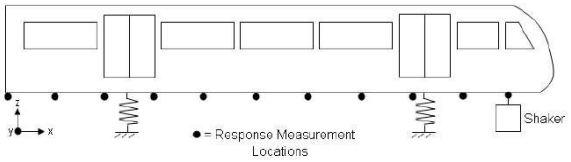


2. Passenger vehicles

Dynamic tests

Dynamic tests can be performed considering vehicles **at rest or in motion**.

The tests carried out with the vehicle at rest involve the use of an **external excitation** through hydraulic actuators, electrodynamic exciters, impact hammers, random movement of people, or even the impact of other vehicles.





Hydraulic actuator



Impact hammer



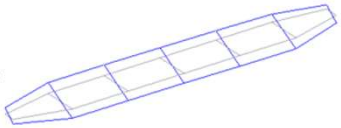
Random movement of people

2. Passenger vehicles

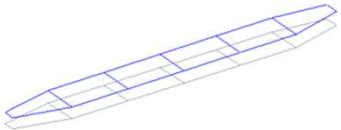
Alfa Pendular dynamic tests

- **Carbody** experimental test (EMEF Contumil facilities)
- Experimental modal identification: rigid body and flexural modes

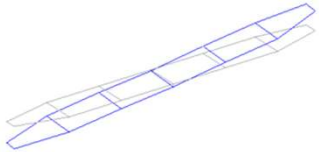




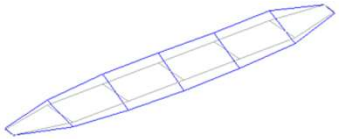
Mode 1 – *f = 1.01 Hz*
Rolling mode



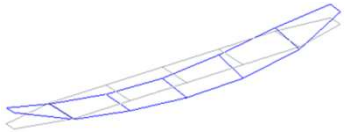
Mode 2 – *f = 1.33 Hz*
Bouncing mode



Mode 3 – *f = 1.59 Hz*
Pitching mode



Mode 4 – *f = 8.38 Hz*
1st torsion mode



Mode 5 – *f = 12.26 Hz*
Bending mode



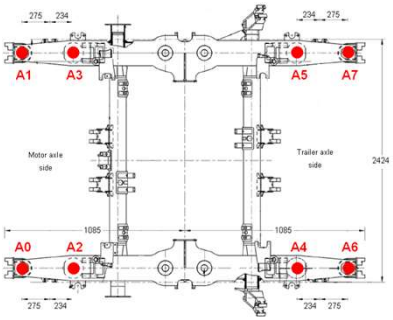


2. Passenger vehicles

Alfa Pendular dynamic tests

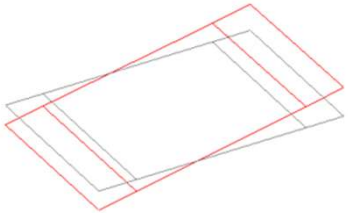
- **Bogie** experimental test (EMEF Entroncamento facilities)
- Experimental modal identification: rigid body modes
- Test performed with and without primary dampers



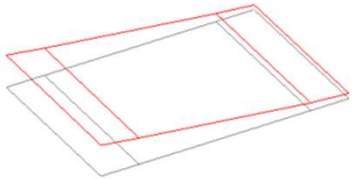




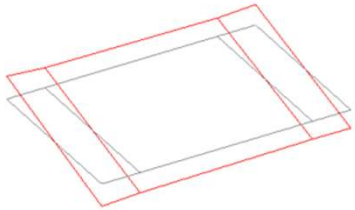




Mode 1 – *f = 11.90 Hz (14.02 Hz)*
Pitching mode



Mode 2 – *f = 17.75 Hz (18.60 Hz)*
Bouncing mode



Mode 3 – *f = 24.48 Hz (25.32 Hz)*
Rolling mode

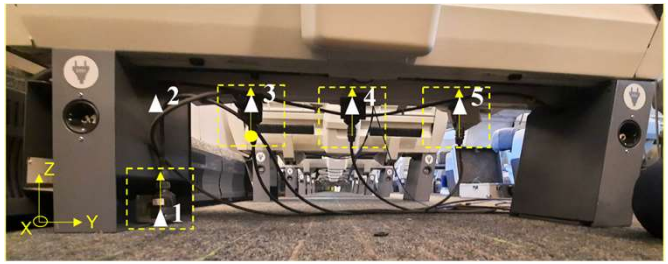
2. Passenger vehicles

Alfa Pendular dynamic tests

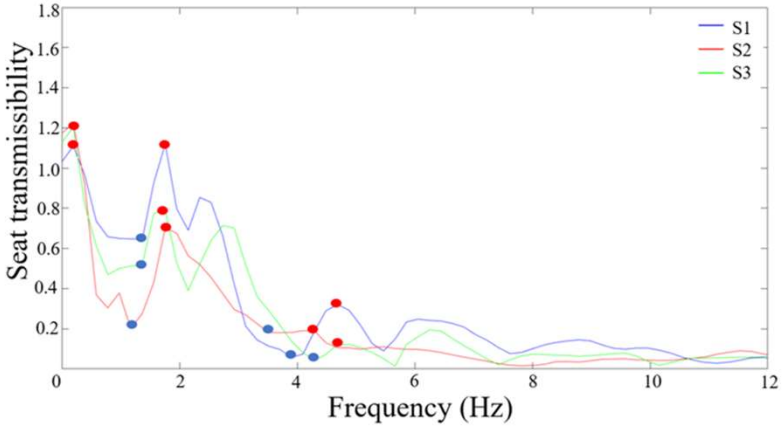
- Experimental modal identification of the **passenger-seat interface**



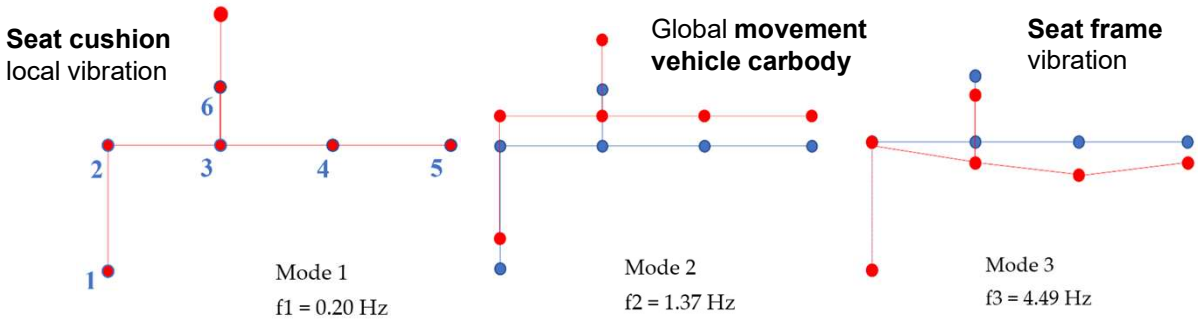




Experimental test setup: seat pad and seat frame accelerometers



Seat transmissibility curves



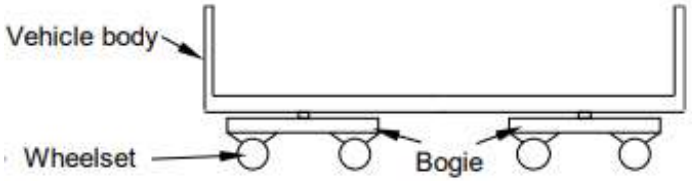
3. Freight vehicles

Types

Bogie vehicles



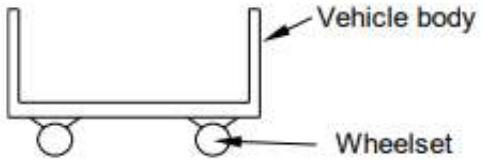




Two-axle vehicles





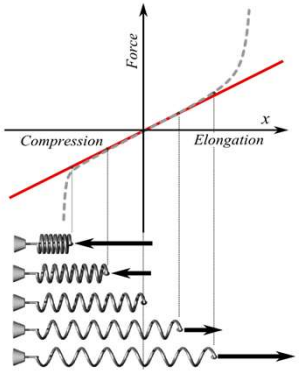


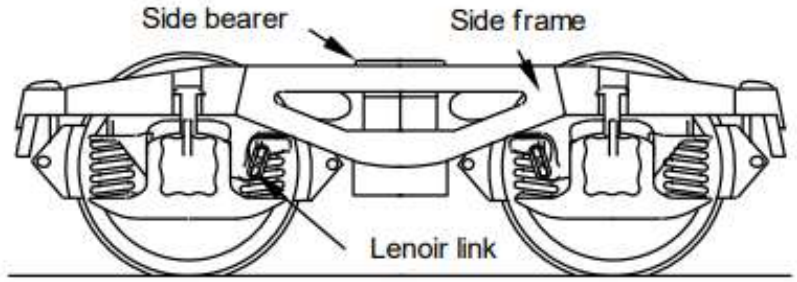
3. Freight vehicles

Primary Suspensions

Coil springs
(common in European bogie vehicles)

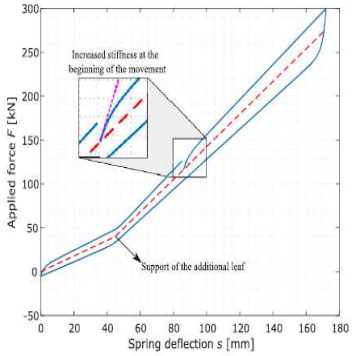


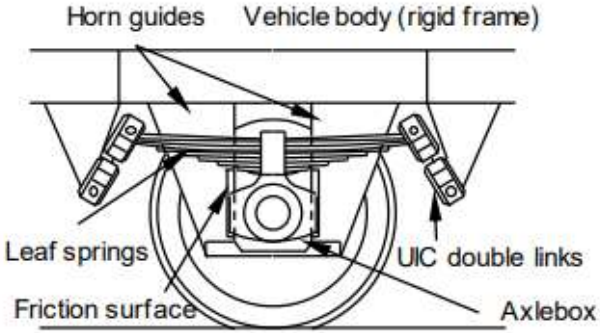




UIC double link leaf springs
(common in European two-axle vehicles)



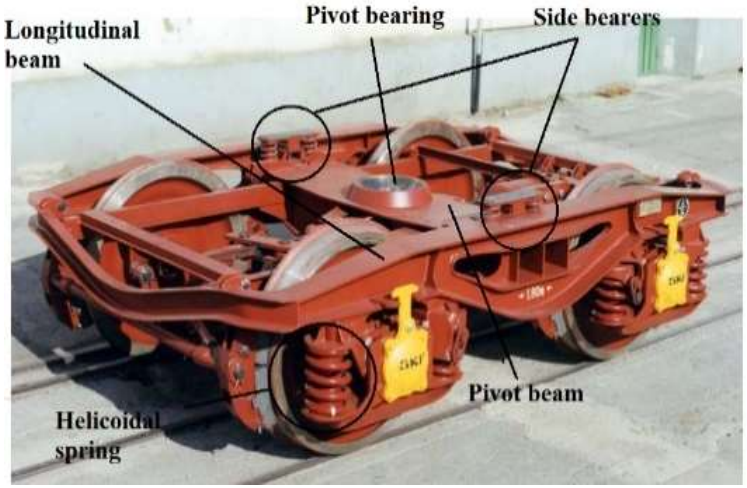


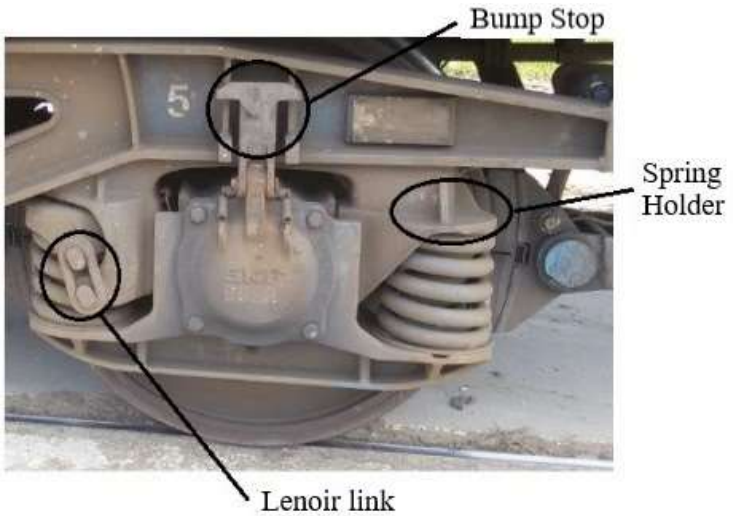


3. Freight vehicles

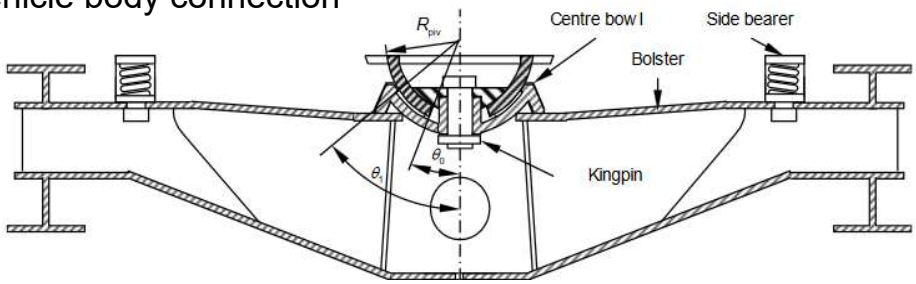
Bogies

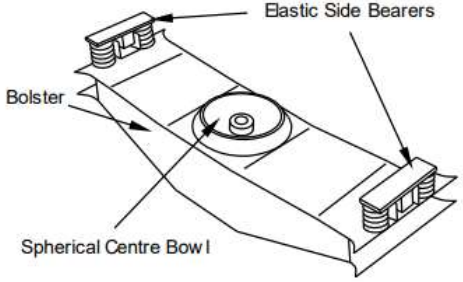
Y25 Bogie





Bogie - vehicle body connection

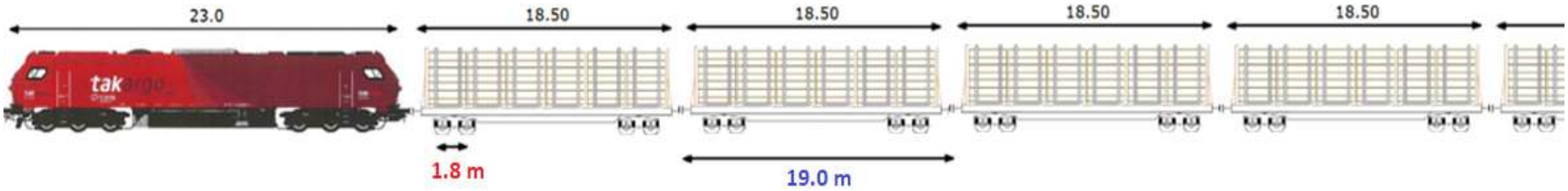


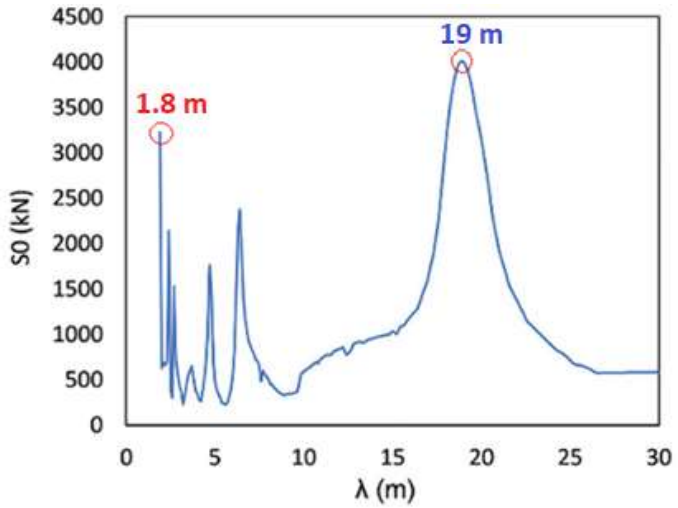


3. Freight vehicles

Dynamic Signature

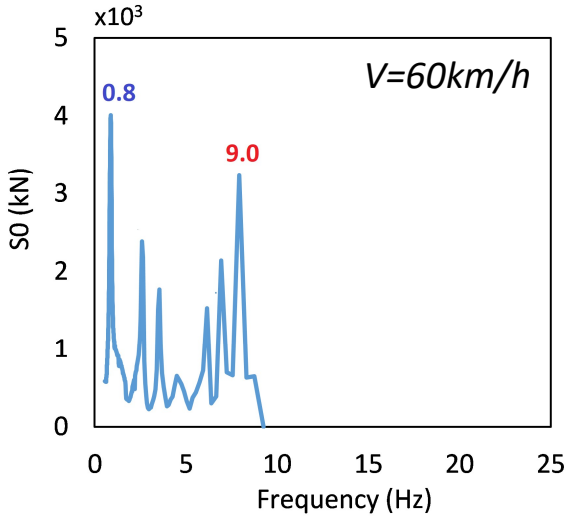
Example Takargo train: locomotive + 14 Sgnss wagons





$f = v/\lambda$

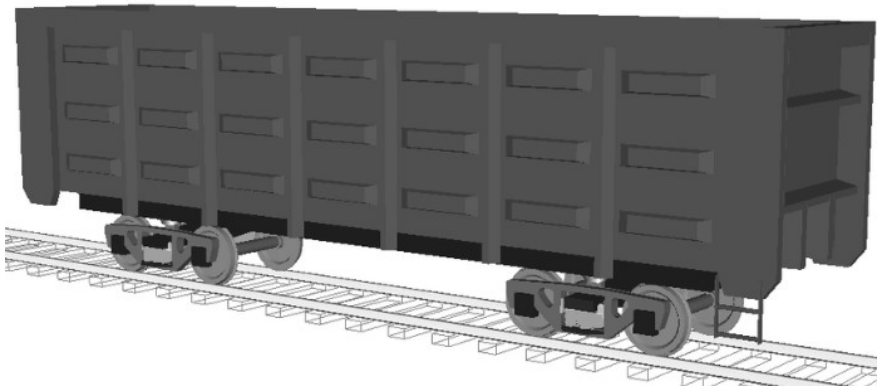
v: velocity
λ: wavelength

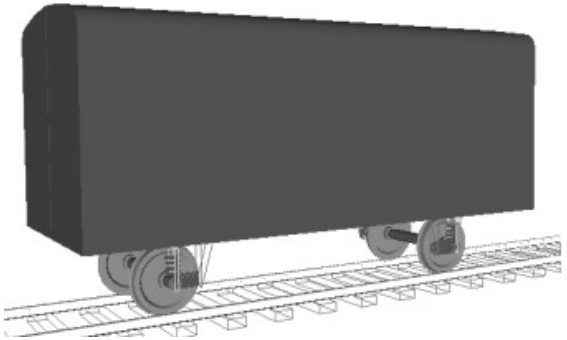


3. Freight vehicles

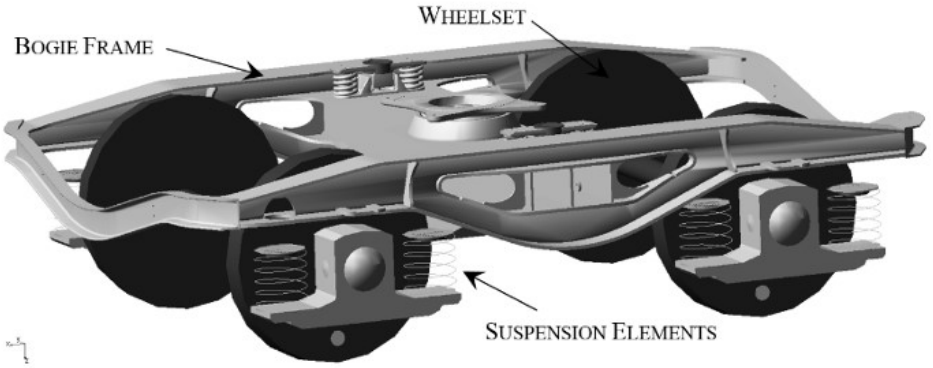
Numerical modelling

Multibody models





Simulation packages:
SIMPACK®
VAMPIRE®
ADAMS-RAIL®



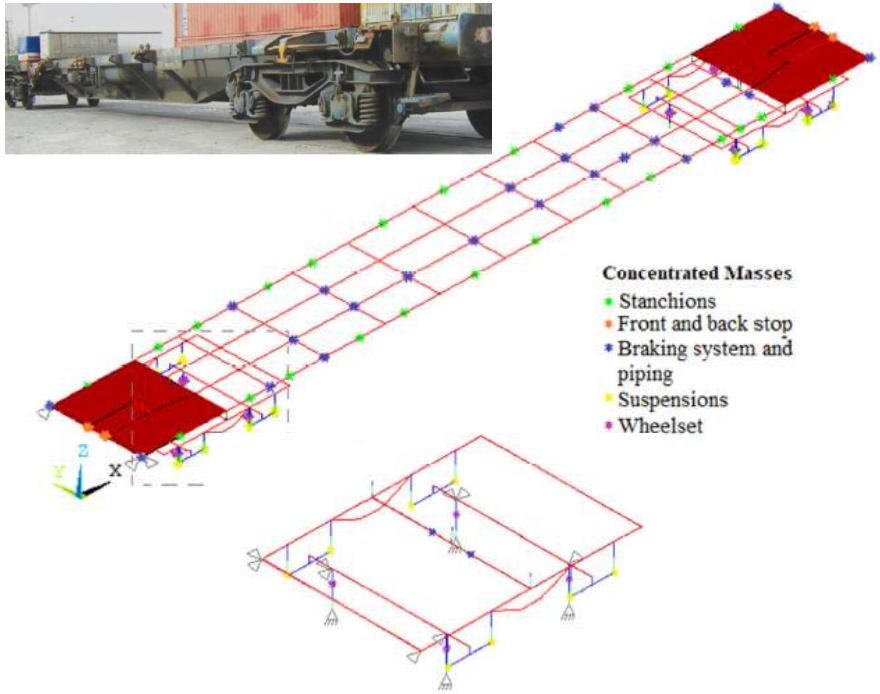
3. Freight vehicles

Numerical modelling

FEM models

Flexible FE models

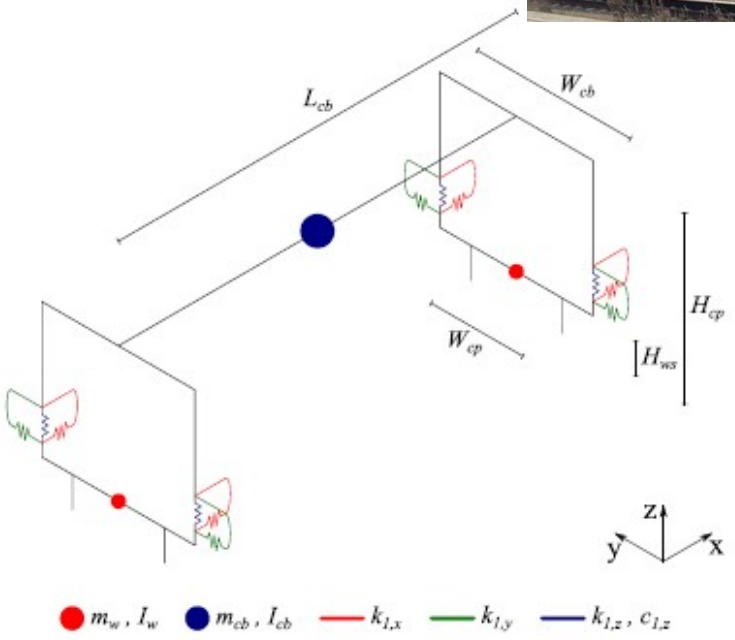
Sgnss Wagon (Silva et al. 2022)



Rigid FE models

Laagrss Wagon (Bragança et al. 2022)



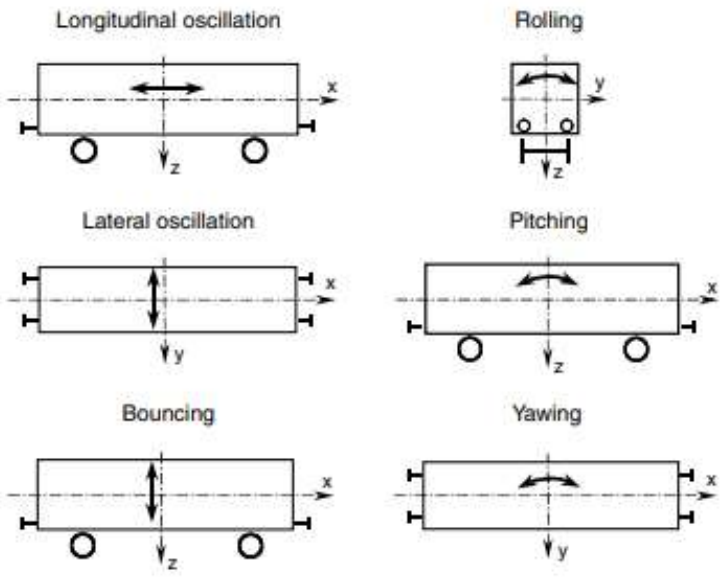


3. Freight vehicles

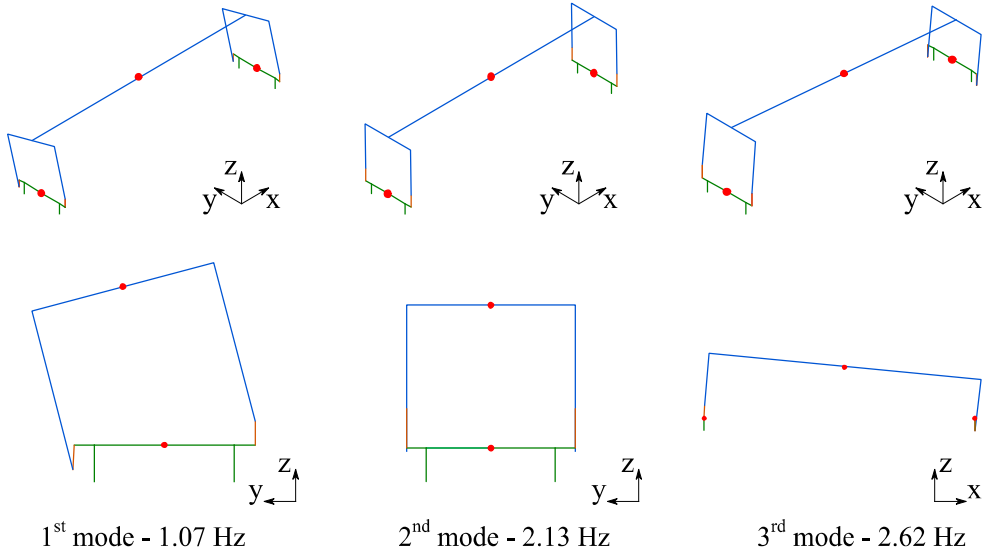
Modal parameters

Rigid body vibration modes

Basic carbody mode shapes



Laagrs model



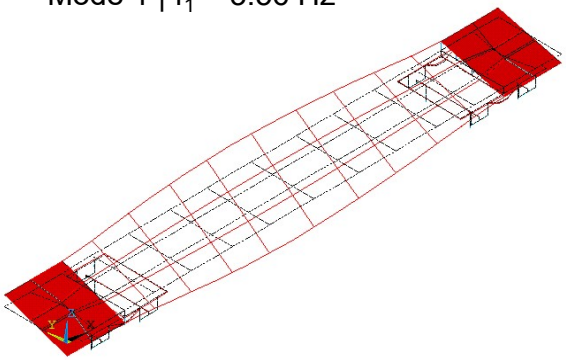
3. Freight vehicles

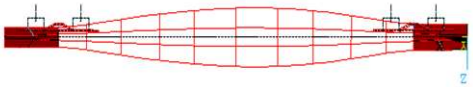
Modal parameters

Bending/torsion vibration modes

Sgnss model

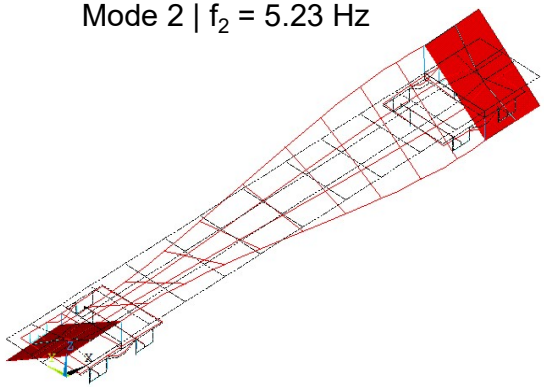
Mode 1 | f_1 = 3.56 Hz

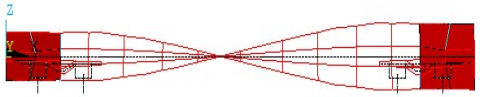




Rolling/Torsion mode

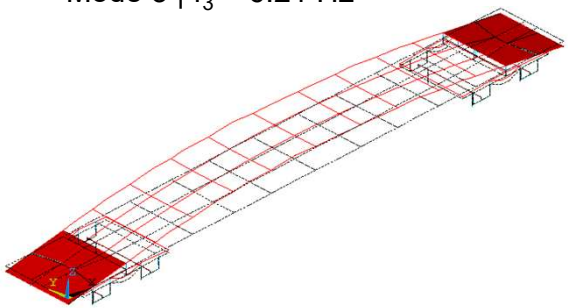
Mode 2 | f_2 = 5.23 Hz





Torsion mode

Mode 3 | f_3 = 6.21 Hz





Bouncing/bending mode

3. Freight vehicles

Dynamic tests

Sgnss wagon tests

- Forced vibration test performed with the vehicle unloaded and loaded and in rest position
- Excitation provided by impact hammers and random movement of people
- Removal of the central stowage to allow workspace
- Symmetrical overload distribution

Loaded condition



Unloaded condition



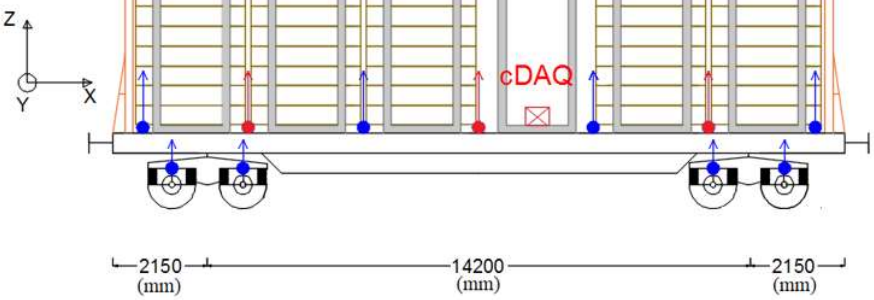
3. Freight vehicles

Dynamic tests

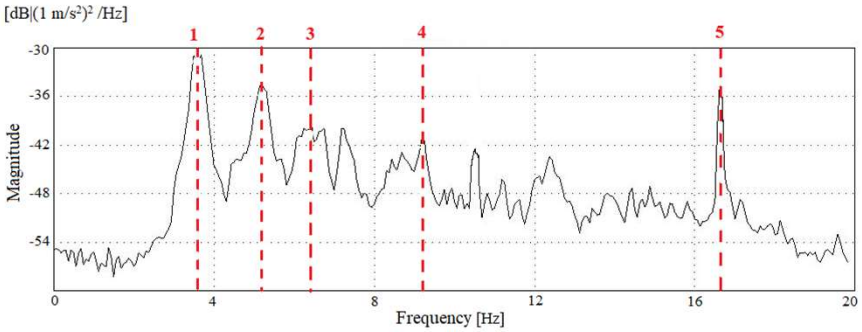
- 16 high-sensitive piezoelectric accelerometers

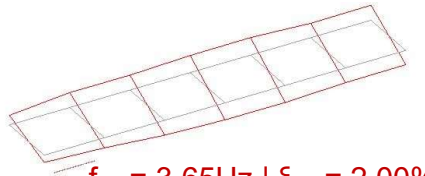
- Accelerometers attached to the base platform with magnetic disks





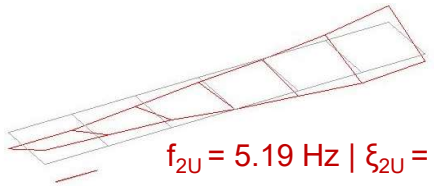
Enhanced Frequency Domain Decomposition method (EFDD)





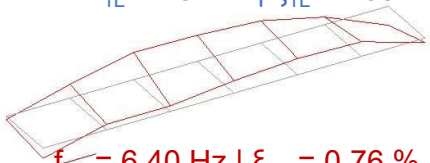
f_{1U} = 3.65Hz | ξ_{1U} = 2.00%

f_{1L} = 1.54Hz | ξ_{1L} = 2.63%



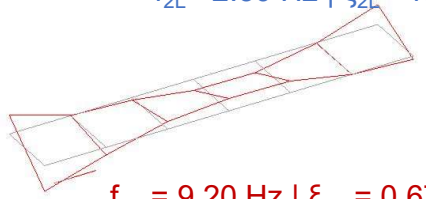
f_{2U} = 5.19 Hz | ξ_{2U} = 1.04 %

f_{2L} = 2.30 Hz | ξ_{2L} = 1.91 %



f_{3U} = 6.40 Hz | ξ_{3U} = 0.76 %

f_{3L} = 3.29 Hz | ξ_{3L} =1.98 %



f_{4U} = 9.20 Hz | ξ_{4U} = 0.67 %

f_{4L} = 4.22 Hz | ξ_{4L} = 0.96 %

4. Anomalies in railway vehicles

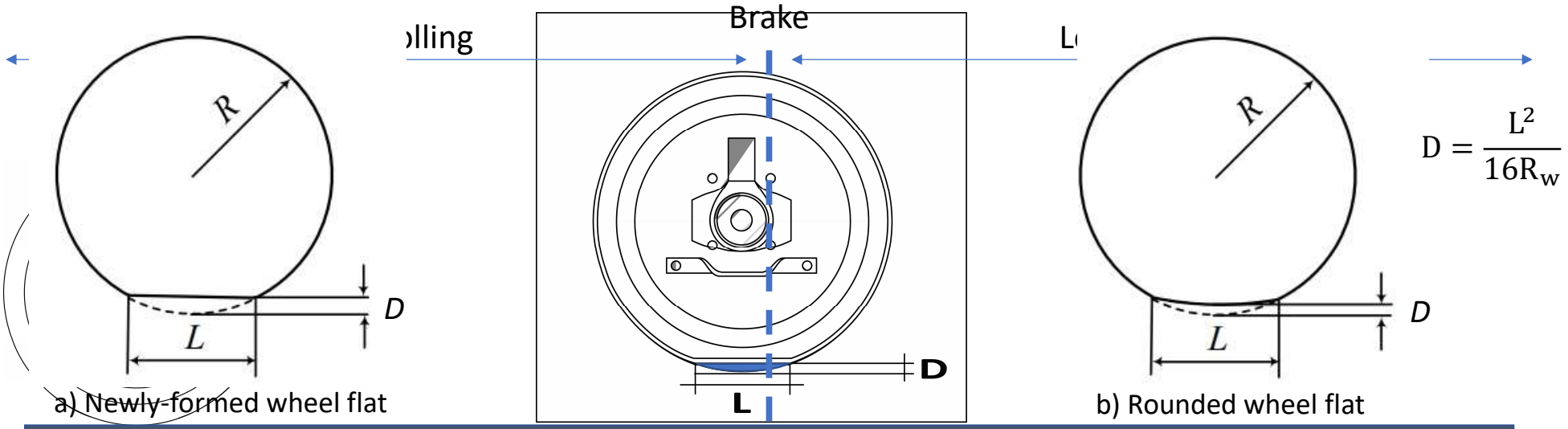
Wheel flat

1) Emergency brake

2) Faulty brakes and wheelset bearings

3) Slip and slide conditions

4) Low wheel-rail adhesion



a) Newly-formed wheel flat

b) Rounded wheel flat

4. Anomalies in railway vehicles

Wheel flat





Classification of the damage

L: Length of the flat (mm)	Severity
10 -20	Low
20 -50	medium
55 - 100	High





4. Anomalies in railway vehicles

Wheel flat

Consequences

1) periodic impact on the wheel-rail contact interface

2) shortening the service life of vehicles and tracks

3) Damage to the infrastructure, namely rail, and sleepers

4) Damage to the train components such as bogies, couplers

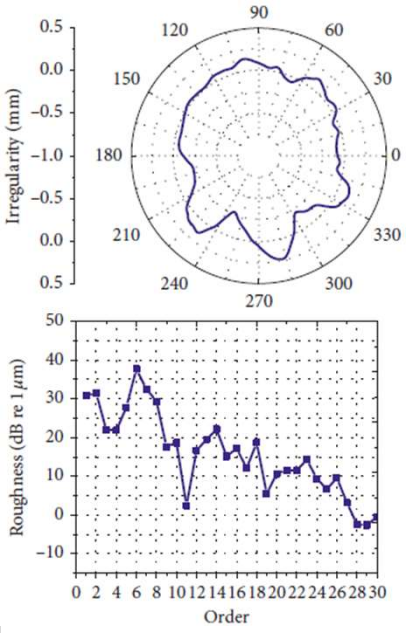
5) generating noise

4. Anomalies in railway vehicles

Polygonization

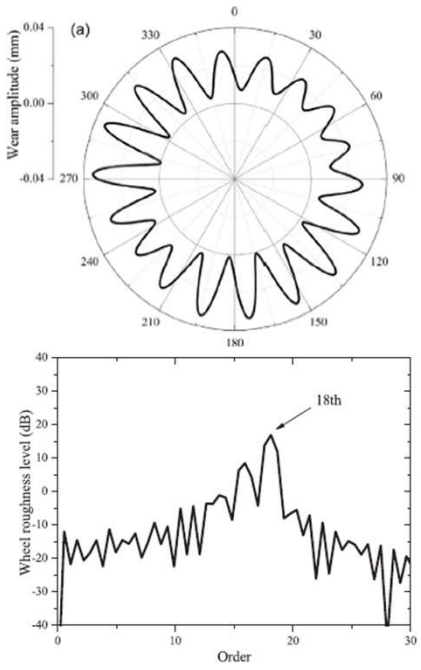
- The **wheel polygonalization** is a periodic radial irregularity or wear around the wheel circumference with wavelength larger than 140 mm and amplitudes > 0.2 mm.

dominant harmonics 6-8



(Cai et al., 2019)

dominant harmonics 18



(Wu et al., 2019)

(Peng, 2020)

Term	Wavelength	Amplitude
Roughness	30-80 mm	10 μm
Polygonization	140 mm-one circle	>0.2 mm



(Bogacz et al., 2016)



(Tao, 2018)

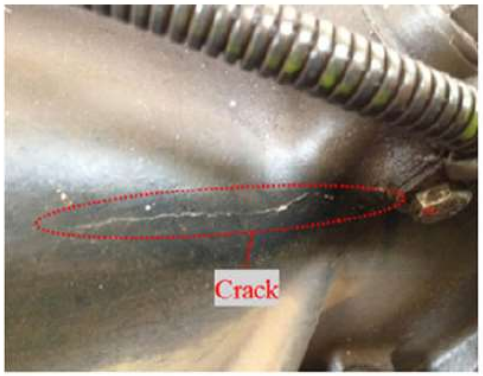


(Wu et al., 2020)

4. Anomalies in railway vehicles

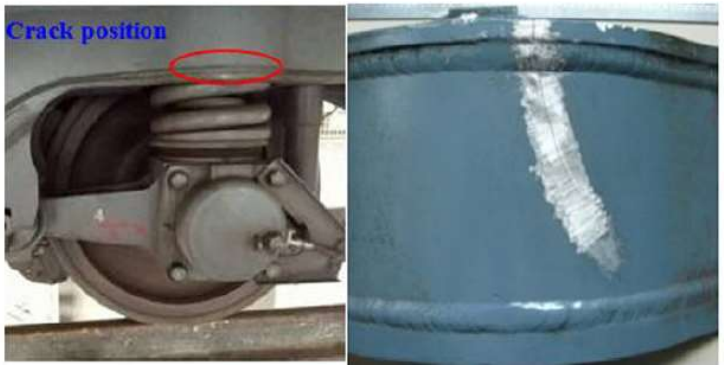
Polygonization



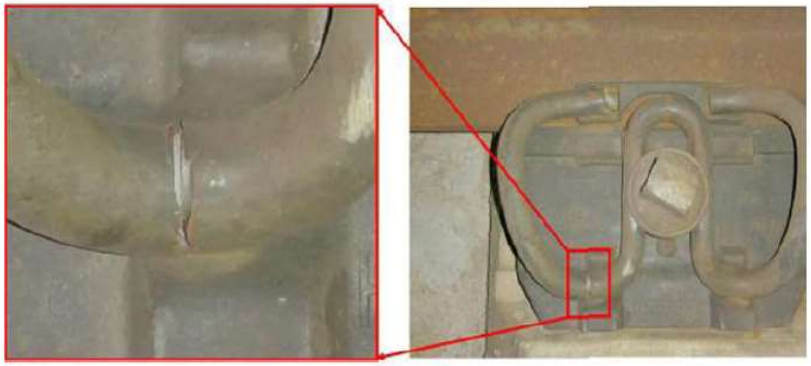












(Tao et al., 2020)

4. Anomalies in railway vehicles

Polygonization

Geometric characterization

$$\lambda = \frac{2\pi R_w}{\theta}, \qquad \theta = 1,2,3 \dots, n$$

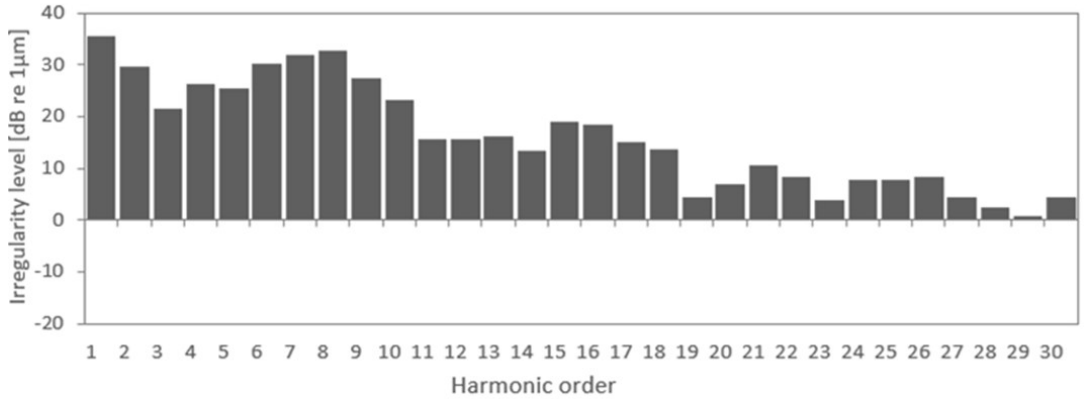
$$A_\theta = \sqrt{2} \cdot 10^{\frac{L_w}{20}} \cdot w_{ref}$$

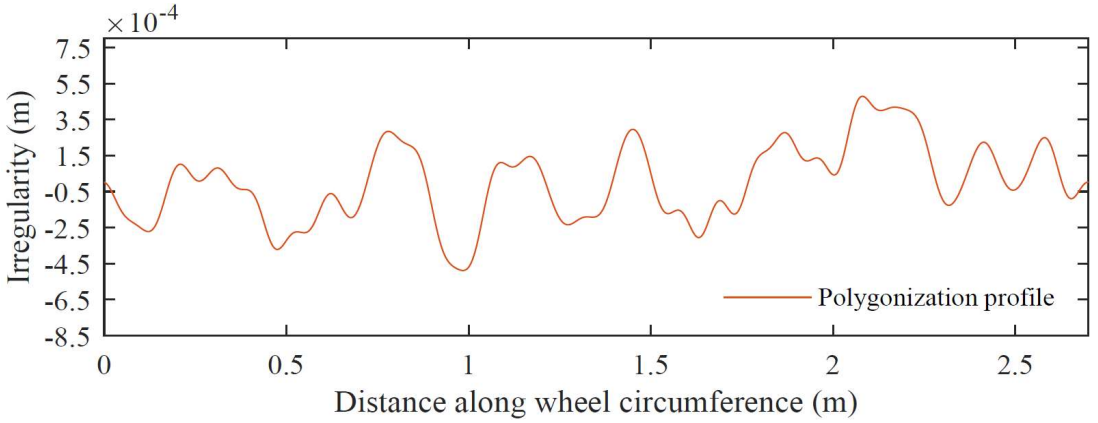
$$w_{ref} = 1\mu m$$

$$w(x_w) = \sum_{\theta=1}^{M} A_\theta \sin\left(\frac{2\pi}{\lambda} x_w + \psi_\theta\right),$$

$w(x_w)$ - irregularity profile;
A_θ- amplitude;
λ - wavelength;
x_w - distance covered by the wheel;
ψ_θ - phase angle.

Pratical example





4. Anomalies in railway vehicles

Unbalanced loads

Loading guidelines of several rail organizations are promulgated to specify the allowed offset values:

Loading Guidelines

Code of practice for the loading and securing of goods on railway wagons

Volume 1

Principles

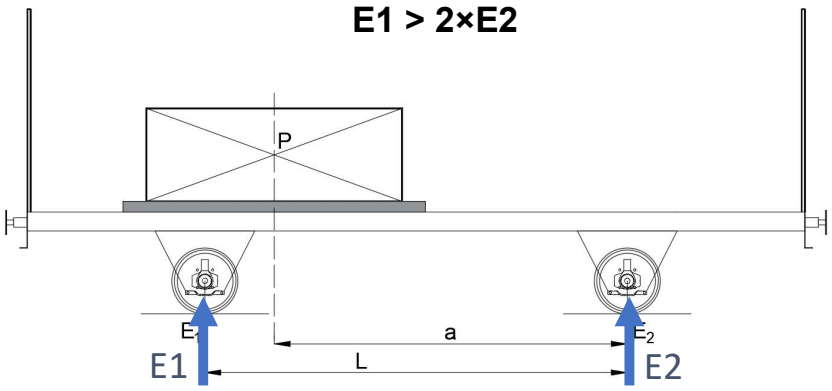
Version 01/04/2022

6th edition

- For **2-axle wagons**: **ratio of 2:1** between the masses per axle;
- For **bogie wagons**: **ratio of 3:1** between the masses per bogie;
- For **all wagons**: **ratio of masses per wheel: 1.25:1**

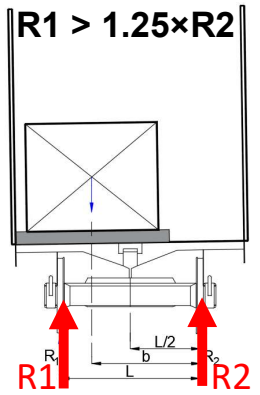
Longitudinal unbalances

E1 > 2×E2



Transversal unbalances

R1 > 1.25×R2



4. Anomalies in railway vehicles

Unbalanced loads

Unbalanced loads is a major factor in the cause of derailments (Rail Accident Investigation Branch (UK))



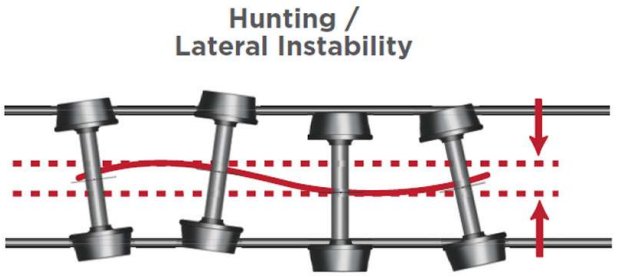






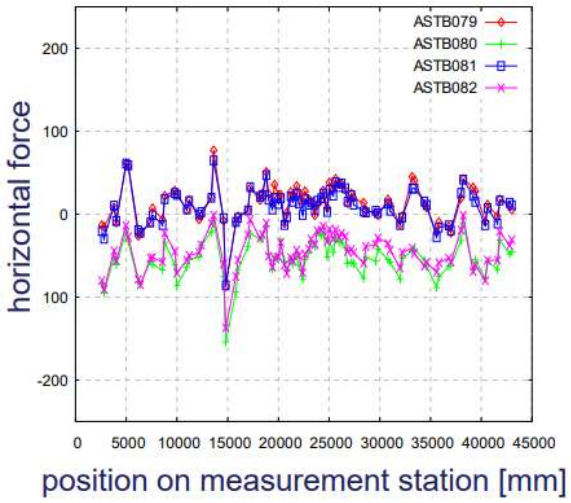
4. Anomalies in railway vehicles

Hunting instability

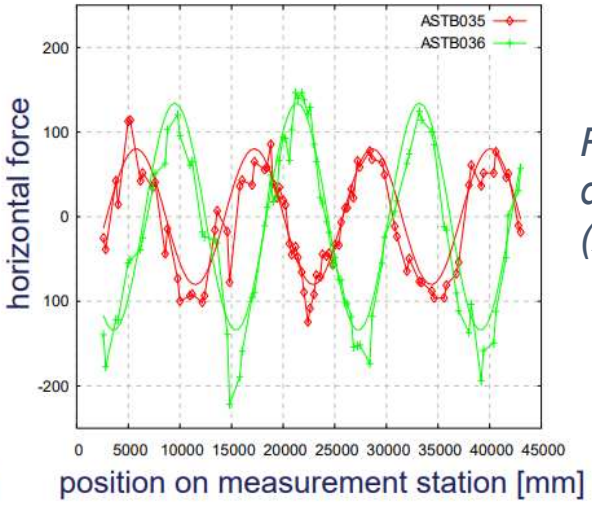


- In railway vehicles, the self-excited lateral oscillations, referred to as **hunting**, begin spontaneously at a threshold speed;
- Above a certain forward speed, called the “Hunting critical speed”, hunting appears as an undamped motion of the wheelset constrained by the wheel flange and the rail;

stochastic



resonance



Results from hunting detector system (ARGOS system)

4. Anomalies in railway vehicles

Hunting instability



References

- Diogo Ribeiro (2012) – "Efeitos Dinâmicos Induzidos por Tráfego em Pontes Ferroviárias: Modelação Numérica, Calibração e Validação Experimental", Dissertação para a obtenção do grau de Doutor em Estruturas de Engenharia Civil, Faculdade de Engenharia da Universidade do Porto, Porto.

- Carlbom, P. - Carbody and passengers in rail vehicle dynamics. Doctoral Thesis, 2000, Department of Vehicle Engineering, KTH - Royal Institute of Technology. Stockholm, Sweden.

- ISO 2631-1 - Mechanical vibration and shock - evaluation of human exposure to whole-body vibration - Part 1: General requirements. Geneva, Switzerland: ISO, 1997.

- Iwnicki, S. - Handbook of railway vehicle dynamics, 2006. London: CRC Press.

- D. Ribeiro, R. Calçada, R. Delgado, M. Brehm, V. Zabel (2013) - "Finite element model updating of a railway vehicle based on experimental modal parameters", Vehicle System Dynamics, Taylor & Francis, 51(6):821-856. DOI: 10.1080/00423114.2013.778416.

- P. Silva, D. Ribeiro, J. Mendes, E. Seabra (2023) – “Modal Identification of Train Passenger Seats Based on Dynamic Tests and Output-Only Techniques”, Applied Sciences, 13(4):2277. DOI: 10.3390/app13042277.

References

- C. Bragança, J. Neto, P.A. Montenegro, D. Ribeiro, H. Carvalho, R. Calçada (2022) - “Calibration and validation of a freight wagon dynamic model in operating conditions and limited experimental data”, Vehicle System Dynamics, 60(9):3024-3050, DOI: 10.1080/00423114.2021.1933091.

- R. Silva, D. Ribeiro, C. Bragança, C. Costa, A. Arêde, R. Calçada (2021) – “Model updating of a freight wagon based on dynamic tests under different loading scenarios”, Applied Sciences, 11(22):10691. DOI: 10.3390/app112210691.

- M. Mohammadi, A. Mosleh, C. Vale, D. Ribeiro, P. Montenegro, A. Meixedo, R. Calçada (2023) – “An Unsupervised Learning Approach for Wayside Train Wheel Flat Detection”. Sensors, 23(4):1910. DOI: 10.3390/s23041910.

- A. Guedes, R. Silva, D. Ribeiro, C. Vale, A. Mosleh, P. Montenegro, A. Meixedo (2023) – “Detection of Wheel Polygonization Based on Wayside Monitoring and Artificial Intelligence”, Sensors, 23(4):2188. DOI: 10.3390/s23042188.

- Cai, W., M. Chi, G. Tao, X. Wu, and Z. Wen, Experimental and Numerical Investigation into Formation of Metro Wheel Polygonalization. Shock and Vibration, 2019. 2019: p. 1538273.

References

- Wu, X., S. Rakheja, W. Cai, M. Chi, A.K.W. Ahmed, and S. Qu, A study of formation of high order wheel polygonalization. Wear, 2019. 424-425: p. 1-14.
- Bogacz R, Frischmuth K. On dynamic effects of wheel–rail interaction in the case of Polygonalisation. Mech Syst Signal Process 2016;79:166–73.
- Peng, B., Mechanisms of Railway Wheel Polygonization. 2020, University of Huddersfield.
- Tao G. Investigation into the formation mechanism of the polygonal wear of HXD electric locomotive wheels [PhD thesis]: Southwest Jiaotong University; 2018.
- Wu, Y., X. Jin, W. Cai, J. Han, and X. Xiao, Key Factors of the Initiation and Development of Polygonal Wear in the Wheels of a High-Speed Train. Applied Sciences, 2020. 10(17): p. 5880.
- Ngigi, R.W., C. Pislaru, A. Ball, and F. Gu, Modern techniques for condition monitoring of railway vehicle dynamics. Journal of Physics: Conference Series, 2012. 364(1): p. 012016.
- Tao, G., Z. Wen, X. Jin, and X. Yang, Polygonisation of railway wheels: a critical review. Railway Engineering Science, 2020. 28(4): p. 317-345.

References

- UIC. Code of Practice for the Loading and Securing of Goods on Railway Wagons; UIC: Paris, France, 2022.
- R. Silva, A. Guedes, D. Ribeiro, C. Vale, A. Meixedo, A. Mosleh, P. Montenegro (2023) - “Early Identification of Unbalanced Freight Traffic Loads Based on Wayside Monitoring and Artificial Intelligence”, Sensors, 23(3):1544. DOI: 10.3390/s23031544.

Monitoring systems

Araliya Mosleh [FEUP]

Contents

1. Introduction
2. Description of monitoring systems
3. Description of the data acquisition system
4. Signal output

1. Introduction

Wheel/rail defects on railway vehicles are documented as a critical source of damage to railway infrastructure.

The presence of geometric defects in the wheels/rails increases:

- Increase Dynamic train-track interaction
- Generate high levels of noise and excessive vibration
- Decrease safety and stability of train
- Increase derailment





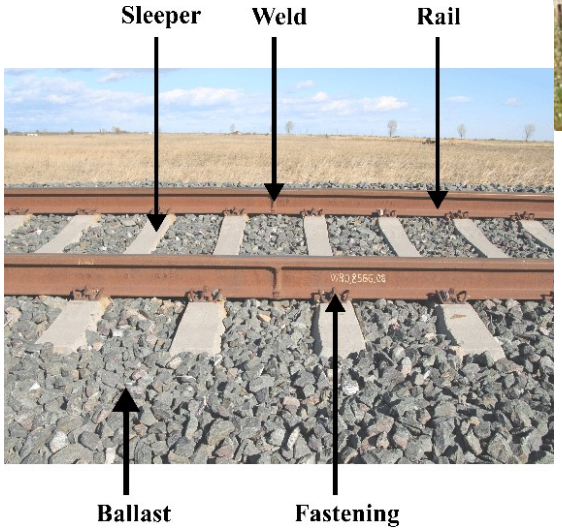




In order to ensure safety and stability, and to minimize maintenance costs, it is recommended to identify damage (wheels/rails) at an early stage.

2. Monitoring systems

On-board condition monitoring system



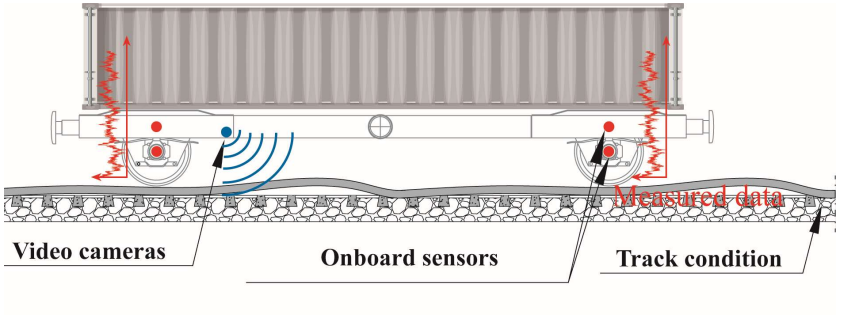


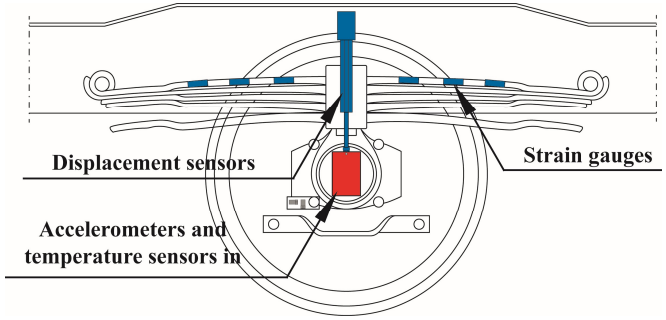
On-board condition monitoring

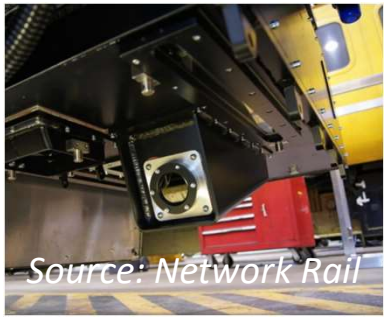
2. Monitoring systems

On-board condition monitoring system

- The objective of an onboard monitoring system is to allow the evaluation of the condition of the vehicle itself, but also from the infrastructure in which the vehicle is running on.
- The vehicle may be instrumented with several kind of sensors, depending on the functions for which the system has been designed for.
- Examples of sensors installed in the vehicle are: accelerometers, inclinometers, displacement sensors (LVDTs), strain gauges, temperature sensors, etc. The vehicle may also contain video-cameras to inspect the track.





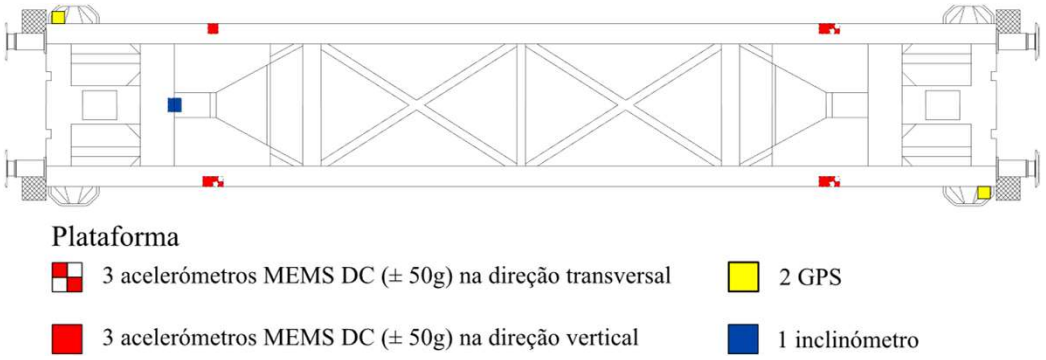


2. Monitoring systems

On-board condition monitoring system

Example of an onboard monitoring system installed in a MEDWAY wagon

Platform instrumentation with accelerometers and inclinometers







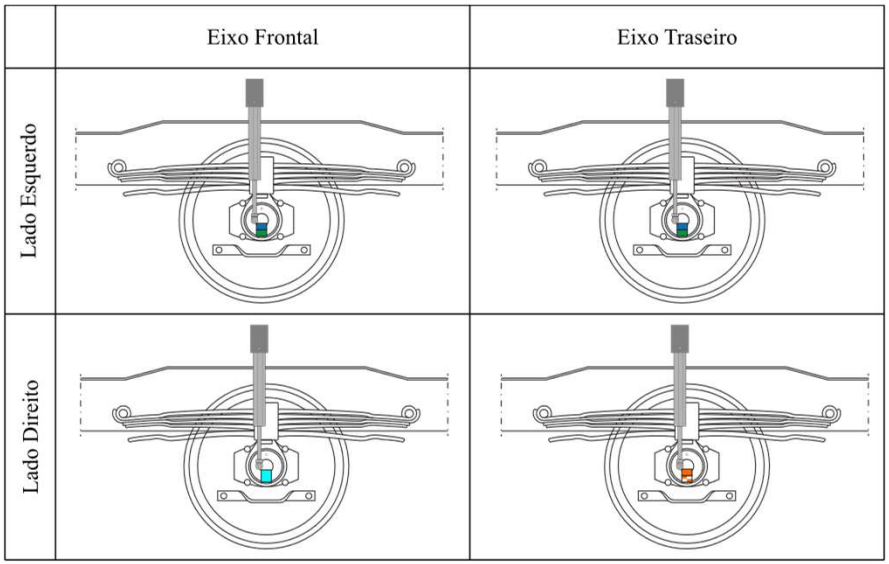


2. Monitoring systems

On-board condition monitoring system

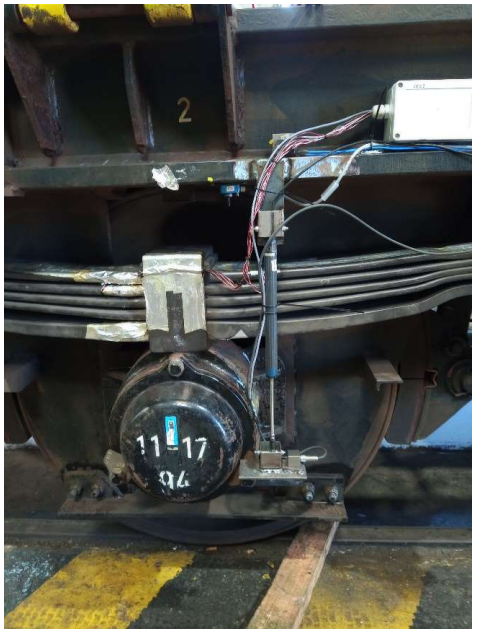
Example of an onboard monitoring system installed in a MEDWAY wagon

Axle boxes instrumentation with accelerometers



Eixos

- 1 acelerómetro MEMS DC (±200 g) triaxial
- 2 acelerómetros (±500 g) na direção vertical
- 1 acelerómetro MEMS DC (±200 g) na direção vertical
- 1 acelerómetro MEMS DC (±200 g) na direção transversal





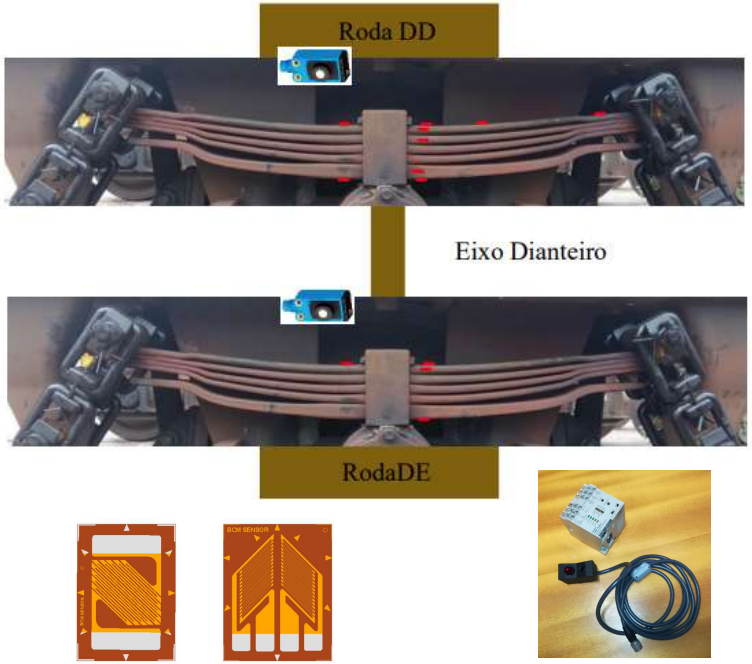


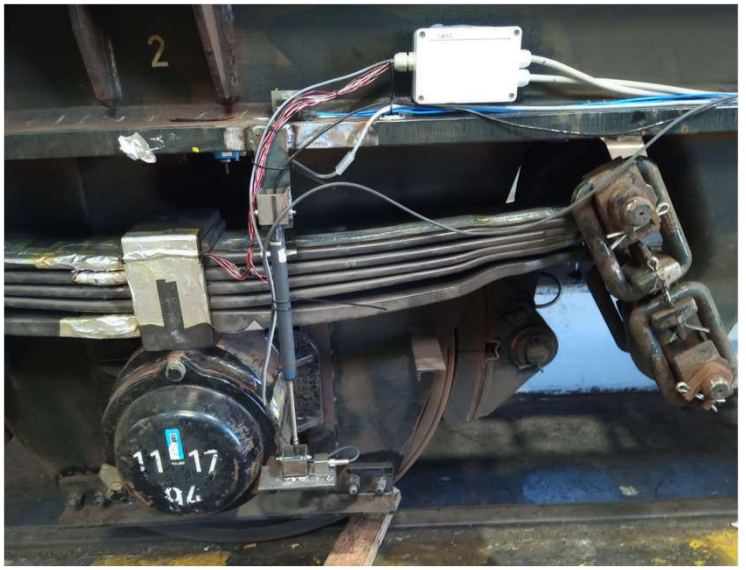
2. Monitoring systems

On-board condition monitoring system

Example of an onboard monitoring system installed in a MEDWAY wagon

Suspensions instrumentation with strain gauges, LVDTs and contactless displacement sensors



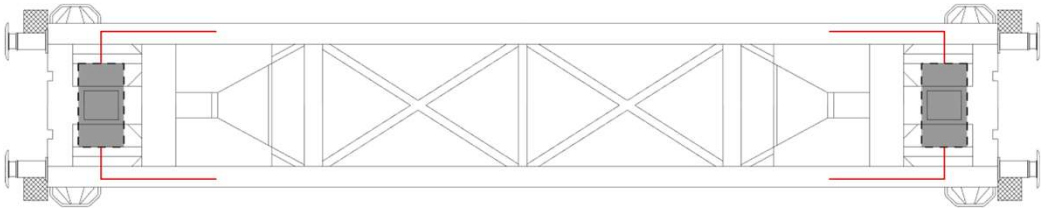


2. Monitoring systems

On-board condition monitoring system

Example of an onboard monitoring system installed in a MEDWAY wagon

Acquisition system and batteries



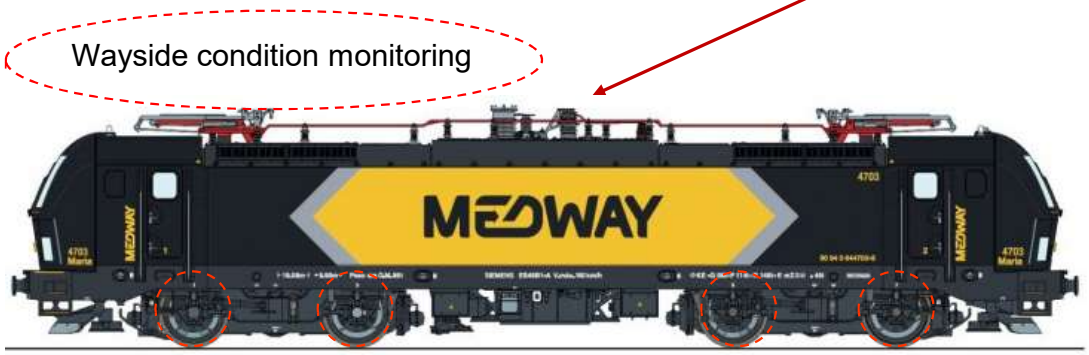




2. Monitoring systems

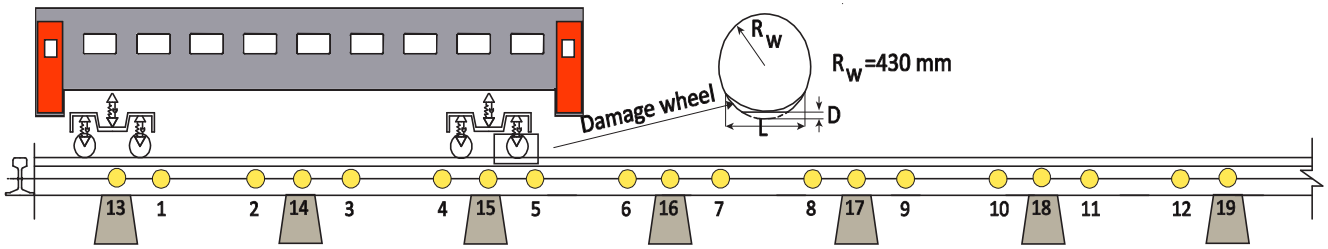
Wayside condition monitoring system



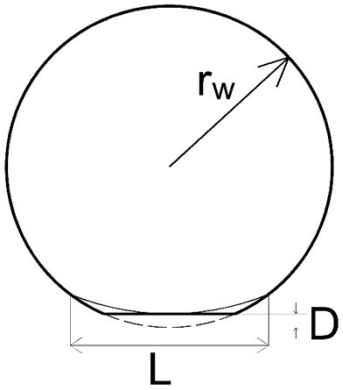


2. Monitoring systems

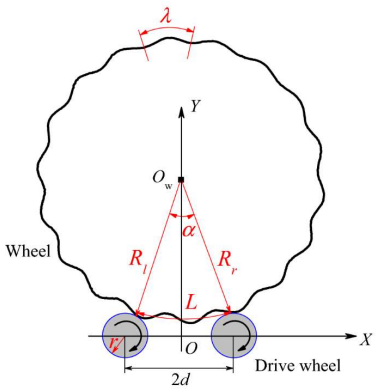
Wayside condition monitoring system







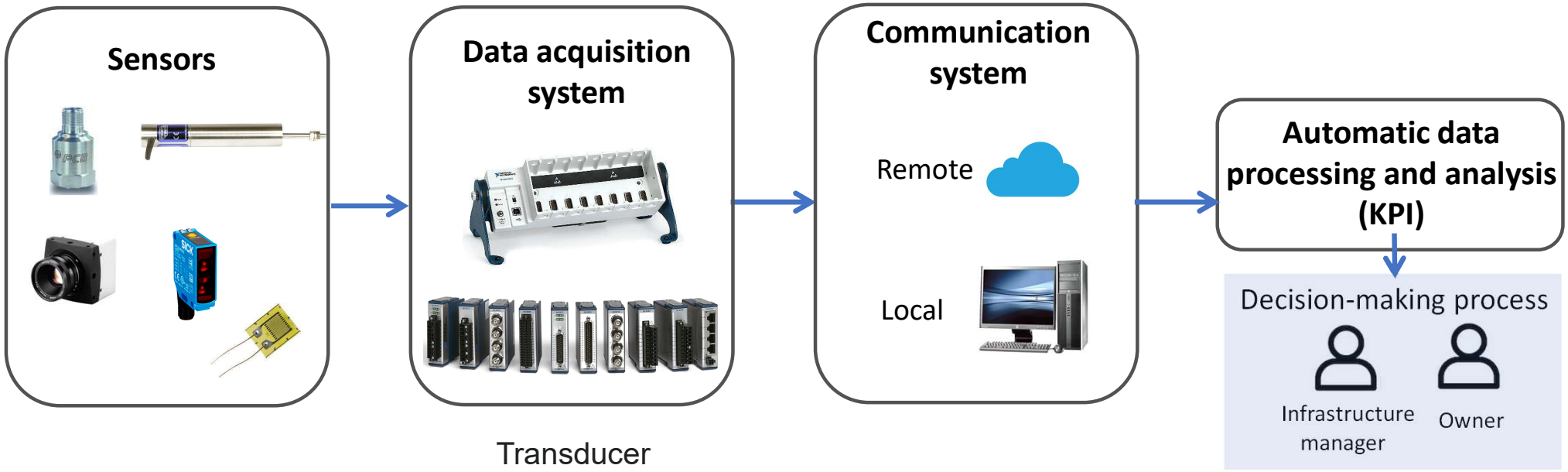
Wheel flat





Wheel with polygonalisation

3. Acquisition system



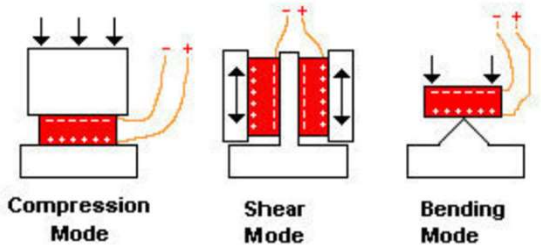
3. Acquisition system

Sensors

Accelerometers - piezoelectric

- **Piezoelectric accelerometers** are based on the property that some crystals have (e.g. quartz), when subjected to a deformation, generate electric charges (**in Volts**) proportional to that deformation.

- The principle of operation is based on three fundamental designs where the crystal (in red) is in **Compression Mode, Shear Mode, or Bending Mode**.



- **Uniaxial** and **triaxial** configurations.

- **Advantages**: high-frequency response, small sized.

- **Disadvantages**: high impedance, low output range (in Volt), limitations in measuring movements with very low frequency and small amplitude components.



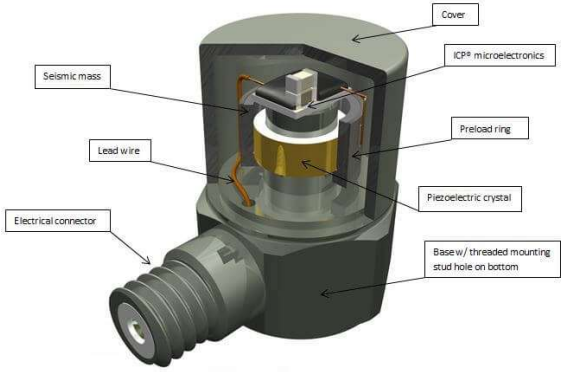


Figure 1: Typical ICP® Accelerometer

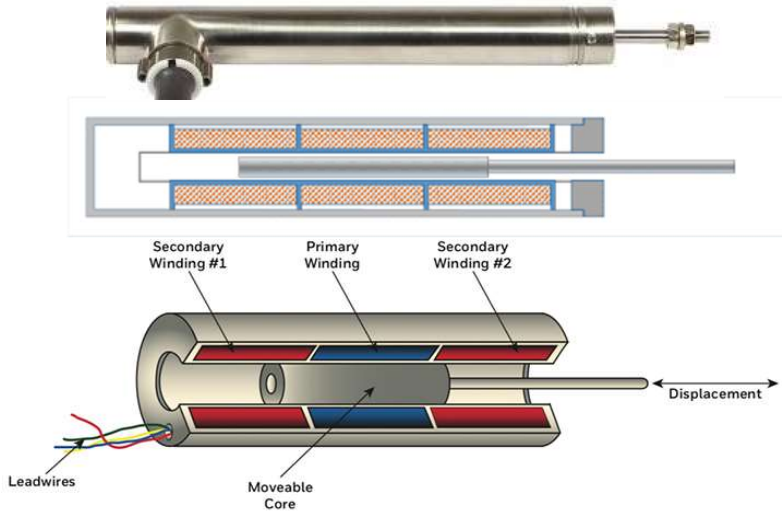
3. Acquisition system

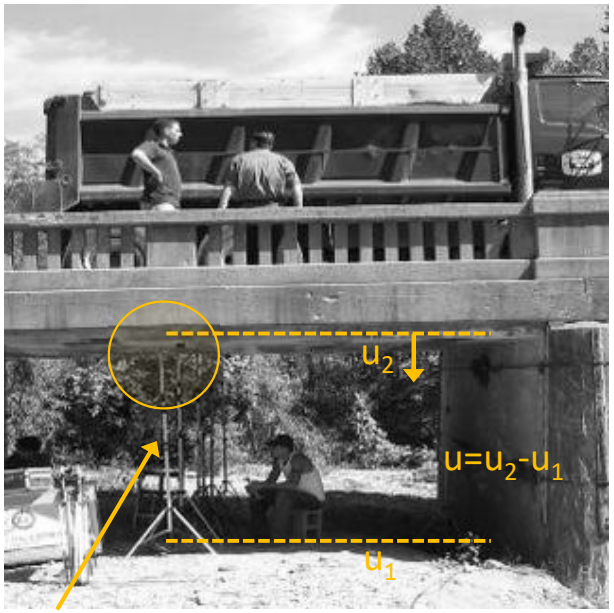
Sensors

Displacement transducers – LVDT

- Typically, in railway bridges, LVDT (Linear Variable Differential Transformer) measures the **relative displacement** between the structure and a reference point (typically the ground).

- The transducer is an electromechanical device which produces an electrical output signal (Volt) proportional to the displacement of its moving part – ferromagnetic core.





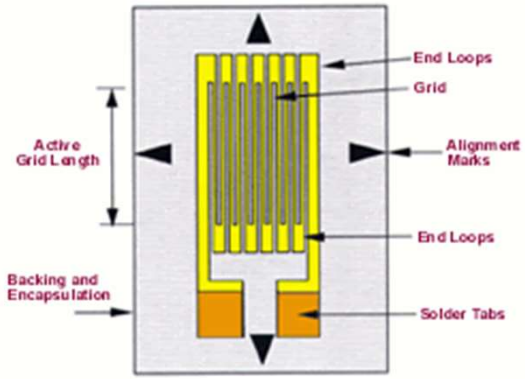
3. Acquisition system

Sensors

Strain gauges

- An electrical resistance strain gauge is a piece of conductor/semiconductor whose **resistance (R) varies directly with the deformation (e)** it is subjected to.

- A strain gauge is a thin and laminated device that can be attached to a variety of materials to measure the applied strain.



Mechanical strain

$$\varepsilon = \frac{\Delta L}{L}$$

→ **Strain gauge** →

Electrical strain

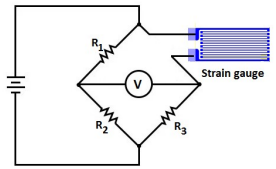
$$\frac{\Delta R}{R} = GF\frac{\Delta L}{L}$$

Gauge Factor

→ **Wheatstone bridge** →

Electrical output

$$\Delta V \infty \frac{\Delta R}{R}$$

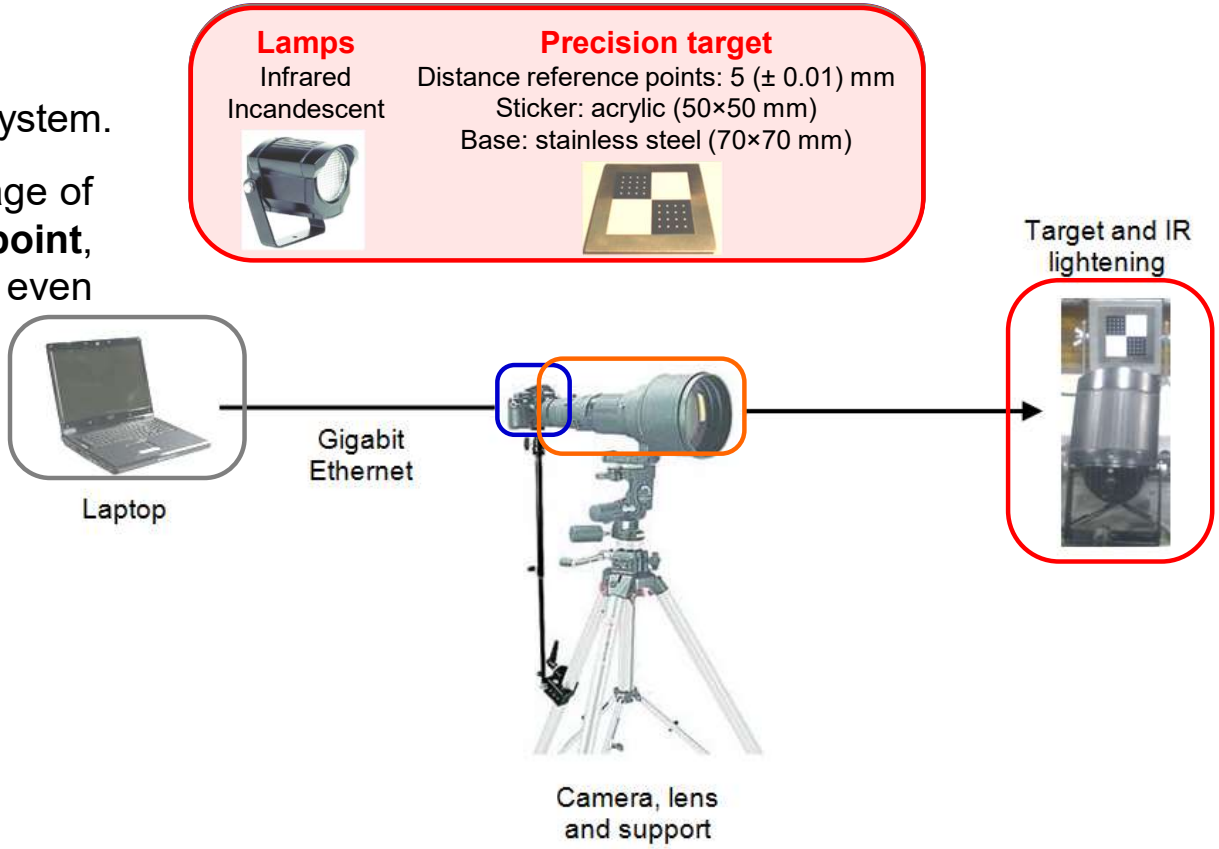


3. Acquisition system

Sensors

Video camera

- **Non-contact** displacement measurement system.
- The non-contact systems have the advantage of being **independent on a reference point**, which in many situations is difficult, or even impossible, to materialize.



3. Acquisition system

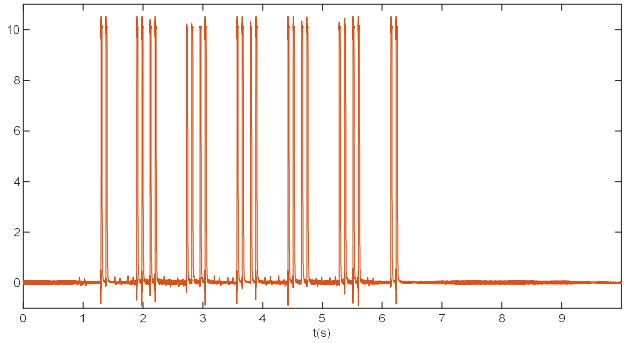
Sensors

Laser

- Precise axle detection and speed estimation.
- Located on the entrance and exit sections of the bridge on track side.
- Laser emitter and receptor (separate components).





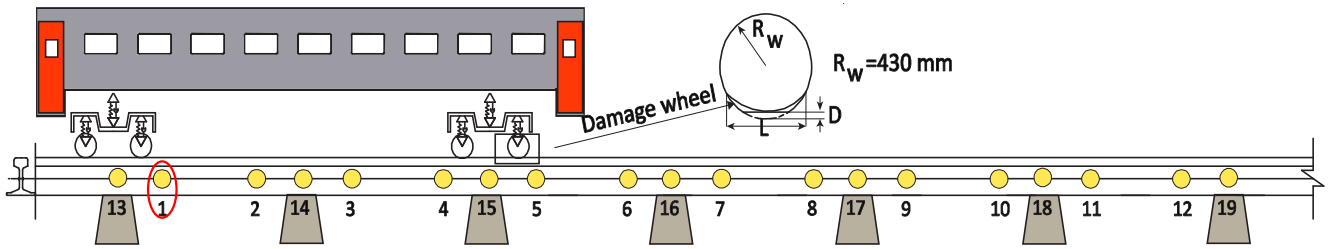


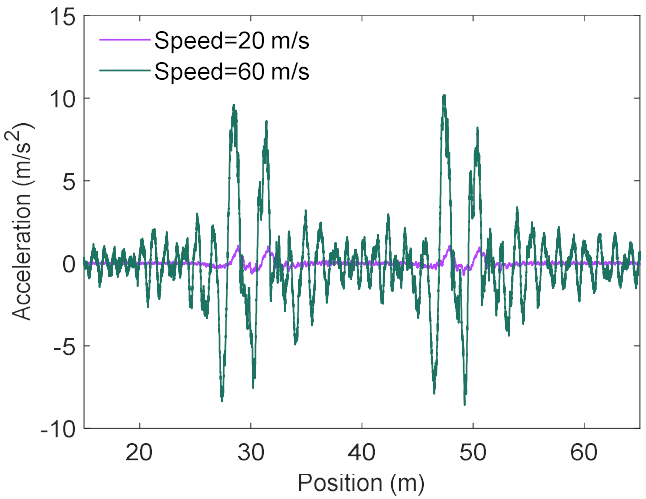
Laser sensor output during a train passage



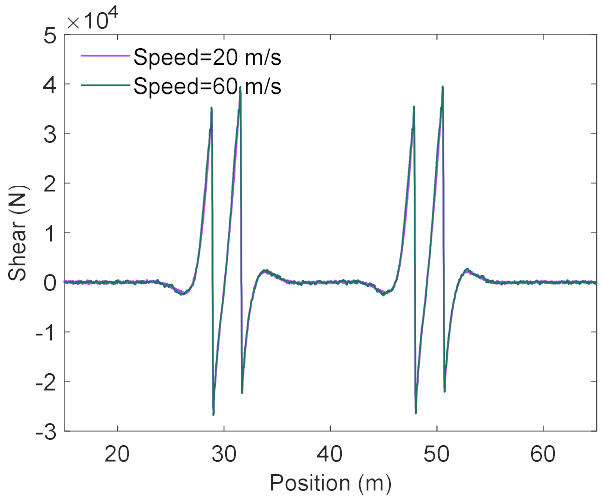
3. Acquisition system

Sensors





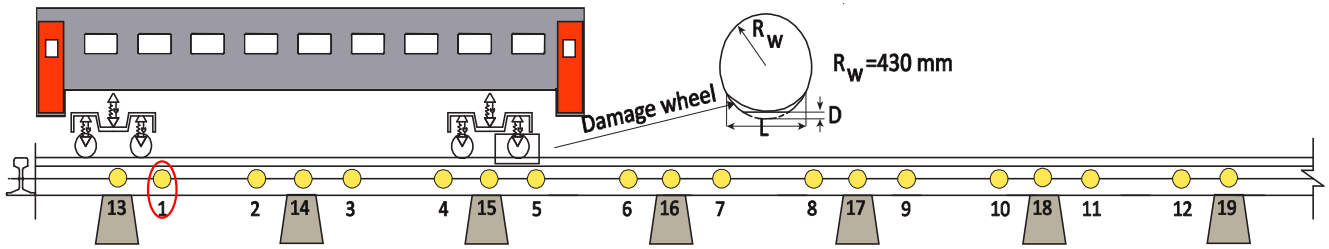
Acceleration

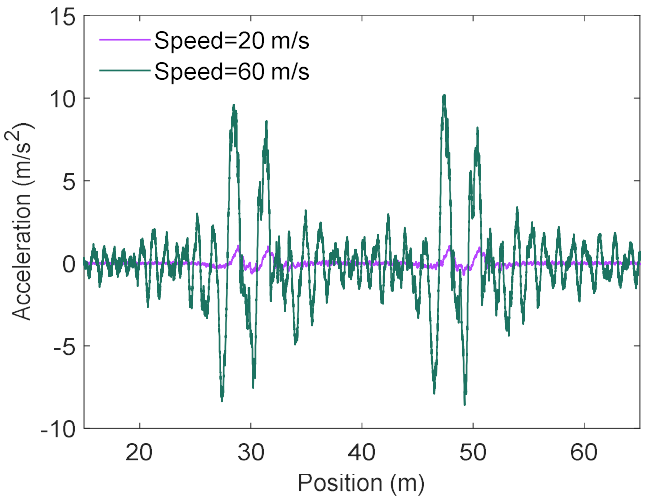


Strain gauge

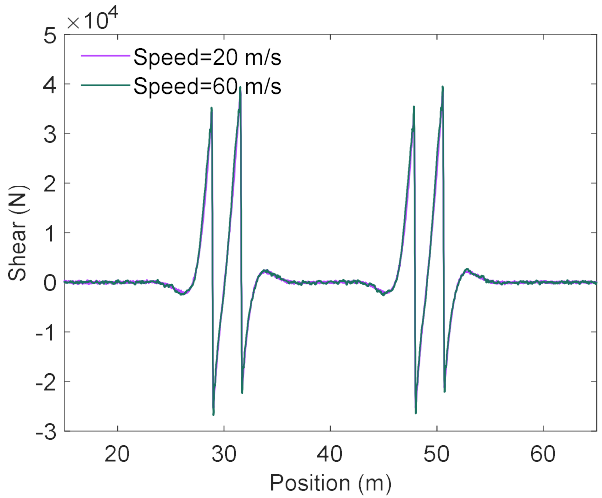
4. Signal output wayside monitoring system – Alfa Pendular

Undamaged wheel





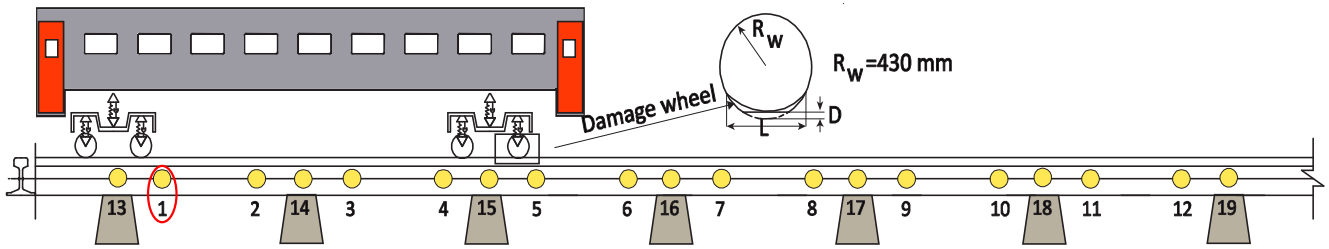
Acceleration

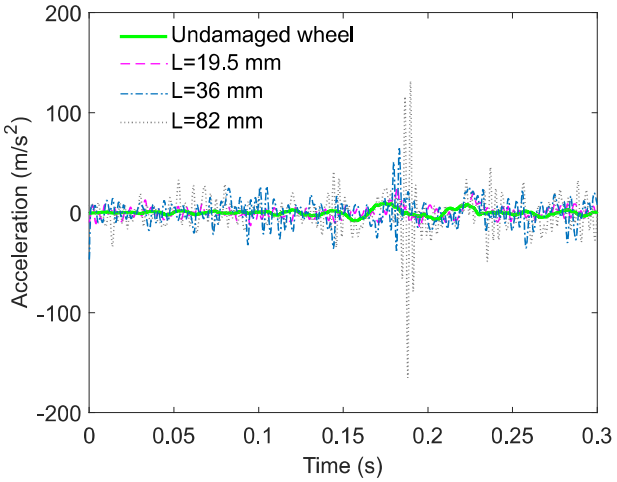


Strain gauge

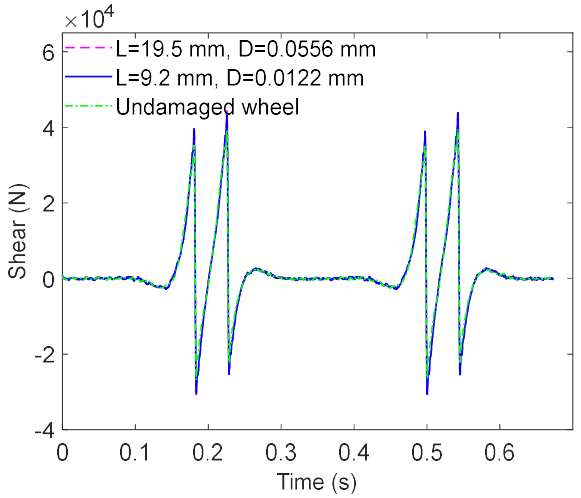
4. Signal output wayside monitoring system – Alfa Pendular

Damaged wheel





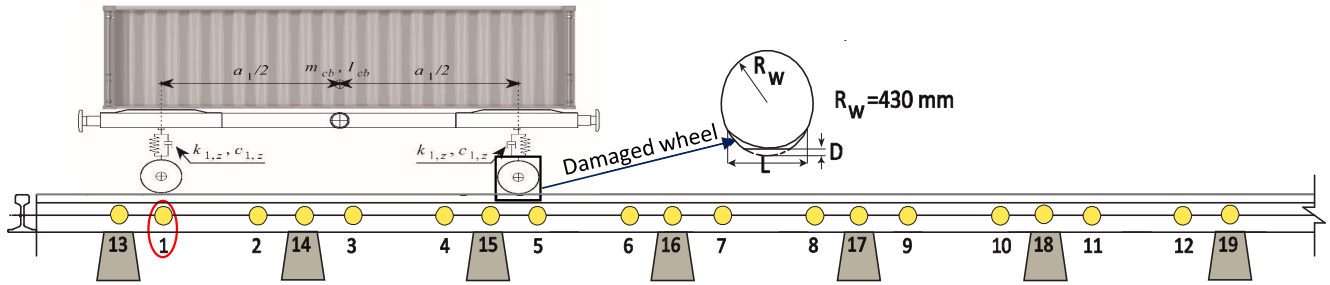
Acceleration

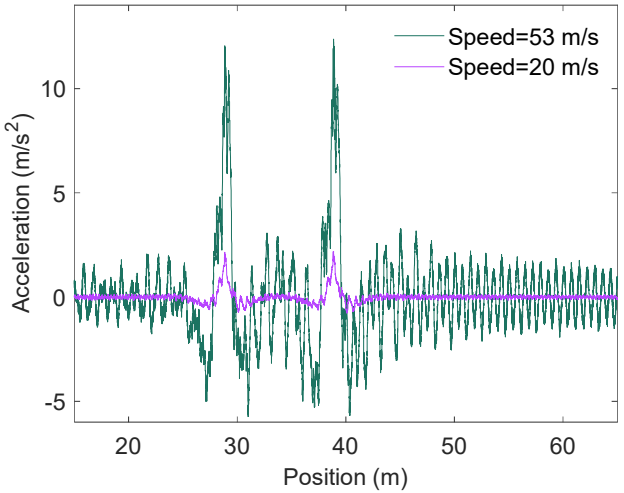


Strain gauge

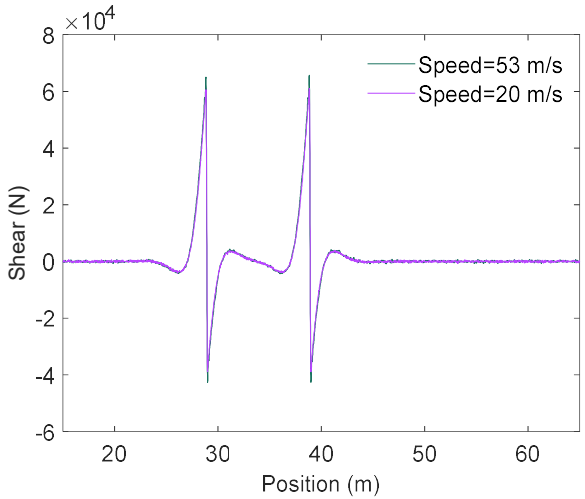
4. Signal output wayside monitoring system – Freight wagon

Undamaged wheel





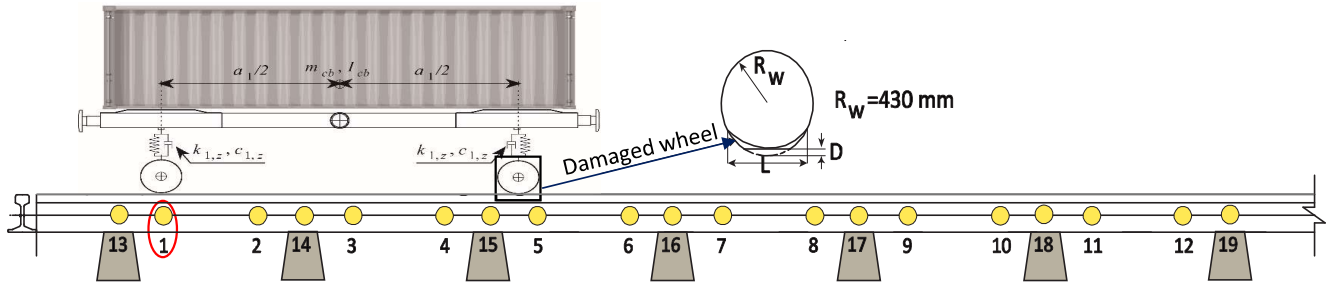
Acceleration

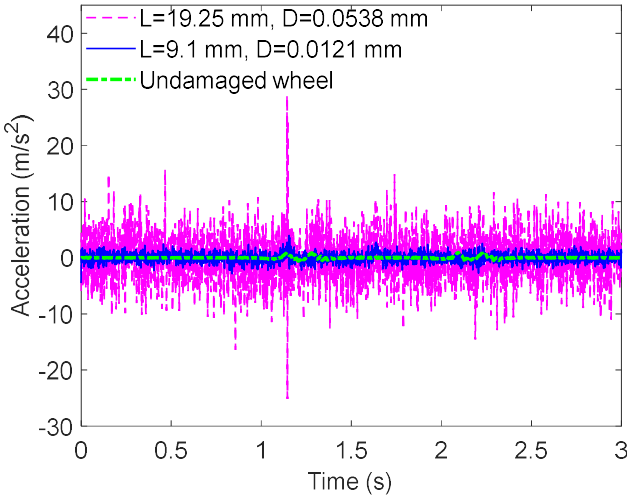


Strain gauge

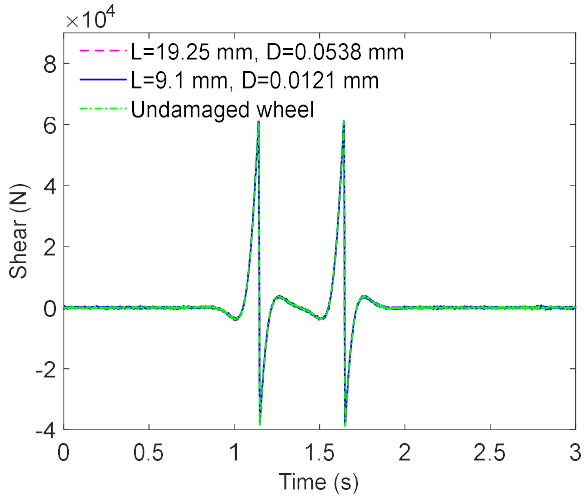
4. Signal output wayside monitoring system – Freight wagon

Damaged wheel





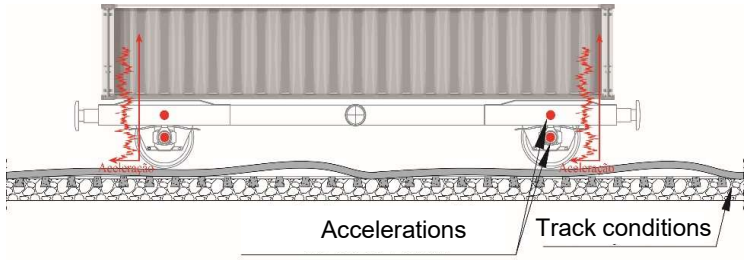
Acceleration

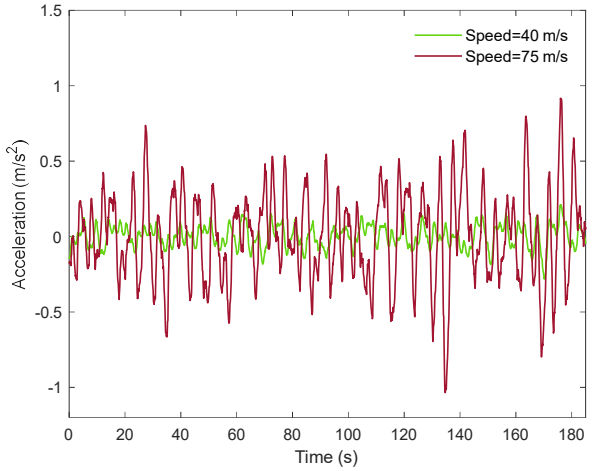


Strain gauge

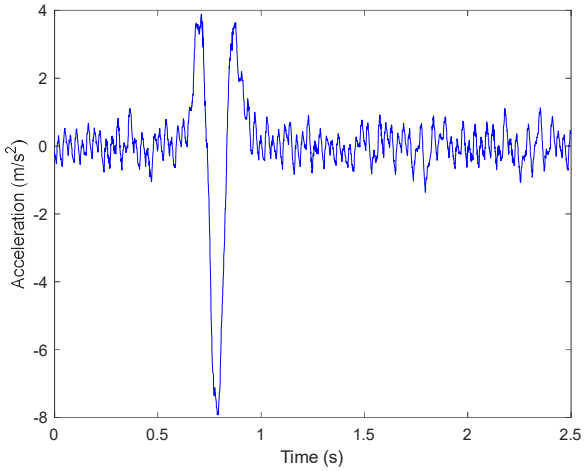
4. Signal output onboard monitoring system – Freight wagon

Damaged and undamaged rail





Acceleration- Undamaged rail



Acceleration- Damaged rail

References

- Mosleh, A., Montenegro, P. Costa, P. Calcada, R., An approach for wheel flat detection of railway train wheels using envelope spectrum analysis. Structure and Infrastructure Engineering, 2021, 17(12): p. 1710-1729, 10.1080/15732479.2020.1832536.

- Wang, Y.W., Y.Q. Ni, Wang, X., Real-time defect detection of high-speed train wheels by using Bayesian forecasting and dynamic model, Mechanical Systems and Signal Processing, 2020. 139: p. 106654, 10.1016/j.ymssp.2020.106654

- Gonçalves, V., Mosleh, A., Vale, C., Montenegro, P., Wheel Out-of-Roundness Detection Using an Envelope Spectrum Analysis, Sensors, 2023, 23 (4):p. 2138, 10.3390/s23042138

- Sun, Q., Chen, C., Kemp, A.H., Brooks, P., An on-board detection framework for polygon wear of railway wheel based on vibration acceleration of axle-box, Mechanical Systems and Signal Processing. 2021,153: p. 107540, 10.1016/j.ymssp.2020.107540

- Mohammadi, M., Mosleh, A., Vale, C., Ribeiro, D., Montenegro, P., Meixedo, A., An Unsupervised Learning Approach for Wayside Train Wheel Flat Detection, Sensors, 2023, 23 (4): p. 1910, 10.3390/s23041910

References

- Mosleh, A., Montenegro, P. Costa, P. Calcada, R., An approach for wheel flat detection of railway train wheels using envelope spectrum analysis. Structure and Infrastructure Engineering, 2021, 17(12): p. 1710-1729, 10.1080/15732479.2020.1832536.

- Krummenacher, G., Soon Ong, C., Koller, S., Kobayashi, S., Buhmann, J., Wheel Defect Detection With Machine Learning, IEEE TRANSACTIONS ON INTELLIGENT TRANSPORTATION SYSTEMS, 2018, 19(4):p. 1176 - 1187, 10.1109/TITS.2017.2720721

- MEDWAY, https://www.medway-iberia.com/pt/pages/transporte-ferroviario-de-mercadorias-multi-modal, accessed in February 2023

- Guedes, A., Silva, R., Ribeiro, R., Vale, C., Mosleh, A., Montenegro, P., Meixedo, Detection of Wheel Polygonization Based on Wayside Monitoring and Artificial Intelligence, Sensors, 2023, 23(4): p. 2188. 10.3390/s23042188.

- Mosleh, A., Meixedo, A., Ribeiro, D., Montenegro, P., Calçada, R., Automatic clustering-based approach for train wheels condition monitoring, International Journal of Rail Transportation, 2022, 10.1080/23248378.2022.2096132

References

- Mosleh, A., Meixedo, A., Ribeiro, D. Montenegro, P. Calcada, R. , Early wheel flat detection: an automatic data-driven wavelet-based approach for railways. Vehicle System Dynamics, 2023, 61(6), 10.1080/00423114.2022.2103436.

- Sun, X., Yang, F., Shi, J., Ke, Z., Zhou, Y., On-Board Detection of Longitudinal Track Irregularity Via Axle Box Acceleration in HSR, IEEEAccess, 2021, 9, :p. 14025 - 14037, 10.1109/ACCESS.2021.3052099

Vehicle-track dynamic interaction
Theoretical background and applications

Pedro Montenegro [FEUP]

Contents

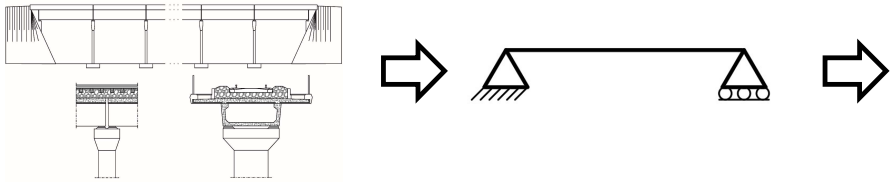
1. Introduction
2. Types of vehicle-track interaction models
3. Formulation of the vehicle-track interaction problem
4. Applications

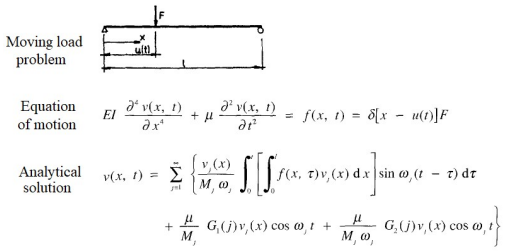
1. Introduction

Methodologies to solve the vehicle-structure dynamic system

The following methodologies can be used to study the vehicle-structure dynamic behavior:

- *Analytical methodologies*

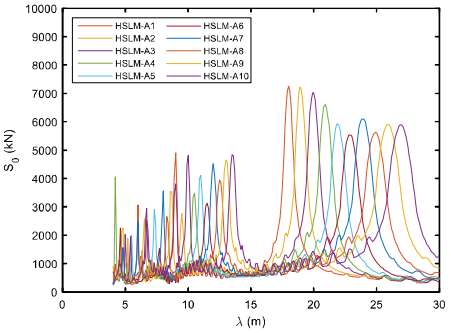




- *Simplified methodologies*

There are two main simplified methodologies developed by the ERRI D214, namely the **Decomposition of Excitation at Resonance (DER method)** and the **Dynamic Residual Influence Line (LIR method)**, both based in the concept of **Train Signature**. The Train Signature represents, the effects of the train in the whole dynamic response.

$$\ddot{y} \le \left(\frac{8\pi f_0^2}{K}\right)\left|\frac{\cos\left(\frac{\pi L}{\lambda}\right)}{\left(\frac{2L}{\lambda}\right)^2-1}\right|\frac{L}{\xi(L+x_{N-1})}\left(\sqrt{\left(\sum_{k=0}^{N-1}P_K\cos\left(\frac{2\pi x_k}{\lambda}\right)\right)^2+\left(\sum_{k=0}^{N-1}P_K sen\left(\frac{2\pi x_k}{\lambda}\right)\right)^2}\right)\left(1-e^{-2\pi\xi\frac{x_{N-1}+L}{\lambda}}\right)$$



1. Introduction

Methodologies to solve the vehicle-structure dynamic system

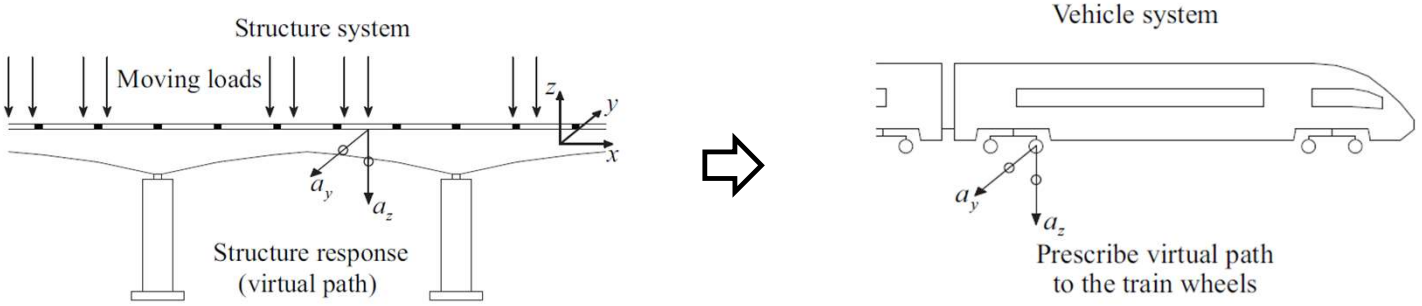
The following methodologies can be used to study the vehicle-structure dynamic behavior:

- *Numerical methodologies based on moving loads*

  The moving loads model assumes that the vehicle's action over the structure may be defined by means of moving loads of fixed magnitude that represent the static load of each wheel or wheelset.

- *Numerical methodologies based on virtual paths*[a]

  First, the virtual path for the vehicle, i.e., the dynamic response of the structure subjected to the action of the vehicle described by a moving load model, is computed. Then, these displacements are prescribed to the wheels of the vehicle to obtain its uncoupled response. Unlike the moving load model, this method allows the calculation, though simplified, of the response of the vehicle, but does not consider the interaction between the two-subsystems.



[a] (Goicolea and Antolín, 2011)

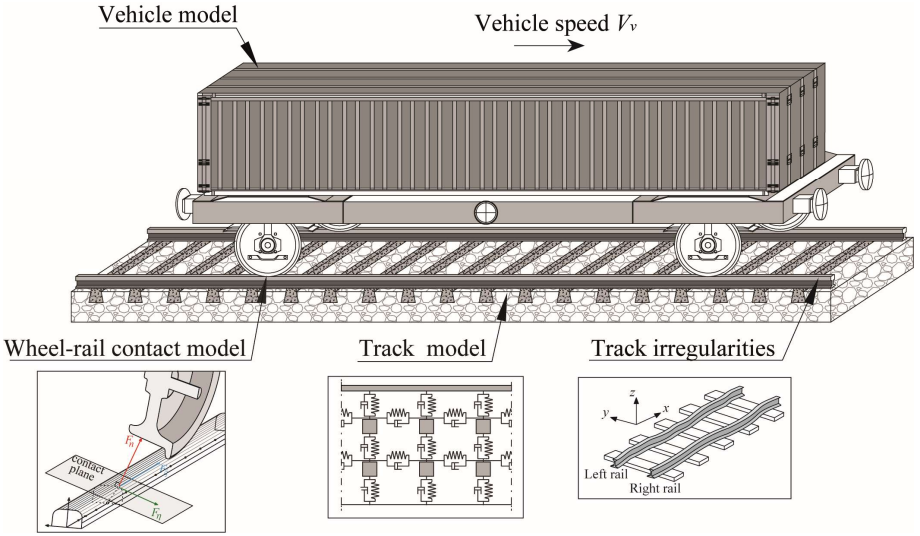
1. Introduction

Methodologies to solve the vehicle-structure dynamic system

The following methodologies can be used to study the vehicle-structure dynamic behavior:

- *Numerical methodologies considering the vehicle-structure interaction*

  Although separated, the vehicle and track/structure form a single system that interact with each other through the contact mechanism that occurs between the wheel and rails. The methodologies that consider the dynamic interaction between these two sub-systems are the most realistic ones, since they can capture the coupled responses from both. The vehicle-structure interaction models are more complex and computationally demanding than the previous ones.

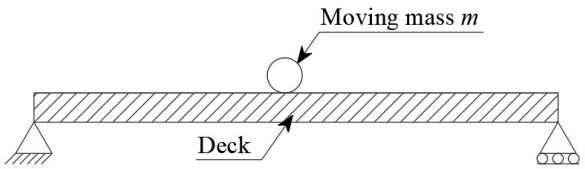


2. Types of vehicle-track interaction models

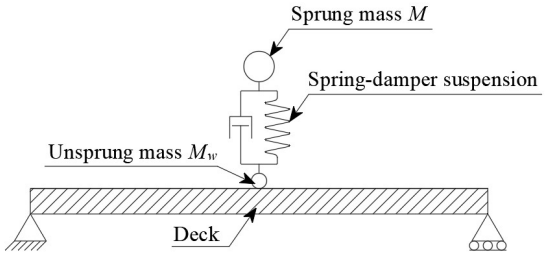
Levels of complexity of the vehicle-structure interaction models

The vehicle-structure interaction models may vary in terms of complexity. The following complexity levels may be defined in order to distinguish them:

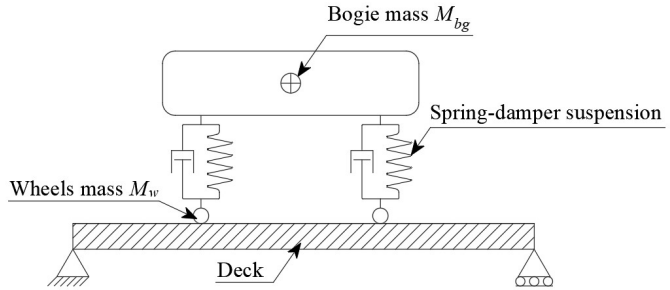
- *Level 1: Moving mass model*



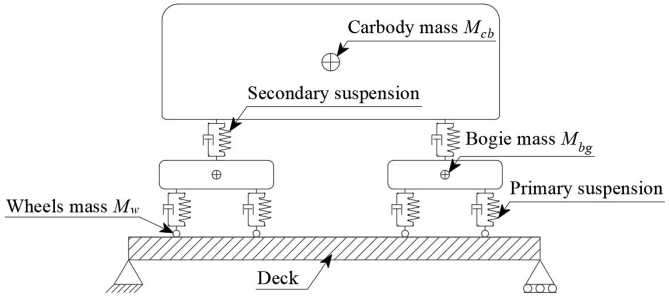
- *Level 2: Moving sprung-mass model*



- *Level 3: Bogie-structure interaction model*



- *Level 4: Vehicle-structure interaction model*

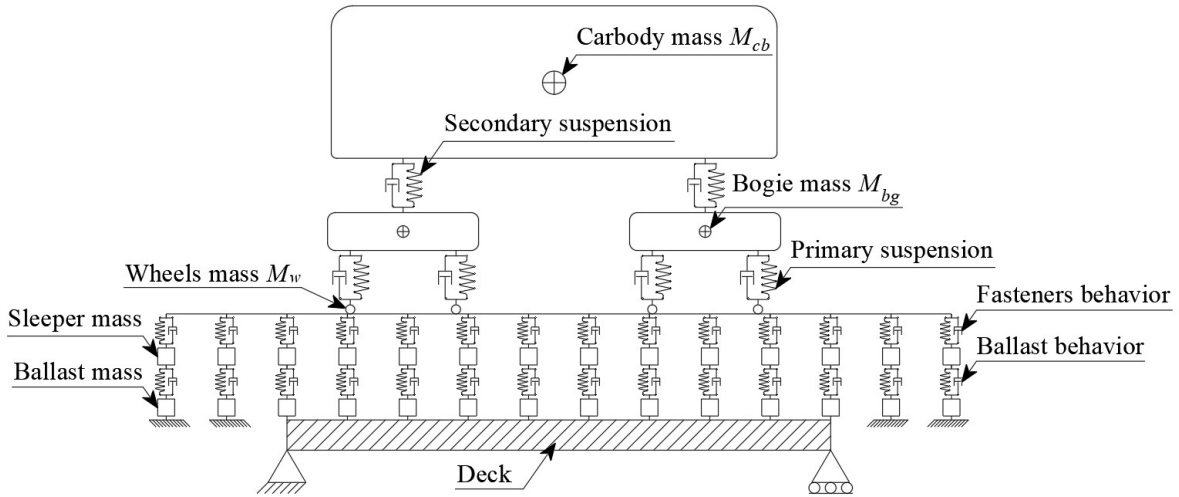


2. Types of vehicle-track interaction models

Levels of complexity of the vehicle-structure interaction models

- *Level 5: Vehicle-track-structure interaction model*

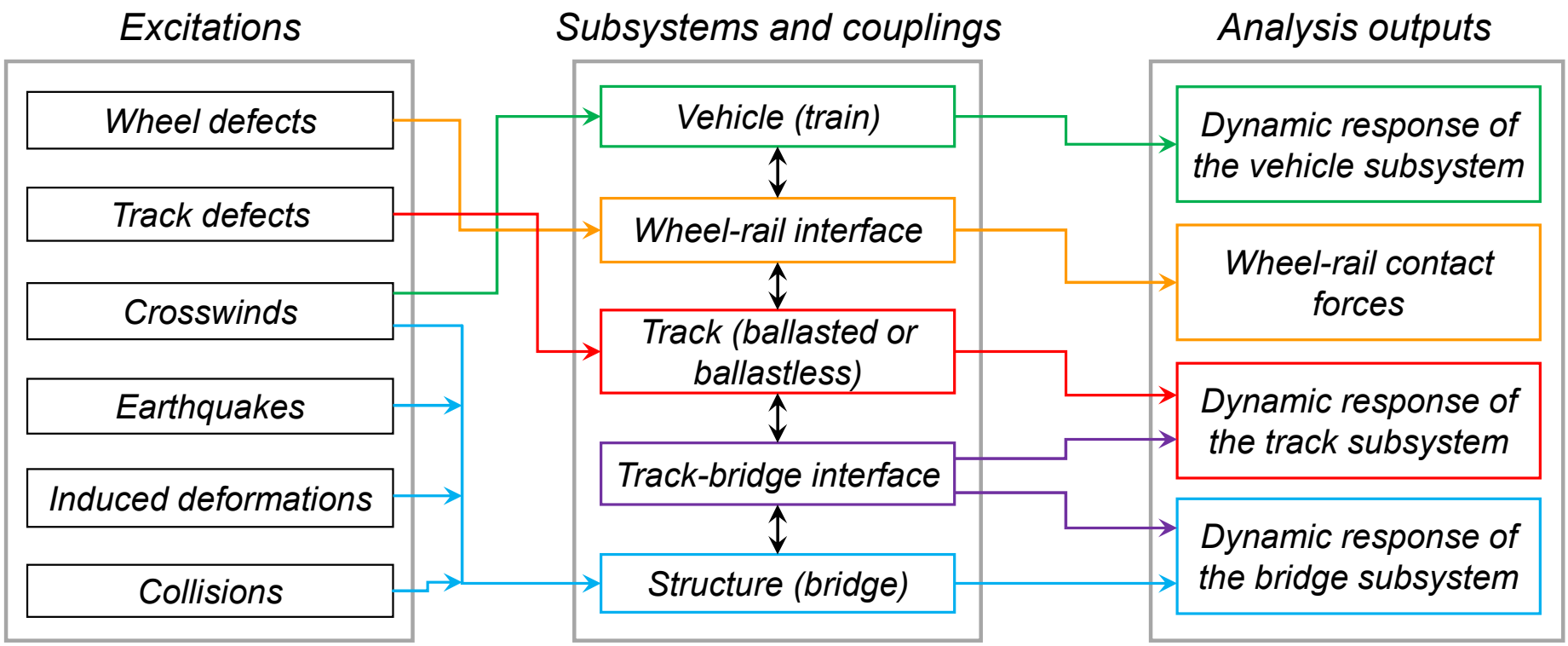
The Vehicle-track-structure interaction model is the most complete one because it considers all the DOF of the vehicle and the composite effect between the structure (bridge) and the track (ballasted or non-ballasted). The vehicle model totalizes 10 DOF in a 2D formulation (vertical motions in each body and pitch rotation in the bogies and carbody), while in a 3D model, this formulation is capable of considering the pitch, rolling and yaw movements, as well.



3. Formulation of the vehicle-track interaction problem

Elements involved in problem

Global overview of the vehicle-track-structure interaction problem



3. Formulation of the vehicle-track interaction problem

Elements involved in problem

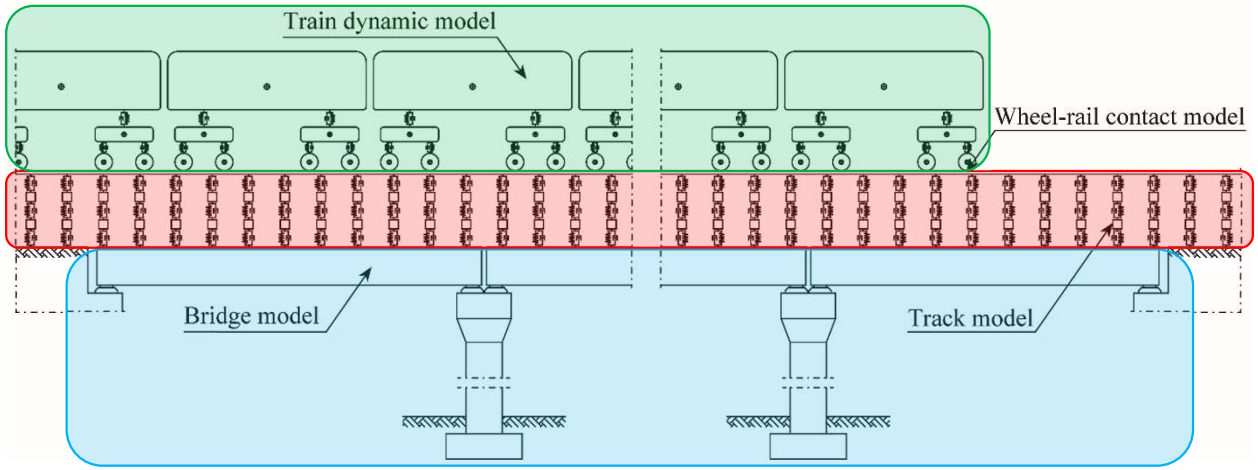
Subsystems in a vehicle-structure interaction model

- The vehicle-structure interaction system is divided in the several subsystems:

i) Subsystem 1: Structure/bridge;

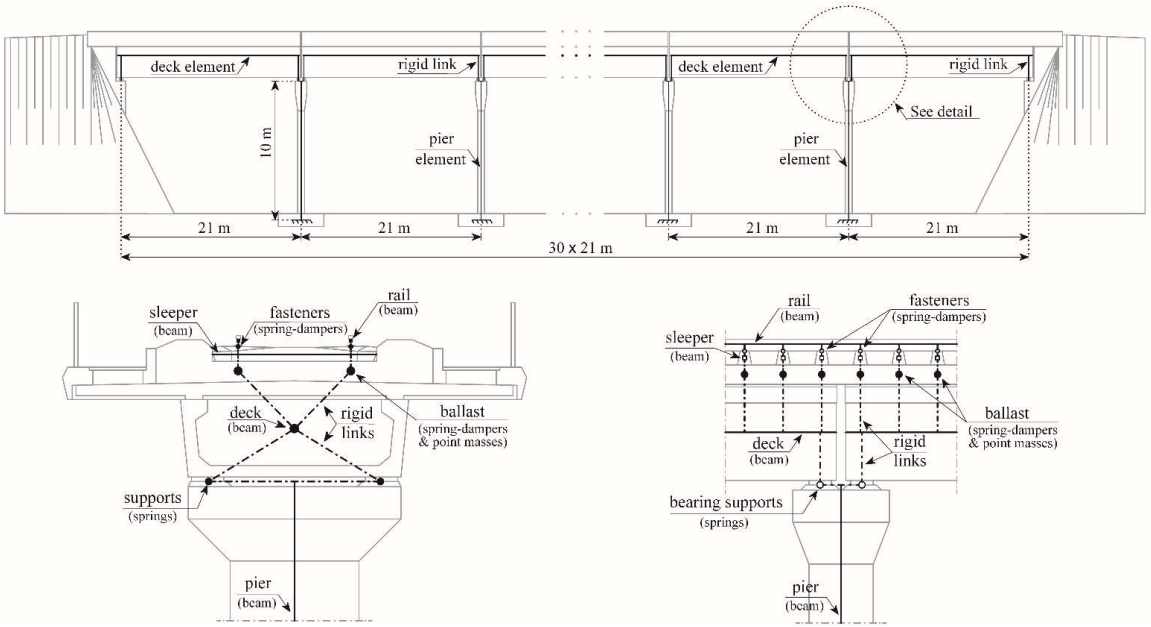
ii) Subsystem 2: Track;

iii) Subsystem 3: Vehicle;

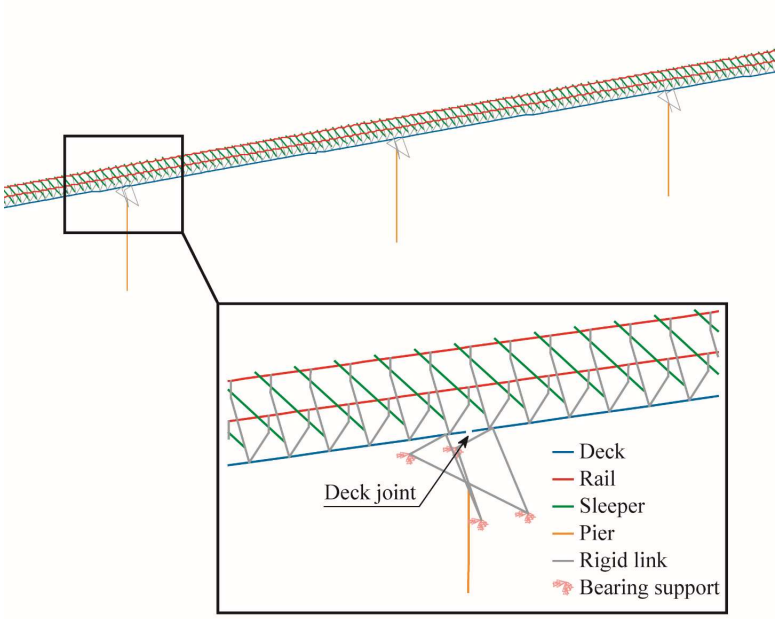


3. Formulation of the vehicle-track interaction problem

Structure-track subsystem modelling



Dynamic model

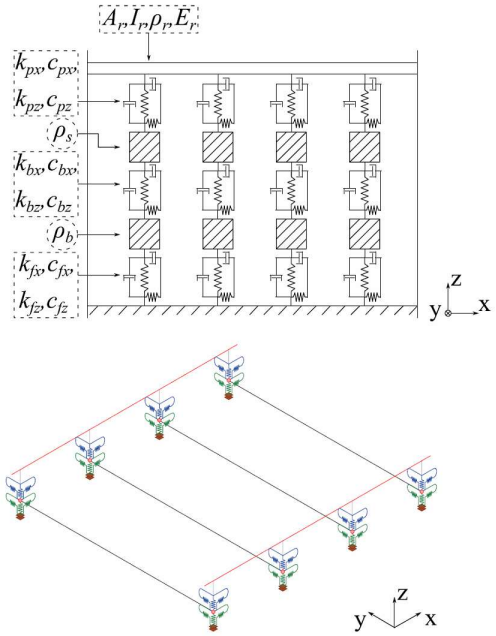


FEM model [a]

[a] Montenegro P.A. et al. (2016)

3. Formulation of the vehicle-track interaction problem

Track subsystem modelling



Ballasted track model

Table 1: Parameters of a ballast track

Designation	Value	Unit	Reference
Ballast's longitudinal stiffness	30	MN/m/m	UIC 774–3-R. (2001)
Ballast's transversal stiffness	7.5	MN/m/m	ERRI D 202/RP 11 (1999)
Ballast's vertical stiffness	100	MN/m/m	ERRI D 202/RP 11 (1999)
Ballast's damping (3 directions)	50	kN.s/m/m	Wu and Yang (2003)
Fastener's longitudinal stiffness	20	MN/m	Zhai, Wang, and Cai (2009)
Fastener's transversal stiffness	20	MN/m	Zhai et al. (2009)
Fastener's vertical stiffness	500	MN/m	ERRI D 214/RP 5 (1999)
Fastener's rotational stiffness	45	kN.m/rad	ERRI D 202/RP 11 (1999)
Fastener's longitudinal damping	50	kN.s/m	Zhai et al. (2009)
Fastener's transversal damping	50	kN.s/m	Zhai et al. (2009)
Fastener's vertical damping	200	kN.s/m	ERRI D 214/RP 5 (1999)

Table 2: Parameters of a ballastless track (slab track)

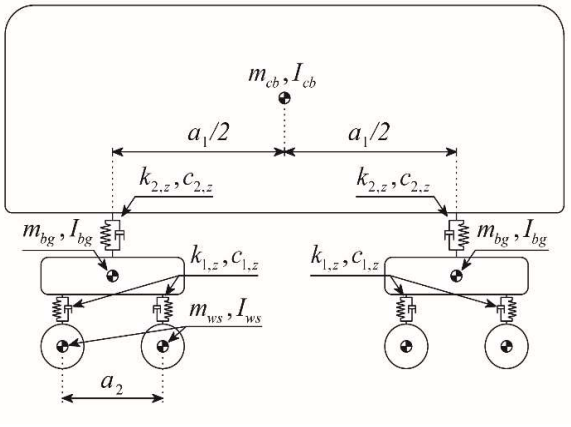
Designation	Value	Unit	Reference
Concrete-asphalt vertical stiffness	17000	MN/m^2	Zhai, We, Song, and Shao (2015)
Fastener's longitudinal stiffness	20	MN/m	Zhai et al. (2009)
Fastener's transversal stiffness	20	MN/m	Zhai et al. (2009)
Fastener's vertical stiffness	500	MN/m	ERRI D 214/RP 5 (1999)
Fastener's rotational stiffness	45	kN.m/rad	ERRI D 202/RP 11 (1999)
Fastener's longitudinal damping	50	kN.s/m	Zhai et al. (2009)
Fastener's transversal damping	50	kN.s/m	Zhai et al. (2009)
Fastener's vertical damping	200	kN.s/m	ERRI D 214/RP 5 (1999)

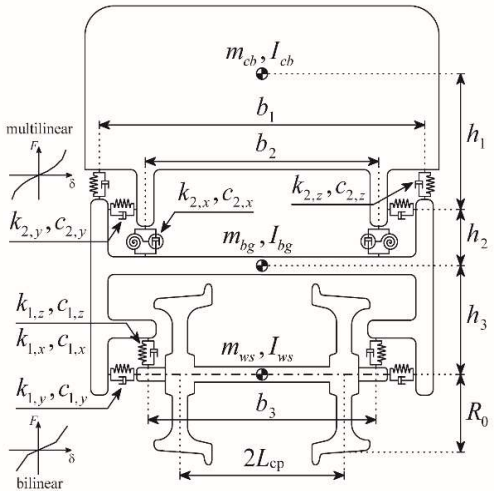
Parameters of a ballasted and ballastless track [a]

[a] Montenegro P.A. et al. (2020a)

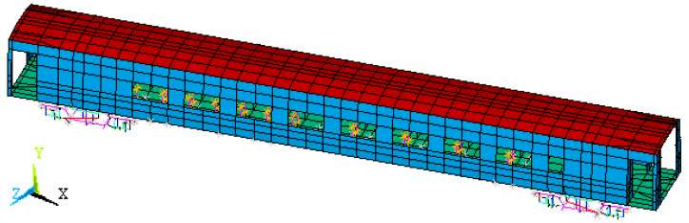
3. Formulation of the vehicle-track interaction problem

Vehicle subsystem modelling

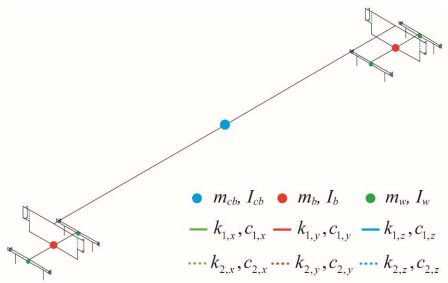


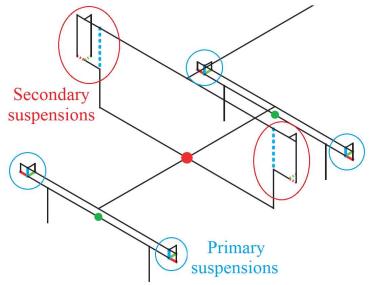


Dynamic model



FEM model [a]





MBS model [b]

[a] Ribeiro et al. (2013)
[b] Montenegro et al. (2020b)

3. Formulation of the vehicle-track interaction problem

Vehicle subsystem modelling



Alfa Pendular (CP - Portugal)



ICE3 (DB - Germany)

Table 1 - Geometrical and mechanical properties of the Alfa Pendular train.

Parameter	Unit	Value
Car body mass, m_{cb}	kg	35640
Car body roll moment of inertia, $I_{cb,x}$	kg.m2	55120
Car body pitch moment of inertia, $I_{cb,y}$	kg.m2	1475000
Car body yaw moment of inertia, $I_{cb,z}$	kg.m2	1477000
Bogie mass, m_b	kg	2829
Bogie roll moment of inertia, $I_{b,x}$	kg.m2	2700
Bogie pitch moment of inertia, $I_{b,y}$	kg.m2	1931.49
Bogie yaw moment of inertia, $I_{b,z}$	kg.m2	3878.76
Wheelset mass, m_w	kg	1711
Wheelset roll moment of inertia, $I_{w,x}$	kg.m2	733.4303
Wheelset yaw moment of inertia, $I_{w,z}$	kg.m2	733.4303
Stiffness of the primary longitudinal suspension, $k_{1,x}$	kN/m	44981.0
Stiffness of the primary transversal suspension, $k_{1,y}$	kN/m	30948.2
Stiffness of the primary vertical suspension, $k_{1,z}$	kN/m	1652.82
Damping of the primary vertical suspension, $c_{1,z}$	kN.s/m	16.739
Stiffness of the secondary longitudinal suspension, $k_{2,x}$	kN/m	4905.0
Stiffness of the secondary transversal suspension, $k_{2,y}$	kN/m	250
Stiffness of the secondary vertical suspension, $k_{2,z}$	kN/m	734.832
Damping of the secondary longitudinal suspension, $c_{2,x}$	kN.s/m	400.0
Damping of the secondary transversal suspension, $c_{2,y}$	kN.s/m	17.5
Damping of the secondary vertical suspension, $c_{2,z}$	kN.s/m	35.0
The static load transmitted by each wheel	kN	64.0
Longitudinal distance between bogies, a_1	m	19
Longitudinal distance between wheelsets, a_2	m	2.7
Transversal distance between vertical secondary suspensions, b_1	m	2.144
Transversal distance between longitudinal secondary suspensions, b_2	m	2.846
Transversal distance between primary suspensions, b_3	m	2.144
Vertical distance between car body center and secondary suspension, h_1	m	0.936
Vertical distance between bogie center and secondary suspension, h_2	m	0.142
Vertical distance between bogie center and wheelset center, h_3	m	0.065
Nominal rolling radius, R_0	m	0.43
Gauge, s	m	1.668

Parameters of a Alfa Pendular [a]

Table 2 - Geometrical and mechanical properties of the ICE3 train.

Parameter	Unit	Value
Car body mass, m_{cb}	kg	53500
Car body roll moment of inertia, $I_{cb,x}$	kg.m2	70000
Car body pitch moment of inertia, $I_{cb,y}$	kg.m2	2621500
Car body yaw moment of inertia, $I_{cb,z}$	kg.m2	2621500
Bogie mass, m_b	kg	3500
Bogie roll moment of inertia, $I_{b,x}$	kg.m2	560
Bogie pitch moment of inertia, $I_{b,y}$	kg.m2	315
Bogie yaw moment of inertia, $I_{b,z}$	kg.m2	1715
Wheelset mass, m_w	kg	1800
Wheelset roll moment of inertia, $I_{w,x}$	kg.m2	1000
Wheelset yaw moment of inertia, $I_{w,z}$	kg.m2	1800
Stiffness of the primary longitudinal suspension, $k_{1,x}$	kN/m	120000
Stiffness of the primary transversal suspension, $k_{1,y}$	kN/m	12500
Stiffness of the primary vertical suspension, $k_{1,z}$	kN/m	1200
Damping of the primary vertical suspension, $c_{1,z}$	kN.s/m	10
Stiffness of the secondary longitudinal suspension, $k_{2,x}$	kN/m	12000
Stiffness of the secondary transversal suspension, $k_{2,y}$	kN/m	240
Stiffness of the secondary vertical suspension, $k_{2,z}$	kN/m	350
Damping of the secondary longitudinal suspension, $c_{2,x}$	kN.s/m	232.7
Damping of the secondary transversal suspension, $c_{2,y}$	kN.s/m	30
Damping of the secondary vertical suspension, $c_{2,z}$	kN.s/m	20
The static load transmitted by each wheel	kN	83.0
Longitudinal distance between bogies, a_1	m	17.5
Longitudinal distance between wheelsets, a_2	m	2.50
Transversal distance between vertical secondary suspensions, b_1	m	2.45
Transversal distance between longitudinal secondary suspensions, b_2	m	2.90
Transversal distance between primary suspensions, b_3	m	2.00
Vertical distance between car body center and secondary suspension, h_1	m	0.50
Vertical distance between bogie center and secondary suspension, h_2	m	0.47
Vertical distance between bogie center and wheelset center, h_3	m	0.10
Nominal rolling radius, R_0	m	0.43
Gauge, s	m	1.435

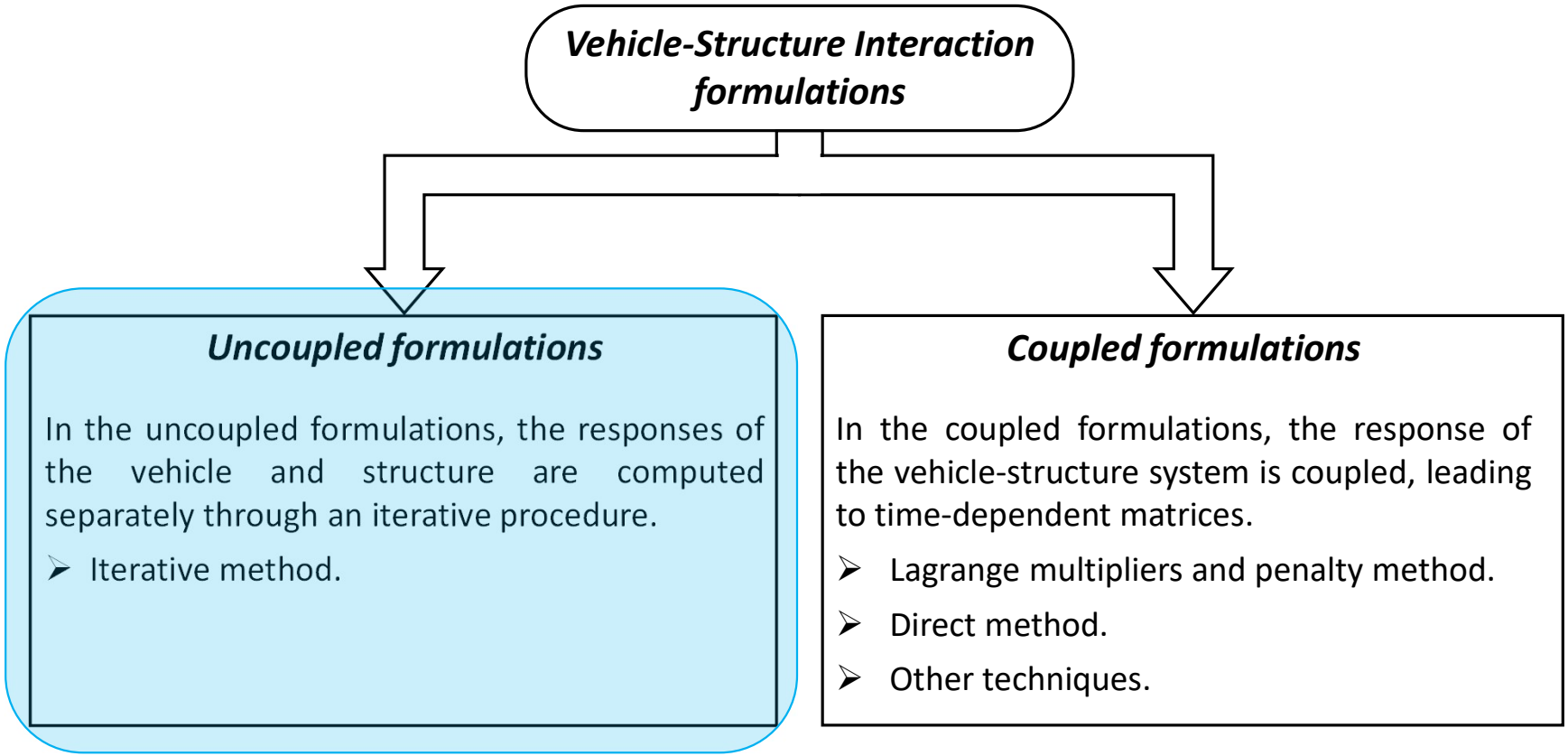
Parameters of a ICE3 [b]

[a] Neto J. et al. (2021)

[b] Peixer M.A. et al. (2021)

3. Formulation of the vehicle-track interaction problem

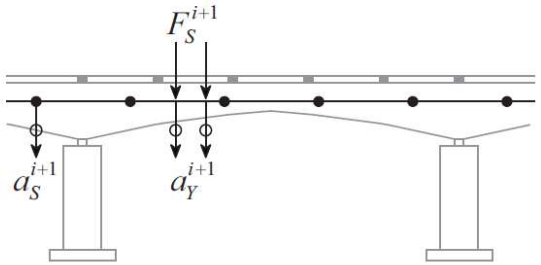
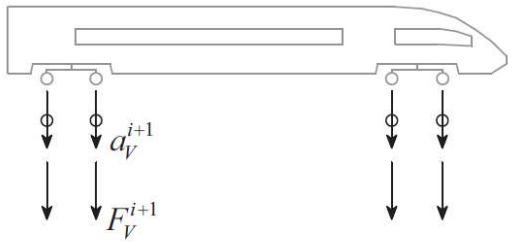
Vehicle-structure coupling



3. Formulation of the vehicle-track interaction problem

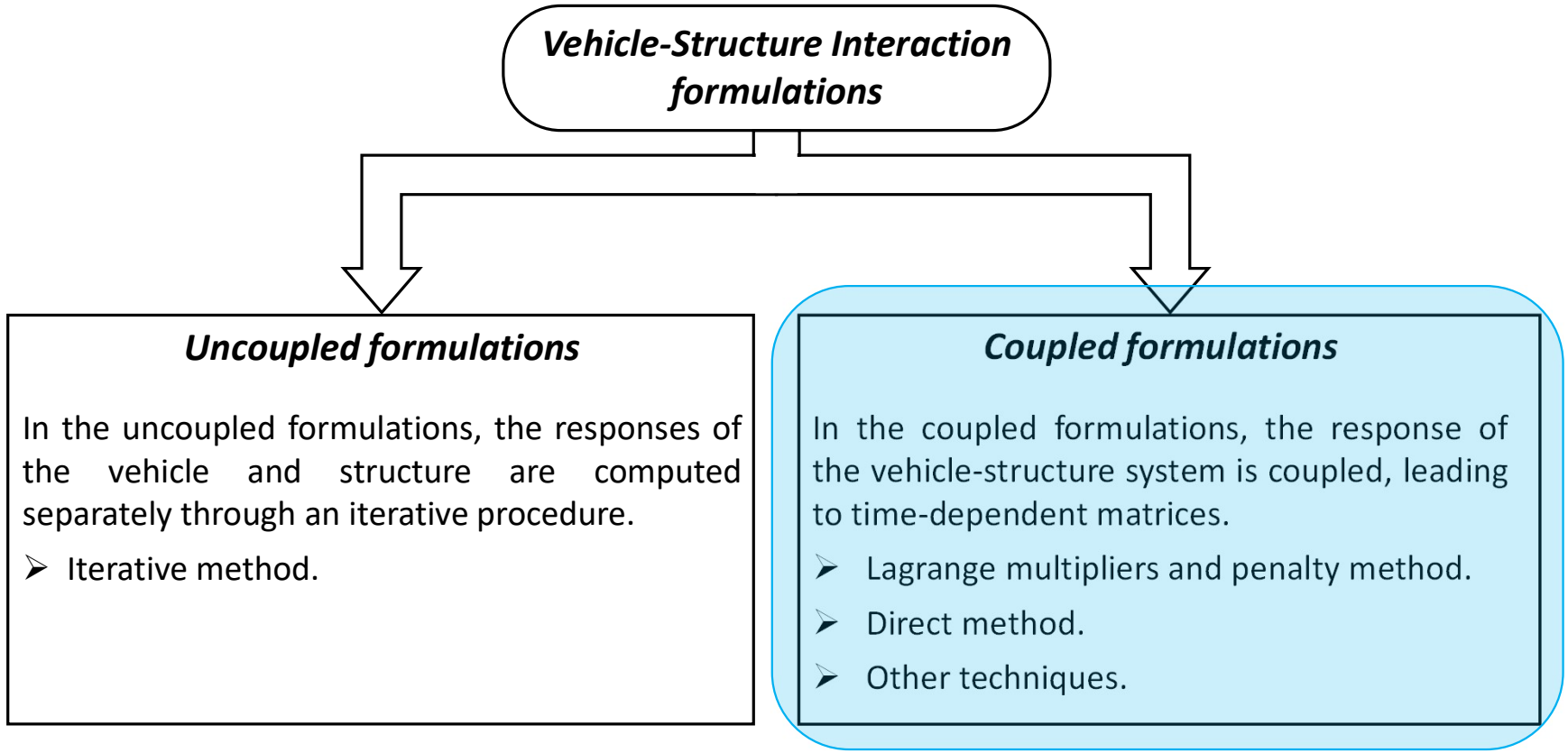
Vehicle-structure coupling

Uncoupled formulations – Iterative method

	Structure	Vehicle
Scheme		
Load	$\mathbf{F}_S^{i+1} = \mathbf{F}_{sta} + \mathbf{F}_{dyn}^{i}$	$\mathbf{a}_V^{i+1} = \mathbf{a}_Y^{i+1} + \mathbf{r}$
Result	$\mathbf{a}_S^{i+1} \rightarrow \mathbf{a}_Y^{i+1}$	$\mathbf{F}_{dyn}^{i+1} = \mathbf{F}_V^{i+1}$
Convergence criterion	$\dfrac{\left\|\mathbf{F}_{dyn}^{i+1} - \mathbf{F}_{dyn}^{i}\right\|}{\left\|\mathbf{F}_{dyn}^{i}\right\|}$	$\begin{cases} \text{if} \le \varepsilon \rightarrow \text{next step} \\ \text{if} > \varepsilon \rightarrow \text{next iteration} \end{cases}$

3. Formulation of the vehicle-track interaction problem

Vehicle-structure coupling

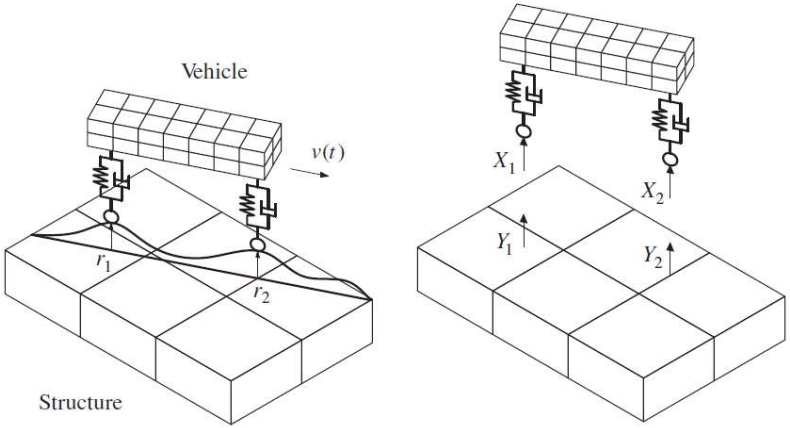


3. Formulation of the vehicle-track interaction problem

Vehicle-structure coupling

Coupled formulations – Direct Method used in vertical interaction

- The Direct Method, proposed by *Neves et al (2012, 2014)*, is a vehicle-structure interaction coupled method in which the **governing equilibrium equations** of the vehicle and structure are **complemented with additional constraint equations** that relate the displacements of the contact nodes of the vehicle with the corresponding nodal displacements of the structure. This method applies the Lagrange multipliers method to the FEM analysis.



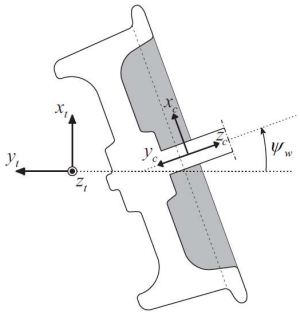
$$\begin{bmatrix} \mathbf{K} & \mathbf{D} \\ \mathbf{H} & 0 \end{bmatrix} \begin{bmatrix} \mathbf{a}^{t+\Delta t} \\ \mathbf{X}^{t+\Delta t} \end{bmatrix} = \begin{bmatrix} \mathbf{F} \\ \mathbf{r} \end{bmatrix} \Longrightarrow \text{Equations of motion}$$
$$\Longrightarrow \text{Constraint equation}$$

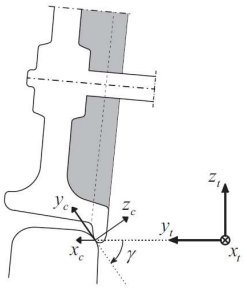
3. Formulation of the vehicle-track interaction problem

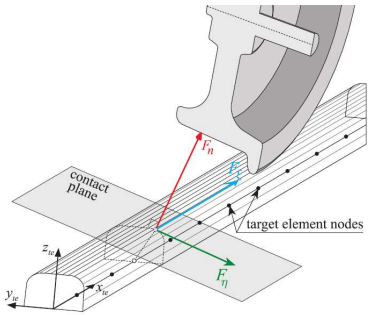
Vehicle-structure coupling

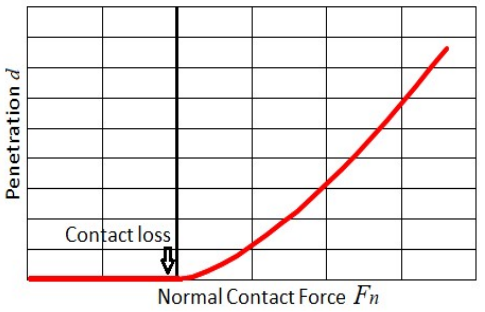
Coupled formulations – Direct Method considering the wheel-rail contact

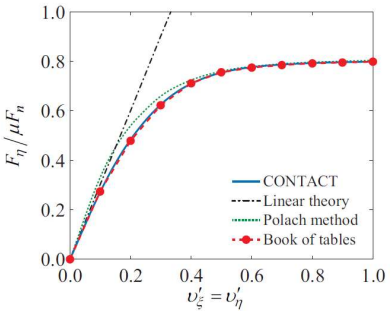
- The original formulation, restricted to vertical interaction, was extended to deal with 3D contact (*Montenegro et al, 2015[a,b]*), which includes the geometry of the wheel and rail and the nonlinear laws for the normal and tangential contact (wheel-rail contact model).
- Both the uncoupled iterative method and the original direct method deal with the nonlinearity that arises from the fact that there are two contacting subsystems. However, the introduction of a wheel-rail contact model brings with it new nonlinearities to the system, namely geometric nonlinearities, nonlinear normal contact forces and nonlinear tangential contact forces.











3. Formulation of the vehicle-track interaction problem

Wheel-rail contact

Problems involved in a wheel-rail contact model

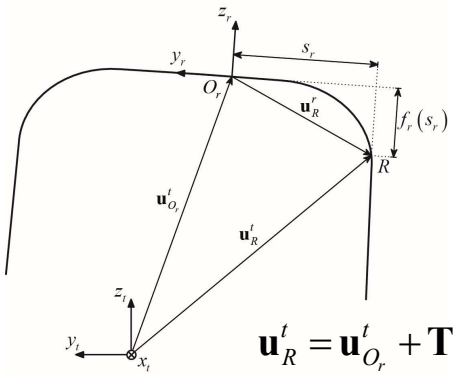
- The wheel rail contact model is divided in three main problems:
  i. Geometric problem: consists of the detection of the contact points between wheel and rail;
  ii. Normal contact problem: results from the compression between the wheel and rail. It is in this phase that the normal forces are computed.
  iii. Tangential contact problem: it is a consequence of the local elasticity of the contacting surfaces and of the rolling friction phenomenon that characterizes the contact between two bodies that roll over each other. The tangential contact forces, also called creep forces, are calculated in this step.
- Assuming that the bodies in contact have the same material properties, the normal and tangential problems can be solved separately.

3. Formulation of the vehicle-track interaction problem

Wheel-rail contact

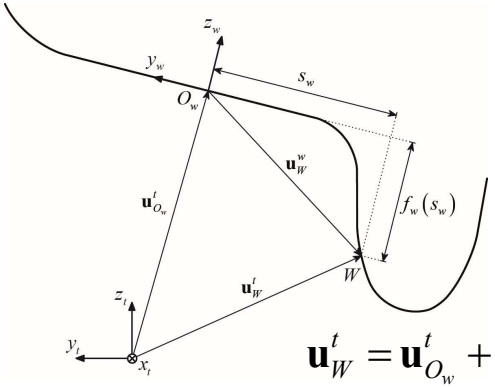
Geometric contact problem

Rail parameterization

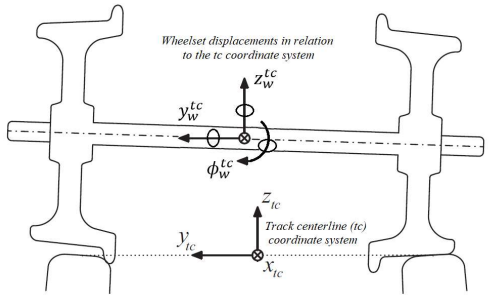


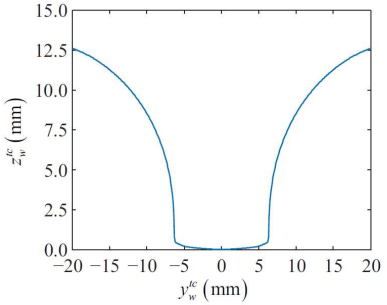
$$\mathbf{u}_R^t = \mathbf{u}_{O_r}^t + \mathbf{T}^{trT}\mathbf{u}_R^r$$

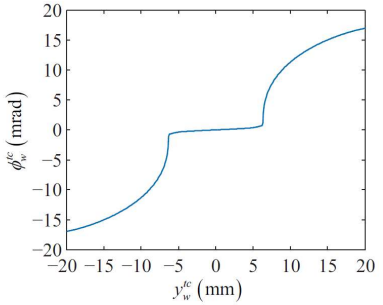
Wheel parameterization



$$\mathbf{u}_W^t = \mathbf{u}_{O_w}^t + \mathbf{T}^{twT}\mathbf{u}_W^w$$







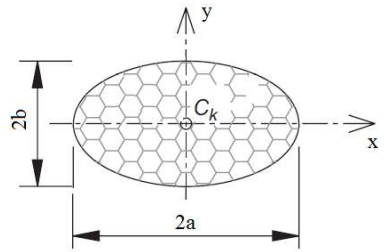
3. Formulation of the vehicle-track interaction problem

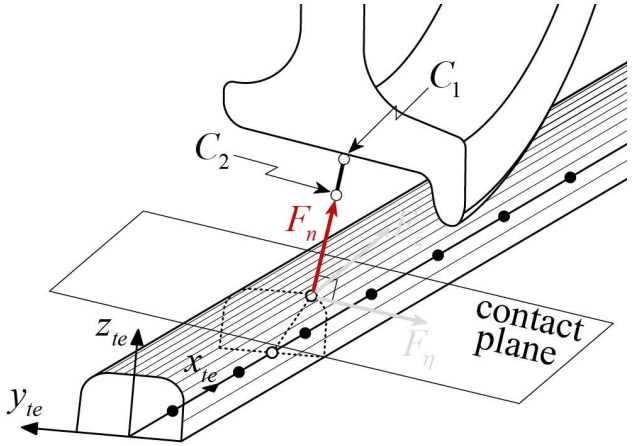
Wheel-rail contact

Normal contact problem

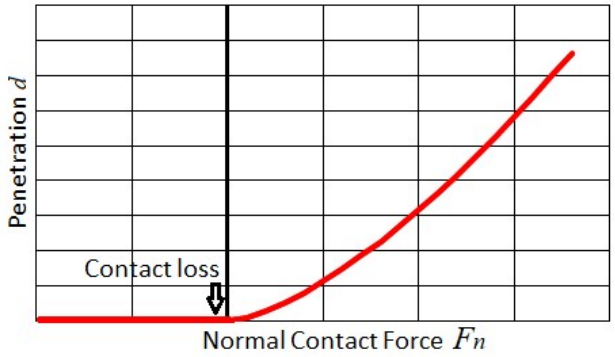
- The normal contact problem consists of computing the contact forces perpendicular to the wheel and rail surfaces at the contact point $\boldsymbol{F_n}$. These forces result from the compression exerted by the wheel to the rail.
- The most used model to define the normal contact is based on the Hertz nonlinear theory, in which the contact area between the two contacting bodies is assumed to be elliptical.

Elliptical contact area





$$F_n = K_h \, d^{3/2}$$

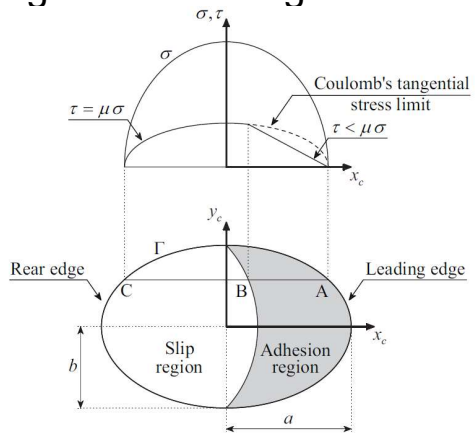


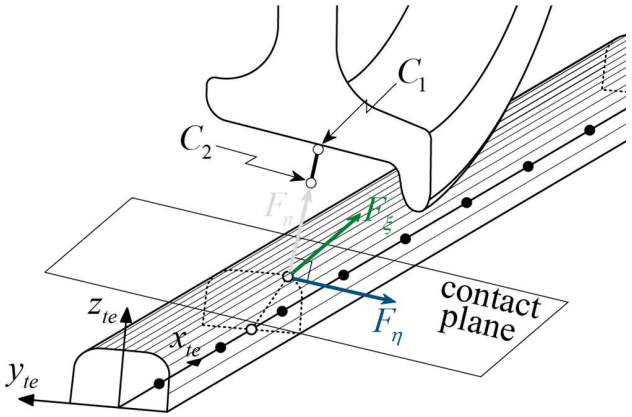
3. Formulation of the vehicle-track interaction problem

Wheel-rail contact

Tangential contact problem

- The tangential contact problem consists of computing the contact forces tangential to the wheel and rail surfaces at the contact point in the longitudinal direction (vehicle's running direction) F_ξ and in the lateral direction F_η . These forces result from the rolling friction phenomenon that characterizes the contact between two bodies compressed against each other that are allowed to roll over each other (a rolling wheel running over a rail)[a-e].





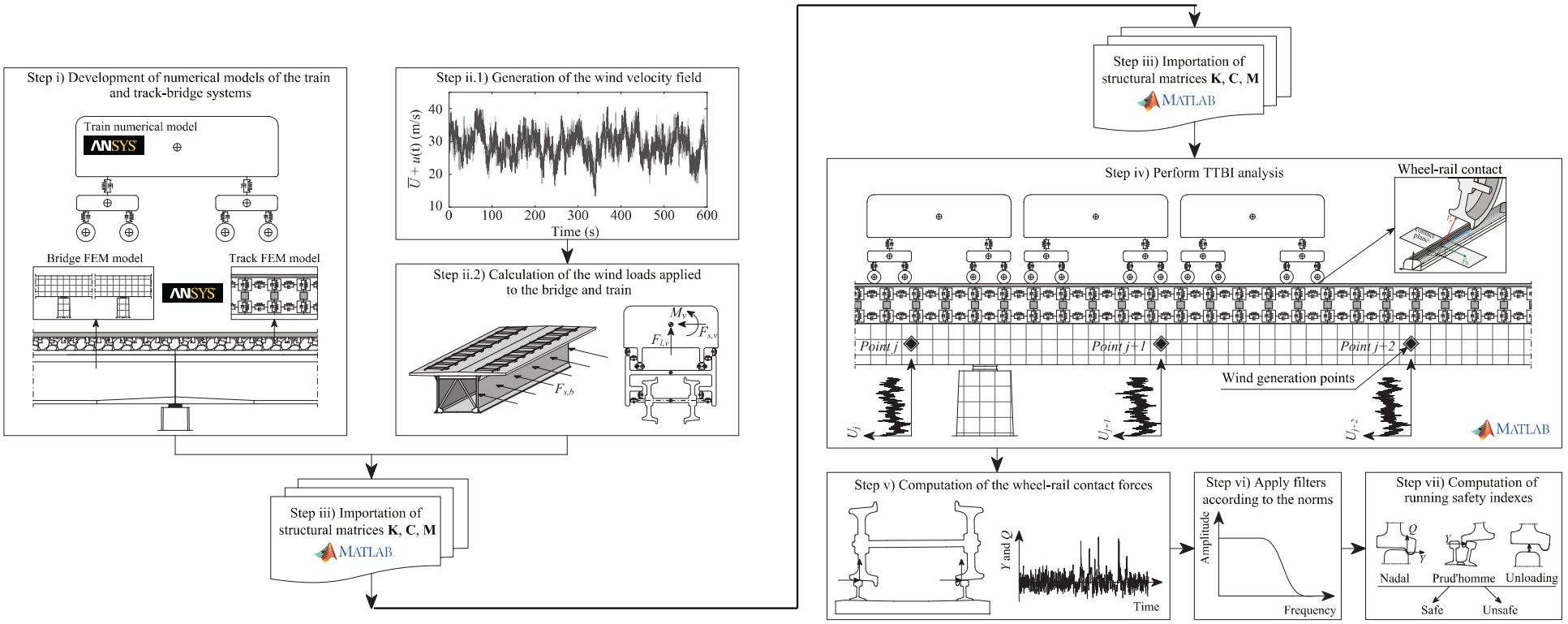
$$F_\eta = \iint_\Gamma \tau_{y_c}\, dx_c\, dy_c$$

$$F_\xi = \iint_\Gamma \tau_{x_c}\, dx_c\, dy_c$$

[a] (Kalker JJ. 1967)
[b] (Kalker JJ. 1682)
[c] (Kalker JJ. 1996)
[d] (Shen et al., 1983)
[e] (Polach O., 1983)

3. Formulation of the vehicle-track interaction problem

VSI – Vehicle-Structure Interaction Analysis code



(Montenegro PA et al., 2015)
(Montenegro PA., 2015)

3. Formulation of the vehicle-track interaction problem

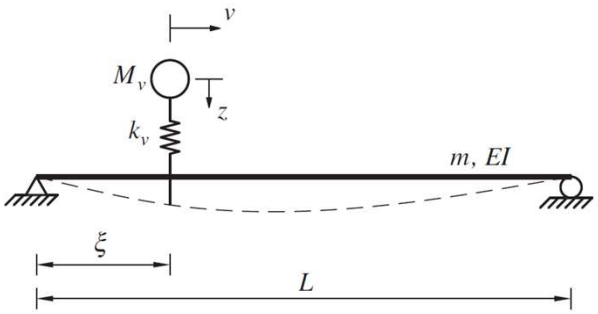
Validation tests used in the VSI software

Validation test 1: Yang beam

- The Yang beam (*Yang and Yaw, 1997*) is a well-known test used to validate the vertical dynamics of any vehicle-structure interaction methodology.
- It consists of a moving sprung mass moving over a simply supported beam. The vertical responses of both the beam midpoint and sprung mass can be obtained by the following semi-analytical governing equations of motion solved by the modal superposition method (*Neves et al, 2012*):

Eq. Motion Beam:
$$\ddot{q}_n(t) + \omega_n^2 q_n(t) + \frac{\delta k_v \phi_n(\xi) \sum_{m=1}^{\infty} \phi_m(\xi) q_m(t)}{M_n} - \frac{\delta k_v \phi_n(\xi) z}{M_n} = \frac{\delta M_v g \phi_n(\xi)}{M_n}$$

Eq. Motion Sprung Mass M_v:
$$M_v \ddot{z} + k_v \left[z - \sum_{m=1}^{\infty} \phi_m(\xi)\, q_m(t) \right] = 0$$

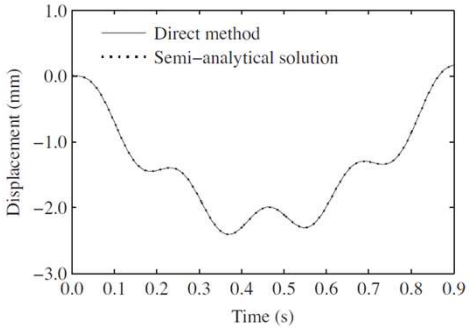


3. Formulation of the vehicle-track interaction problem

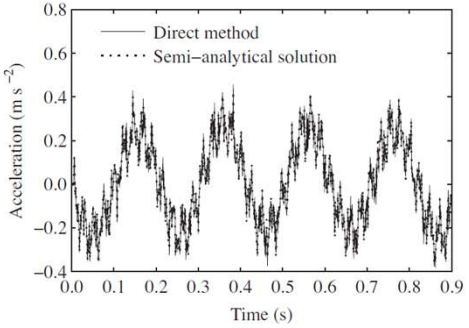
Validation tests used in the VSI software

Validation test 1: Yang beam

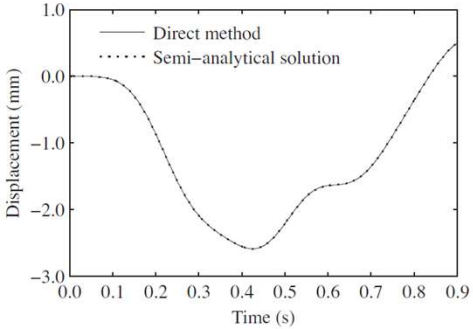
Vertical displacement of the beam's midpoint



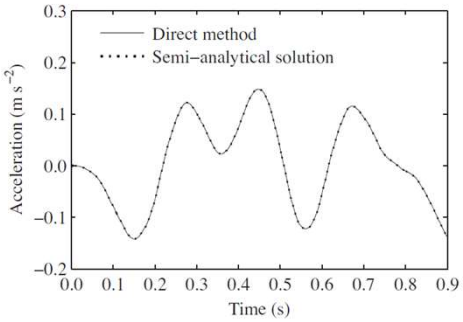
Vertical acceleration of the beam's midpoint



Vertical displacement of the sprung mass



Vertical acceleration of the sprung mass

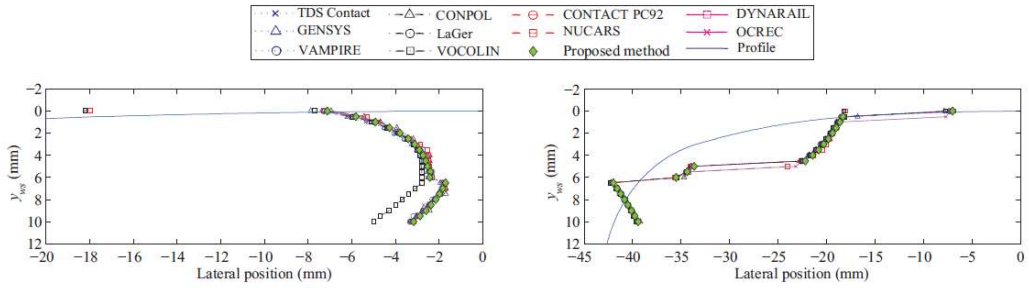


3. Formulation of the vehicle-track interaction problem

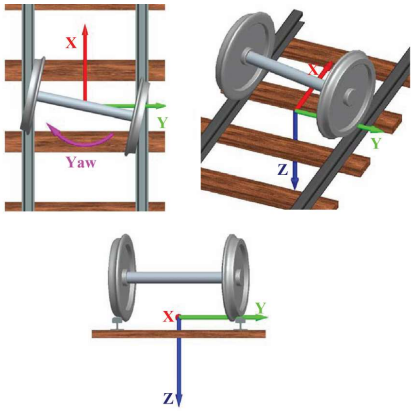
Validation tests used in the VSI software

Validation test 2: Manchester benchmarks

- The Manchester Metropolitan University (*Shackleton and Iwnicki, 2008*) conducted a series of tests with ten railway vehicle MBS softwares and compared the results. These softwares vary in terms of the wheel-rail contact model adopted. Note that these benchmarks were intended to validate the contact model in a rigid track, since they do not consider flexibility of the structure (pure MBS simulation). The algorithm developed by *Montenegro et al. (2015)*[a,b,c] proved to be in a good agreement with the majority of the tested softwares.



Rail lateral contact positions according to the lateral displacement of the wheelset y_{ws}

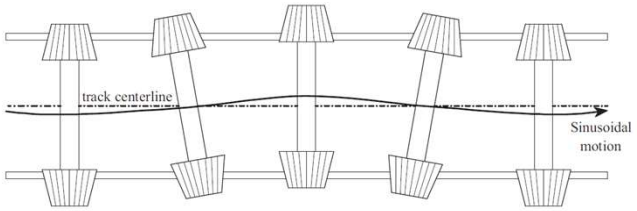


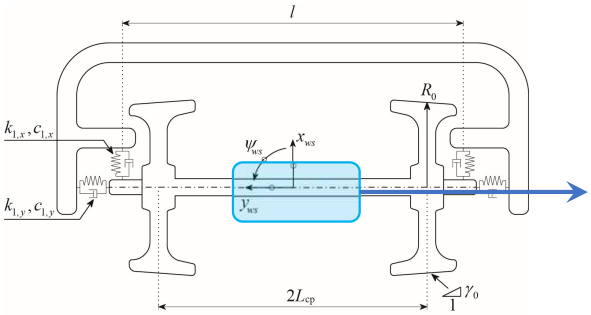
[a] (Montenegro PA et al., 2015)
[b] (Montenegro PA., 2015)
[c] (Montenegro PA et al., 2023)

3. Formulation of the vehicle-track interaction problem

Validation tests used in the VSI software

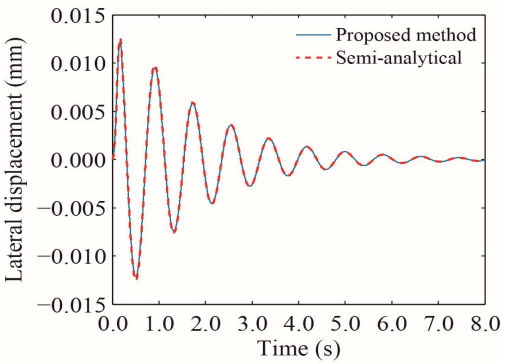
Validation test 3: Hunting stability analysis of a suspended wheelset



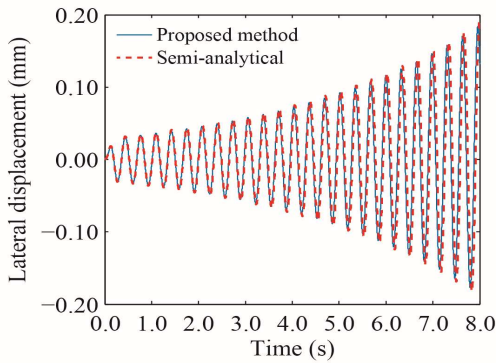


Lateral displacements of the wheelset y_{ws}

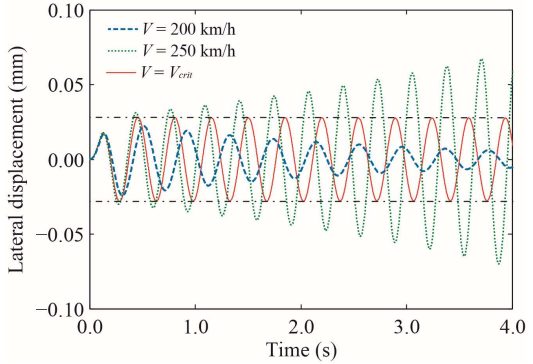
Lateral response for V=100km/h



Lateral response for V=250km/h



Lateral responses for 3 speeds



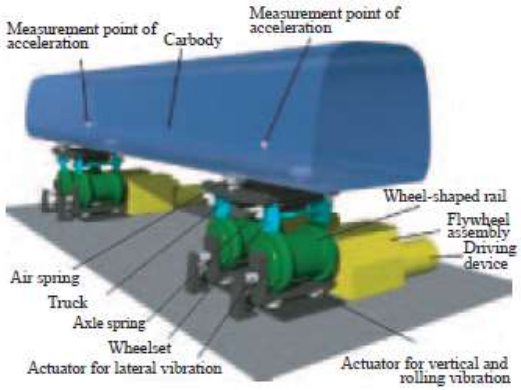
(Montenegro PA et al., 2023)

3. Formulation of the vehicle-track interaction problem

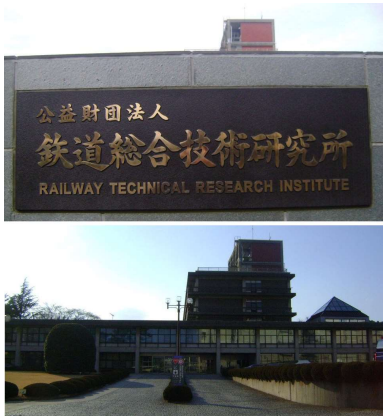
Validation tests used in the VSI software

Validation test 4: Simulation of a test rig experiment

- The test was carried out in the rolling stock test plant of the RTRI, Tokyo, Japan.







- The four wheel-shaped rails of the test rig, controlled by independent actuators, can simulate different types of rail deviations and allows speeds up to 500 km/h.
- The test consisted of measuring lateral accelerations inside the carbody of a prototype Shinkansen vehicle in real scale running at 300 km/h.

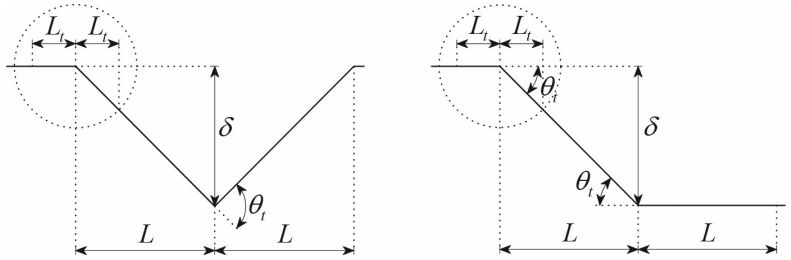
3. Formulation of the vehicle-track interaction problem

Validation tests used in the VSI software

Validation test 4: Simulation of a test rig experiment

- The algorithm developed by *Montenegro et al. (2015)*[a,b,c] proved to be in a good agreement with the experimental results.

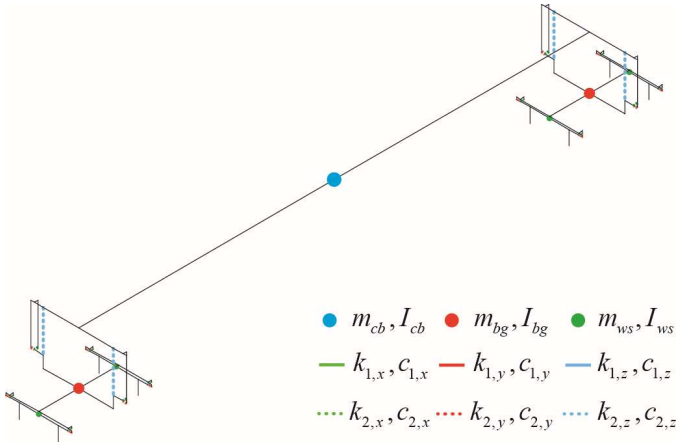
Track deflection shapes imposed by the actuators (δ = 8mm)



Bending shape

Translation shape

Model of the vehicle



[a] (Montenegro PA et al., 2015)
[b] (Montenegro PA., 2015)
[c] (Montenegro PA et al., 2023)

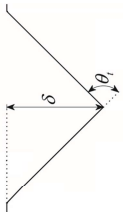
3. Formulation of the vehicle-track interaction problem

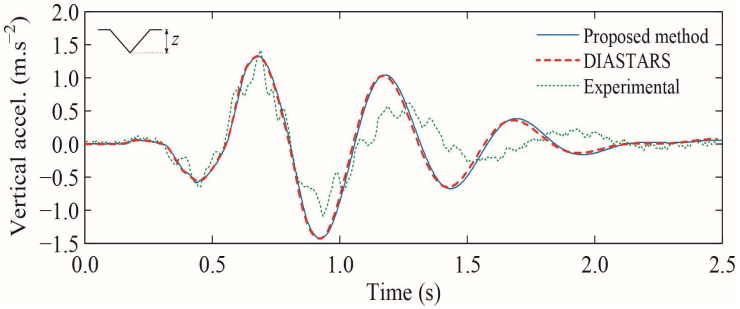
Validation tests used in the VSI software

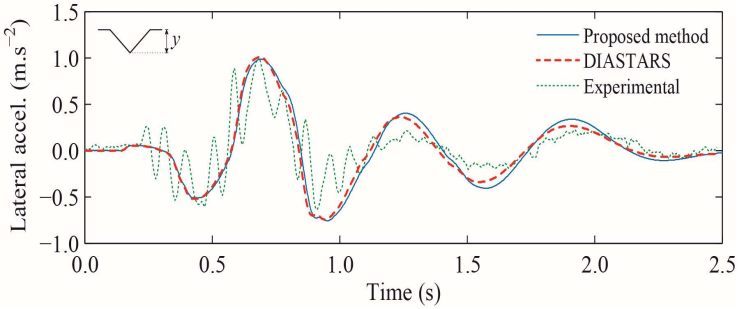
Validation test 4: Simulation of a test rig experiment

Vertical accelerations | *Lateral accelerations*

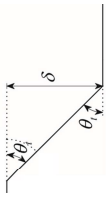
Bending shape: L = 20m

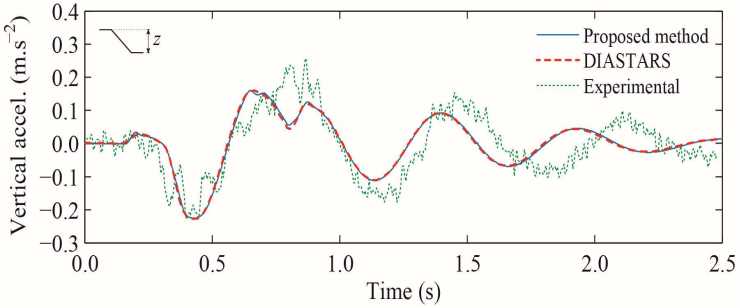


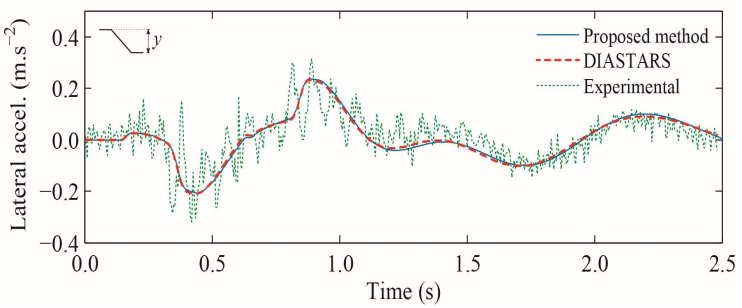




Translation shape: L = 20m







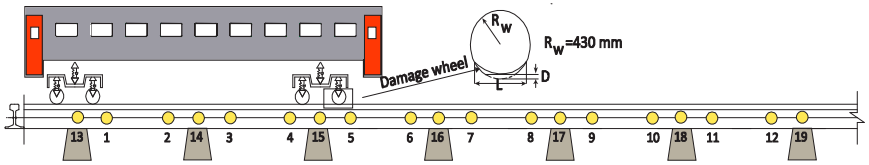
[a] (Montenegro PA et al., 2015)
[b] (Montenegro PA., 2015)
[c] (Montenegro PA et al., 2023)

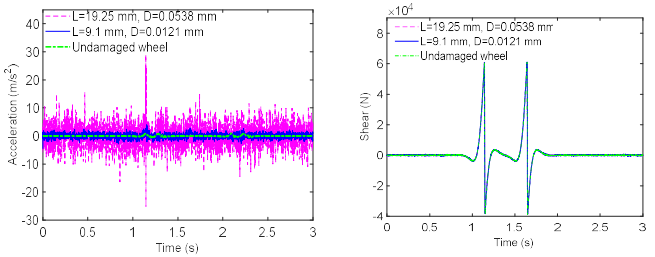
4. Applications

Type of applications

- The vehicle-structure interaction models may be used in a wide range of scenarios, such as:

i. Analysis of the bridge and/or track dynamic response.





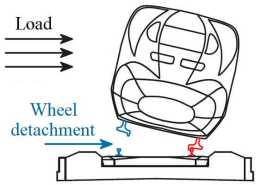
ii. Riding comfort analysis through the analysis and post-processing of the carbody accelerations;

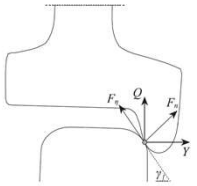
$$a^W(t) = \sqrt{\frac{1}{T}\int_{t-T}^{t} a_W^2(\tau)d\tau}$$

Comfort scale according to EN12299 (2009)

Sensation	*Lower bound of N_{MV}*	*Upper bound of N_{MV}*
Very comfortable	-	1.5
Comfortable	1.5	2.5
Medium	2.5	3.5
Uncomfortable	3.5	4.5
Very uncomfortable	4.5	-

iii. Running safety analysis through the derailment criteria computed from the WR contact forces;





$$\xi_N = \frac{Y}{Q} \leq 0.8 \quad ; \quad \xi_U = 1 - \frac{Q}{Q_0} \leq 0.9$$

References

- Goicolea JM, Antolín P. Dynamic effects of railway traffic due to lateral motion in long viaducts with high piers, COMPDYN 2011 - 3rd ECCOMAS Thematic Conference on Computational Methods in Structural Dynamics and Earthquake Engineering, Corfu, Greece, 2011.
- Montenegro P.A. et al. (2016). "Running safety assessment of trains moving over bridges subjected to moderate earthquakes". Earthquake Eng & Structural Dyn, 45, 483–504.
- Montenegro P.A. et al. (2020a). "Stability of a train running over the Volga river high-speed railway bridge during crosswinds". Structure and Infrastructure Eng, 16(8), 1121-1137.
- Ribeiro et al. (2013). "Running safety assessment of trains moving over bridges subjected to moderate earthquakes". Earthquake Engineering & Structural Dynamics, 45, 483–504.
- Montenegro et al. (2020b). "Dynamic effects on a train-bridge system caused by stochastically generated turbulent wind fields". Engineering Structures, 211, 1-16.
- Neto J. et al. (2021). "Evaluation of the train running safety under crosswinds - a numerical study on the influence of the wind speed and orientation considering the normative Chinese Hat Model". I. J. of Rail Transp, 9(3), 204-231.

References

- Peixer M.A. et al. (2021). "Running safety evaluation of a train moving over a high-speed railway viaduct under different track conditions". Engineering Failure Analysis, 121, 105133.
- Neves SGM, Azevedo AFM, Calçada R. A direct method for analyzing the vertical vehicle–structure interaction, Engineering Structures 2012; 34: 414-420.
- Neves SGM, Montenegro PA, Azevedo AFM, Calçada R. A direct method for analyzing the nonlinear vehicle–structure interaction, Engineering Structures 2014; 69: 83-89.
- Montenegro PA, Neves S, Calçada R, Tanabe M, Sogabe M. Wheel-rail contact formulation for analyzing the lateral train-structure dynamic interaction, Comp & Strct 2015a; 152: 200-214.
- Montenegro PA. A methodology for the assessment of the train running safety on bridges. PhD Thesis, Faculty of Engineering of the University of Porto, Porto, Portugal; 2015b.
- Kalker JJ. On the rolling contact of two elastic bodies in the presence of dry friction. PhD thesis, Delft University of Technology, Delft, The Netherlands; 1967.

References

- Kalker JJ. A fast algorithm for the simplified theory of rolling contact, Vehicle System Dynamics 1982; 11: 1-13.
- Kalker JJ. Book of tables for the Hertzian creep-force law, 2nd Mini Conference on Contact Mechanics and Wear of Wheel/Rail Systems, Budapest, Hungary; 1996.
- Shen ZY, Hedrick JK, Elkins JA. A comparison of alternative creep force models for rail vehicle dynamic analysis, Vehicle System Dynamics 1983; 12: 79-83.
- Polach O. A fast wheel-rail forces calculation computer code, Vehicle System Dynamics 1999; 33: 728-739.
- Yang YB, Yau JD. Vehicle-bridge interaction element for dynamic analysis, Journal of Structural Engineering 1997; 123: 1512-1518.
- Shackleton P, Iwnicki S. Comparison of wheel–rail contact codes for railway vehicle simulation: (…) Manchester Contact Benchmark and initial results, Veh Sys Dyn 2008; 46: 129-149.
- Montenegro PA, Calçada R. Wheel-rail contact model for railway vehicle structure interaction applications: development and validation, Railway Engineering Science 2023, in press.

Machine Learning Methodologies for Damage Identification

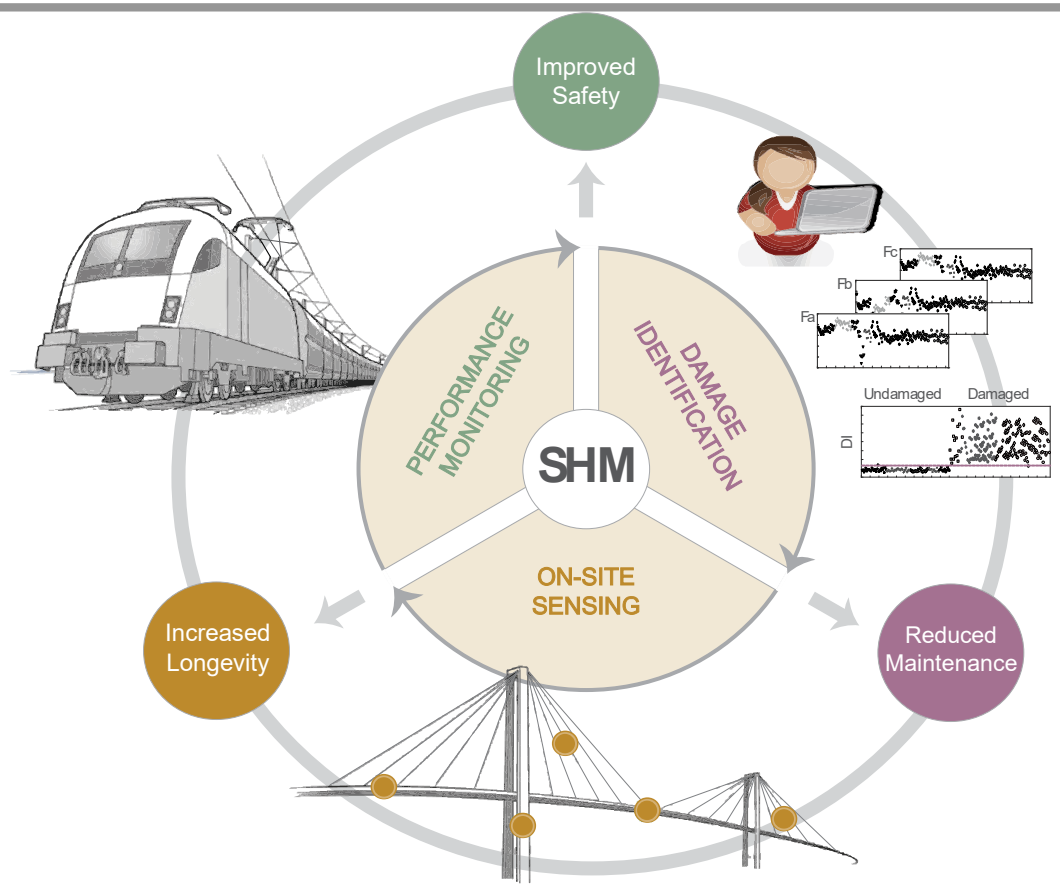
Andreia Meixedo [FEUP], Maria de Lurdes Simões [FEUP], Diogo Ribeiro [ISEP], Araliya Mosleh [FEUP], Rúben Silva [FEUP], António Guedes [ISEP]

Contents

1. Introduction
2. Theoretical Background
3. Machine Learning Methodology
4. Case studies

1. Introduction

Structural Health Monitoring (SHM) for Damage Identification represents a promising strategy in the ongoing challenge of achieving sustainable infrastructural systems since it has the potential to identify damage before it becomes critical, enabling early preventive actions to be taken to minimize costs.

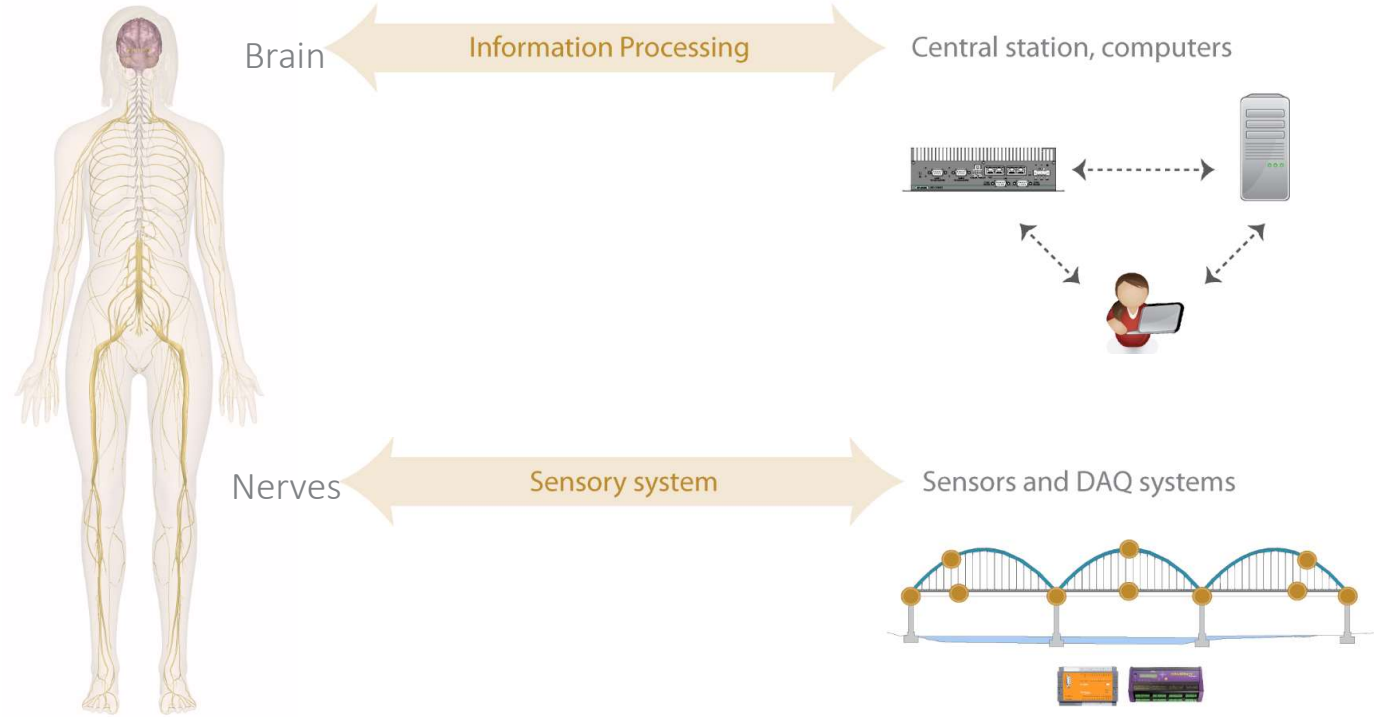


The goal is to achieve economical, efficient and intelligent technologies to manage the operation and maintenance of infrastructure.

2. Theoretical Background

Structural Health Monitoring (SHM)

The basic idea of SHM is to build up a system like the human nervous system, where the brain (computer) processes the information and defines actions (maintenance activities), and the nerves (sensors) feel the pain (damage).



2. Theoretical Background

Hierarchical structure of damage identification

SHM techniques can be classified into one of the following levels, according to their ability to answer the following questions:

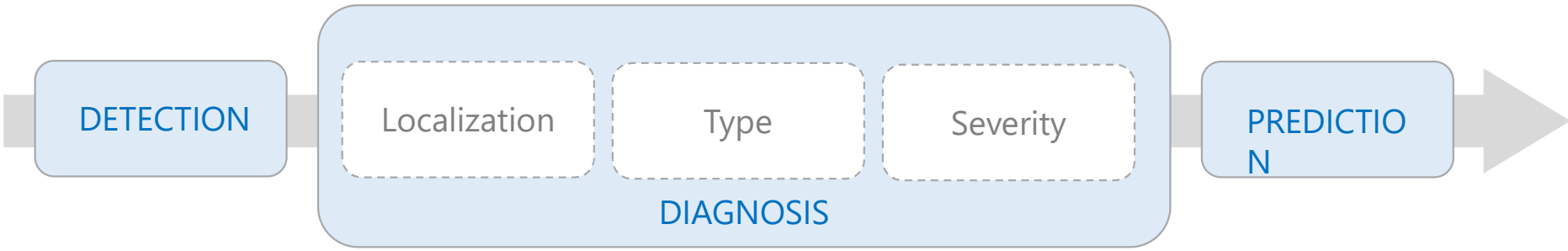
Level 1: Is the damage present in the structural system (detection)?

Level 2: Where is the damage located (localization)?

Level 3: What kind of damage is present (type)?

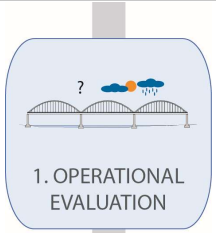
Level 4: What is the extent of damage (severity)?

Level 5: What is the residual lifetime (prediction)?



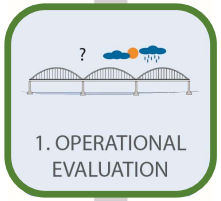
2. Theoretical Background

SHM Strategy for Damage Identification



2. Theoretical Background

SHM Strategy for Damage Identification



1. What are the life safety and/or economic justifications for performing SHM?
2. How is damage defined for the system being monitored?
3. What are the operational and environmental conditions under which the monitored structural system functions?
4. What are the limitations on acquiring data in the operational environment?

2. Theoretical Background

Hierarchical structure of damage identification

SHM techniques can be classified into one of the following levels, according to their ability to answer the following questions:

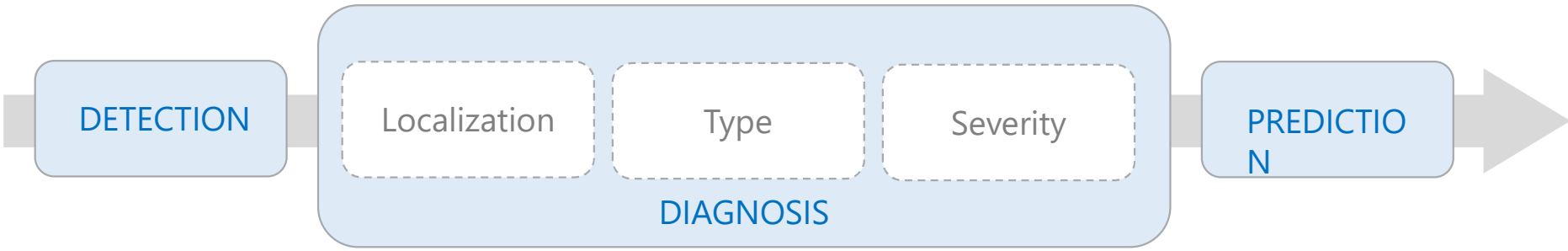
Level 1: Is the damage present in the structural system (detection)?

Level 2: Where is the damage located (localization)?

Level 3: What kind of damage is present (type)?

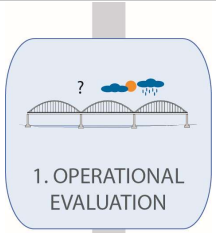
Level 4: What is the extent of damage (severity)?

Level 5: What is the residual lifetime (prediction)?



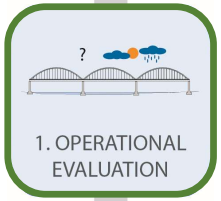
2. Theoretical Background

SHM Strategy for Damage Identification



2. Theoretical Background

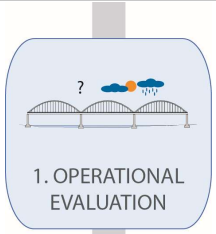
SHM Strategy for Damage Identification



1. What are the life safety and/or economic justifications for performing SHM?
2. How is damage defined for the system being monitored?
3. What are the operational and environmental conditions under which the monitored structural system functions?
4. What are the limitations on acquiring data in the operational environment?

2. Theoretical Background

SHM Strategy for Damage Identification





Types and amount of data to be collected:
- a. Sensors' placement,
- b. Data acquisition, storage and transmittal system.

Periodicity in data acquisition:
- a. Only after extreme events,
- b. Periodic intervals,
- c. Continuous.

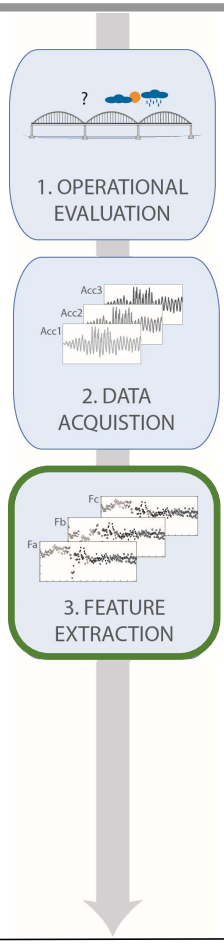
Monitoring typologies:
- a. Static-based,
- b. Vibration-based,
- c. Both.

Sources of variability:
- a. environmental conditions,
- b. data reduction conditions,

Data modelling and cleansing procedures

2. Theoretical Background

SHM Strategy for Damage Identification



Physical models for feature extraction:
- a. Linear VS nonlinear,
- b. Purely experimental or analytical/experimental

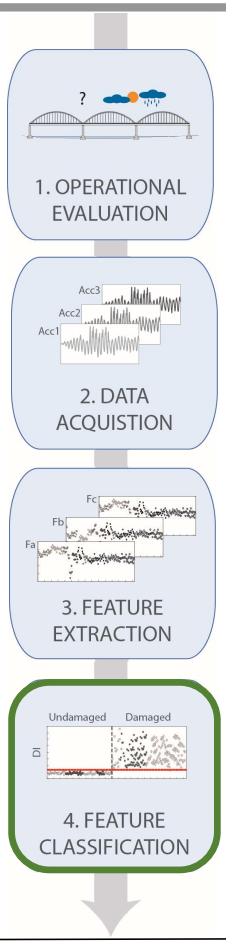
Basis for feature selection:
- a. Numerical analysis,
- b. Past experience

Damage-sensitive features based on:
- a. Static measurements,
- b. Vibration measurements,
- c. Both

Data modelling, fusion and compression

2. Theoretical Background

SHM Strategy for Damage Identification



Choose an approach:

a. Novelty identification is an inverse problem (model-based)

b. Novelty identification is a forward problem (data-driven)

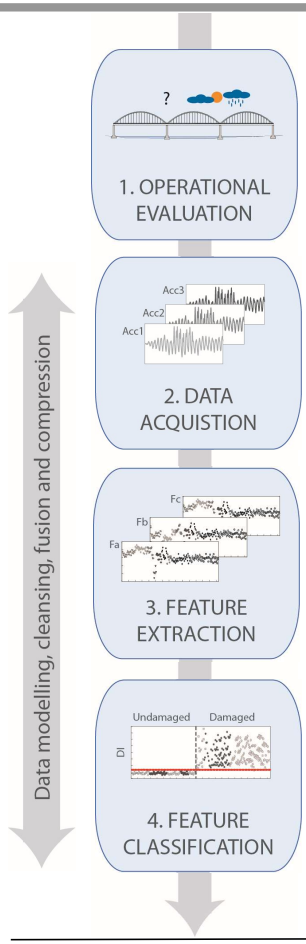
Build a statistical model for feature discrimination based on

a. Supervised learning (data available from undamaged and damaged state)

b. Unsupervised learning (data available from baseline state)

2. Theoretical Background

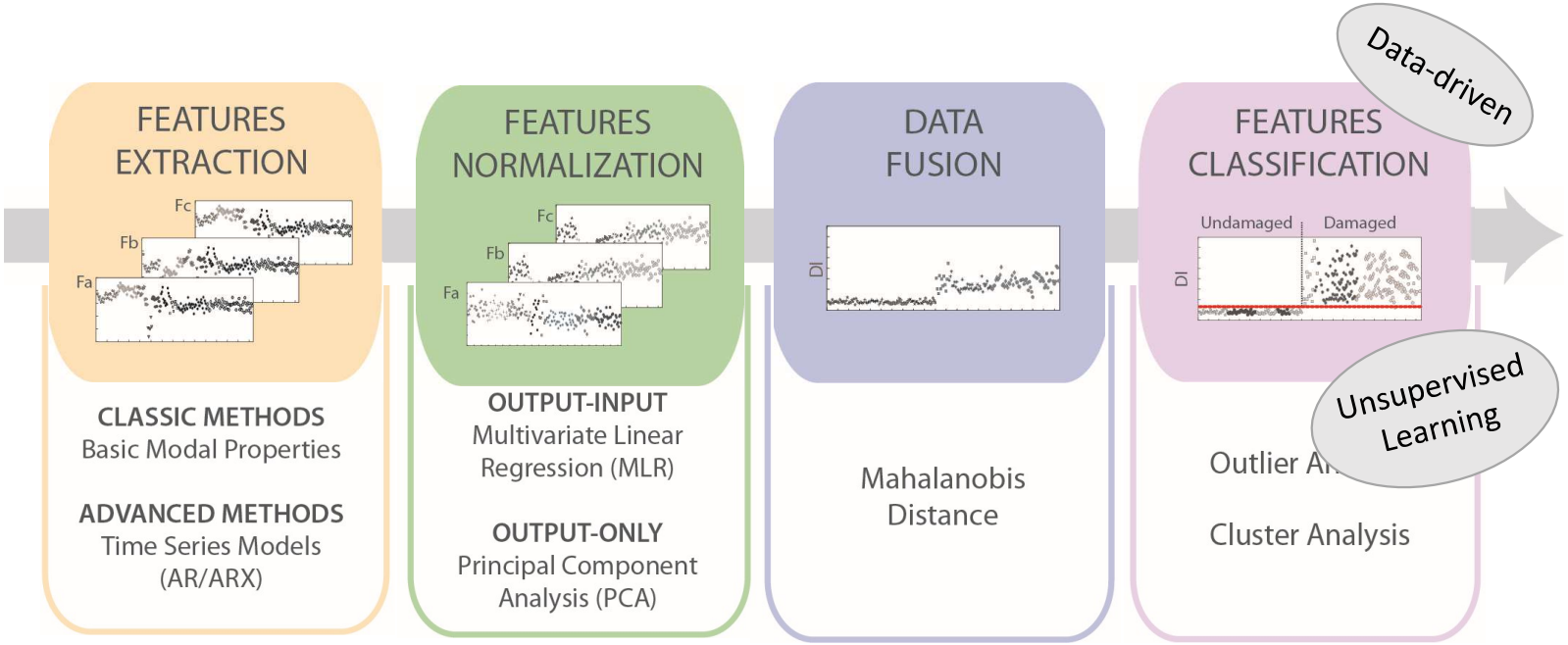
SHM Strategy for Damage Identification



MACHINE LEARNING METHODOLOGY FOR DAMAGE IDENTIFICATION

3. Machine Learning Methodology

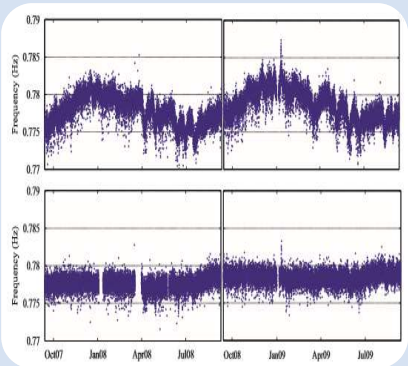
Steps description



3. Machine Learning Methodology

Features Extraction – Classic Methods

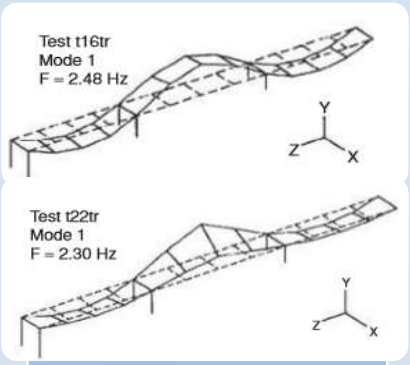
(Magalhães et al., 2011)



Frequency changes

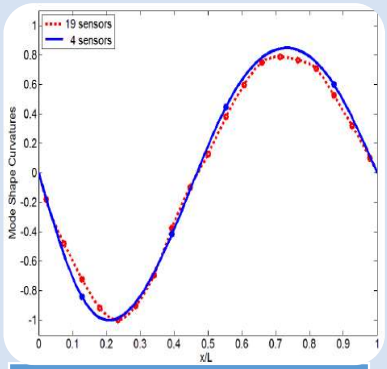
This approach assumes that damage causes changes in structural stiffness which, in turn, alter natural frequencies.

Farrar, C. & Worden, K. (2013)



Mode shape changes

Unlike natural frequencies, modal shapes can provide spatial information (location) of damage. Also, changes in them are more sensitive to local damage.



Mode shape curvature changes

The idea is that second derivatives of modal shapes are more sensitive to variations caused by structural damage.

3. Machine Learning Methodology

Features Extraction – Classic Methods

ADVANTAGES	DISADVANTAGES
• Easy to implement; • Easy to understand; • Easy to extract from raw data (dynamic signals); • Low statistical uncertainty in the measured values (robustness in modal identification).	• Low sensitivity to early damages; • Requires the observation of a high number of dof when the structures are complex; • For complex systems (such as real-world structures), it is hardly possible to obtain the spatial information of structural changes; • Difficulty in finding damage close to the bearings.

3. Machine Learning Methodology

Features Extraction – Advanced Methods

AutoRegressive (AR) model

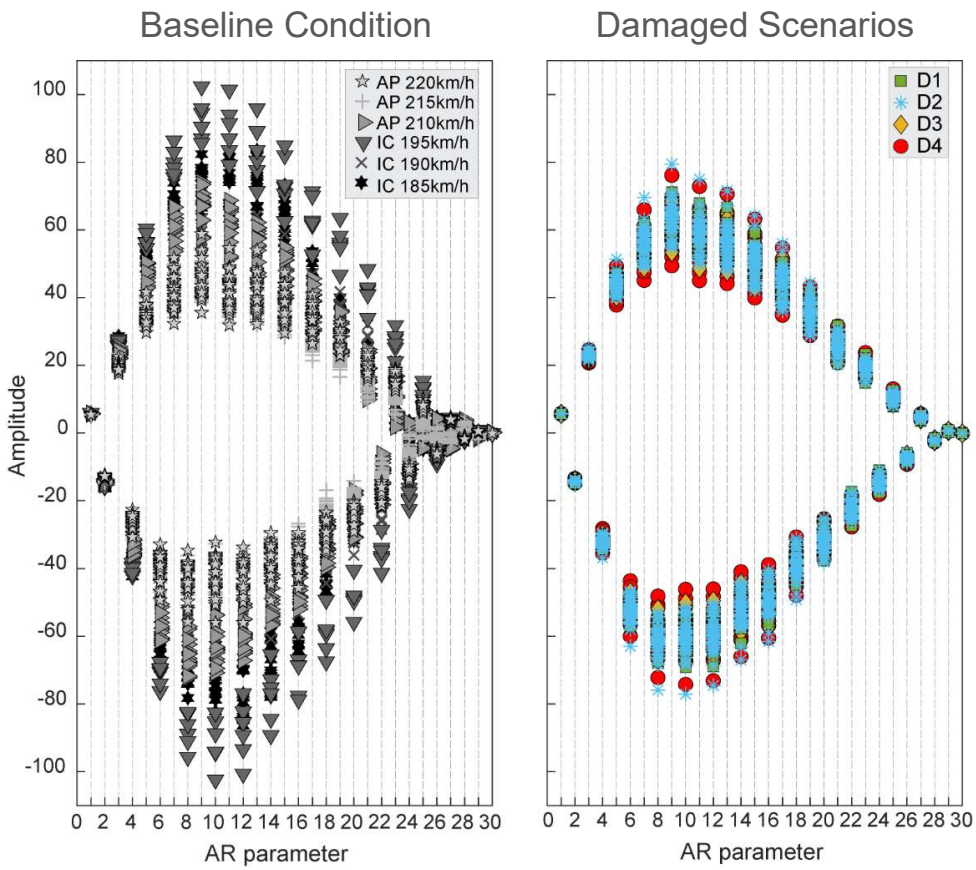
The Autoregressive Model, usually designated AR(p), where p is the order of the model, is a linear time series model defined as:

$$y_j = \sum_{i=1}^{n_a} a_i y_{j-i} + \varepsilon_j$$

where y_j , the current value of the response, is defined as a linear combination of n_a previous response values linearly combined by the coefficients a_i.

Typical time series lead to an overdetermined set of equations that must be solved to obtain estimates of the AR coefficients (Yule-Walker and least-squares methods).

The appropriate model order can be determined by several methods (Akaike's information criterion, partial autocorrelation function, SVD, etc.)



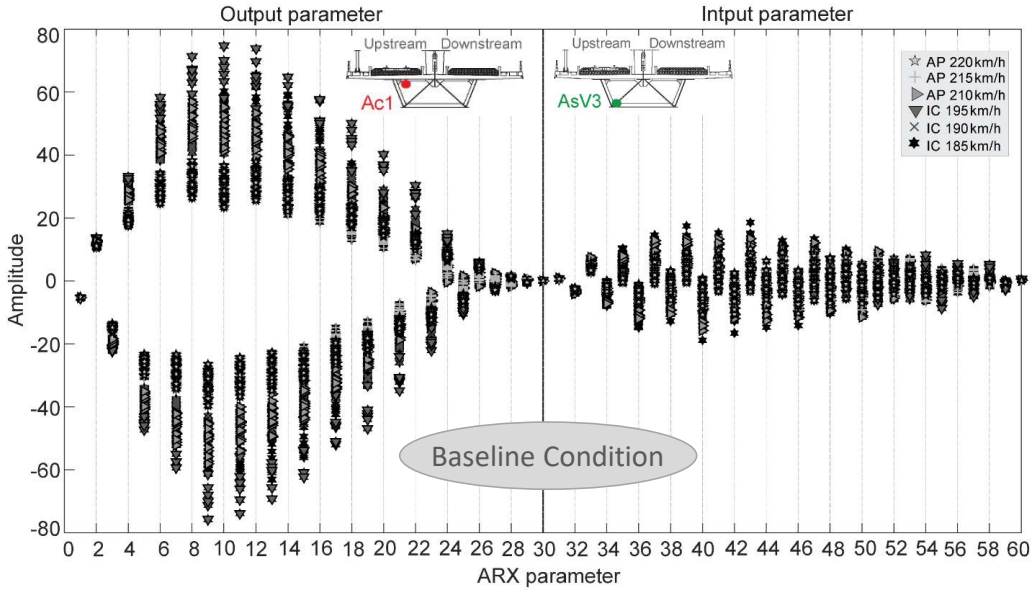
3. Machine Learning Methodology

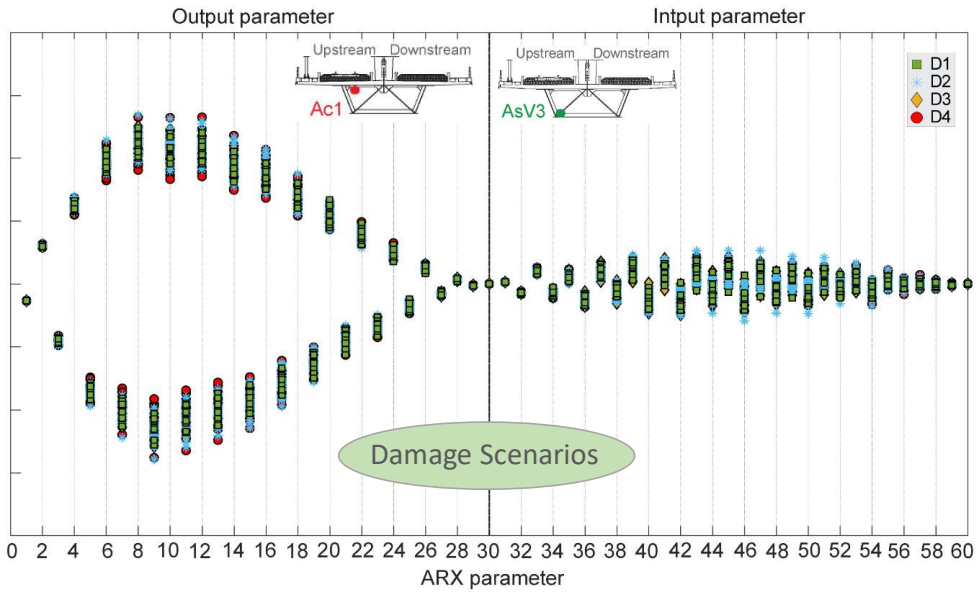
Features Extraction – Advanced Methods

AutoRegressive eXogenous (ARX) model

The ARX model regresses the current measurement upon finite measurements of its past and upon an exogenous input series, where y_j, x_j, and ε_j are output, input, and error terms of the model at the signal value j, respectively. On the other hand, n_a, n_b and a_i, b_k represent the orders and the parameters of the output and input data, respectively.

$$y_j = \sum_{i=1}^{n_a} a_i y_{j-i} + \sum_{k=1}^{n_b} b_k x_{j-k} + \varepsilon_j$$





3. Machine Learning Methodology

Features Extraction – Advanced Methods

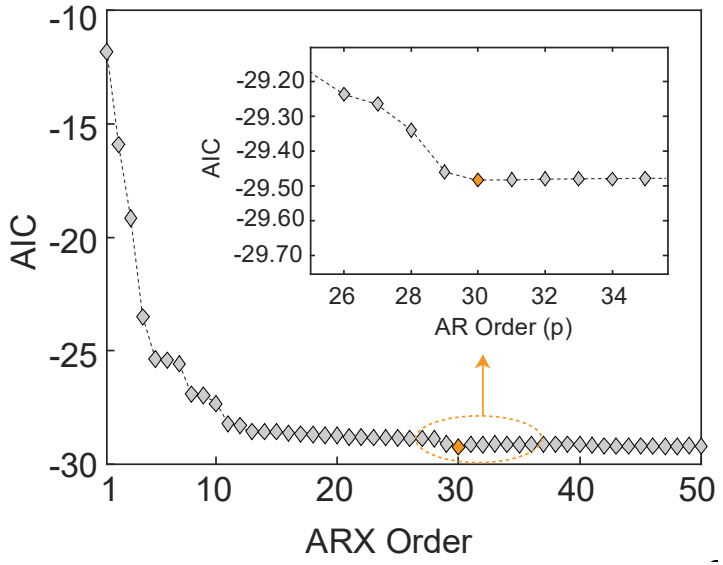
AutoRegressive eXogenous (ARX) model order

Akaike's information criterion (AIC)

The AIC is a measure of the goodness-of-fit of an estimated statistical model that is based on the trade-off between fitting accuracy and number of estimated parameters. In the context of ARX models this criterion assume the form:

$$AIC = N_t \, ln \, \varepsilon + 2N_p$$

where N_p is the number of estimated parameters, N_t the number of predicted data points, and ε=SSR/N_t the average sum-of-square residual (SSR) errors. To find out an optimum order, one should examine a wide range of orders and choose a number with the minimum AIC value.



3. Machine Learning Methodology

Features Extraction – Advanced Methods

AutoRegressive eXogenous (ARX) model order

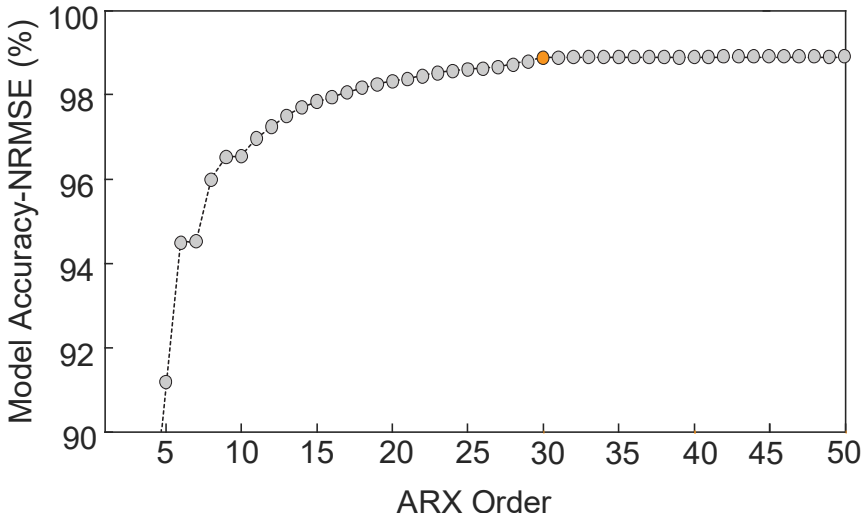
Normalized Root Mean Square Error (NRMSE)

NRMSE fitness value can also be used to quantify the model accuracy according to the ARX order defined.

$$NRMSE = 1 - \frac{\sum_{i=1}^{n}(y_i - \hat{y}_i)^2}{\sum_{i=1}^{n}(y_i - \bar{y})^2}$$

where, y_i is the measured data, $\hat{y}_i$ is the simulated data through the ARX model, and $\bar{y}$ is the mean of the measured dataset.

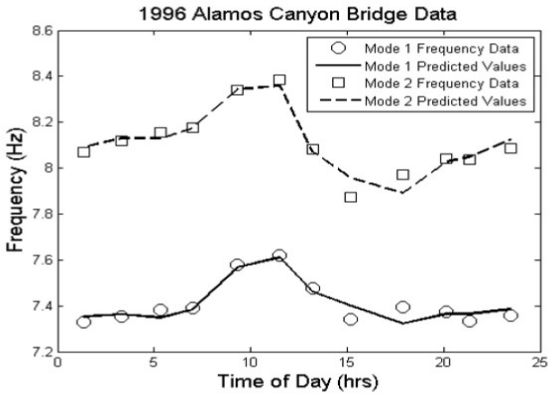
To find out an optimum order, one should examine a wide range of orders and choose a number with the maximum NRMSE value.



3. Machine Learning Methodology

Features Normalization

(Figueiredo, 2010)



FEATURES NORMALIZATION APPROACHES

Regression-based methods (Input-output)

- Multivariate Linear Regression (MLR)
- Multi-layer Perceptron (MLP)

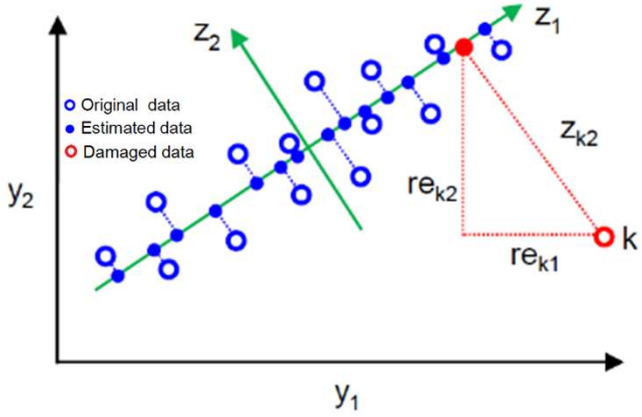
Environmental and operational actions need to be measured.

Latent-variable methods (Output only)

- Principal Component Analysis (PCA)
- Auto Associative Neural Networks (AANN)

Suppress independent actions using only structural measurements

(Santos, 2014)



3. Machine Learning Methodology

Features Normalization

Multivariate Linear Regression (MLR)

The MLR model uses a set of measured environmental and operational variations (EOVs) as inputs and delivers a matrix output that represents the estimated (or predicted) features.

Given *m* features, *n* baseline simulations and *s* operational / environmental actions, the multivariate regression model is expressed by the following:

$$Y = X \cdot \hat{w} + \varepsilon_{MLR}$$

***n-by-m* output matrix of predicted features**

***n-by-(s+1)* EOVs matrix**

***n-by-m* regression error**

***(s+1)-by-m* matrix of coefficients that weights EOVs input**

The coefficients of the model parameters $\hat{w}$ are obtained through the least squares method and given by the following equation:

$$\hat{w} = (X^T \cdot X)^{-1} \cdot X^T \cdot Y$$

Once the model is calibrated, i.e., the optimal weights are evaluated, new data can be used as input ($\hat{X}$) and the residual error matrix $\hat{\varepsilon}_{MLR}$, which corresponds to the damage-sensitive features from which the EOVs effects are removed, is denoted by:

$$\hat{\varepsilon}_{MLR} = Y - \hat{X} \cdot \hat{w}$$

3. Machine Learning Methodology

Features Normalization

Principal Component Analysis (PCA)

A Principal Component Analysis (PCA) uses an orthogonal transformation to convert a set of measurements of correlated events (***v*** measured events with ***n*** observations each) into a set of values of linearly uncorrelated variables called **principal components** (***q*** components).

$$Z_{(n\times q)} = X_{(n\times v)}\, U_{(v\times q)} \qquad \text{with:} \quad X = \begin{bmatrix} x_1^1 & x_1^2 & \dots & x_1^v \\ x_2^1 & x_2^2 & \dots & x_2^v \\ \vdots & \vdots & \dots & \vdots \\ x_n^1 & x_n^2 & \dots & x_n^v \end{bmatrix}$$

Matrix with data in the transformed space

Matrix with data in the original space

Transformation Matrix

The transformation matrix U can be obtained by means of a singular value decomposition (SVD) of the covariance matrix C:

$$C = U\,\Lambda\,V^T \qquad \text{with:} \quad C = \begin{bmatrix} var(x^1) & cov(x^1,x^2) & \dots & cov(x^1,x^v) \\ cov(x^2,x^1) & var(x^2) & \dots & cov(x^1,x^v) \\ \vdots & \vdots & \ddots & \vdots \\ cov(x^v,x^1) & cov(x^v,x^2) & \dots & var(x^v) \end{bmatrix}$$

Diagonal matrix w/ principal components values

3. Machine Learning Methodology

Features Normalization

Principal Component Analysis (PCA)

In case of removing some of the principal components the inverse transformation can give the correspondent re-projected data (X'):

$$X' = X\ U\ U^T$$

where matrix U includes only the principal vectors of interest.

The number of principal components of interest depends of the problem type.

Typically, the principal components associated with the **environmental and operational factors** **have larger values because are normally associated with parts of the time records with higher amplitudes and limited duration.**

Whereas variations related to other effects, especially those of small magnitude, such as **early-damage**, **may be summarized in latter components.**

Since the aim is to detect damage, which has generally a local effect, the feature normalization procedure consists of **removing the most significant principal components from the features** and **retaining the rest for subsequent statistical analysis**.

3. Machine Learning Methodology

Data Fusion

Mahalanobis Distance

The Mahalanobis Distance (MD) was selected since it is based on the AR/ARX parameters' centre and covariance, therefore enabling additional sensitivity if these quantities are computed using only the features extracted from the baseline conditions.

With this approach, the **MD measures the distance between the representative baseline and each set of features extracted**.

Smaller MD values represent greater similarities with the representative baseline, while higher values reveal greater differences, and, therefore, more dissimilar structural conditions.

The analytical expression of Mahalanobis Distance for each simulation i is given by:

$$MD_i = \sqrt{(x_i - \bar{x}) \cdot {S_x}^{-1} \cdot (x_i - \bar{x})^T}$$

where x_i is a vector of *m* features representing the potential damage/outlier, $\bar{x}$ is the matrix of the means of the features estimated on baseline simulations, and S_x is the covariance matrix of the baseline simulations.

The MD can be applied in two different stages: stage 1: **to merge features**; stage 2: **to merge sensors**.

3. Machine Learning Methodology

Features Classification

Outlier Analysis

Generally, the literature assumes that the Mahalanobis squared distance can be approximated by a chi-squared distribution in n-dimensional space, thus the **Mahalanobis distance can be approximated by a normal (or Gaussian) distribution and an outlier analysis can be performed based on a statistical threshold.**

A confidence boundary (CB) to detect a damage index (DI) that constitutes an outlier can be estimated by the Gaussian inverse cumulative distribution function (ICDF) considering a mean $\bar{\mu}$ and standard deviation σ of the baseline feature vector, and for a level of significance α. The inverse function can be defined in terms of the Gaussian cumulative distribution function (CDF) as follows:

$$CB = invF(1-\alpha)$$

Where,

$$F(x|\bar{\mu},\sigma) = \frac{1}{\sigma\sqrt{2\pi}}\int_{-\infty}^{x} e^{-\frac{1}{2}\left(\frac{x-\bar{\mu}}{\sigma}\right)^2} dy, for\ x\epsilon\mathbb{R}$$

Thus, **a feature is considered to be an outlier when its DI is equal or greater than CB**. It is important to note that the selection of α carries a trade-off between the Type I error (false positive indication of damage) and the Type II error (false-negative indication of damage).

3. Machine Learning Methodology

Features Classification

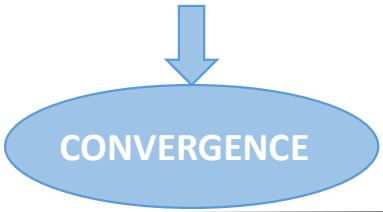
Cluster Analysis

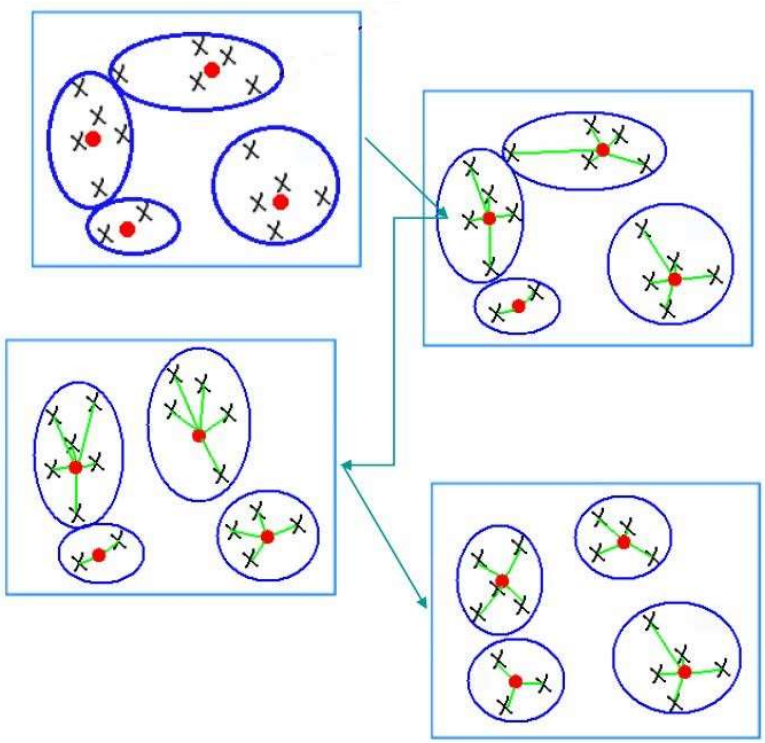
Silhouette Index

Validity Index that allows to assess which partition is the most suitable for representing the data's structures.
The higher the Silhouette, the more compact and separate are the clusters. Hence, its maximal value indicates the optimal partition.

K-means method

1. Random initialization of the *k* **clusters**;
2. Calculation of **distances** between each feature and the nearest **cluster**;
3. Clusters update:
   Minimization of the square of the sum of **distances** between features





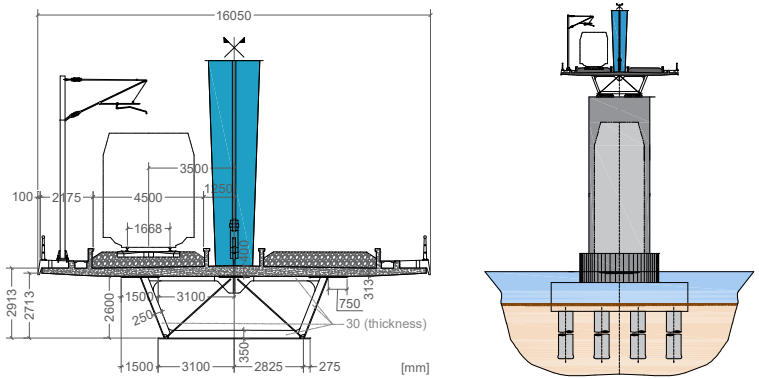
(Cury et al., 2012)

4. Case studies

Bridge Health Monitoring

Alcácer do Sal Bridge

- Composite bowstring-arch bridge with a concrete slab laid over a steel box girder;
- 3 parabolic arches connected to each span of the deck by 18 hangers;
- Total length of 480 m divided in 3 continuous spans;
- The deck is fixed on pier P1, whereas on piers P2, P3 and P4 only the transverse movements of the deck are restrained;
- Only the upstream track is currently in operation.



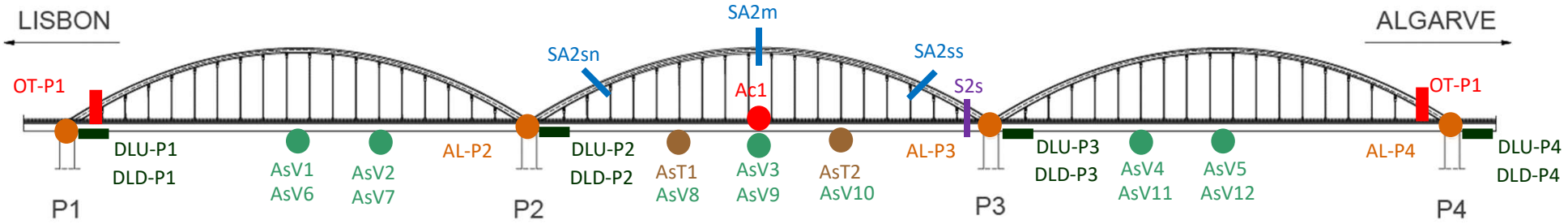


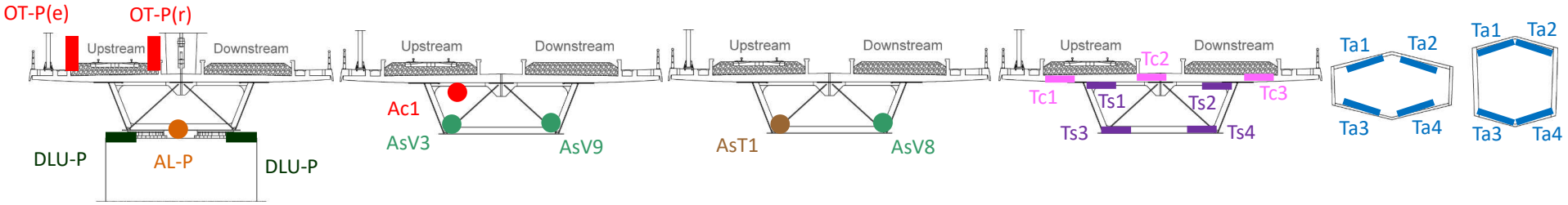


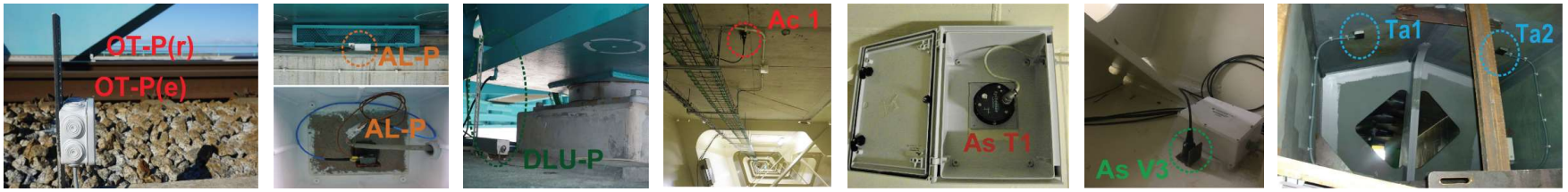
4. Case studies

Bridge Health Monitoring

Dynamic Monitoring System



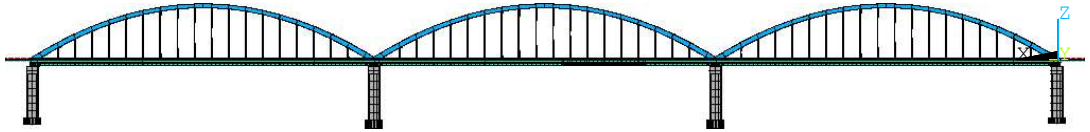


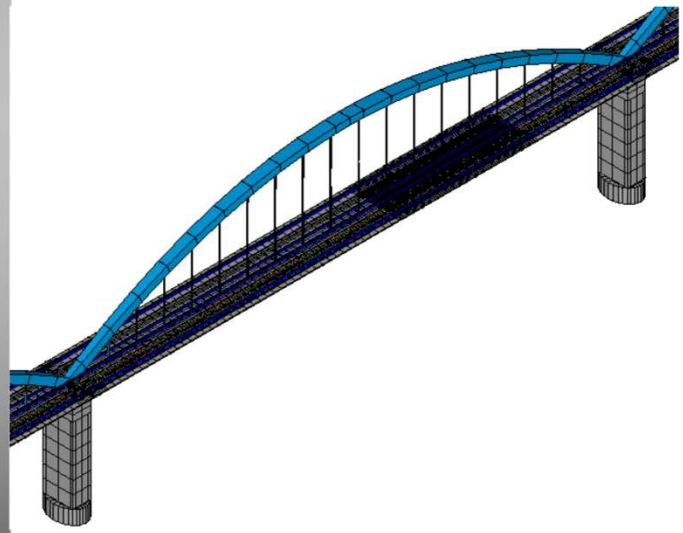


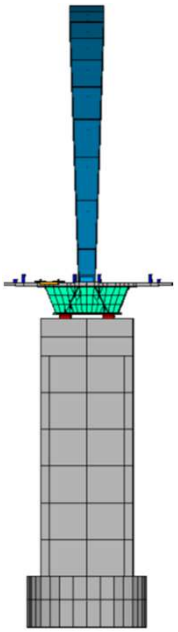
4. Case studies

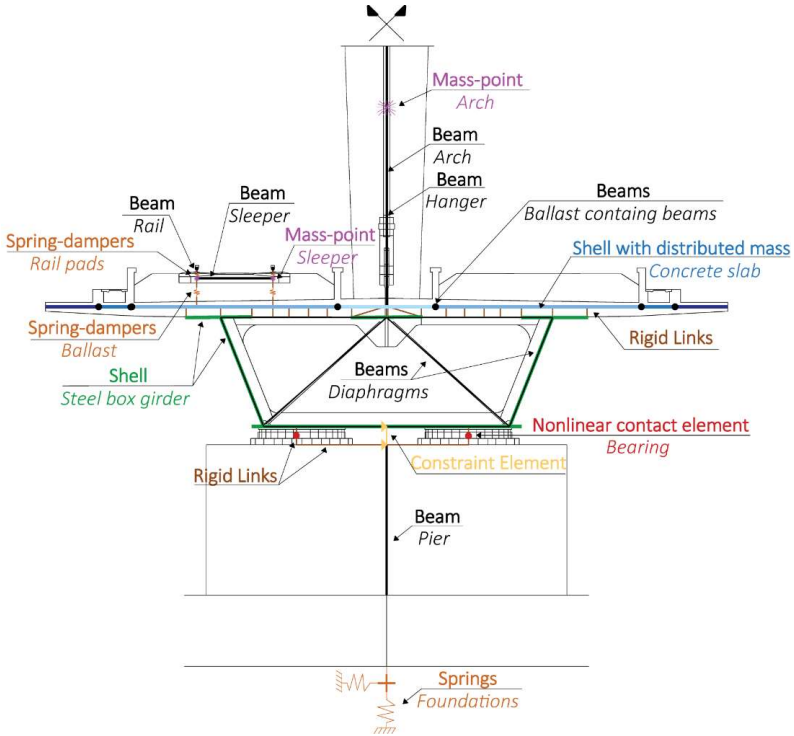
Bridge Health Monitoring

Numerical Modelling









4. Case studies

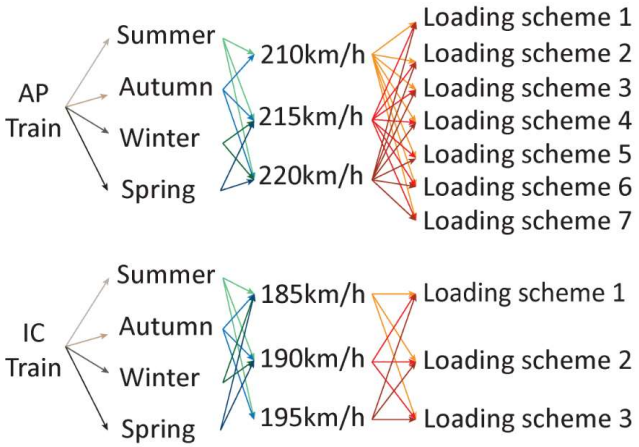
Bridge Health Monitoring

Simulation of baseline and damaged scenarios

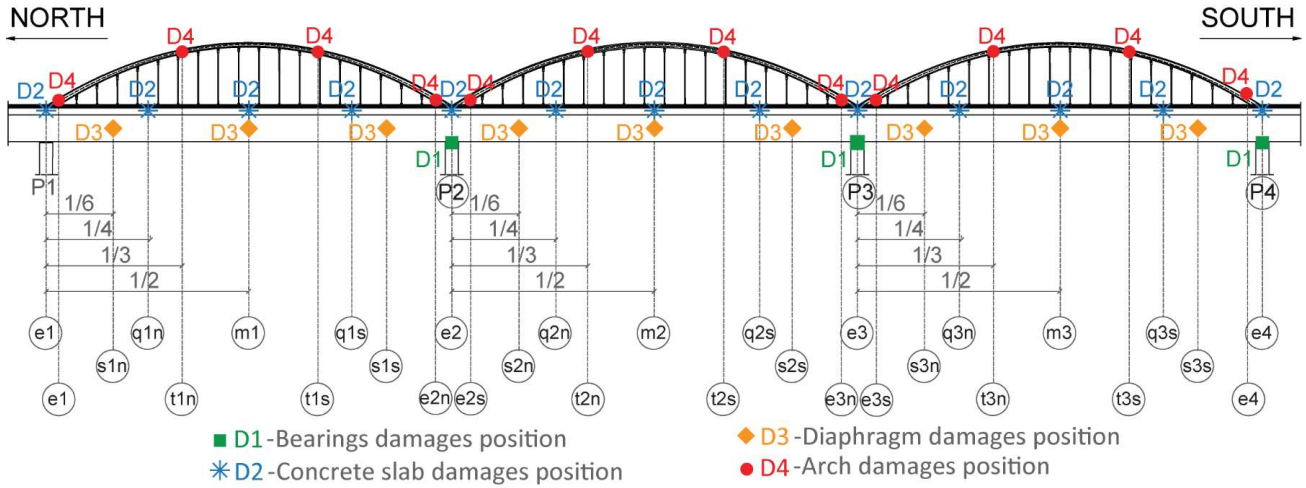
Different combinations for the baseline condition, that aim at reproducing the bridge responses considering the variability of train type, speed, temperature actions, and loads, were simulated.

Damage severities of 5%, 10% and 20% of stiffness reductions in the concrete slab, diaphragm and arches were simulated, as well as friction increases in the movements of the bearing devices from a reference value of 1.5% to 1.8%, 2.4%, 3.0% and the full restraint of these elements.

Baseline Condition



Types of Damages

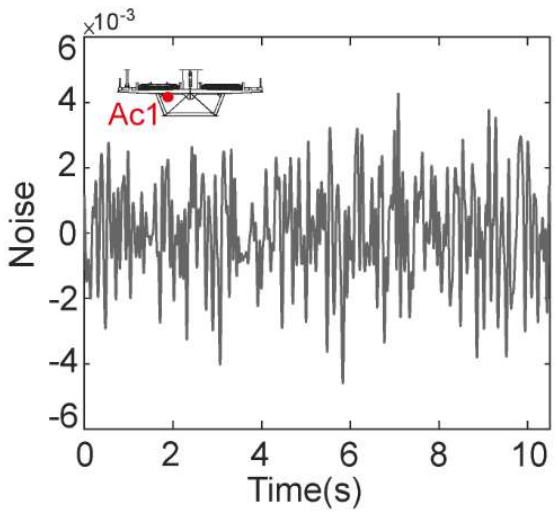


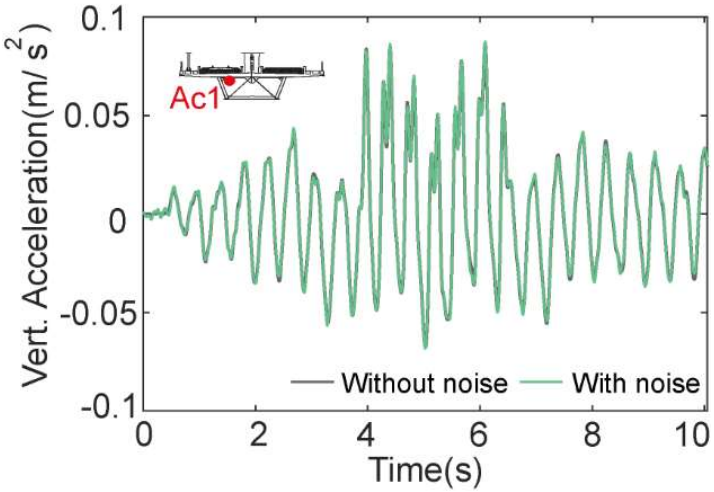
4. Case studies

Bridge Health Monitoring

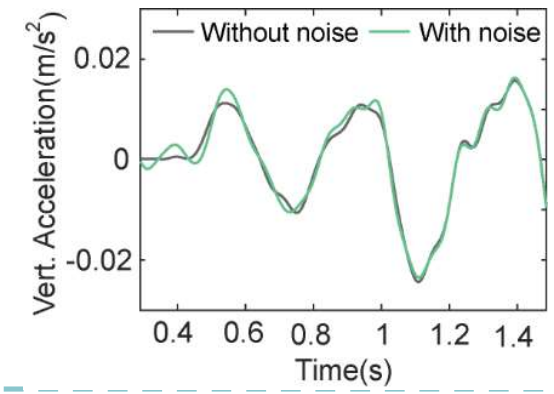
Noise Distribution

To obtain the most similar and reliable reproduction of the real SHM data, the noise measured on site by each accelerometer was added to the corresponding numerical output.





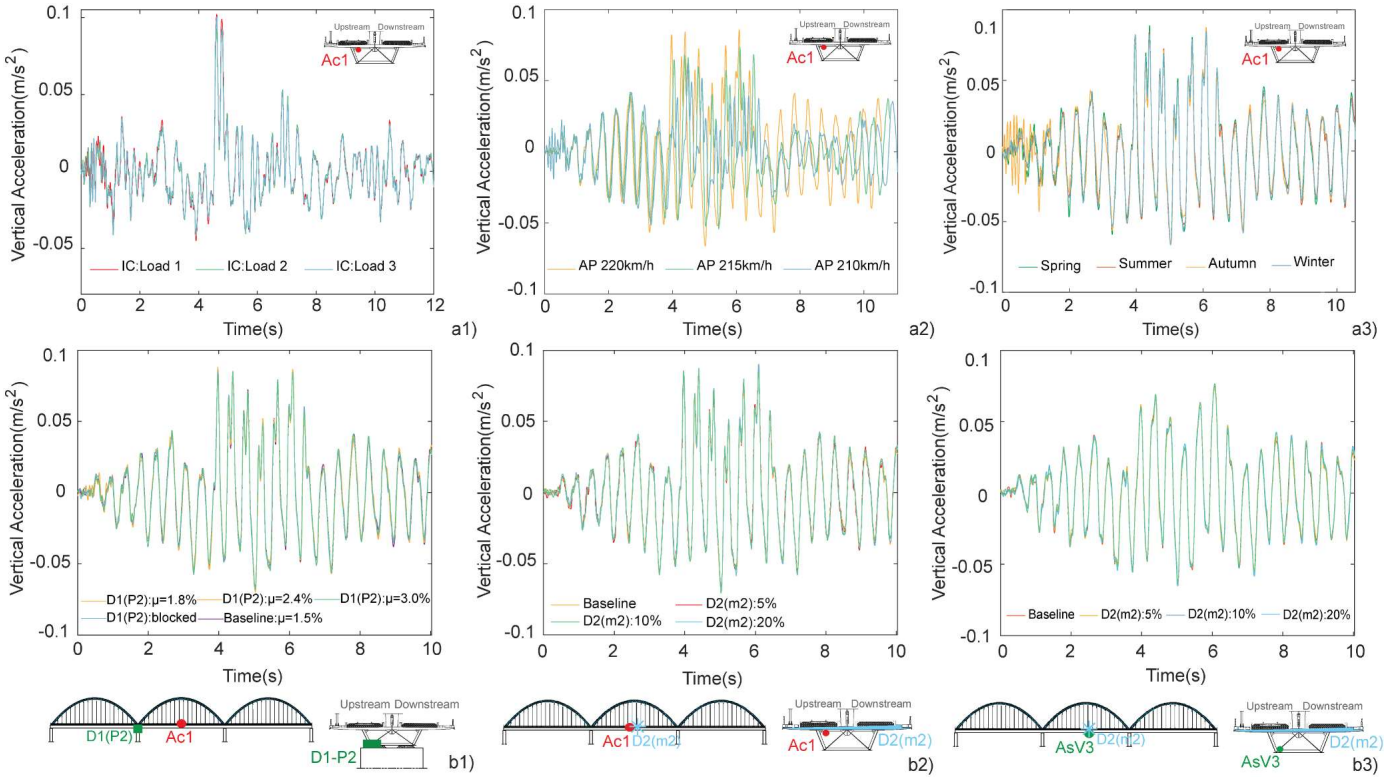
Window



4. Case studies

Bridge Health Monitoring

Numerical Simulation



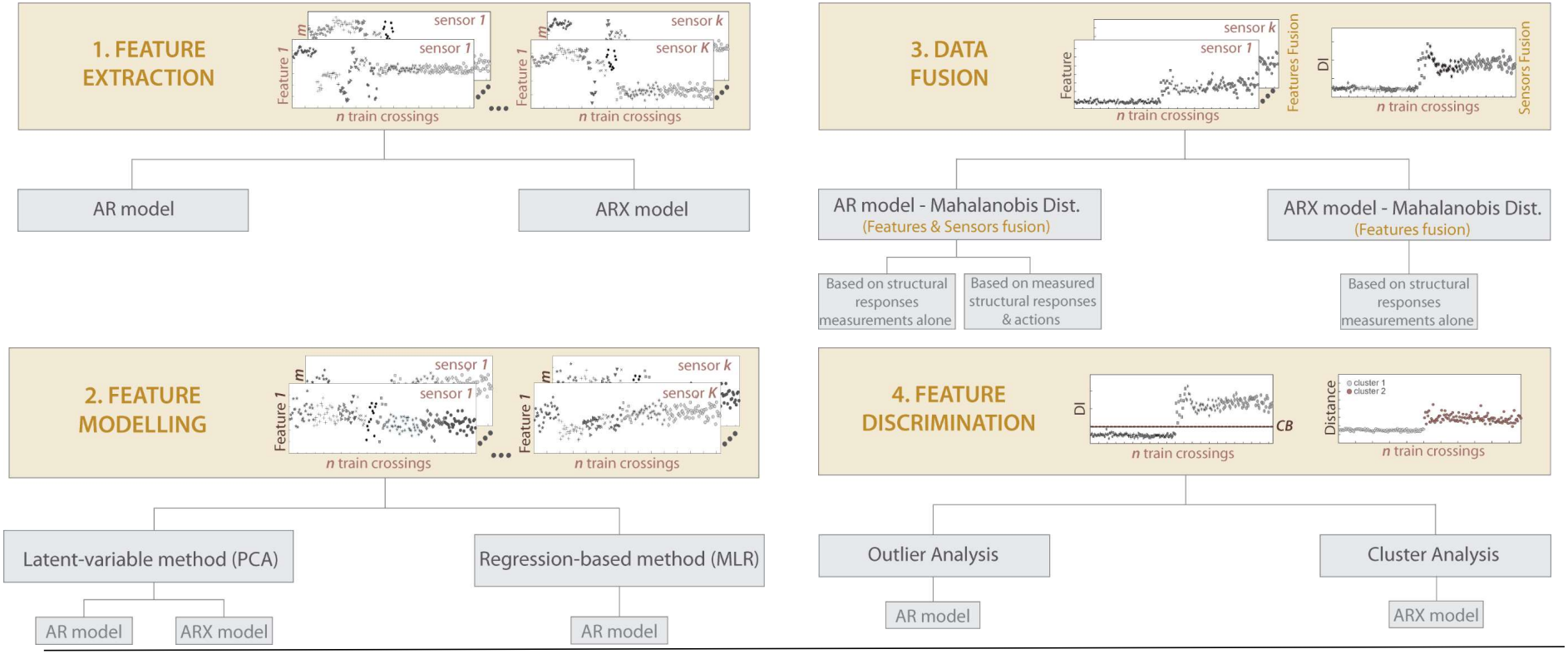
Baseline Condition

Damaged Scenarios

4. Case studies

Bridge Health Monitoring

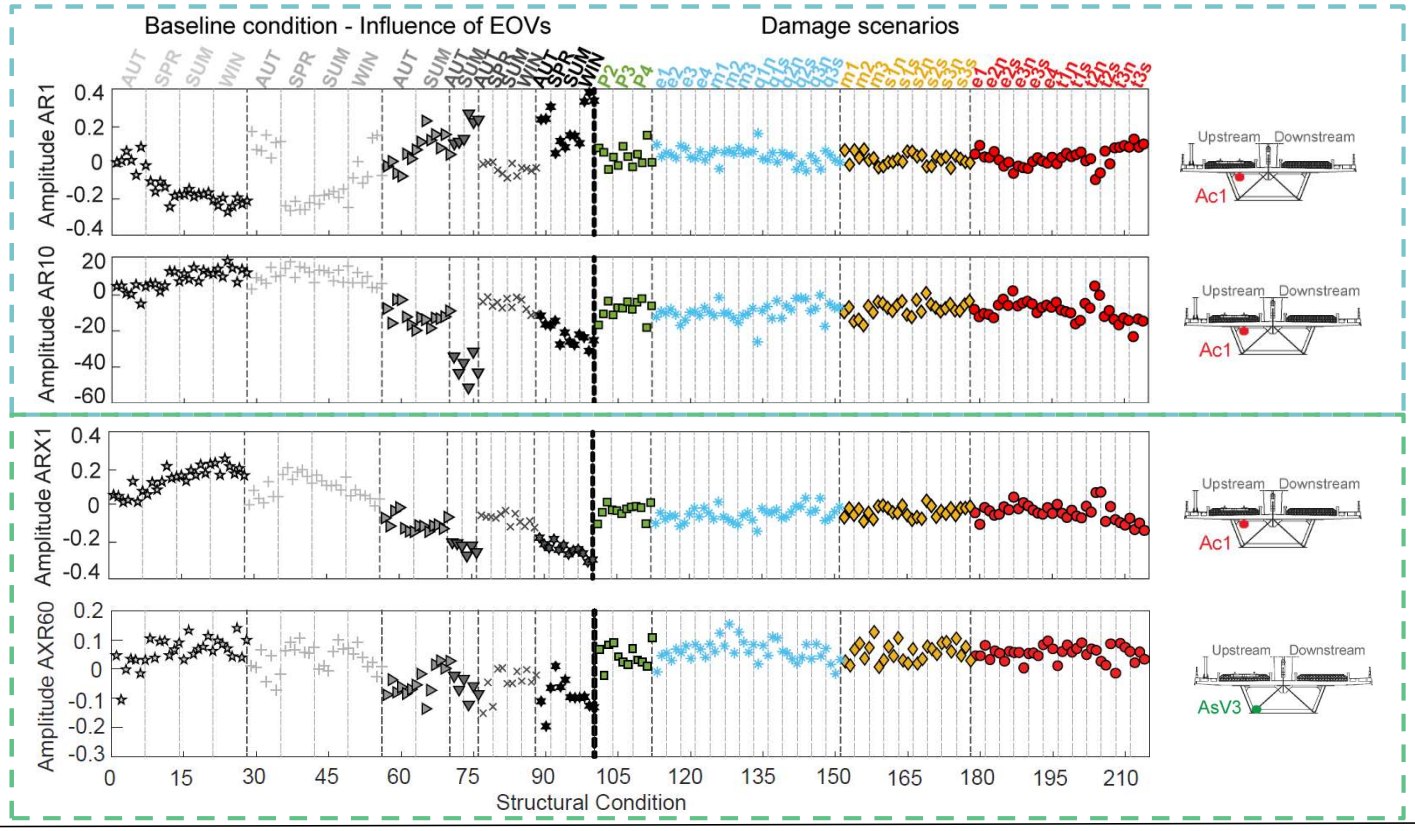
Machine Learning Methodology



4. Case studies

Bridge Health Monitoring

Features Extraction



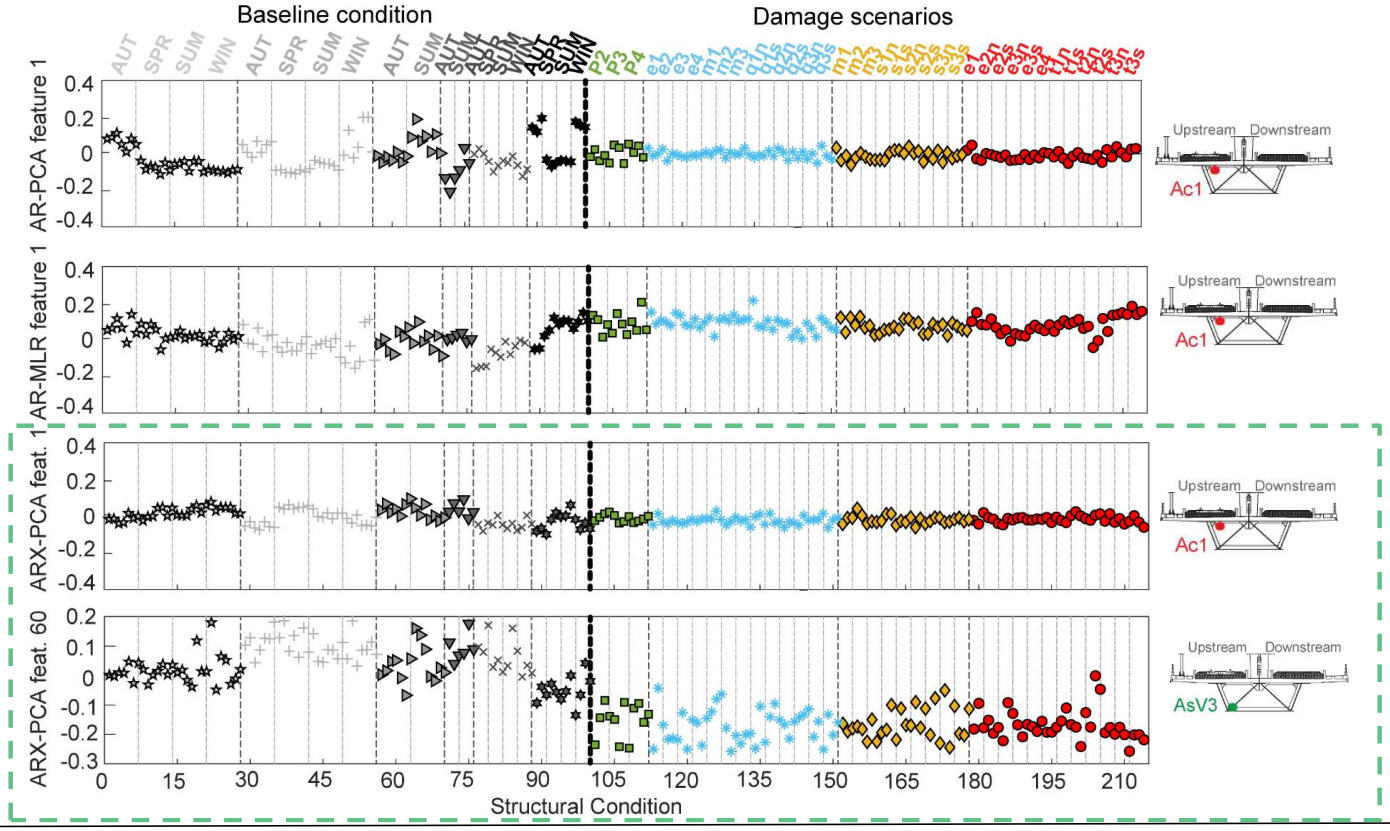
AR parameters

ARX parameters

4. Case studies

Bridge Health Monitoring

Features Normalization



AR PCA

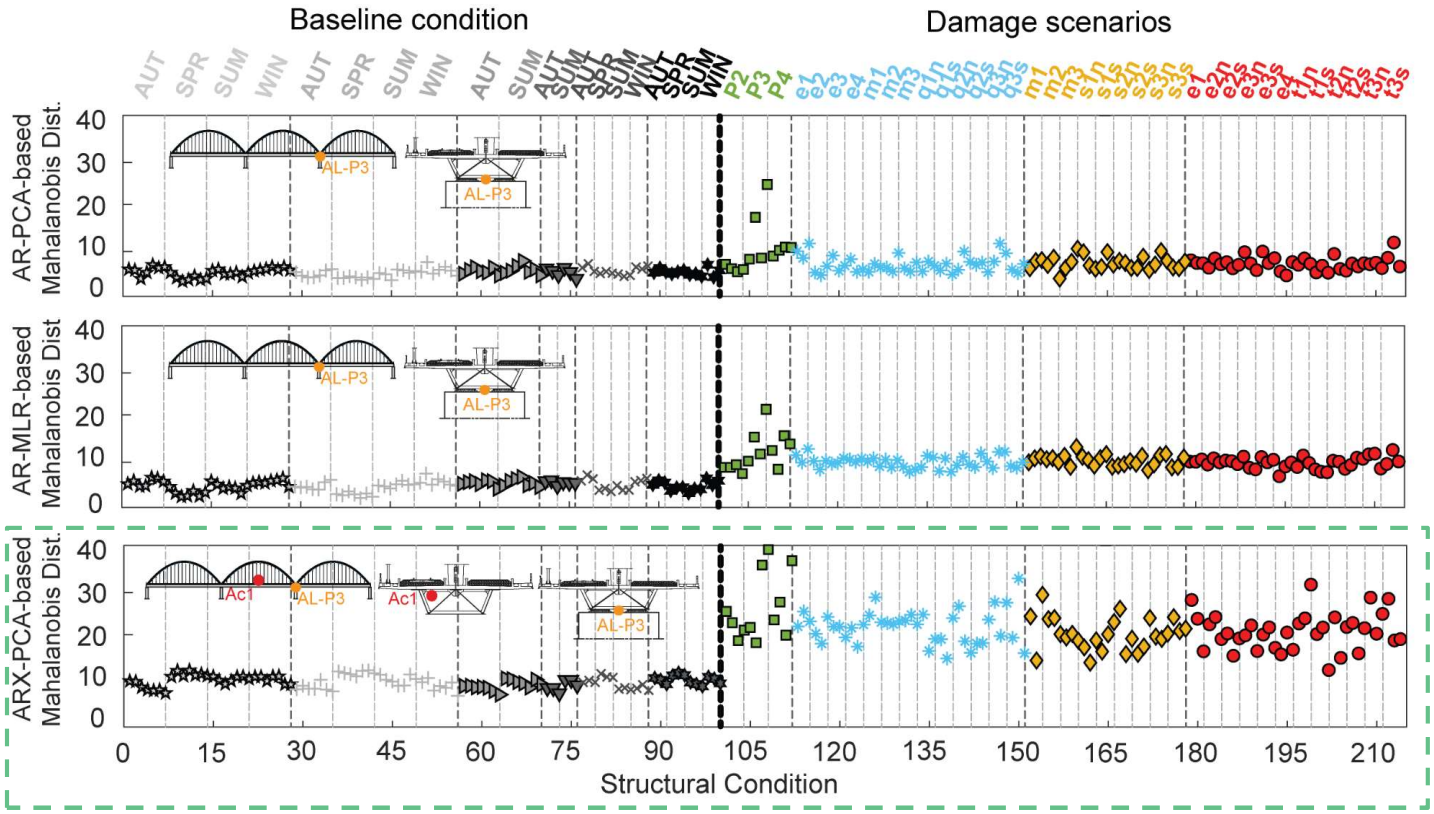
AR MLR

ARX PCA

4. Case studies

Bridge Health Monitoring

Features Fusion



AR PCA

AR MLR

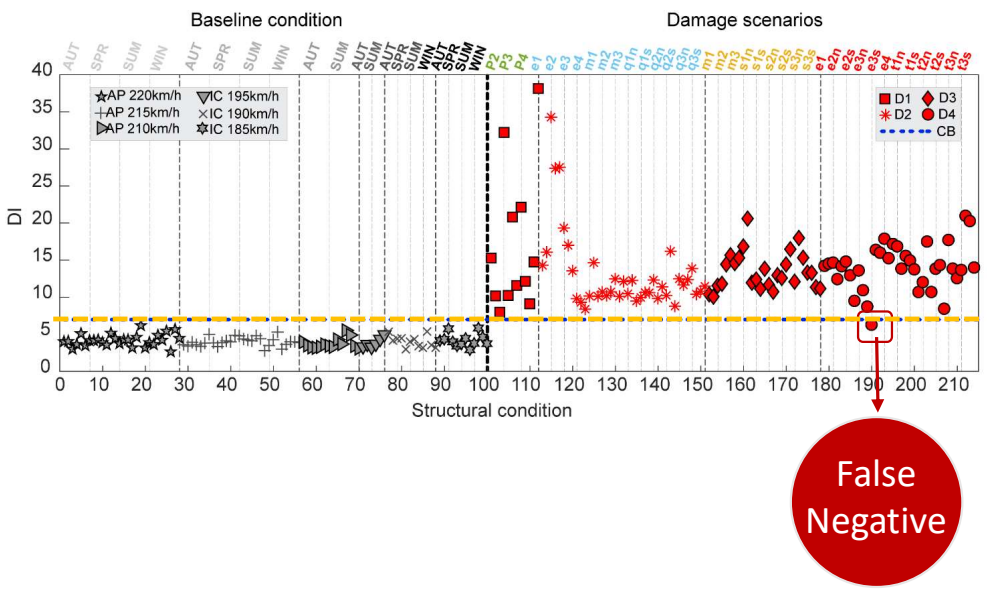
ARX PCA

4. Case studies

Bridge Health Monitoring

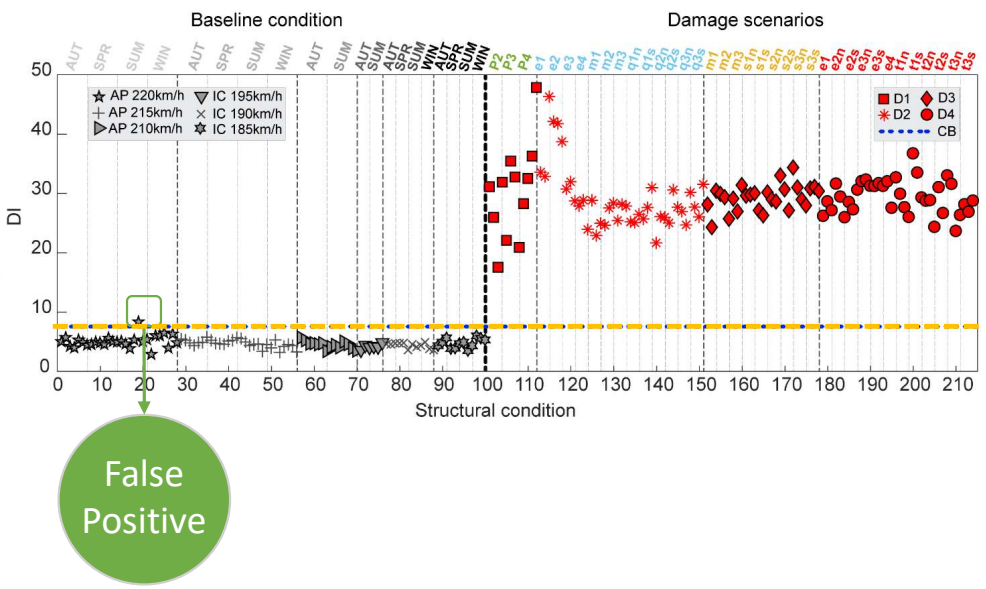
Features Classification – Outlier Analysis

AR-PCA



False Negative

AR-MLR



False Positive

4. Case studies

Bridge Health Monitoring

Features Classification – Cluster Analysis

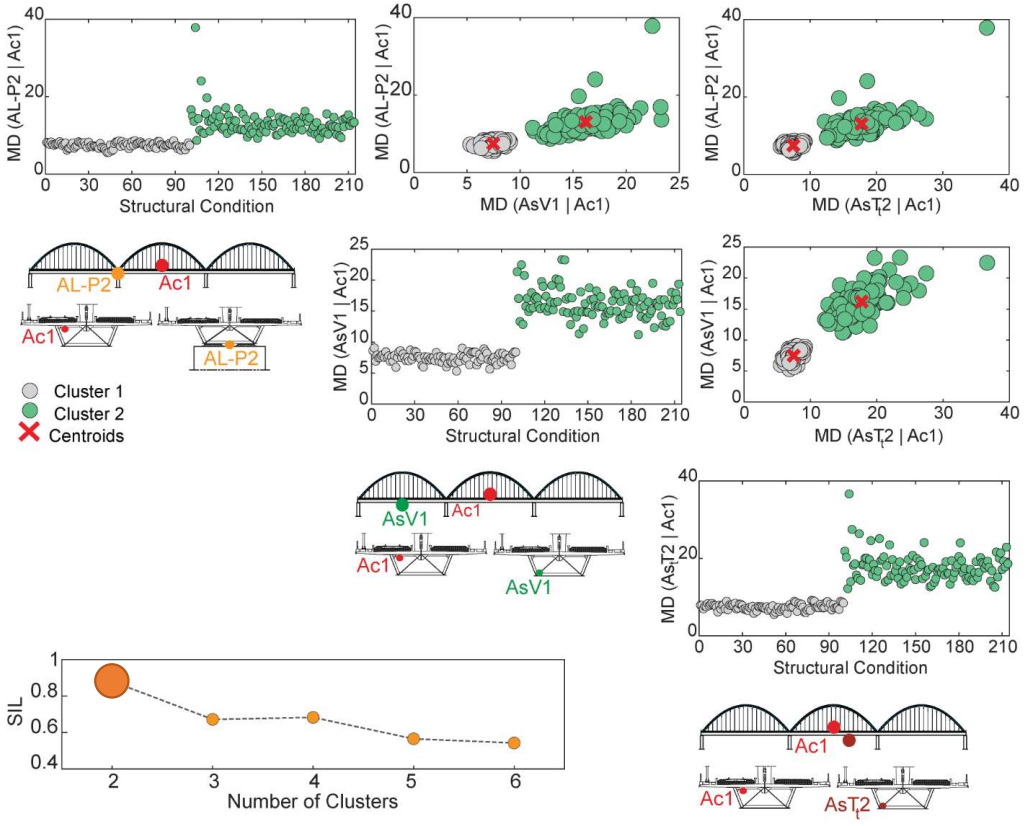
The aim of the clustering process is to divide a dataset into groups, which must be **as compact and separate as possible**.

The application of the **k-means** is exemplified here using the ARX-PCA-based features after fusion for each sensor cluster.

The **SIL indices** extracted from five cluster partitions exhibit a **maximum for k=2 clusters**.

It can be observed the dissimilarity between the two centroids of three different combinations of sensors, while the plots in the diagonal of this figure show that the two clusters found for each couple of sensors are separated when the simulated damages start.

The clusters have the advantage of allowing a **multidimensional representation of the features**, unlike the Mahalanobis distance, which is unidimensional.



4. Case studies

Wayside Monitoring





Wheel Flat Identification



Wheel Polygonization Detection

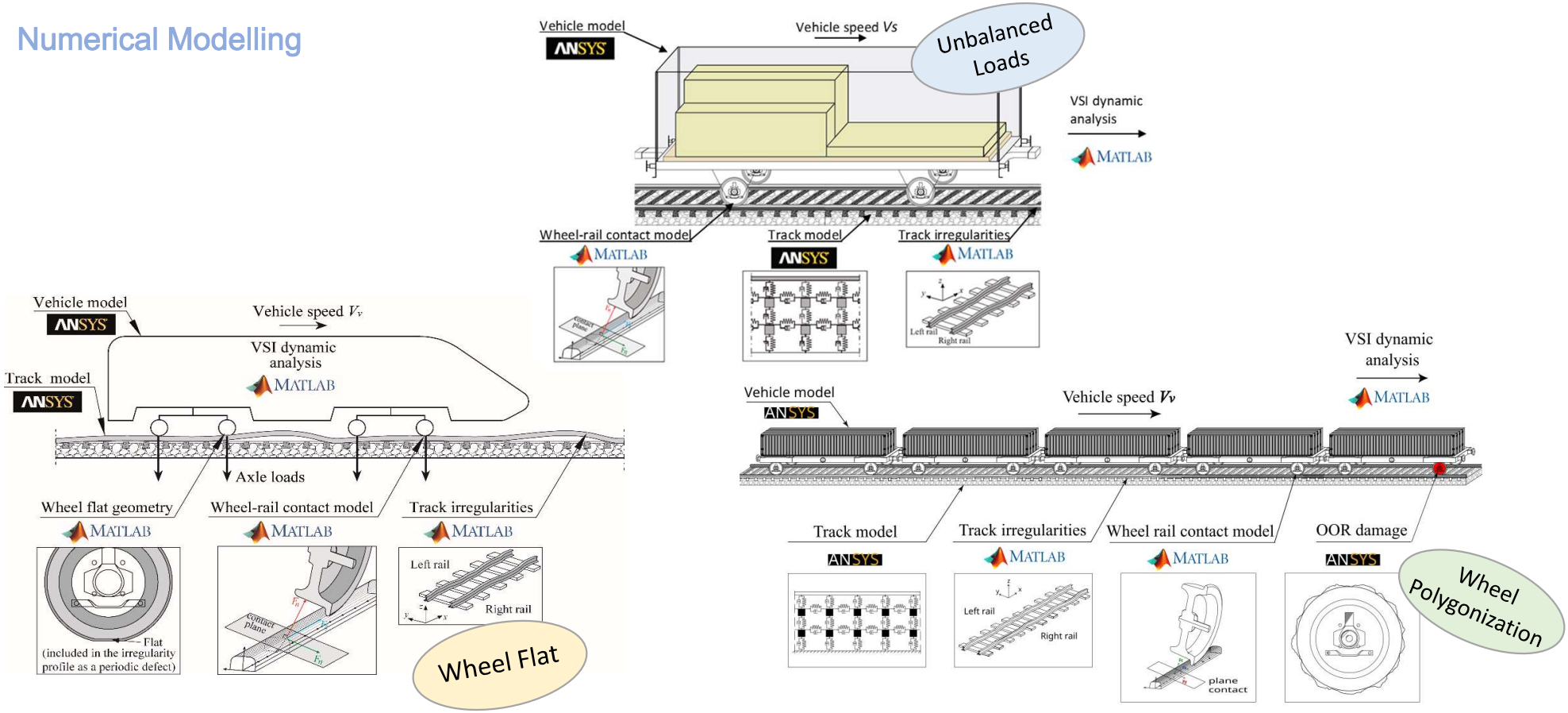


Unbalanced Loads Detection

4. Case studies

Wayside Monitoring

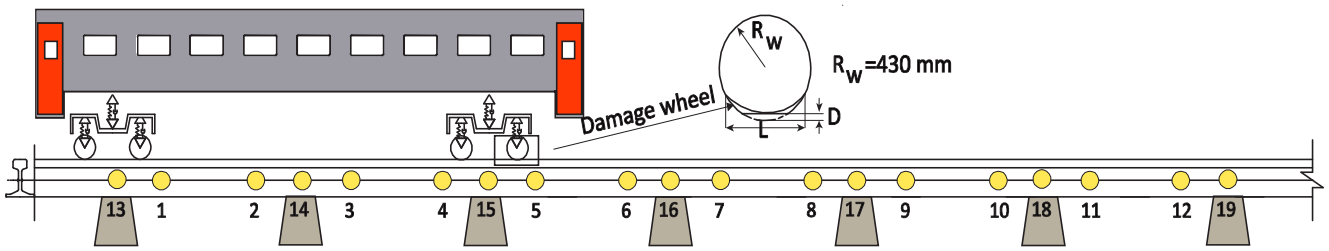
Numerical Modelling



4. Case studies

Wayside Monitoring – Wheel flat identification

Virtual monitoring system



Baseline scenarios

Alfa Pendular

3 types of loading scheme

10 unevenness profiles

v = 20 to 60 m/s

noise = 5%

Total: 100 baseline scenarios

Damage scenarios

Alfa Pendular

1 type of loading scheme

1 unevenness profile

v = 60 m/s

noise = 5%

Flat lengths: 10-20 mm

25-50 mm

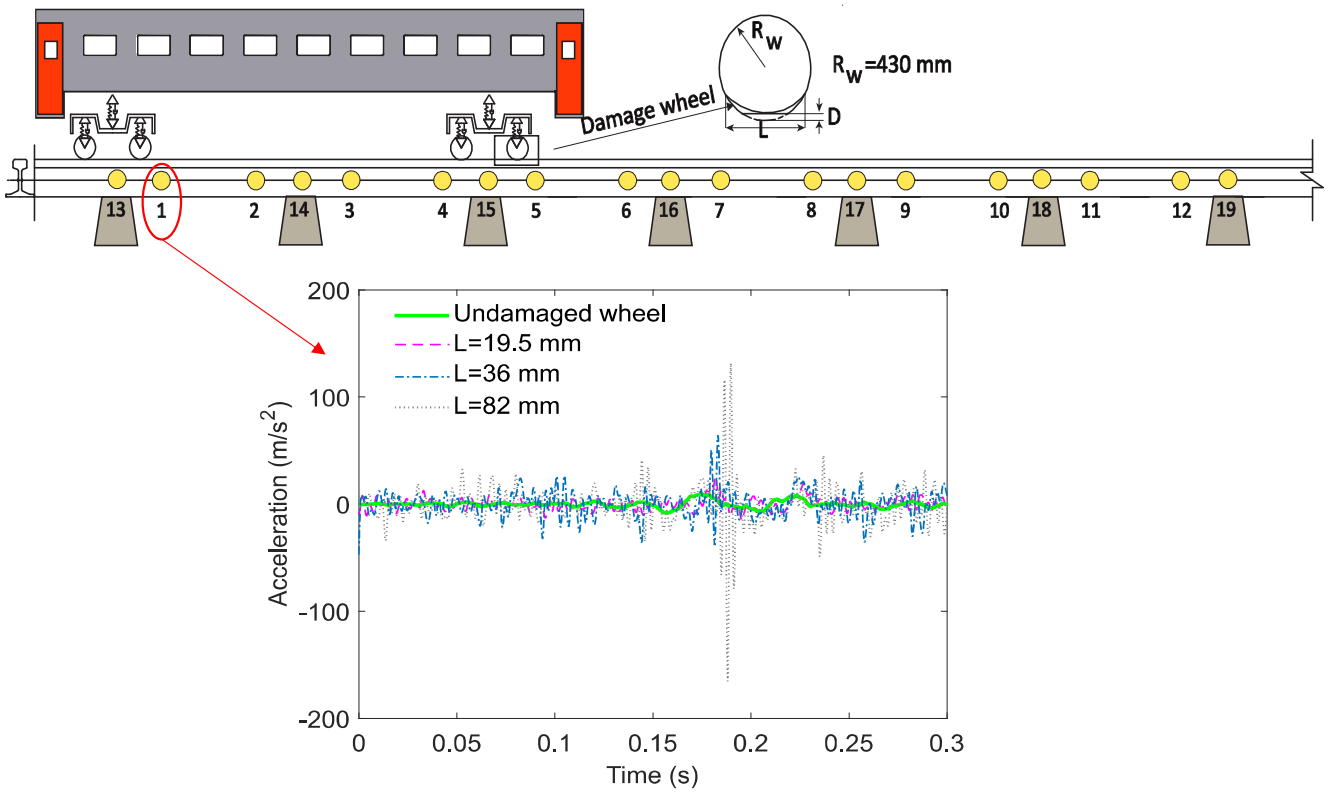
55-100 mm

Total: 150 damage scenarios

4. Case studies

Wayside Monitoring – Wheel flat identification

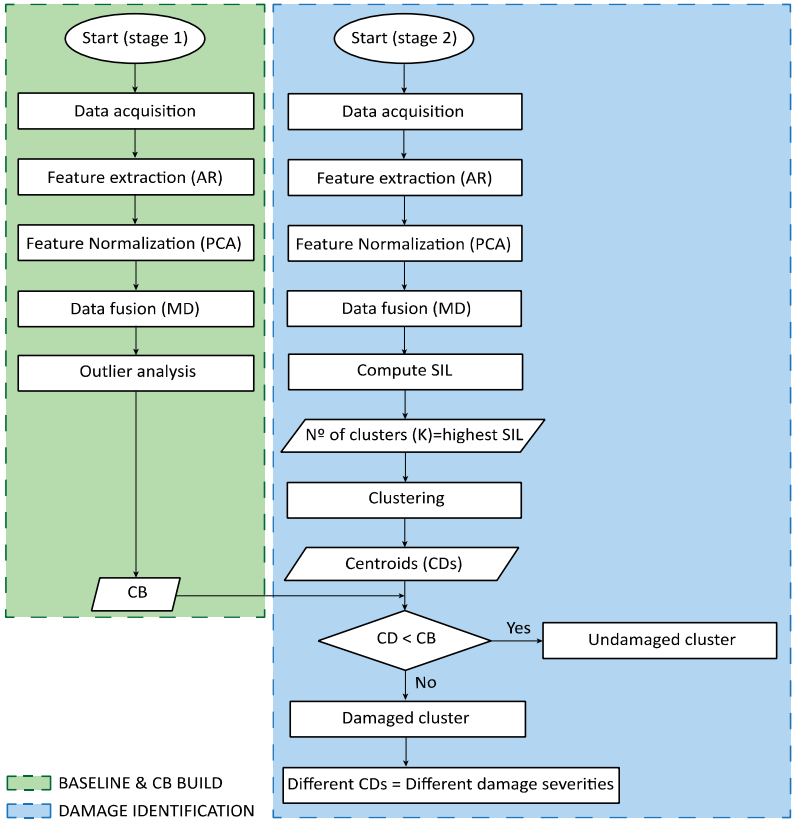
Virtual monitoring system



4. Case studies

Wayside Monitoring – Wheel flat identification

Machine Learning Methodology



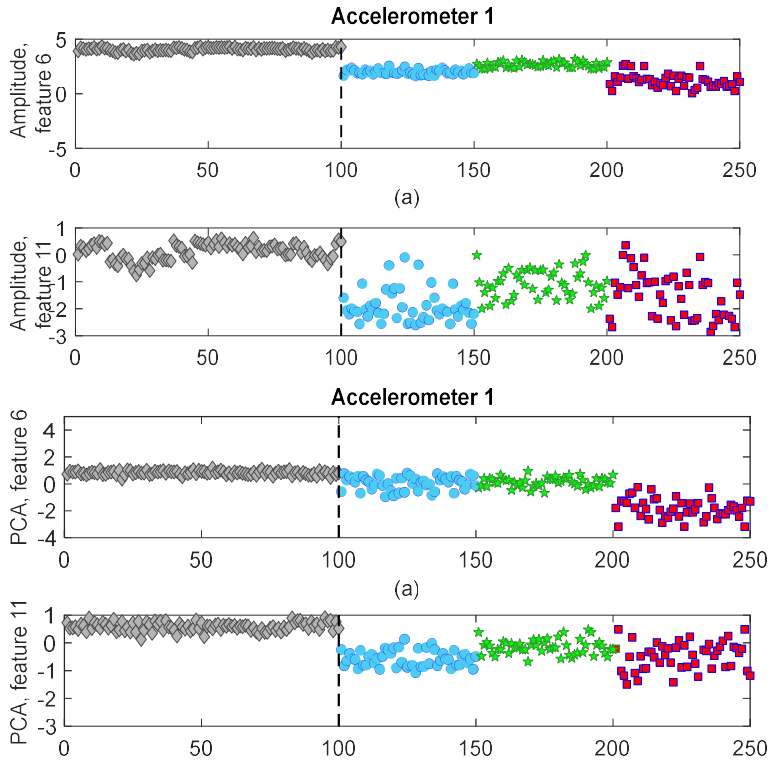
4. Case studies

Wayside Monitoring – Wheel flat identification

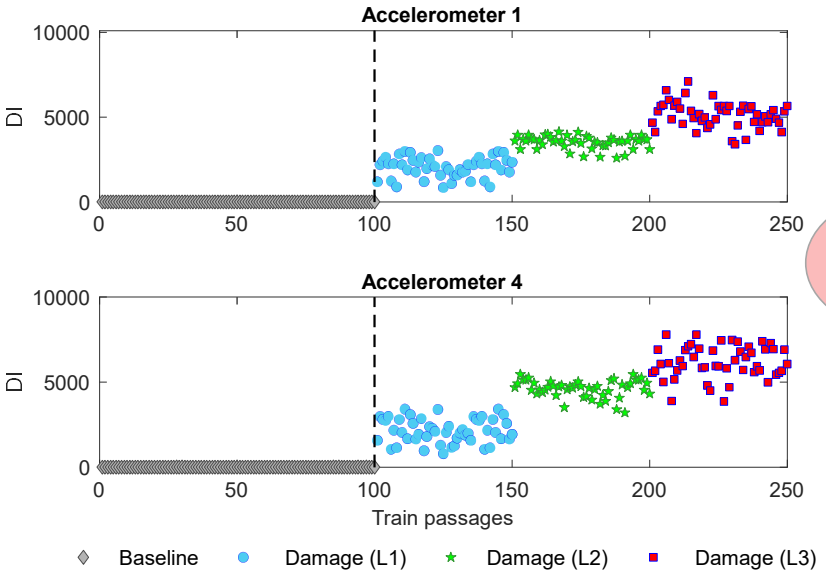
Machine Learning Methodology

Features Extraction

Features Normalization



Features Fusion

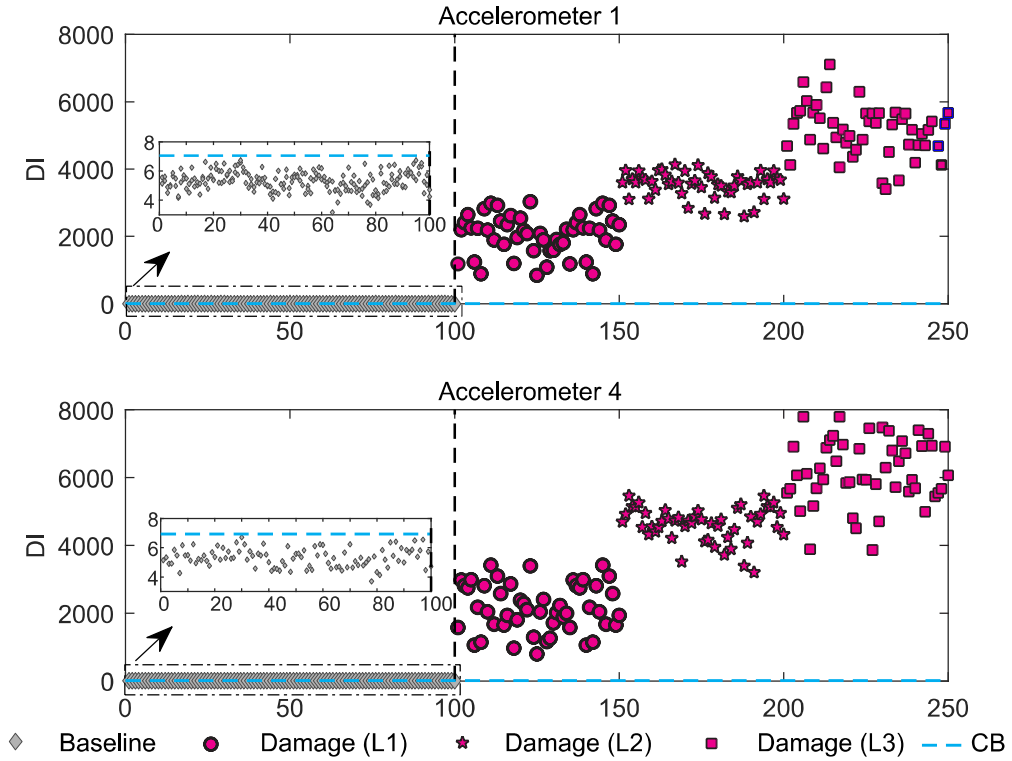


4. Case studies

Wayside Monitoring – Wheel flat identification

Machine Learning Methodology

Outlier Analysis

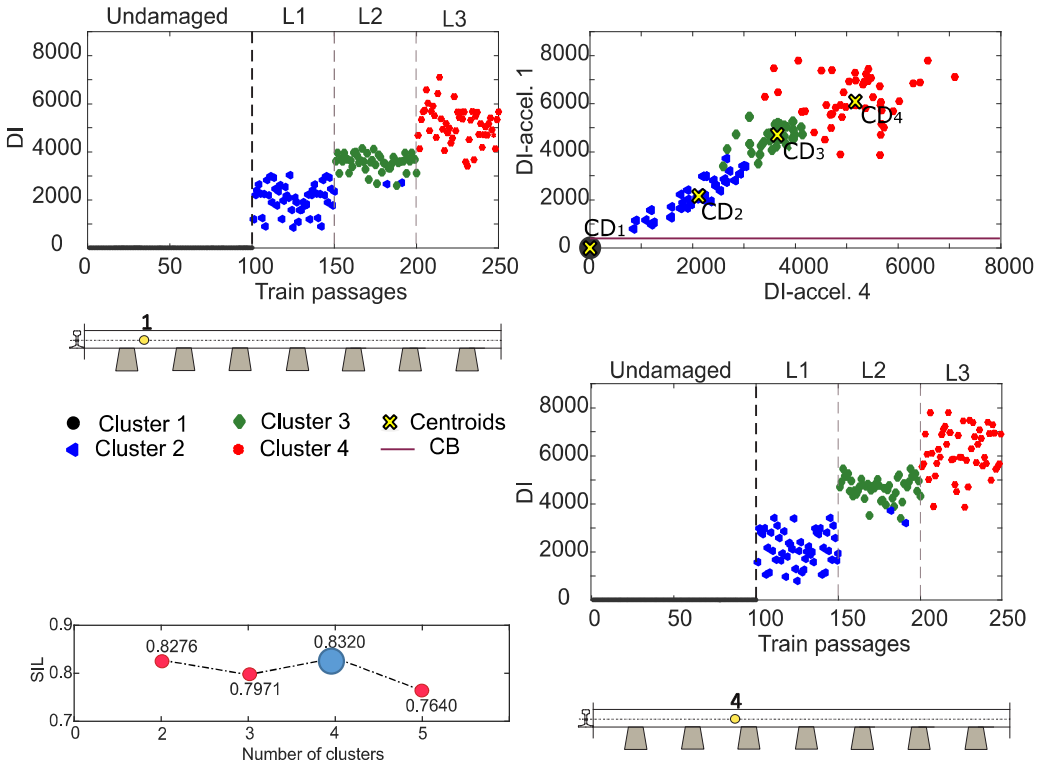


4. Case studies

Wayside Monitoring – Wheel flat identification

Machine Learning Methodology

Cluster Analysis



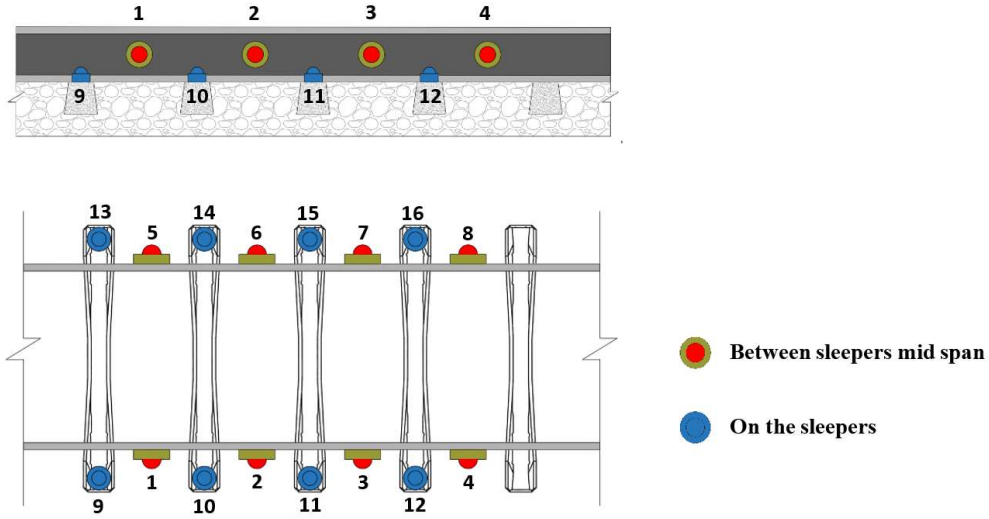
4. Case studies

Wayside Monitoring – Wheel polygonization detection

Virtual monitoring system

The numbers 1-to-4 and 5-to-8 represent the position of the measurement points mounted on the rail between two sleepers on the right and left sides, respectively.

Accelerations over the sleepers are measured by sensors located on positions 9-to-12 and 13-to-16.

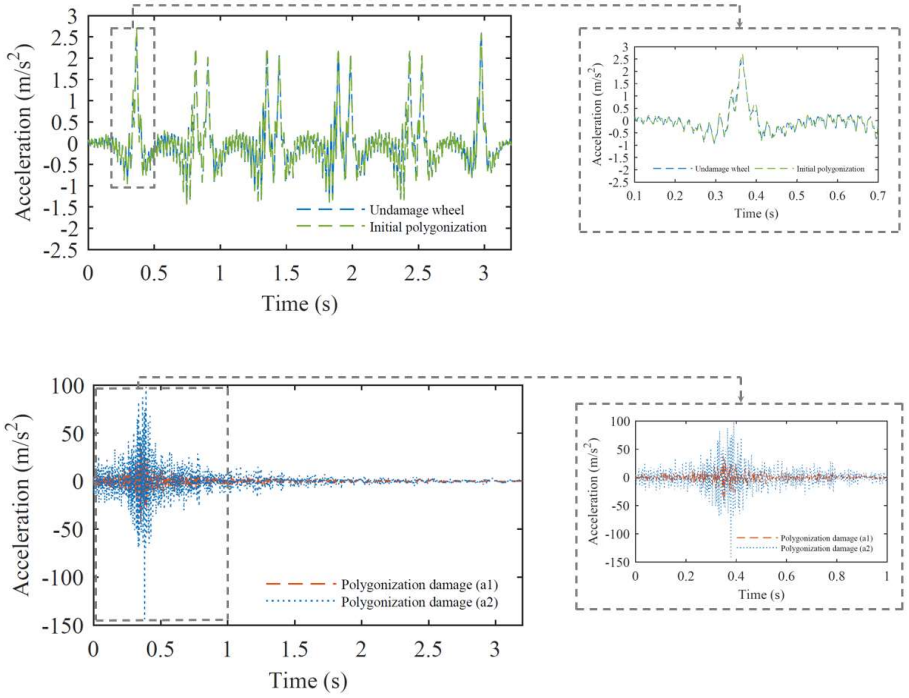


4. Case studies

Wayside Monitoring – Wheel polygonization detection

Baseline Condition and Damaged Scenarios

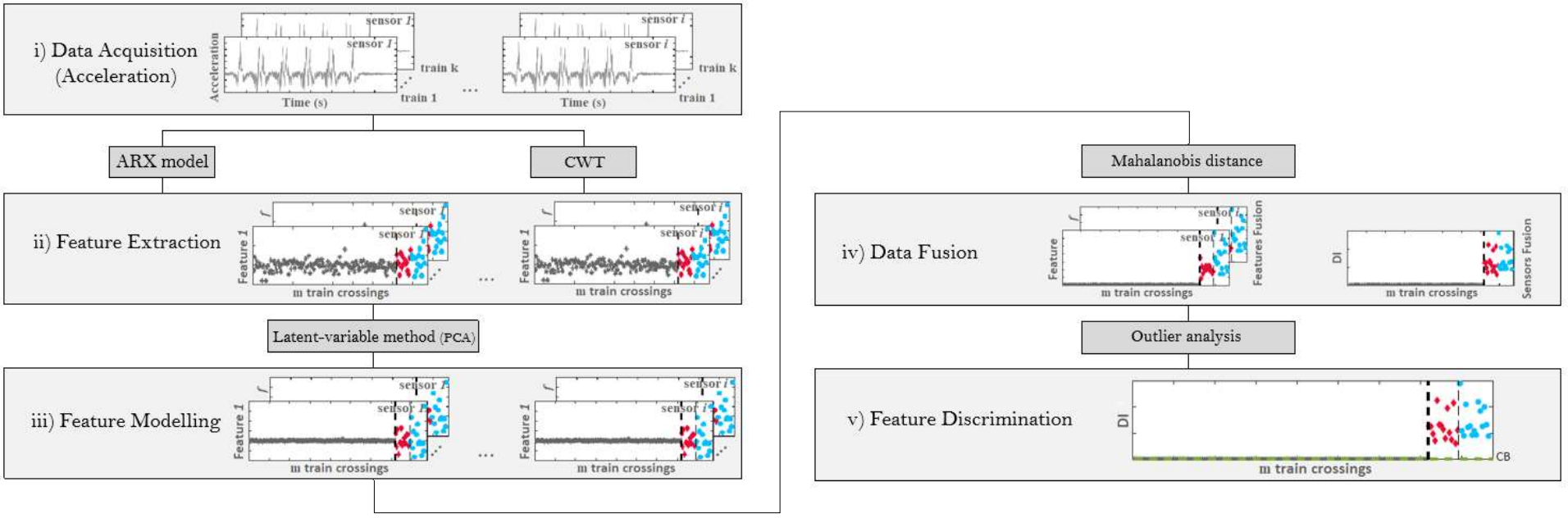
	Undamaged scenarios/healthy wheel		Damaged scenarios
	Perfect wheel	**Initial polygonal wheel**	**Polygonization wheel**
Vehicle	five freight wagons of the Laagrss type		
Number of loading schemes	6	1 (full load)	1 (full load)
Unevenness profile	4	1	1
Speed range	40-120 km/h	80 km/h	80 km/h
Noise ratio	5%	5%	5%
Location of defect		1st wagon 3rd wagon 5th wagon	1st wagon
Amplitude of defect (W)	-	0.035 mm	0.2-0.6 mm 0.8-1.2 mm
Total analyses	**113**	**30**	**30**



4. Case studies

Wayside Monitoring – Wheel polygonization detection

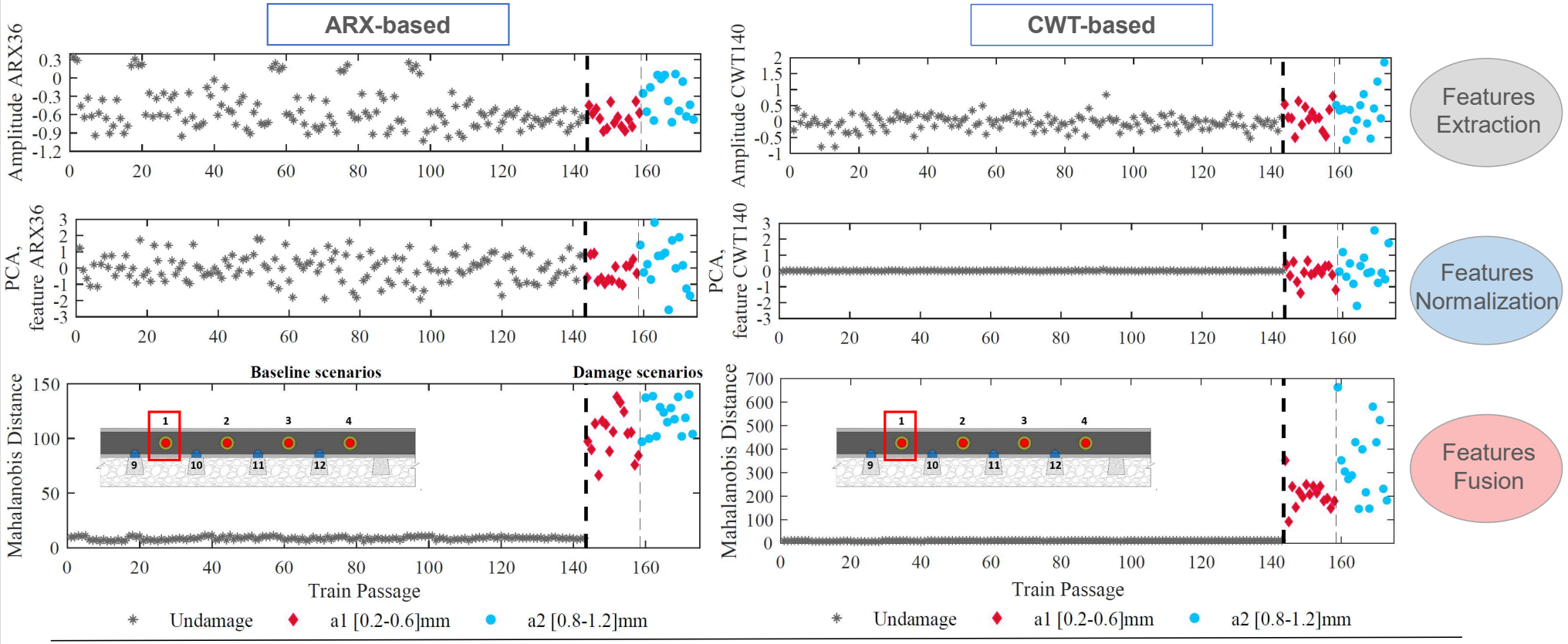
Machine Learning Methodology



4. Case studies

Wayside Monitoring – Wheel polygonization detection

Machine Learning Methodology



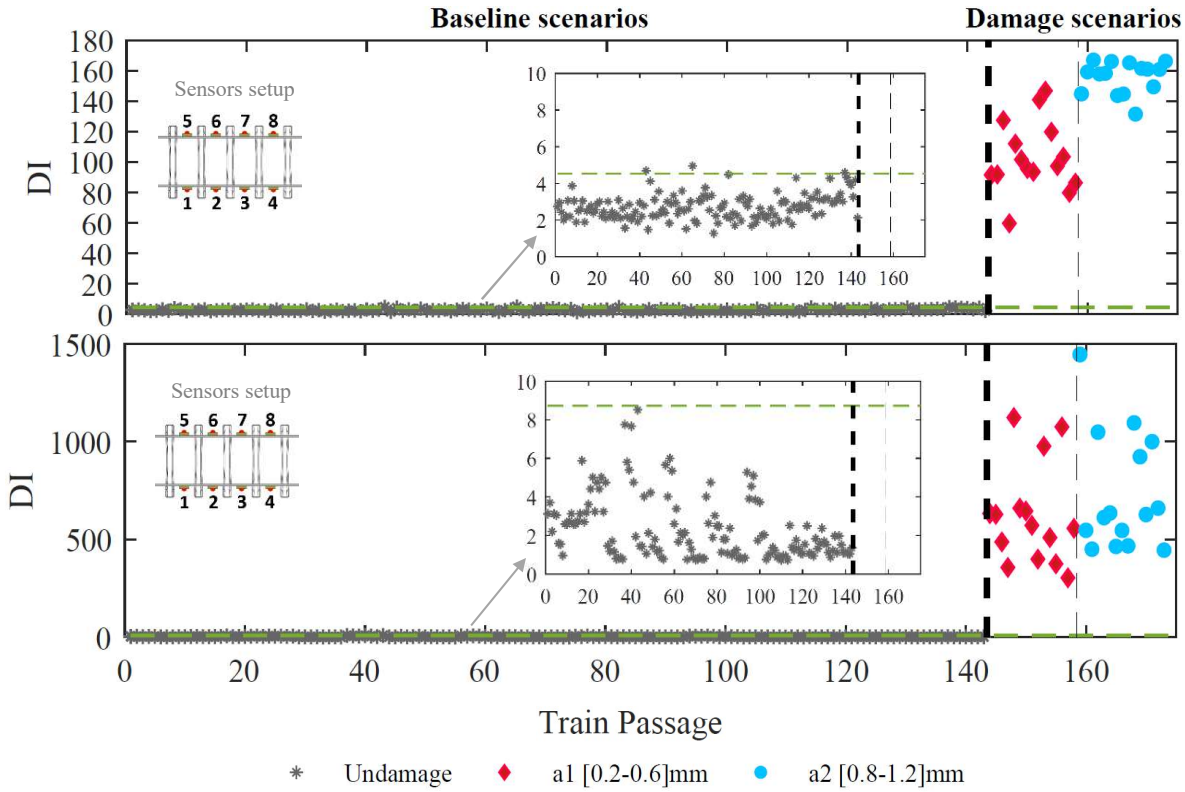
4. Case studies

Wayside Monitoring – Wheel polygonization detection

Machine Learning Methodology

ARX-based

CWT-based



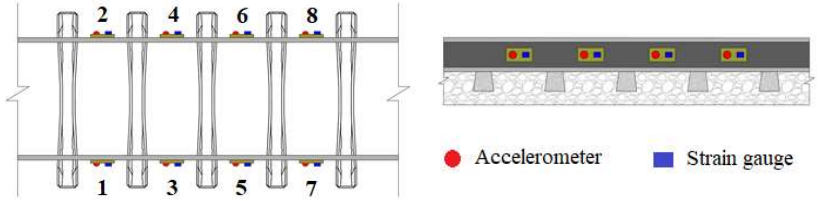
Sensors Fusion
+
Outlier Analysis

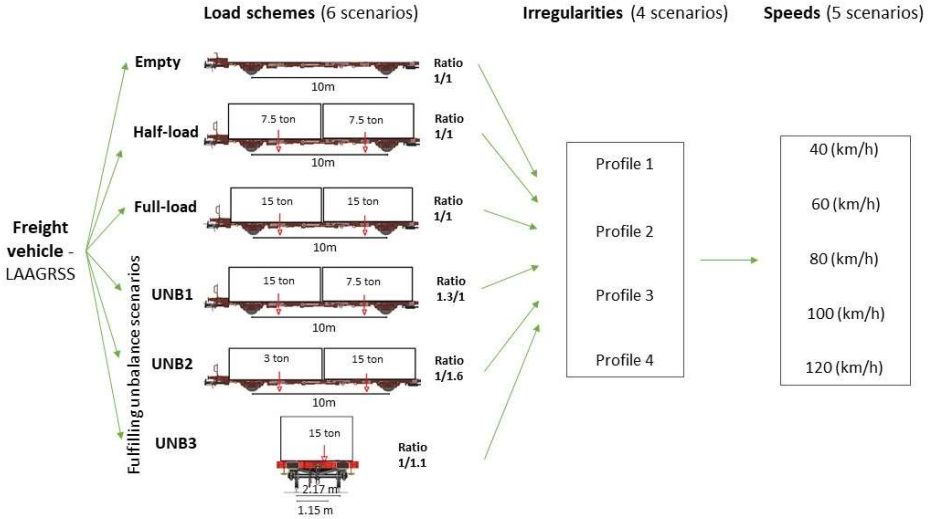
4. Case studies

Wayside Monitoring – Unbalanced loads identification

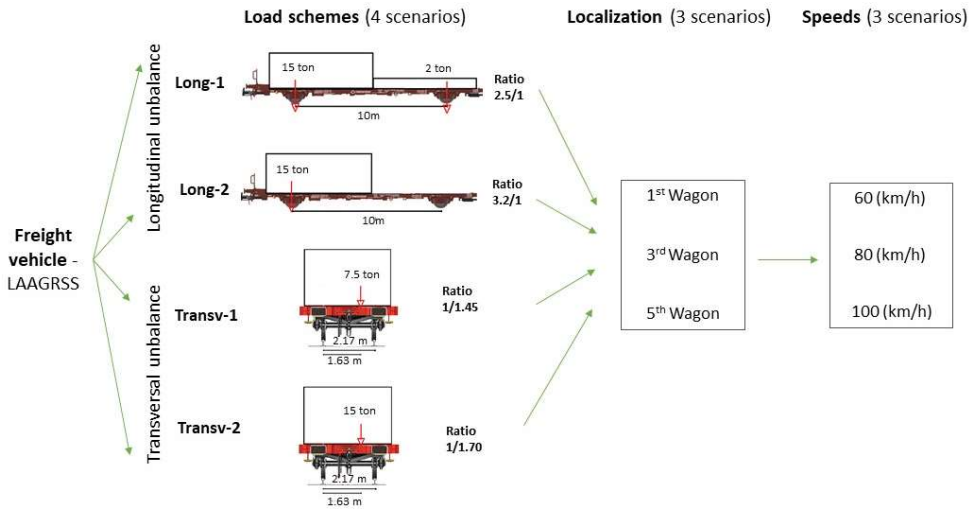
Virtual wayside monitoring system and load scenarios

The system is composed by a set of 8 accelerometers and 8 strain gauges mounted on the rail at mid-span between two sleepers.





Baseline Condition

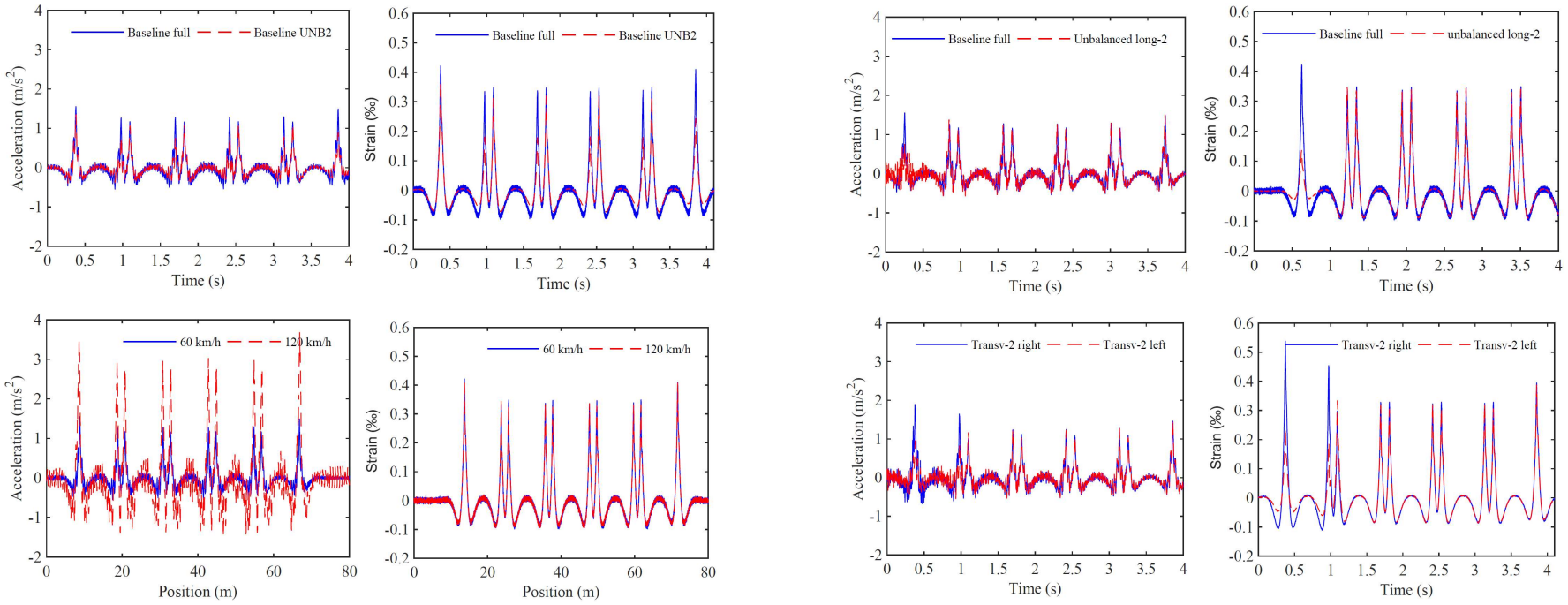


Unbalanced load Scenarios

4. Case studies

Wayside Monitoring – Unbalanced loads identification

Baseline Condition and Unbalanced load Scenarios



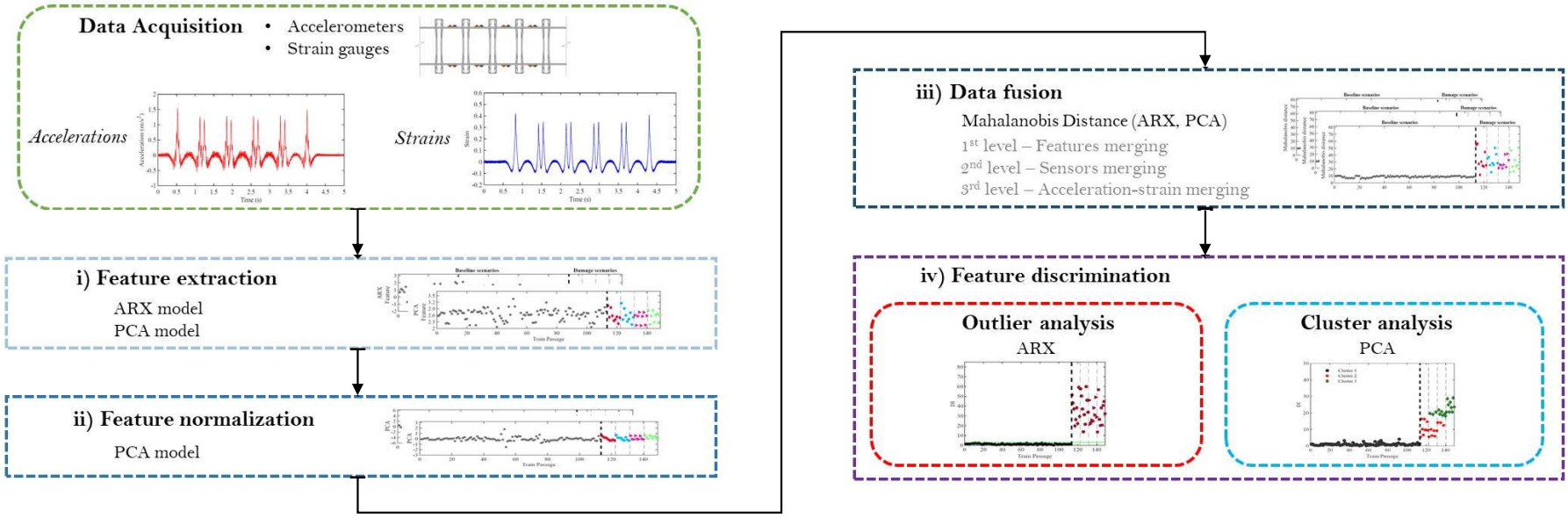
Baseline Condition

Unbalanced load Scenarios

4. Case studies

Wayside Monitoring – Unbalanced loads identification

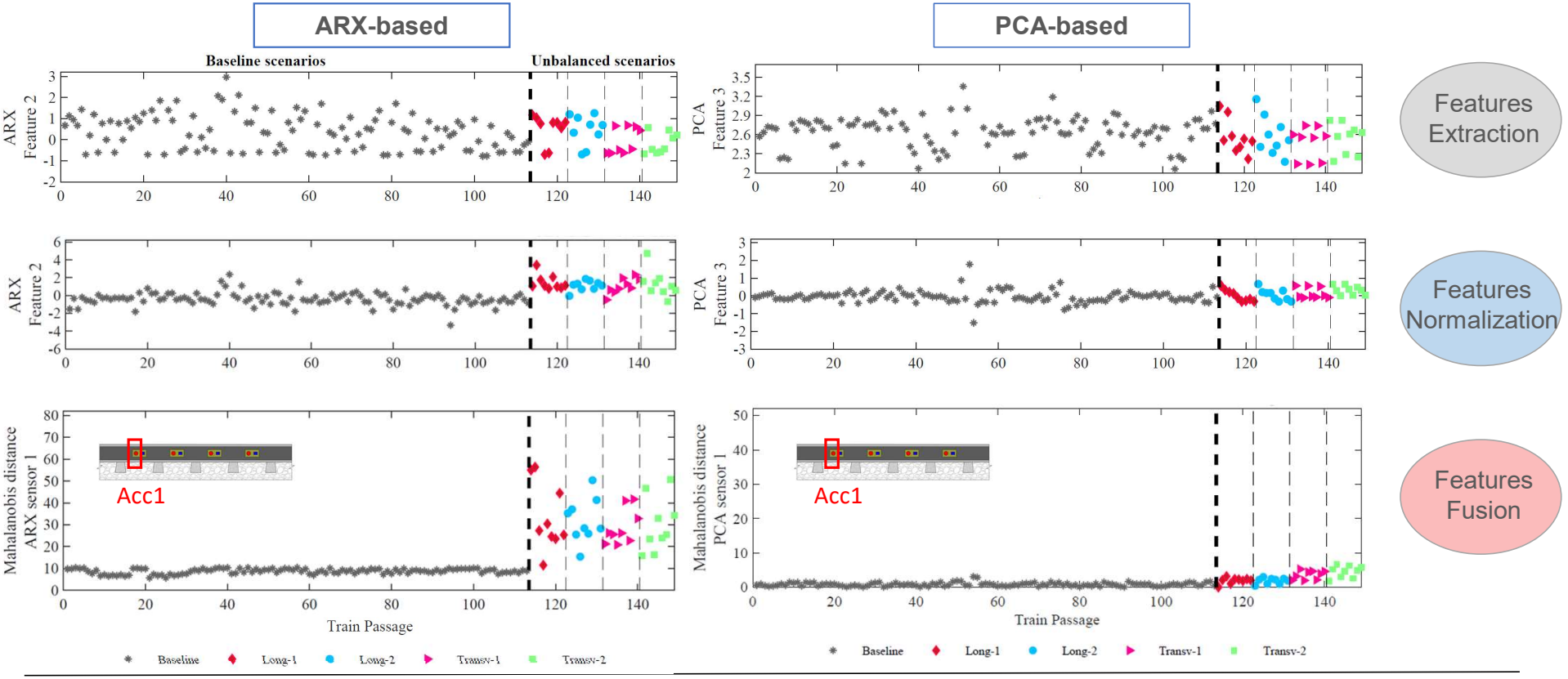
Machine Learning Methodology



4. Case studies

Wayside Monitoring – Unbalanced loads identification

Machine Learning Methodology



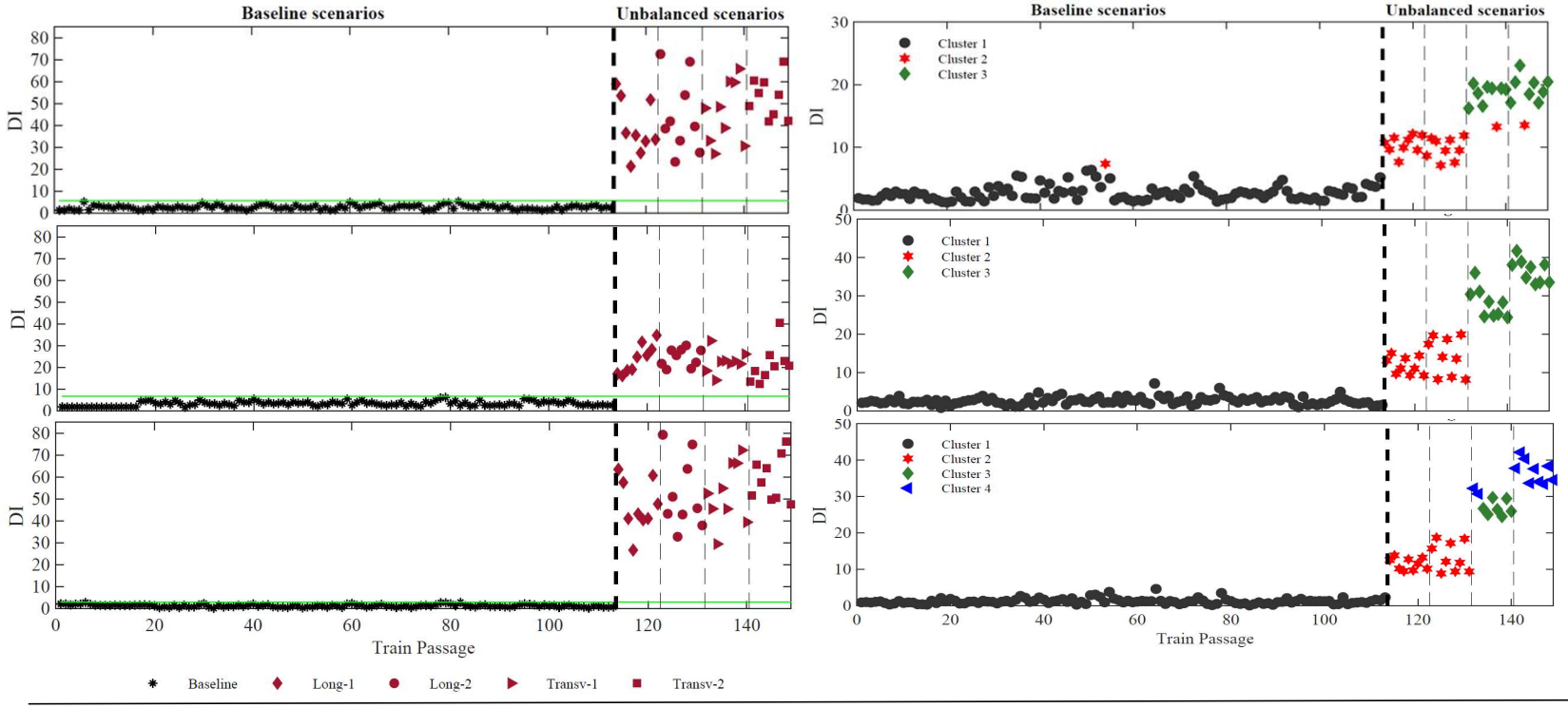
4. Case studies

Wayside Monitoring – Unbalanced loads identification

Machine Learning Methodology

Outlier Analysis | ARX-based

Cluster Analysis | PCA-based



Accelerometers Fusion

Strains Fusion

Acc+Strain Fusion

References

- Meixedo, A. (2021). Damage identification in railway bridges based on train induced dynamic responses. PhD Thesis. Faculty of Engineering - University of Porto, Portugal.

- Meixedo A, Santos J, Ribeiro D, et al. (2021) Damage detection in railway bridges using traffic-induced dynamic responses. Engineering Structures.238:112189; 10.1016/j.engstruct.2021.112189.

- Meixedo A, Santos J, Ribeiro D, et al. (2022) Online unsupervised detection of structural changes using train–induced dynamic responses. Mechanical Systems and Signal Processing. 165:108268; 10.1016/j.ymssp.2021.108268.

- Magalhães, F., Cunha, A. & Caetano, E., (2011). Vibration based structural health monitoring of an arch bridge: from automated OMA to damage detection, Mechanical Systems and Signal processing, doi:10.1016/j.ymssp.2011.06.011.

- Farrar, C. & Worden, K. (2013). Structural Health Monitoring – A machine learning approach, 1st ed, John Wiley & Sons Ltd, UK.

References

- Figueiredo, E., (2010). Damage Identification in Civil Engineering Infrastructure under Operational and Environmental Conditions. University of Porto, Faculty of Engineering.
- Santos, J. (2014). Smart Structural Health Monitoring Techniques for Novelty Identification in Civil Engineering Structures. PhD Thesis. Instituto Superior Técnico - University of Lisbon.
- Cury, A., Cremona, C., & Dumoulin, J. (2012). Long-term monitoring of a PSC box girder bridge: Operational modal analysis, data normalization and structural modification assessment. Mechanical Systems and Signal Processing, 33, 13–37. https://doi.org/10.1016/j.ymssp.2012.07.005.
- Mosleh, A., Montenegro, P. Costa, P. Calcada, R., An approach for wheel flat detection of railway train wheels using envelope spectrum analysis. Structure and Infrastructure Engineering, 2021, 17(12): p. 1710-1729, 10.1080/15732479.2020.1832536.
- Mosleh, A., Meixedo, A., Ribeiro, D. Montenegro, P. Calcada, R. , Early wheel flat detection: an automatic data-driven wavelet-based approach for railways. Vehicle System Dynamics, 2023, 61(6), 10.1080/00423114.2022.2103436.

References

- Guedes, António; Silva, Ruben; Ribeiro, Diogo; Vale, Cecília; Mosleh, A.;Montenegro, P. A.; Meixedo, Andreia. Autor correspondente: Guedes, António."Detection of Wheel Polygonization Based on Wayside Monitoring and Artificial Intelligence". Sensors 23 4 (2023): 2188. http://dx.doi.org/10.3390/s23042188.

- Silva, Ruben; Guedes, António; Ribeiro, Diogo; Vale, Cecília; Meixedo, Andreia; Mosleh, A.; Montenegro, P. A.. Autor correspondente: Silva, Ruben. "Early Identification of Unbalanced Freight Traffic Loads Based on Wayside Monitoring and Artificial Intelligence". Sensors 23 3 (2023): 1544. http://dx.doi.org/10.3390/s23031544.

Acknowledgments